

**Montana Water Center
Annual Technical Report
FY 2009**

Introduction

The Montana University System Water Center is located at Montana State University in Bozeman, was established by the Water Resources Research Act of 1964. Each year, the Center's Director at Montana State University works with the Associate Directors from the University of Montana - Missoula and Montana Tech - Butte to coordinate statewide water research and information transfer activities. This is all in keeping with the Center's mission to investigate and resolve Montana's water problems by sponsoring research, fostering education of future water professionals and providing outreach to water professionals, water users and communities.

To help guide its water research and information transfer programs, the Montana Water Center seeks advice from an advisory council to help set research priorities. During the 2009 research year, the Montana Water Research Advisory Council members were: Gretchen Rupp, Director and Steve Guettermann, Assistant Director for Outreach, Montana Water Center

Marvin Miller, Montana Bureau of Mines & Geology and MWC Associate Director

Don Potts, University of Montana and MWC Associate Director

Mark Aagenes, Montana Trout Unlimited, Conservation Director

Jeff Tiberi, Montana Association of Conservation Districts, Executive Director

J. P. Pomnichowski, Montana State Legislator

Daniel Sullivan, Montana Department of Agriculture, Technical Services Bureau Chief

Tyler Trevor, Montana University System, Associate Commissioner

Mike Volesky, Montana Governor's Office, Natural Resources Policy Advisor

Larry Dolan, Hydrologist - Montana Department of Natural Resources and Conservation

Hal Harper, Chief Policy Advisory - Governor's Office

John Kilpatrick, Director - Montana Water Science Center; U.S. Geological Survey

Mark Lere, Fisheries Division - Montana Fish, Wildlife & Parks

Bonnie Lovelace, Water Protection Bureau Chief Montana Department of Environmental Quality

Research Program Introduction

Through its USGS funding, the Montana Water Center partially funded three new water research projects and continued funding for three other projects for faculty at three of Montana's state university campuses. The Montana Water Center requires that each faculty research project directly involve students in the field and/or with data analysis and presentations. This USGS funding also provided research fellowships to four students involved with water science and hydro engineering. Here is a brief synopsis of their work, with the second year research projects listed first.

Completed Research Projects Dr. Winsor Lowe of the University of Montana and his team was awarded \$6,930 for studying "The Importance of Ecologically Connected Streams to the Biological Diversity of Watersheds: a case study in the St. Regis River subbasin, Montana." This project promises to have impact in how the state will address its obligations under the national Clean Water Act.

Dr. Stephen Parker, chemistry professor at Montana Tech of the University of Montana, and his team studied diel (24 h) and seasonal differences in the concentration and stable carbon isotope composition of dissolved inorganic and organic carbon in the Clark Fork and Big Hole Rivers of southwestern Montana. Dr. Parker received \$8,586.00.

Dr. Andrew Wilcox in the Department of Geosciences at the University of Montana is capitalizing on the rare opportunity to study river channel changes following the removal of a 100 year old hydroelectric dam with his project "Evolution of channel morphology and aquatic habitat in the Middle Clark Fork River following removal of Milltown Dam." Wilcox was funded \$15,818.00.

First Year Research Projects Dr. Wyatt Cross and Dr. Brian McGlynn of Montana State University's Department of Land Resources and Environmental Sciences received \$16,740. Their project, "Tracking Human-Derived Nitrogen through Stream Food Webs in a Rapidly Developing Mountain Watershed," will continue with data gathering and analysis.

Dr. Elizabeth Meredith of Montana Tech of the University of Montana began work on "Quantification of Coal-Aquifer Baseflow in Montana Rivers Using Carbon Isotopes." Dr. Meredith received \$14,500.00.

Dr. Gary Icopini and his team, also of Montana Tech of the University of Montana, were awarded \$12,210 for their work "Organic Wastewater Chemicals in Ground Water and Blacktail Creek, Summit Valley, Montana."

Student Fellowships Victoria Balfour, a PhD student in the University of Montana's College of Forestry and Conservation, was awarded \$1,500 for continuing work on her thesis titled "Variability in Wildfire Ash Characteristics: Implications for Post-fire Runoff, Erosion, and Water Quality."

Alaina Garcia, a triple major senior in engineering, mathematics and Spanish at Montana State University received \$1,000 for developing a prototype of study "A More Efficient Micro Turbo that Utilizes a Tesla Turbine Technology."

Able Mashamba, a PhD candidate in Montana State University's Department of Land Resources and Environmental Sciences, used his \$1,000 fellowship to study on "Bayesian Uncertainty and Sensitivity Analysis for Complex Environmental Models, with Applications in Watershed Management."

Bryan Swindell, a master's degree student studying Paleoecology at Montana State University, also received \$1,000 to further his study of climate change using "Tree-ring based reconstruction of Bighorn River Flow During the Last Millennium."

ng and the temporal variability in the concentration and stable carbon isotope composition of dissolved inorganic and organ

Carbon cycling and the temporal variability in the concentration and stable carbon isotope composition of dissolved inorganic and organic carbon in streams

Basic Information

Title:	Carbon cycling and the temporal variability in the concentration and stable carbon isotope composition of dissolved inorganic and organic carbon in streams
Project Number:	2006MT89B
Start Date:	3/1/2006
End Date:	9/1/2009
Funding Source:	104B
Congressional District:	At large
Research Category:	Climate and Hydrologic Processes
Focus Category:	Geochemical Processes, Hydrogeochemistry, Water Quality
Descriptors:	
Principal Investigators:	Stephen Parker, Douglas Cameron

Publications

There are no publications.

Temporal Variability in the Concentration and Stable Carbon Isotope Composition of Dissolved Inorganic and Organic Carbon in Two Montana, USA Rivers

Stephen R. Parker · Simon R. Poulson · M. Garrett Smith ·
Charmaine L. Weyer · Kenneth M. Bates

Received: 27 February 2009 / Accepted: 30 July 2009
© Springer Science+Business Media B.V. 2009

Abstract Here we report diel (24 h) and seasonal differences in the concentration and stable carbon isotope composition of dissolved inorganic (DIC) and organic carbon (DOC) in the Clark Fork (CFR) and Big Hole (BHR) Rivers of southwestern Montana, USA. In the CFR, DIC concentration decreased during the daytime and increased at night while DOC showed an inverse temporal relationship; increasing in the daytime most likely due to release of organic photosynthates and decreasing overnight due to heterotrophic consumption. The stable isotope composition of DIC ($\delta^{13}\text{C}$ -DIC) became enriched during the day and depleted over night and the $\delta^{13}\text{C}$ -DOC displayed the inverse temporal pattern. Additionally, the night time molar rate of decrease in the concentration of DOC was up to two orders of magnitude smaller than the rate of increase in the concentration of DIC indicating that oxidation of DOC was responsible for only a small part of the increase in inorganic carbon. In the BHR, in two successive years (late summer 2006 & 2007), the DIC displayed little diel concentration change, however, the $\delta^{13}\text{C}$ -DIC did show a more typical diel pattern characteristic of the influences of photosynthesis and respiration indicating that the isotopic composition of DIC can change while the concentration stays relatively constant. During 2006, a sharp night time increase in DOC was measured; opposite to the result observed in the CFR and may be related to the night time increase in flow and pH also observed in that year. This night time increase in DOC, flow, and pH was not observed 1 year later at approximately the same time of year. An in-stream mesocosm chamber used during 2006 showed that the night time increase in pH and DOC did not occur in water that was isolated from upstream or hyporheic contributions. This result suggests that a “pulse” of high DOC and pH water was advected to the sampling site in the BHR in 2006 and a model is proposed to explain this temporal pattern.

S. R. Parker (✉) · M. G. Smith · C. L. Weyer · K. M. Bates
Department of Chemistry and Geochemistry, Montana Tech of The University of Montana,
1300 W. Park St., Butte, MT 59701, USA
e-mail: sparker@mtech.edu

S. R. Poulson
Department of Geological Sciences and Engineering, University of Nevada-Reno, 1664 N. Virginia St.,
Reno, NV 89557-0138, USA

Keywords Dissolved organic carbon · Carbon isotopes · Dissolved inorganic carbon · Diel

1 Introduction

Investigations over the past 20 years have shown that diel (24 h) changes in the concentration of chemical species in flowing systems are reproducible processes that play an integral role in the health and water quality of river systems. Healthy rivers can exhibit large diel pH, dissolved O₂ (DO), and CO₂ cycles that are largely driven by aquatic plants and microbes which alternately consume or produce CO₂ depending on whether photosynthesis or respiration is the dominant process (Odum 1956; Pogue and Anderson 1994; Nagorski et al. 2003; Parker et al. 2005, 2007a). These short term variations are driven by the daily photoperiod, which influences: aquatic photoautotrophs; instream temperature cycles; changes in dissolved gas gradients between air and water; and affect either directly or indirectly concentration changes in metals and metalloids (e.g., Nimick et al. 2003, 2005; Jones et al. 2004; Gammons et al. 2005; Parker et al. 2007a, b and references therein). While researchers investigating the mechanisms influencing diel processes have provided great insight into the “driving forces” behind these daily changes, there is still much that is not well understood. By gaining deeper insight into the underlying mechanisms controlling diel concentration changes of important dissolved and particulate species we will be able to develop a better fundamental understanding of how streams function. This knowledge will help scientists, resource managers and others make better predictions on how streams will respond to shifting conditions caused by climate change, changing agricultural practices, restoration activities, nutrient fluxes and development.

Previous work has demonstrated that there is a significant and reproducible diel cycle in the stable isotope composition of dissolved inorganic carbon ($\delta^{13}\text{C-DIC}$) in both the Clark Fork River (CFR) and Big Hole River (BHR) in Montana, USA as well as a substantial cycle in the ^{18}O composition of dissolved molecular oxygen ($\delta^{18}\text{O-DO}$) in the BHR and other streams (Parker et al. 2005, 2007a, 2009). These daily changes in the isotope composition of the DIC and DO are caused by the combined effects of photosynthesis and respiration of aquatic plants and microbes as well as gas-exchange and groundwater influx. Additionally, $\delta^{13}\text{C-DIC}$ has been used as a tracer of the origins and sources of carbon in watersheds (e.g., Gaiero et al. 2005), but these data must be used carefully since substantial diel changes in $\delta^{13}\text{C-DIC}$ can occur (up to 4.5‰, Parker et al. 2009).

Dissolved organic carbon (DOC) represents a significant pool of reduced carbon in most aquatic ecosystems that is readily available to heterotrophic microorganisms as an energy source (McKnight et al. 1997; Volk et al. 1997). It has also been suggested that the DOC pool may be the largest source of carbon for microbial activity (Kaplan and Bott 1982; Hobbie 1992). Additionally, it has been shown that different size classes of DOC molecules exist and that the distribution can change over a diel period (Amon and Benner 1996; Zeigler and Fogel 2003). Depending on the size and composition of the DOC some classes of molecules may be more refractory than others and consequently consumed at different rates (Thurman 1985; Zeigler and Fogel 2003).

The types and concentration of the DOC can have a significant influence on the chemical composition of surface waters such as the bioavailability of metal ions and the absorption of

light in the visible and UV ranges (McKnight et al. 1997). Much of the literature examining DOC in rivers has concentrated on sources of organic carbon and its fate and transport to downstream areas (e.g., Thurman 1985; Olivie-Lanquet et al. 2001; Bianchi et al. 2004, 2007; Hood et al. 2005; Dalzell et al. 2007). Several researchers have shown that diel changes in DOC concentration occur in streams and can be attributed to daily changes in the level of productivity of algal communities (e.g., Manny and Wetzel 1973; Kaplan and Bott 1982; Harrison et al. 2005; Spencer et al. 2007). However, there is little literature that reports investigations of temporal changes in DOC and the ^{13}C -composition of DOC ($\delta^{13}\text{C}$ -DOC) simultaneously on a diel scale in surface waters (Zeigler and Fogel 2003). Since community respiration is using the DOC as a carbon source and other aquatic species are producing organic molecules as a consequence of their daily productivity, it is reasonable to expect changes in the isotopic composition of the DOC as it is influenced by the daily changes in the rates of metabolic activity (Barth and Veizer 1999; Zeigler and Fogel 2003; Zeigler and Brisco 2004).

DOC can include water soluble forms of amino acids, carbohydrates, organic acids, alcohols as well as fulvic and humic acids (Thurman 1985). Sources of DOC in streams can include decomposition of detrital organic matter, importation of organics from external (allochthonous) sources and in-stream production by aquatic plants and microbes (autochthonous). Microbes using DOC as a carbon source will produce CO_2 from respiration with a carbon isotope signature characteristic of the organic carbon substrate (Clark and Fritz 1997). In temperate regions, plant organic matter, that serves as the carbon source for microbial respiration has a $\delta^{13}\text{C}$ of -20 to -30% (Clark and Fritz 1997). In contrast, atmospheric CO_2 has $\delta^{13}\text{C}$ of -7 to -8.5% (NOAA 2008) and consequently DIC produced by gas exchange will be isotopically enriched compared to that produced by respiration.

A significant portion of DOC in natural waters falls in the category of natural organic matter (NOM), and most of the NOM fits into the operationally defined subcategories of fulvic acids (FA) and humic acids (HA; Thurman 1985; Macalady 1998). The fulvic and humic acids as well as other organic acids are well known for their ability to complex metal ions in solution (Saar and Weber 1982; Clapp et al. 1998). It is known that the fulvic and humic acids can contribute to daily variations in surface water iron concentrations by affecting Fe redox cycling through changes in the photoreactivity of Fe in the aqueous system (Voelker et al. 1997; Hrcir and McKnight 1998).

In this study, we investigated diel changes in the concentration of DOC and DIC in two different rivers systems (CFR and BHR). These rivers are geographically close but exhibited approximately inverse diel patterns in the concentration of DOC during the late summer of 2006. An in-stream mesocosm chamber was used in the BHR during 2006 to compare diel cycles and levels of DOC and DIC that were isolated from the flowing water column or hyporheic water exchanges. A follow-up study was conducted in the BHR 1 year later to assess the reproducibility of the diel DOC pattern observed the previous year. Additionally, in order to identify possible sources of DOC in the BHR a series of seeps (streamside springs) and shallow sediment water was sampled during the follow-up work in 2007. The rates of DOC consumption and DIC production in the CFR were compared in order to determine what portion of the inorganic carbon being produced resulted from the oxidation of DOC. The $\delta^{13}\text{C}$ -DOC was examined in the CFR as well as the $\delta^{13}\text{C}$ -DIC in the CFR and BHR. These isotope results are used here in conjunction with the seep and chamber data to investigate the relationship of the diel changes in DOC and DIC to the processes influencing these changes. Models are presented to help interpret the

diel behavior of DOC in the CFR and the differences in the diel behavior of DOC observed in the BHR between 2006 and 2007.

2 Field Sites

2.1 CFR Site

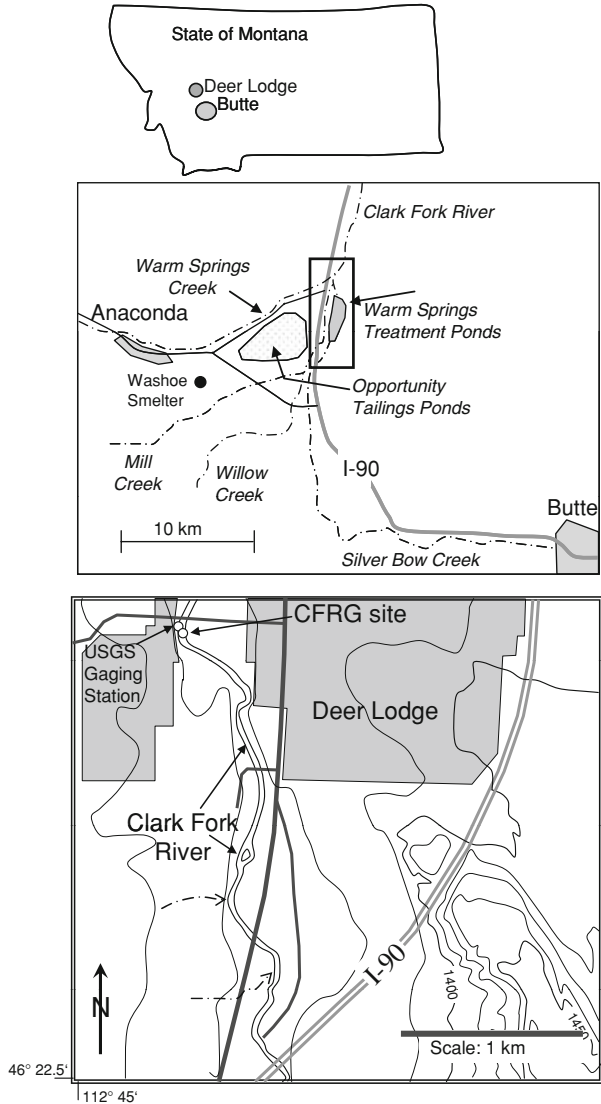
The field site on the Clark Fork River ($46^{\circ}23'51''\text{N}$; $112^{\circ}44'33''\text{W}$; sampling site CFRG) was within the city limits of Deer Lodge, MT and directly across from the USGS gaging station (Fig. 1, USGS Gage #12324200, 1,372 m elevation). Streamflow measurements were taken from the USGS gaging station which records every 15 min. The Clark Fork here is a second order stream with a discharge of roughly $0.6\text{--}60\text{ m}^3\text{ s}^{-1}$ depending on the time of year. The river in the study reach has moderate alkalinity ($\sim 3,200\text{--}3,700\text{ }\mu\text{eq l}^{-1}$; Parker et al. 2007a) and a pH range of about 8.0–9.0 during the summer months. Aquatic plants are dominated by *Cladophora* and diatom algae (Watson 1989). The mining and smelting centers of Butte and Anaconda are situated at the headwaters of the upper Clark Fork River along Silver Bow and Warm Springs Creeks, respectively (Fig. 1) such that the floodplain and streambed of the upper Clark Fork River contain highly elevated quantities of metals and metalloids (e.g., Fe, Cu, Zn, Pb, Cd, As) deposited as the result of mining, milling, and smelting activities (Moore and Luoma 1990). Currently, most of the heavy metal load in Silver Bow Creek is removed by a lime treatment facility at Warm Springs (Fig. 1). However, elevated concentrations of dissolved arsenic have been measured in the water exiting the treatment ponds ($>40\text{ }\mu\text{g L}^{-1}$) during summer base-flow periods (Duff 2001; Gammons et al. 2007). Diel changes in the concentration of metals and arsenic in the upper CFR have been previously characterized (Brick and Moore 1996; Parker et al. 2007a; Gammons et al. 2007).

2.2 BHR Site

The field site near the Mudd Creek Bridge on the Big Hole River ($45^{\circ}48'28''\text{N}$, $113^{\circ}18'51''\text{W}$; sampling site BHRG) was about 50 m upstream from the USGS gaging station (Fig. 2; USGS Gage #6024540, 1795 m). Annual flows range from 5 to $140\text{ m}^3\text{ s}^{-1}$ depending on time of year. Flow data for this site was obtained from the USGS gaging station which records discharge every 15 min. The BHR is a headwater tributary to the Missouri River and is a free-flowing river draining a sparsely-populated, high elevation basin ($\sim 1,900\text{ m}$ above sea level) of approximately $7,200\text{ km}^2$ in extent. This river is relatively pristine and there is little historical impact from mining or industrial sources. The principal activities in the basin are agriculture and recreation.

Previous work (Gammons et al. 2001; Ridenour 2002; Wenz 2003; Parker et al. 2005) has summarized the general geochemical characteristics of the Big Hole River. Overall, the Big Hole River at Mudd Creek Bridge can be classified as a Na–Ca–bicarbonate water, with alkaline pH and low to moderate alkalinity ($1,500\text{--}1,800\text{ }\mu\text{eq L}^{-1}$). The lower alkalinity of the BHR versus the CFR described above results in lower buffering capacity of the BHR stream water that often leads to larger ranges in and higher absolute values of pH during summer low flow periods.

Fig. 1 Location map of the upper Clark Fork River showing Butte, MT; Anaconda, MT; Warm Springs Ponds, Opportunity Ponds and the CFRG sampling site on the Clark Fork River near Deer Lodge, Montana, USA



3 Methods

3.1 Field Methods

3.1.1 Clark Fork River

Diel sample collection on the CFR began on 27 July 2006 at 11:15 and continued until 13:15 on 28th of July. All times are reported as local time (MDT, GMT—0600).

In situ temperature, pH, specific conductivity (SC), dissolved oxygen (DO) concentration and percent O₂ saturation were measured at each sampling time with a Hydrolab MS-5 datasonde (Luminescent DO probe) or an In Situ Troll 9000 (Clark DO probe) as

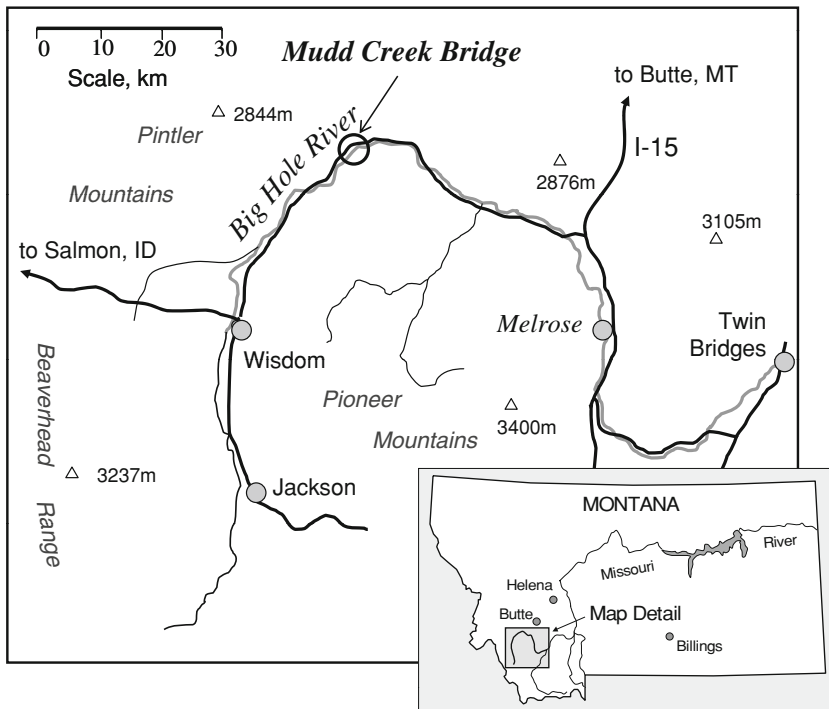


Fig. 2 Site map showing the Mudd Creek Bridge sampling area of the Big Hole River located in southwestern Montana, USA

well as a hand-held meter (WTW 340i). The instruments were calibrated according to the manufacturer's specifications.

Several samples were collected for laboratory analysis of DO using the Winkler method (Wetzel and Likens 1991). Unfiltered water was collected in 500 mL glass bottles with no head space and stored on ice until analysis in the laboratory within 48 h. The results of these analyses were compared to the DO measurements using hand and in situ instruments (shown in results).

Water was sampled from the main stem of the river in a well mixed, rapidly flowing reach approximately 0.5 m deep, 3 m from shore and at a depth approximately half way between surface and bottom. Filtration was done using a peristaltic pump and disposable 142 mm diameter 0.1 μm cellulose-ester filter membranes (for further details see Gammons et al. 2005). Samples (filtered) for DOC analysis were collected in 250 mL amber bottles that had been acid washed (5% HNO_3), triple rinsed with deionized water and oven dried (100°C). Filtered samples for ^{13}C -isotope analysis of dissolved inorganic carbon ($\delta^{13}\text{C}$ -DIC) were collected in 125 or 250 mL acid-washed, oven dried, glass bottles with no head-space and the DIC was precipitated in the laboratory as SrCO_3 after Usdowski et al. (1979).

A detector was used to measure photosynthetically active radiation (PAR) flux values (400–700 nm, $\mu\text{E m}^{-2} \text{s}^{-1}$) which were based on the manufacturer's calibration of the sensor. The PAR went to zero at 21:00 h in the evening and rose above zero at 06:30 in the morning. This *dark* period (zero PAR) is represented by the shaded region on all diel graphs.

All samples collected in the field were stored on ice, in sealed plastic bags and returned to the laboratory immediately following the field work.

3.1.2 Big Hole River

Two separate diel samplings occurred on the BHR approximately 1 year apart: 8 to 9 August 2006 and 31 July to 1 Aug 2007. Sampling was performed similar to that described in the previous section on the Clark Fork site. Alkalinity was measured in the field using a Hach titrator and standardized H_2SO_4 . Samples from seeps above the main sampling site were collected with a clean 60 mL syringe that was triple rinsed with sample water and then filtered using 0.2 μm PES syringe filters into glass bottles. Sediment pore water was collected at two locations near the sampling site with a 60 mL syringe that was inserted approximately 12 cm into the shallow sediments in the middle of the river. The syringe plunger was very slowly withdrawn to minimize water from being pulled around the barrel of the syringe from the above river; taking 2–3 min to fill the 60 mL volume. This water was filtered using 0.2 μm PES filters into glass bottles.

An isolation chamber was used during the 2006 sampling that was made from a 10 cm inside diameter clear acrylic plastic cylinder 22 cm long. One end was sealed and the other end was removable (both clear acrylic). Each end had a tubing connector fastened to a drilled and threaded hole in the center. Prior to the start of the diel sampling, the chamber was filled approximately half-full with cobbles ranging from 2 to 10 cm in diameter collected from the sampling site that were covered with attached periphyton and biofilms. The chamber lid was sealed with silicone vacuum grease and held in place with an elastic strap. Clear plastic tubing was used to connect the chamber to a peristaltic pump mounted on a tethered platform in the river, then to a low volume flow chamber on a datasonde and back to the chamber. The chamber and datasonde were placed on the river bottom at a depth of ~ 0.5 m. At the beginning of the sampling period, the chamber was flushed with river water, filled and purged to remove most of the trapped air. The chamber water was sampled every 2 h as described previously for DOC and DIC; then flushed and refilled with fresh river water. The datasonde connected to the chamber recorded pH, temperature, DO, and SC every 30 min throughout the diel period.

3.2 Analytical Methods

A pre-concentration step for samples for $\delta^{13}\text{C}$ -DOC analysis was performed by evaporating 250 mL of filtered river water to near-dryness at 50°C and resuspending in 4 mL of 1% H_3PO_4 .

The SrCO_3 precipitates (described above) for $\delta^{13}\text{C}$ -DIC and the DOC concentrates for $\delta^{13}\text{C}$ -DOC were analyzed using a Eurovector elemental analyzer interfaced to a Micromass Isoprime stable isotope ratio mass spectrometer after Harris et al. (1997) and Gandhi et al. (2004), respectively. Replicate analyses (three per sample set) indicated an average relative standard deviation (RSD) of 0.95‰ for $\delta^{13}\text{C}$ -DOC and 0.55‰ for $\delta^{13}\text{C}$ -DIC.

All analyses for total carbon (TC) and DOC were performed at Montana Tech using an Ionics (Model 1505) Total Carbon Analyzer (combustion method). All samples for TC analysis used filtered, unacidified water. Samples for DOC analysis used filtered water that was acidified to 1% (v/v) with concentrated H_3PO_4 and sparged for 5 min with N_2 . These samples were then sparged in the instrument for an additional 3 min with CO_2 -free air and analyzed. Standards were prepared from a stock solution of $1,000 \text{ mg l}^{-1}$ potassium hydrogen phthalate (KHP) prior to each analysis. All glassware used for carbon analyses

was acid-washed and oven dried prior to use (100°C). DIC was determined by subtracting DOC concentration from TC. Replicate analyses indicated an RSD of 5% for DOC and DIC.

3.3 Modeling

The partial pressure of dissolved (wet) CO₂ ($p\text{CO}_2$, μatm) was calculated for the CFR and BHR with the modeling program CO₂SYS (Lewis and Wallace 1998) using the temperature, pH and either the total alkalinity or DIC to determine the carbon speciation.

4 Results and Discussion

4.1 Clark Fork River

4.1.1 Field Results

Temperature, flow, pH, and specific conductivity from the diel sampling on the CFR in 2006 are shown in Fig. 3. A diel pH change of approximately 0.6 units (range 7.8–8.4) was observed which is attributed to daytime net consumption of CO₂ by aquatic photosynthesis and night time production of CO₂ by community respiration. The temperature reached a daytime maximum of 24.6°C and night time minimum of 16.5°C. A diel change in flow of approximately 13% was observed most likely due to evapo-transpiration in the streamside riparian zones (Bond et al. 2002). The dissolved oxygen reached a daytime high of 158% of saturation (385 $\mu\text{mol L}^{-1}$) and a night time low of 65% (164 $\mu\text{mol L}^{-1}$). DO concentrations ($n = 3$) determined by Winkler titration were in good agreement with instrument readings (Fig. 3c). The $p\text{CO}_2$ was above atmospheric partial pressure ($\sim 252 \mu\text{atm}$) during the whole diel period; decreasing during the day and increasing at night (Fig. 3c).

4.1.2 DOC and DIC

DOC showed a 1.8-fold diel change in concentration from a minimum of 124 to a maximum of 231 $\mu\text{mol C L}^{-1}$ (Fig. 4a). At the same time the average concentration of DIC was ~ 52 -times higher than that of the DOC. The DIC showed a ~ 5 -fold diel change in concentration from a minimum of 3.4 to a maximum of 17.0 mmol C L^{-1} (Fig. 4a). The diel change in DOC is most likely produced by release of soluble organic carbon compounds (i.e., amino acids, sugars, organic acids) by photosynthetic organisms during the daytime (Kaplan and Bott 1982; Vymazal 1994 and references therein) followed by consumption of those soluble organics by heterotrophic microbes during the night. The gradual increase in DOC after about 23:00 suggests a net accumulation due heterotrophic processing of larger insoluble organics from sediments or particulates (Zeigler and Fogel 2003). The DIC concentration decreased during the daytime due to removal of CO₂ by photosynthesis and increased at night due to community respiration.

The molar ratio of DIC/DOC reached a minimum of 16 at $\sim 17:00$ and a maximum of 104 at $\sim 06:00$ the following morning (Fig. 4b). This large increase in DIC relative to DOC at night suggests that oxidation of DOC contributed only a small part of the increase in DIC and that the majority of DIC was produced from other sources (e.g., aerobic or anaerobic respiration of microbes within the sediment bed; or groundwater influx). The

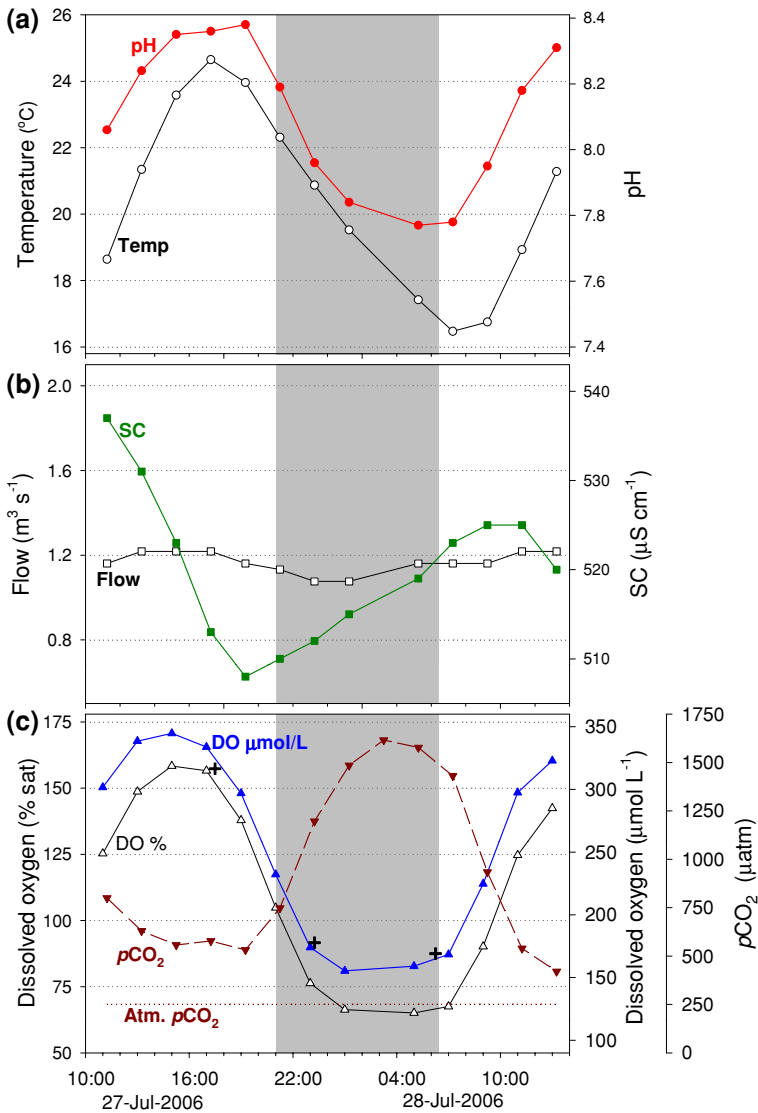


Fig. 3 Temperature and pH (a), specific conductivity (SC) and flow (b), dissolved oxygen (% saturation and $\mu mol L^{-1}$) and pCO_2 (c) at the Clark Fork River sampling site in Deer Lodge, MT. The cross marks (+) indicate Winkler DO measurements (see methods) performed to verify O_2 concentrations from instruments. Shaded bars in all diel graphs represent night time as determined by PAR signal of zero

rates of change in the concentration of DIC and DOC between sampling times can be compared to better understand how these two parameters were changing relative to each other (Fig. 4c). For example, at 19:15 the $\Delta DOC/\Delta t$ is about $-4.8 \mu mol C L^{-1} h^{-1}$ while the $\Delta DIC/\Delta t$ is approximately $1530 \mu mol C L^{-1} h^{-1}$; the concentration of DIC is increasing ~ 316 times faster than the concentration of DOC is decreasing. This also suggests that the majority of the increase seen in DIC was from sources other than the oxidation of the measured DOC.

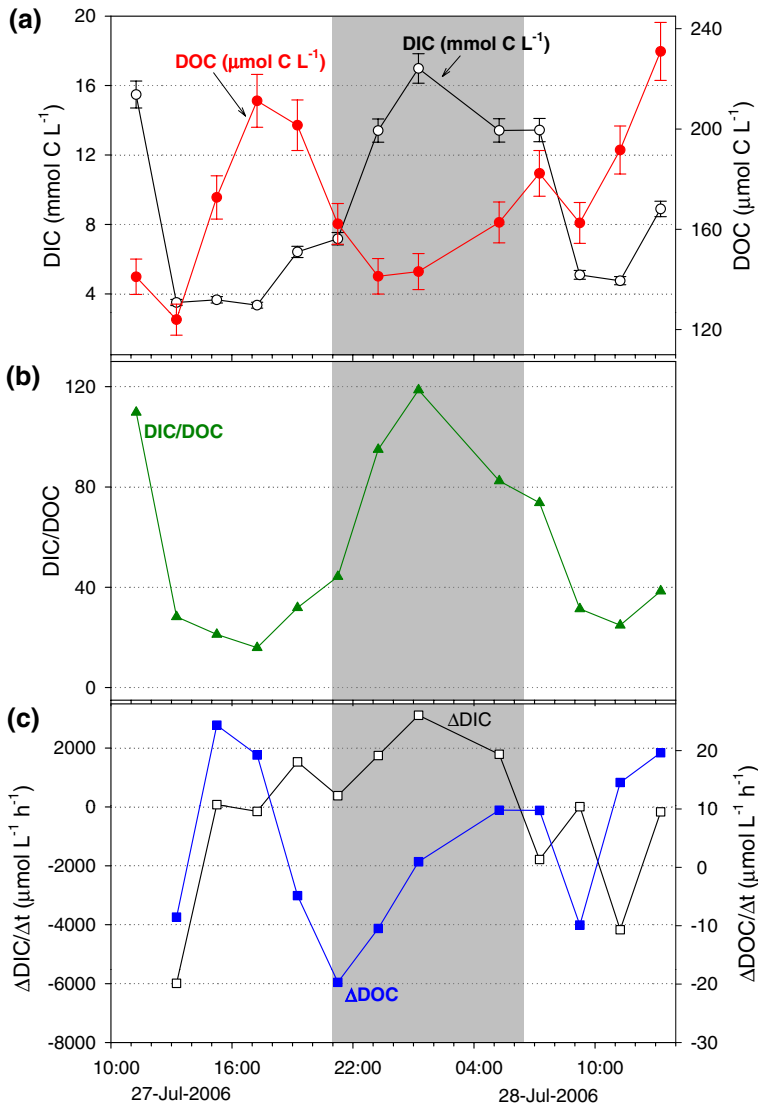


Fig. 4 DOC ($\mu\text{mol C L}^{-1}$) and DIC (mmol C L^{-1}) at CFRG during diel sampling in 2006 (a); molar ratio of DIC to DOC at CFRG (b) and the rate of change in DIC ($\text{mmol C L}^{-1} \text{h}^{-1}$) and DOC ($\mu\text{mol C L}^{-1} \text{h}^{-1}$) (c). Error bars represent 5% RSD based on replicate determinations

4.1.3 $\delta^{13}\text{C}$ -DOC and $\delta^{13}\text{C}$ -DIC

The isotopic composition of DOC ($\delta^{13}\text{C}$ -DOC) and DIC ($\delta^{13}\text{C}$ -DIC) also showed changes over the sampling period (Fig. 5). Diel changes in $\delta^{13}\text{C}$ -DIC have been observed previously in the CFR and BHR (Parker et al. 2005, 2007a). Photosynthesis removes CO_2 during the day with a reported isotopic depletion of about -29% (Falkowski and Raven 1997); such that the residual DIC becomes isotopically enriched. Gas-exchange with atmospheric

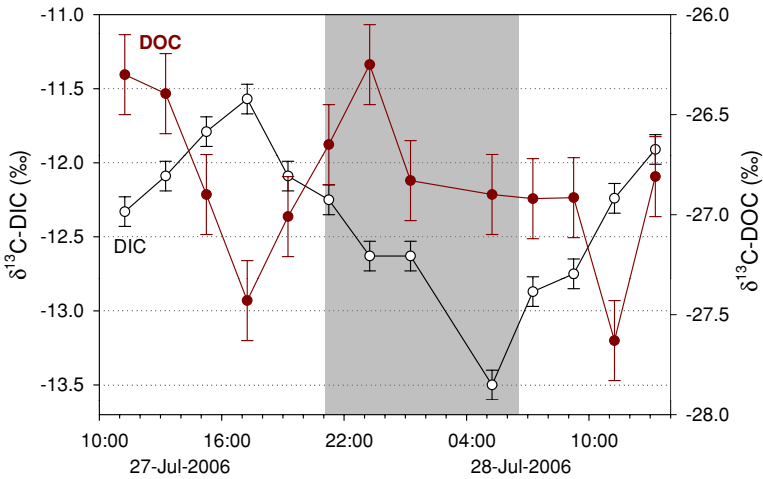


Fig. 5 $\delta^{13}\text{C-DOC}$ and $\delta^{13}\text{C-DIC}$ values measured during diel sampling in the CFR. Error bars represent a RSD of 0.95% for $\delta^{13}\text{C-DOC}$ and 0.55% for $\delta^{13}\text{C-DIC}$

CO_2 ($\delta^{13}\text{C} = -7$ to -8.5‰) will tend to elevate the $\delta^{13}\text{C-DIC}$ which had an average value over the diel period of -12.4‰ . However, as reported in Sect. 4.1.1 the $p\text{CO}_2$ was above atmospheric levels during the diel period such that the net flux of CO_2 would have been from the water to the atmosphere for the 24-h period. Diffusional fractionation associated with CO_2 outgassing should have caused the $\delta^{13}\text{C-DIC}$ to become isotopically heavier but the opposite was observed, with the $\delta^{13}\text{C-DIC}$ becoming increasingly depleted over night. This is consistent with community respiration being the dominant process which was influencing the $\delta^{13}\text{C-DIC}$.

The $\delta^{13}\text{C-DOC}$ showed the inverse isotopic diel trend to that of the DIC. The concentration of DOC increased during the day (Fig. 4a) due to soluble organics that were “leaking” from photosynthetic organisms and since photosynthesis discriminates against ^{13}C it follows that the DOC produced during this time will be isotopically depleted. Zeigler and Fogel (2003) suggested that the daytime decrease in $\delta^{13}\text{C-DOC}$ observed in a tidal wetland was due to the exudation of carbohydrates produced by phytoplankton and macrophytes. As photosynthesis decreased in the late afternoon ($\sim 17:00$), community respiration consumed this pool of soluble (isotopically light) organics, discriminating against the heavier isotope (kinetically) such that the remaining DOC pool becomes isotopically enriched (concentration decreasing, Fig. 4a). It is also possible that these “leaking”, isotopically light photosynthates such as carbohydrates are more readily bio-available and are used first for respiration (Zeigler and Fogel 2003). After $\sim 23:00$ the isotopic composition of the pool stabilizes at approximately -26.9‰ . The $\delta^{13}\text{C}$ of the local aquatic and streamside vegetation was not measured during this study, but temperate region C_3 plants should have an isotope composition in the range of -20 to -30‰ (Clark and Fritz 1997). Consequently, this $\delta^{13}\text{C-DOC}$ plateau from 01:00 to 09:00 may reflect the DOC being produced by microbial degradation of detritus with an isotope signature typical of temperate region vegetation. This is consistent with the increase in DOC concentration after 23:00 (discussed above) being due to heterotrophic degradation of organic detritus accumulated within the sediment bed.

During the night as community respiration consumes the isotopically light DOC and insoluble organic matter in the sediments, it produces light CO_2 which causes the $\delta^{13}\text{C}$ -DIC to continue dropping until photosynthesis reverses the trend starting about 06:30 (Parker et al. 2009).

4.2 Big Hole River

4.2.1 Field and Isolation Chamber Results

Diel samplings were conducted on the BHR in two successive years during late summer, low flow conditions (2006 and 2007) within 8 days of the same date each year (Fig. 6). The hydrographs for a 6–7-day period bracketing the sampling for the 2 years show that the average flow in 2007 was about 1.7-times higher than in 2006 during the sampling period and that different temporal flow patterns were present in the 2 years (Fig. 7). The flow during the diel sampling period in 2006 showed a ~ 2.7 -fold minimum to maximum increase and exhibited a sharp decrease during the late afternoon ($\sim 17:00$) followed by a gradual increase with a maximum at about 01:00–03:00 (Fig. 6b). The flow in 2007 showed a ~ 1.3 -fold minimum to maximum increase during the sampling period with a gradual decrease throughout the afternoon reaching a minimum about 21:00 through 02:00 followed by a gradual increase through the following morning (Fig. 6e). The 2007 pattern is more typical of one expected to be produced by evapo-transpiration from productive

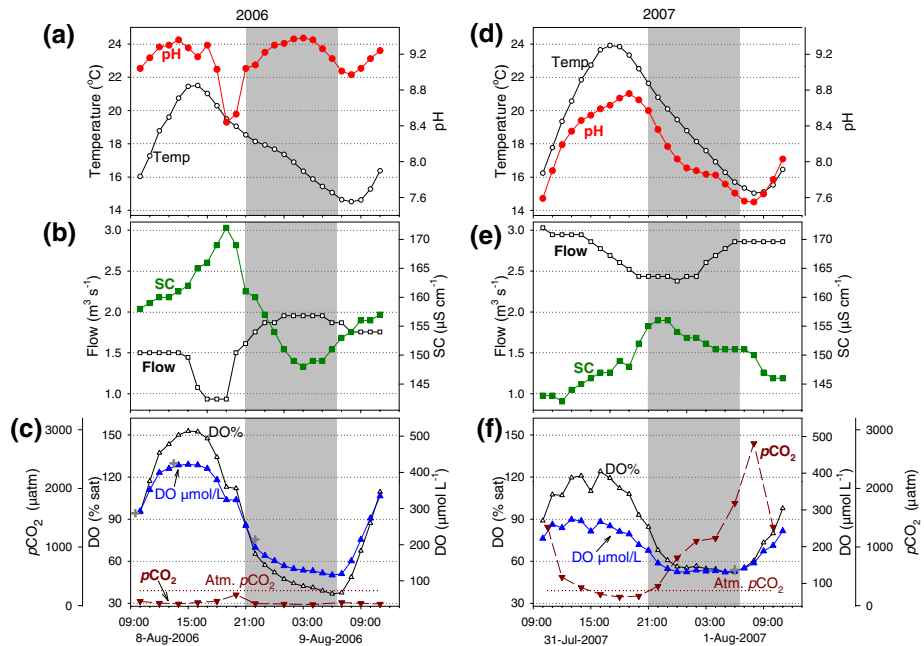


Fig. 6 Temperature and pH (a; 2006) and (d; 2007); flow and specific conductivity (SC) (b; 2006) and (e; 2007); and dissolved oxygen (% saturation and $\mu\text{mol L}^{-1}$) (c; 2006) and (f; 2007) for the BHR. The cross marks (+) indicate Winkler DO measurements (see methods) performed to verify O_2 concentrations from instruments

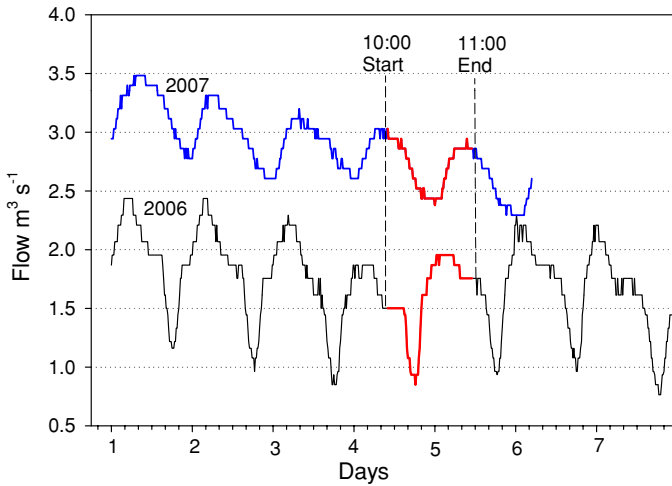


Fig. 7 Hydrographs (USGS gage data) for the BHR site for a 6–7 day period around the field work in 2006 and 2007. *Red lines* show the sampling period in both years and *dashed lines* show the approximate starting (10:00) and ending (11:00) times for sampling

upstream riparian zones (Bond et al. 2002) while the pattern observed in 2006 is not well understood (discussed below).

The pH variation observed in 2006 is very unusual with a sharp pH drop in late afternoon ($\sim 17:00$), at approximately the same time that the flow dropped (Fig. 6a). This was followed by a gradual increase in pH with a maximum at $\sim 03:00$; approximately the same time that the flow peaked in 2006. The late afternoon decrease in flow in 2006 described above was also accompanied by a sharp increase in specific conductivity (SC) at the same time ($\sim 18:00$, Fig. 6b). The SC dropped after this time with a minimum at $\sim 03:00$, the same time that the flow reached a maximum. The behavior of DO in 2006 was “normal” with the exception of a small shoulder at approximately 19:00 which corresponds to the sharp flow decrease in the late afternoon (Fig. 6c). In contrast to the CFR described above, the $p\text{CO}_2$ in the BHR in 2006 was below atmospheric levels ($\sim 252 \mu\text{atm}$) for the 24-h sampling period (Fig. 6c) which is due to the high pH (avg. 9.1) and high productivity as shown by the large diel change in O_2 concentration (37–152% sat.) during this base flow period. The late afternoon drop in pH described above ($\sim 17:00$) was mirrored by a small increase in $p\text{CO}_2$ followed by a night time decrease as the pH began to rise. This is an unusual $p\text{CO}_2$ pattern since it usually increases over night due to community respiration and decreasing pH, as observed in the CFR (Fig. 3c).

In 2007, the changes in flow, SC, and pH were more typical of “normal” stream behavior (Fig. 6d, e). The diel change in DO was not as large in 2007 as in 2006 and was possibly modulated by the larger flow (Fig. 6f). Maximum stream temperature was higher in 2007 than 2006 which also decreased O_2 solubility. The $p\text{CO}_2$ during 2007 was above atmospheric levels except for a brief period in the afternoon ($\sim 16:00$ – $20:00$) and showed a more “typical” pattern (Fig. 6f). The higher $p\text{CO}_2$ levels are in part due to the lower pH values in 2007 (avg. 8.1) versus 2006 (avg. 9.1).

An isolation chamber with stream water plus cobbles and attached periphyton was used during the 2006 sampling (Fig. 8a). This allowed a comparison of temperature, pH, and DO between the river and water in the chamber which was isolated from chemical species

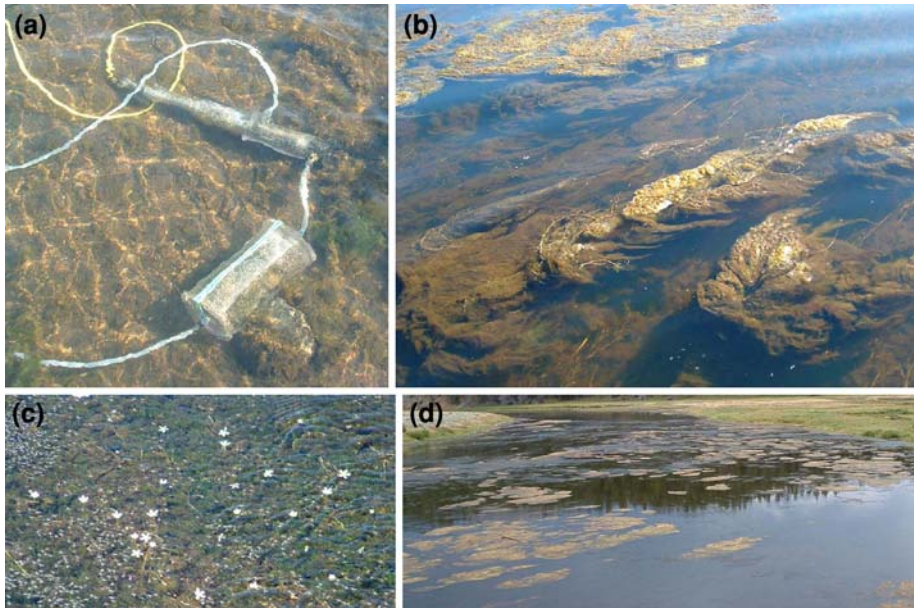


Fig. 8 Pictures of the isolation chamber (a), streaming algal mats (b), area of *Ranunculus aquatilis* (river buttercups, c) and river with algal mats near sampling area (d) in the BHR

transported to the sampling site from upstream or from hyporheic discharge (Fig. 9). Consequently, the observed changes in chemistry of the chamber water were dominated by interactions with the enclosed benthic materials. Temperature and DO both in the chamber and in the river were similar through the diel period although at night the DO in the chamber did reach a minimum of about $31 \mu\text{mol L}^{-1}$ versus $115 \mu\text{mol L}^{-1}$ in the river (Fig. 9a, c). This night time difference in DO was most likely due to the absence of gas exchange with the atmosphere in the chamber. The pH in the chamber did not show the same unusual pattern displayed in the river (Fig. 9b). Since the chamber was refilled with river water every 2 h, it does show evidence of a subdued version of the decrease in pH seen in the river at $\sim 19:00\text{--}20:00$. The pH in the water isolated in the chamber showed a 0.13 unit change in pH versus 0.86 units in the river in the time period from 17:00 to 19:00. Since the pH profile in the chamber was similar to the more typical pattern found in river systems (i.e., CFR Fig. 3a) and that it was refilled with river water every 2 h emphasizes the temporal period over which the pH modification can occur. The $p\text{CO}_2$ in the chamber (Fig. 9c), similar to pH, showed a more typical diel behavior and did not show the small increase around 19:00 as was seen in the river. The potential causes of these differences in the diel pH and $p\text{CO}_2$ patterns in 2006 between the river and the chamber will be discussed in the next section.

4.2.2 DOC and DIC

A 4.6-fold minimum to maximum diel change in DOC in the BHR was observed in 2006 while no regular diel change in DOC concentration was observed in 2007 (Fig. 10a, b). The night time peak in DOC concentration in 2006 occurred at $\sim 01:00$, which coincides

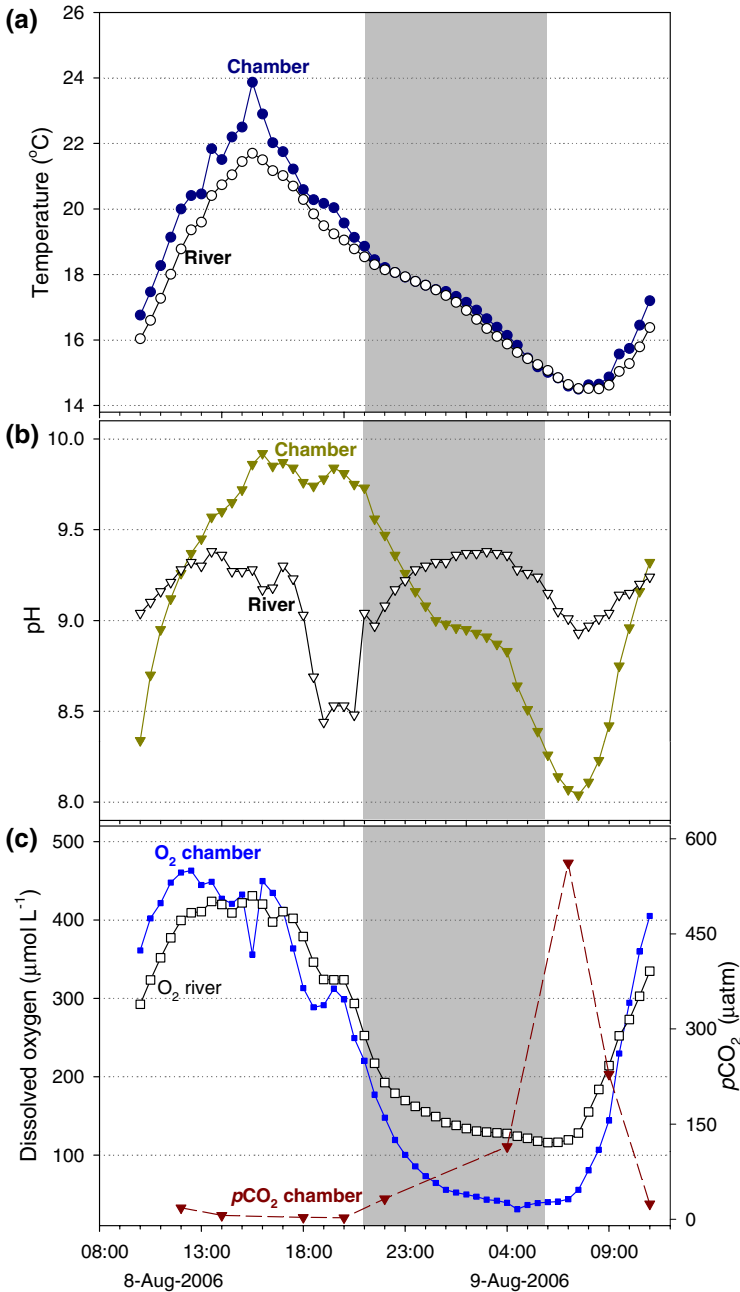


Fig. 9 Temperature (a), pH (b) and dissolved oxygen (% saturation and $\mu\text{mol L}^{-1}$) (c) for the isolation chamber and BHR during the 2006 sampling

approximately with the timing of the maximum values reached by both flow and pH (Fig. 6a, b). At the same time, the concentration of DIC both in 2006 and 2007 did not change significantly over the diel period. The load of DOC (concentration \times flow) in 2006

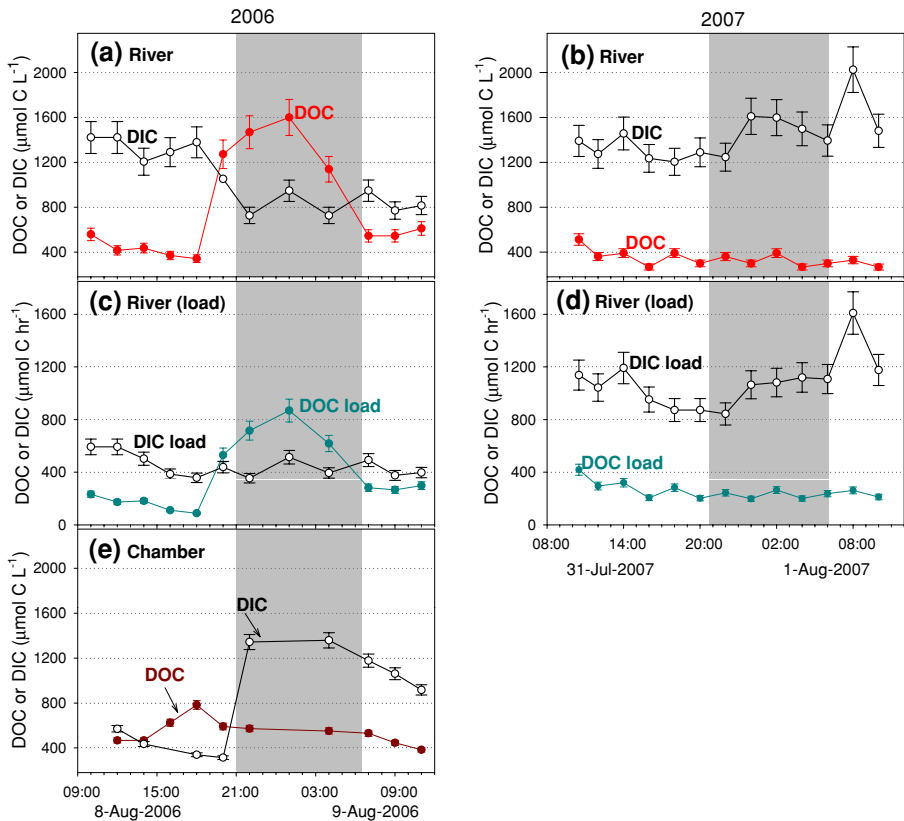


Fig. 10 Concentrations DIC and DOC in the BHR in 2006 (a) and 2007 (b); load of DOC and DIC in the BHR in 2006 (c) and 2007 (d); and DOC and DIC in the isolation chamber during 2006 (e). Error bars represent 5% RSD based on replicate determinations

shows the same night time increase with a maximum at $\sim 01:00$ when the flow peaked while there was no change in load of DOC over the diel period in 2007 (Fig. 10c, d). This indicates that the diel change in concentration in 2006 (Fig. 10a) was not an artifact of the change in flow (Fig. 6b) since the load of DOC increased simultaneously. Although the average load of DIC in 2007 was about 2.4 times higher than in 2006 there was no apparent regular diel pattern in either year (Fig. 10c, d).

One possible explanation for this significant late afternoon/night time increase in DOC in 2006 and not in 2007 may be linked to the unusual flow pattern observed in 2006. After the late afternoon decrease in flow in 2006 ($\sim 17:00$; Fig. 6b), the following increase may have included a groundwater influx from bank-storage and/or benthic sediments. This water may have carried additional concentrations of DOC from decaying organic matter producing the DOC increase observed in the river. In order to better address the DOC concentration and pH of bank storage/sediment pore waters during the 2007 sampling, water was collected from seeps (small springs) along the river bank as well as pore water withdrawn from the shallow stream bottom sediments. The seeps were on both sides of the river between 300 and 800 m upstream from the sampling site. The seeps all had higher

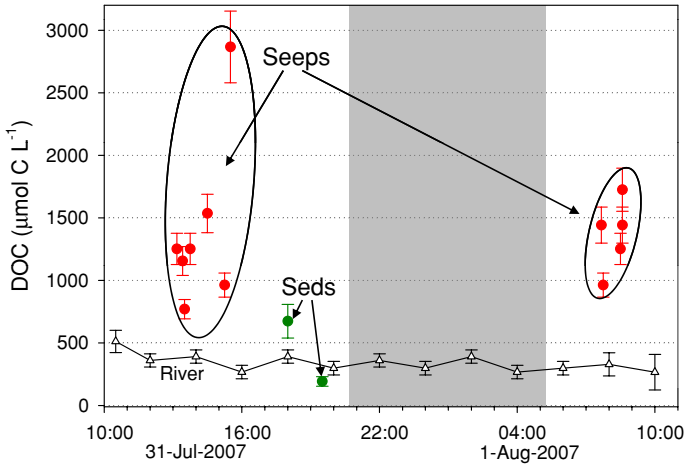


Fig. 11 Concentration of DOC ($\mu\text{mol C L}^{-1}$) in seeps (red), shallow sediments (green) and the BHR (open triangles) during the 2007 sampling site

DOC concentrations and lower pH values than the river water at the sampling site (Fig. 11; Table 1). The average DOC concentration of the seeps was $1,385 \mu\text{mol C L}^{-1}$ while the average DOC in the river over the diel period was $341 \mu\text{mol C L}^{-1}$. The DOC concentration of the shallow sediment water sampled was similar to that of the river (Fig. 11), which is characteristic of shallow, short range hyporheic flow paths (Poole et al. 2008). The average pH of the seep waters was 6.8 while the average pH of the river during the 2007 diel sampling was 8.1 (9.1 in 2006). This suggests that if the night time increase in DOC in 2006 was due to a significant influx of bank storage water, then the pH should have decreased simultaneously; not increased. This is not to suggest that streamside/groundwater contributions of DOC and other solutes did not occur but that those contributions were relatively constant while the large night time increase in DOC was produced by a separate process.

Another hypothesis that has been considered to explain the large diel changes in flow that have been observed periodically during late summer in the BHR has been the presence of large stretches of algae and macrophytes (*Ranunculus aquatilis* and other species) that float to the surface during the day while they are actively photosynthesizing, effectively forming an “in-stream” dam (see Fig. 8b–d). At night these photosynthetic organisms sink toward the bottom allowing the trapped water to flow down the river as a wave. This model is consistent with stream flow observations in this reach of the river during a similar flow regime in 2005 when the river stage (water level) increased and the flow decreased (C. Gammons personal communication). This might explain the decrease in flow in the late afternoon during 2006 followed by an increase in water at night from upstream as the in-stream damming action ceased. This pulse of water that was retarded by the plants and algae during the day may have been higher in pH due to photosynthetic removal of CO_2 and contain higher amounts of DOC due to leakage of organic photosynthates as discussed above in Sect. 4.1.2.

This model that conceptualizes a “wave” of water moving down the river can be further analyzed by looking at the SC of the water over the diel period. The average diel SC of the river was significantly lower in 2006 ($157 \mu\text{S cm}^{-1} \pm 6.7$; $n = 51$) than that of the seeps

Table 1 Concentrations of DOC from seeps and sediments from the Big Hole River sampled during 2007

Site	<i>T</i> (°C)	pH	SC	DO % sat	DO $\mu\text{mol/L}$	DOC $\mu\text{mol C/L}$	Location
Seep 1a	20.8	6.76	130	75.2	165	1,252	N 45°48.429'; W 113°19.147'
Seep 1b	NA	NA	NA	NA	NA	1,442	N 45°48.429'; W 113°19.147'
Seep 2a	25.2	6.88	129	105.2	206	1,155	N 45°48.433'; W 113°19.164'
Seep 2b	NA	NA	NA	NA	NA	963	N 45°48.433'; W 113°19.164'
Seep 3	19.5	6.23	157	52.0	117	770	N 45°48.433'; W 113°19.174'
Seep 4	23.0	7.12	157	135.5	288	1,252	N 45°48.436'; W 113°19.195'
Seep 5a	20.1	6.91	622	0.9	2.0	1,536	N 45°48.708'; W 113°19.564'
Seep 5b	11.7	7.05	608	43.9	119	1,252	N 45°48.708'; W 113°19.564'
Seep 6	23.4	6.91	167	104.7	214	964	N 45°48.439'; W 113°19.196'
Seep 7	15.6	6.23	124	123.4	278	2,867	N 45°48.439'; W 113°19.203'
Seep 8	11.4	6.83	582	25.0	68	1,442	N 45°48.712'; W 113° 19.579'
Seep 9	10.1	7.40	617	58.8	165	1,725	N 45°48.707'; W 113°19.567'
Sed 1	NA	NA	NA	NA	NA	674	N 45°48.450'; W 113°18.750'
Sed 2	NA	NA	NA	NA	NA	193	N 45°48.450'; W 113°18.750'

All seeps are between 300 and 800 m upstream from BHR sampling site

T temperature; pH in standard units; *SC* specific conductivity ($\mu\text{S/cm}$); *NA* not available

sampled in 2007 (avg. $329 \mu\text{S cm}^{-1}$; range: 124–622). Additionally, the effect of the higher *SC* of the seeps on the river *SC* was investigated with a synoptic survey through the sampling area in 2007. This survey showed consistently higher conductivity water near the stream banks (avg. $157 \pm 4.6 \mu\text{S cm}^{-1}$, $n = 8$) than in the middle of the channel (avg. $147 \pm 3.9 \mu\text{S cm}^{-1}$, $n = 49$) which shows that additions of water from streamside areas were entering the river. Assuming that the chemistry of the seep/groundwater was similar in the 2 years, the increase in *SC* of the river observed in 2006 (Fig. 6b) during the late afternoon when the flow decreased is consistent with a lower volume of river water (lower *SC*) relative to groundwater (higher *SC*). This was then followed by a decrease in *SC* as the flow increased in the first part of the night ($\sim 21:00$ – $01:00$; Fig. 6b) possibly related to an increase in the volume of river water being advected into the sampling area relative to the groundwater contributions.

In further support of this model, the *DOC* concentration and *pH* in the isolation chamber did not display the same night time increase observed in the river in 2006 (Fig. 10e). This difference in *DOC* and *pH* behavior between the chamber and the river is consistent with the model described above suggesting that a “slug” of water migrated downstream that was higher in *pH*; passing the BHR sampling site between 17:00 and 01:00. If the increase in *DOC* and *pH* was produced by aquatic vegetation in the direct area of the sampling site, it should have been observed at some level in the chamber as well as in the river. Additionally, the *DIC* concentration in the chamber showed a pattern that is more “typical” of productive systems with the *DIC* decreasing during the day, while photosynthesis is the dominant metabolic process, resulting in a net removal of CO_2 ; followed by increasing CO_2 at night as community respiration returns it to the water column (Fig. 10e). This was the same pattern observed for the *DIC* concentration in the CFR (Fig. 4a).

Another possible cause of the large and reproducible abnormal flow cycle observed in 2006 could have been a significant daily change in irrigation withdrawals upstream from

the sampling site. The hydrologist for the Montana Department of Natural Resources and Conservation indicated: (1) that there was no one irrigation structure that could remove that amount of water upstream from our site; (2) that the irrigators generally don't turn their ditches on and off, especially on a regular schedule; and (3) most irrigators were not withdrawing water at that time of year due to low flows (M. Roberts personal communication). Consequently it seems unlikely that there was any anthropogenic cause of the flow pattern observed in 2006.

These explanations for the abnormal flow, pH, and DOC behavior observed in 2006 are currently the focus of a continued investigation to better understand the hydrology and biogeochemistry of the upper Big Hole River.

4.2.3 Isotope Composition of DIC

The $\delta^{13}\text{C}$ -DIC was determined for both the 2006 and 2007 samplings in the BHR (Fig. 12). The pattern is typical of $\delta^{13}\text{C}$ -DIC reported previously (Parker et al. 2005, 2009) and similar to those observed in 2006 on the CFR (Fig. 5). There was no discernible diel pattern in DIC concentration in the BHR both during 2006 and 2007 and at the same time the minimum to maximum isotope composition change was ~ 3.3 and 2.7% in 2006 and 2007, respectively. Additionally, the $\delta^{13}\text{C}$ -DIC in 2006 did not show any influence of the aberrant pH and flow cycle (Fig. 8a, b) which appears to have been associated with the diel change in DOC (Fig. 9a). Diel changes in $\delta^{13}\text{C}$ -DIC are influenced by isotopically light CO_2 produced by community respiration, consumption of CO_2 by photosynthesis, gas exchange with the atmosphere, influx of groundwater and dissolution of carbonate minerals. Groundwater contributions of DIC do not appear to be significant in controlling the diel changes in $\delta^{13}\text{C}$ -DIC in 2006 and 2007 in the BHR at this site since these changes are not correlated with the flow cycles. The daytime increases in $\delta^{13}\text{C}$ -DIC have been attributed to kinetic fractionation associated with the consumption of CO_2 by photosynthesis. Since the average pH in 2006 was ~ 1 unit higher than in 2007 the $p\text{CO}_2$ was significantly lower in 2006 versus 2007 (Fig. 6e, f). In 2006 the $p\text{CO}_2$ was below atmospheric levels during the whole diel period while in 2007 the $p\text{CO}_2$ dipped below atmospheric levels during a brief period in the afternoon. During this afternoon period in 2007 when the $p\text{CO}_2$ was low, the net flux of CO_2 would have been from the atmosphere to the water which would have raised the $\delta^{13}\text{C}$ -DIC toward an equilibrium value of -1 to $+3\%$. However, the maximum afternoon $\delta^{13}\text{C}$ -DIC in 2006 and 2007 was -11.5% and -10.5% , respectively, indicating that a balance of metabolic processes was most significant in determining the isotopic composition of inorganic carbon. At night the $\delta^{13}\text{C}$ -DIC both in 2006 and in 2007 decreased during the period when respiration was the only metabolic process operating. In 2006 the $p\text{CO}_2$ remained below atmospheric levels during the whole diel period (Fig. 6c) while in 2007 $p\text{CO}_2$ increased well above atmospheric equilibrium over night (Fig. 6f). Gas exchange in 2006 at night should have resulted in a net influx of atmospheric CO_2 which should have caused an increase in $\delta^{13}\text{C}$ -DIC but since the $\delta^{13}\text{C}$ -DIC continued to decrease, community respiration producing light CO_2 must have been the most significant process affecting the isotope values. In 2007 the night time $p\text{CO}_2$ increased well above atmospheric levels which should have resulted in a net efflux of CO_2 from the water to the air. Diffusional fractionation associated with outgassing should have caused the $\delta^{13}\text{C}$ -DIC to increase but it continued to decrease overnight indicating again that community respiration was again the most significant process influencing the $\delta^{13}\text{C}$ -DIC in the absence of photosynthesis. This emphasizes the dynamic nature of the inorganic carbon pool. While the concentration is not changing in a regular manner, the isotopic

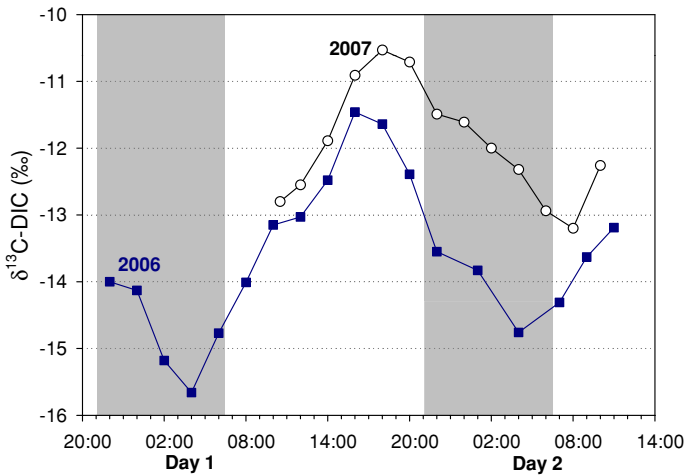


Fig. 12 $\delta^{13}\text{C-DIC}$ at the BHR site during the 2006 (blue squares) and 2007 (open circles) during diel samplings. Error bars represent 3% RSD based on duplicate determinations

composition of the pool was being modified by changing metabolic rates in this highly productive system and this was reflected by the diel pattern of $\delta^{13}\text{C-DIC}$.

5 Conclusions

Diel concentration cycles in DOC were observed in both the CFR and the BHR in 2006 but very different temporal patterns were observed in these two rivers. No change in DOC concentration was observed at the same location in the BHR approximately 1 year later (2007) suggesting that the presence of diel changes in DOC concentration are dependent on conditions that can change from year-to-year such as different flow regimes (Fig. 6b, e). The average flow in the BHR in 2007 was ~ 1.7 times higher than in 2006 and had a different temporal pattern suggesting that the presence of the observed diel changes in DOC may be linked to circumstances present during extreme low, base flow conditions. During these extreme low flow events the volume of water in the river is low in relation to the mass of attached periphyton which could amplify effects such as instream damming caused by aquatic plants and algae. These hydrologic and biogeochemical dynamics are not well understood and are the subjects of further study.

The DOC cycle in the BHR in 2006 reached a maximum concentration at $\sim 01:00$, which is approximately the time that the flow reached its maximum (Fig. 6b, 7). The pH during the 2006 sampling showed an unusual bi-phasic pattern with a maximum around 14:00 and then again at about 02:00. Between these two maximums there was a steep drop in pH with a minimum at $\sim 17:00$; coincident with the steep drop in flow. Normally pH will reach a minimum in the early morning ($\sim 07:00$ in 2007, Fig. 6d). This pH increase during the night could not have been caused *directly* by photosynthesis removing CO_2 from the water. However, since the flow increased at the same time this pattern is consistent with a mass of water moving into this reach that was chemically modified (higher pH, lower conductivity). Two hypotheses that have been suggested above to explain these data are: (1) increased flow from streamside regions and/or benthic sediments at night as evapo-transpiration decreased;

and (2) the possibility that algae and macrophytes in upstream reaches float up and partially dam the river during the day due to photosynthesis and then sink at night, releasing the water. The second hypothesis has been suggested to explain the large diel changes in flow previously observed in this middle reach of the BHR of up to $2.8 \text{ m}^3 \text{ s}^{-1}$ (100% minimum to maximum) in a period of as little as 2 h (USGS gage data, not shown). These large flow cycles observed in the past have had similar timing and trends to those of the 2006 flow reported in this study.

The first explanation is partially supported by preliminary results of samples collected from a number of seeps along the BHR above the sampling site in 2007. The water from these seeps had DOC concentrations ~ 4 -times higher on the average than the river (Fig. 11). At the same time water extracted from shallow benthic sediments had DOC concentrations similar to that of the river. The pH of the water from the seeps was in general lower than that of the river (avg., 6.8 vs. 8.1; Table 1). Consequently, this makes it seem unlikely that the increase in pH in conjunction with the increase in DOC observed in 2006 was due to a large influx of water from bank storage in streamside areas above the sampling site.

The latter explanation predicts a “slug” of water moving downstream that would be of higher pH due to photosynthetic removal of CO_2 during the day and have a higher concentration of DOC due to leakage of soluble organic photosynthates. It is interesting to note that the $\delta^{13}\text{C}$ -DIC during both 2006 and 2007 had the same pattern and in 2006 appeared to show no influence from the observed flow and pH increase during the night (Fig. 11). This suggests that the biologic processing of inorganic carbon is acting at a time scale resulting in a “normal” $\delta^{13}\text{C}$ -DIC pattern.

In the CFR, the DOC showed an inverse temporal pattern to that observed in the BHR in 2006. The DOC in the CFR reached a maximum concentration at $\sim 16:00$ which is consistent with “leakage” of photosynthates during this active photosynthetic period. The $\delta^{13}\text{C}$ -DOC became isotopically depleted during the afternoon most likely due to incorporation of “light” organics produced by photosynthesis and then became enriched during the night as microbial oxidation of DOC consumed lighter carbon containing compounds at a faster rate. It is also possible that the isotopically heavier DOC is in part a different class of compounds that was more recalcitrant and less readily oxidized than the isotopically lighter, recently synthesized compounds. Additionally, a comparison of the rates of change in the concentration of DOC and DIC indicates that the night time increase in DIC can not be solely attributed to microbial oxidation of DOC.

This study emphasizes the importance of the need for a better understanding of the dynamic nature of diel changes in the concentration of both dissolved inorganic and organic species in rivers. It also underscores the fact that different patterns of DOC concentration can occur seasonally in the same aquatic system. Additionally, it demonstrates a need to better quantify the types of organic compounds included in the DOC pool in relation to both the isotopic composition as well as how readily available these forms are for heterotrophic oxidation. These results also highlight the fact that significant short term temporal changes in DOC can occur and monitoring protocols for DOC need to take diel concentration changes into account. Also, predicting diel concentration patterns based on prior behavior may not always be reliable as shown by the BHR results for 2006 and 2007.

The night time pH maximum observed in the BHR during 2006 that coincided with the large concentration increase of DOC suggests that these two occurrences may have been caused by the same process which is also related to the simultaneous increase in flow. Unfortunately, these “anomalous” flow occurrences don’t happen every year as seen in 2007 but do need to be further investigated when they do happen. This may lead to

significant insight into the function and response of riverine systems to drought/low flow and changing land use conditions.

Acknowledgments We thank Heiko Langer, David Nimick and Blaine McClesky for their help with analytical work. Chris Gammons has been an invaluable resource of information on the CFR and BHR and provided productive critical insight for this work. This work was funded by the Montana Water Center through a grant from the USGS 104(b) Water Resources Research Program as well as the Montana Tech Undergraduate Research Program. S. Poulson was funded by NSF, EAR-0738912. This manuscript was greatly improved by the comments of two anonymous reviewers.

References

- Amon RMW, Benner R (1996) Bacterial utilization of different size classes of dissolved organic matter. *Limnol Oecoaogr* 41:41–51
- Barth JAC, Veizer J (1999) Carbon cycle in St. Lawrence aquatic ecosystems at Cornwall (Ontario), Canada: seasonal and spatial variations. *Chem Geol* 159:107–128
- Bianchi TS, Filley T, Dria K, Hatcher PG (2004) Temporal variability in sources of organic carbon in the lower Mississippi River. *Geochim Cosmochim Acta* 68:959–967
- Bianchi TS, Wysocki LA, Stewart M, Filley TR, McKee BA (2007) Temporal variability in terrestrial-derived sources of particulate organic carbon in the lower Mississippi River and its upper tributaries. *Geochim Cosmochim Acta* 71:4425–4437
- Bond BJ, Jones JA, Moore G, Phillips N, Post D, McDonnell JJ (2002) The zone of vegetation influence on baseflow revealed by diel patterns of streamflow and vegetation water use in a headwater basin. *Hydrol Process* 16:1671–1677
- Brick CM, Moore JN (1996) Diel variation of trace metals in the upper Clark Fork River, Montana. *Environ Sci Technol* 30:1953–1960
- Clapp CE, Hayes MHB, Senesi N, Griffith SM (eds) (1998) Humic substances and organic matter in soil and water environments: characterization, transformations, and interactions. International Humic Substances Society, Inc., St. Paul
- Clark ID, Fritz P (1997) Environmental isotopes in hydrogeology. Lewis Pub, New York
- Dalzell BJ, Filley TR, Harbor JM (2007) The role of hydrology in annual organic carbon loads and terrestrial organic matter export from a Midwestern agricultural watershed. *Geochim Cosmochim Acta* 71:1448–1462
- Duff BC (2001) Arsenic treatability study utilizing aeration and iron adsorption-coprecipitation at the Warm Springs Ponds. MS thesis, Montana Tech. Butte, MT USA
- Falkowski PG, Raven JA (1997) Aquatic photosynthesis. Blackwell Sciences, Malden
- Gaiero D, Probst JL, Depetris PJ, Gauthier-Lafaye F, Stille P (2005) $\delta^{13}\text{C}$ tracing of dissolved inorganic carbon sources in Patagonian rivers (Argentina). *Hydrol Process* 19(17):3321–3344
- Gammons CH, Ridenour R, Wenz A (2001) Diurnal and longitudinal variations in water quality along the Big Hole River and tributaries during the drought of August, 2000. Mont Bur Mines Geol 424:39 Open-File Report
- Gammons CH, Nimick DA, Parker SR, Cleasby TE, McClesky RB (2005) Diel behavior of iron and other heavy metals in a mountain stream with acidic to neutral pH: Fisher Creek, MT, USA. *Geochim Cosmochim Acta* 69:2505–2516
- Gammons CH, Grant TM, Nimick DA, Parker SR, DeGrandpre MD (2007) Diel changes in water chemistry in an arsenic-rich stream and treatment-pond system. *Sci Total Env* 384:433–451
- Gandhi H, Wiegner TN, Ostrom PH, Kaplan LA, Ostrom NE (2004) Isotopic (^{13}C) analysis of dissolved organic carbon in stream water using an elemental analyzer coupled to a stable isotope mass spectrometer. *Rapid Commun Mass Spectrom* 18:903–906
- Harris D, Porter LK, Paul EA (1997) Continuous flow isotope ratio mass spectrometry of carbon dioxide trapped as strontium carbonate. *Commun Soil Sci Plant Anal* 28:747–757
- Harrison JA, Matson PA, Fendorf SE (2005) Effects of a diel oxygen cycle on nitrogen transformations and greenhouse gas emissions in a eutrophied subtropical stream. *Aquat Sci* 67(3):308–315
- Hobbie JE (1992) Microbial control of dissolved organic carbon in lakes—research for the future. *Hydrobiologia* 229:169–180
- Hood E, Williams MW, McKnight DM (2005) Sources of dissolved organic matter (DOM) in a rocky mountain stream using chemical fractionation and stable isotopes. *Biogeochemistry* 74(2):231–255

- Hrncir DC, McKnight D (1998) Variation in photoreactivity of iron hydroxides taken from an Acidic Mountain Stream. *Environ Sci Technol* 32:2137–2141
- Jones CA, Nimick DA, McCleskey B (2004) Relative effect of temperature and pH on diel cycling of dissolved trace elements in Prickly Pear Creek, Montana. *Water Air Soil Pollut* 153:95–113
- Kaplan LA, Bott TL (1982) Diel fluctuations of DOC generated by algae in a piedmont stream. *Limnol Oceanogr* 27(6):1091–1100
- Lewis E, Wallace DWR (1998) Program developed for CO₂ system calculations. ORNL/CDIAC-105. Carbon Dioxide Information Analysis Center, Oak Ridge National Laboratory, U.S. Department of Energy, Oak Ridge, Tennessee; <http://cdiac.ornl.gov/oceans/co2rprt.html>
- Macalady DL (ed) (1998) Perspectives in environmental chemistry. Oxford University Press, New York
- Manny BA, Wetzel RG (1973) Diurnal changes in dissolved organic and inorganic carbon and nitrogen in a hardwater stream. *Freshw Biol* 3:31–43
- McKnight DM, Harnish R, Wershaw RL, Baron JS, Schiff S (1997) Chemical characteristics of particulate, colloidal and dissolved organic material in Loch Vale Watershed, Rocky Mountain National Park. *Biogeochemistry* 36:99–124
- Moore JN, Luoma SN (1990) Hazardous wastes from large-scale metal extraction. *Environ Sci Technol* 24:1279–1285
- Nagorski SA, Moore JN, McKinnon TE, Smith DB (2003) Scale-dependent temporal variations in stream water geochemistry. *Environ Sci Technol* 37:859–864
- Nimick DA, Gammons CH, Cleasby TE, Madison JP, Skaar D, Brick CM (2003) Diel cycles in dissolved metal concentrations in streams—occurrence and possible causes. *Water Resour Res* 39:1247. doi: [10.1029/WR001571](https://doi.org/10.1029/WR001571)
- Nimick DA, Cleasby TE, McCleskey RB (2005) Seasonality of diel cycles of dissolved trace metal concentrations in a Rocky Mountain Stream. *Env Geol* 47:603–614
- NOAA (2008) Climate monitoring and diagnostics laboratory, carbon cycle greenhouse gases 2008. <http://www.cmdl.noaa.gov/ccgg/iadv>
- Odum HT (1956) Primary production in flowing waters. *Limnol Oceanogr* 1:102–117
- Olivie-Lanquet G, Gruau G, Dia A, Riou C, Jaffrezic A, Henin O (2001) Release of trace elements in wetlands: role of seasonal variability. *Water Res* 35(4):943–952
- Parker SR, Poulson SR, Gammons CH, DeGrandpre MD (2005) Biogeochemical controls on diel cycling of stable isotopes of dissolved oxygen and dissolved inorganic carbon in the Big Hole River, Montana. *Environ Sci Technol* 39:7134–7140. doi: [10.1021/es0505595](https://doi.org/10.1021/es0505595)
- Parker SR, Gammons CH, Poulson SR, DeGrandpre MD (2007a) Diel changes in pH, dissolved oxygen, nutrients, trace elements, and the isotopic composition of dissolved inorganic carbon in the upper Clark Fork River, Montana, USA. *Appl Geochem* 22:1329–1343. doi: [10.1016/j.apgeochem.2007.02.007](https://doi.org/10.1016/j.apgeochem.2007.02.007)
- Parker SR, Gammons CH, Jones CA, Nimick DA (2007b) Role of hydrous iron oxide formation in attenuation and diel cycling of dissolved trace metals in a stream affected by acid rock drainage. *Water Air Soil Pollut* 181:247–2663. doi: [10.1007/s11270-006-9297-5](https://doi.org/10.1007/s11270-006-9297-5)
- Parker SR, Gammons CH, Poulson SR, Weyer CL, Smith MG, Babcock JN, Oba Y (2009) Diel behavior of stable isotopes (18-O & 13-C) of dissolved oxygen and dissolved inorganic carbon in Montana, USA rivers, and in a mesocosm experiment. *Chemical Geology*. doi: [10.1016/j.chemgeo.2009.06.016](https://doi.org/10.1016/j.chemgeo.2009.06.016)
- Parkhurst DL, Appelo CAJ (1999) User's guide to PHREEQC (Version 2)—a computer program for speciation, batch-reaction, one-dimensional transport, and inverse geochemical calculations: U.S. Geological Survey Water-Resources Investigations Report 99-4259: 310, http://wwwbr.cr.usgs.gov/projects/GWC_coupled/phreeqc/
- Pogue TR, Anderson CW (1994) Processes controlling dissolved oxygen and pH in the Upper Willamette River Basin. US Geol Surv. Water-Resources Investigations Report 95-4205
- Poole GC, O'Daniel SJ, Jones KL, Woessner WW, Bernhardt ES, Helton AM, Stanford JA, Boer BR, Beechie TJ (2008) Hydrological spiraling: the role of multiple interactive flow paths in stream ecosystems. *River Res Applic* 24(7):1018–1031. doi: [10.1002/rra.1099](https://doi.org/10.1002/rra.1099)
- Ridenour R (2002) A seasonal and spatial chemical study of the Big Hole River, Southwest Montana. M.S. Thesis, Montana Tech of The University of Montana, Butte, MT
- Saar RA, Weber JH (1982) Fulvic acid: modifier of metal-ion chemistry. *Environ Sci Technol* 16:510A–517A
- Spencer RGM, Pellerin BA, Bergamaschi BA, Downing BD, Kraus TEC, Smart DR, Dahlgren RA, Hernes PJ (2007) Diurnal variability in riverine dissolved organic matter composition determined by in situ optical measurements in the San Joaquin River (California, USA). *Hydrol Process* 21:3181–3189. doi: [10.1002/hyp.6887](https://doi.org/10.1002/hyp.6887)
- Thurman EM (1985) Organic geochemistry of natural waters. Kluwer Acad. Pub, Boston

- Usdowski E, Hoefs J, Menschel G (1979) Relationship between ^{13}C and ^{18}O fractionation and changes in major element composition in a recent calcite-depositing spring—a model of chemical variations with inorganic CaCO_3 precipitation. *Earth Planet Sci Lett* 42:267–276
- Voelker BM, Morel BM, Sulzberger B (1997) Iron redox cycling in surface waters: effects of humic substances and light. *Environ Sci Technol* 31:1004–1111
- Volk CJ, Volk CB, Kaplan LA (1997) Chemical composition of biodegradable dissolved organic matter in streamwater. *Limnol Oceanogr* 42(1):39–44
- Vymazal J (1994) *Algae and element cycling in wetlands*. Lewis Publishers, CRC Press, Inc., Boca Raton, p 222
- Watson V (1989) Maximum levels of attached algae in the Clark Fork River. *Proc Mont Acad Sci* 49:27–35
- Wenz AC (2003) Diurnal variations in the water quality of the Big Hole River. M.S. Thesis, Montana Tech of The University of Montana, Butte, MT
- Wetzel RG, Likens GE (1991) *Limnological analysis*, 2nd edn. Springer-Verlag, NY
- Zeigler SE, Brisco SL (2004) Relationships between the isotopic composition of dissolved organic carbon and its bioavailability in contrasting Ozark streams. *Hydrobiologia* 513:153–169
- Zeigler SE, Fogel ML (2003) Seasonal and diel relationships between the isotopic compositions of dissolved and particulate organic matter in freshwater ecosystems. *Biogeochemistry* 64:25–52

The Importance of Ecologically Connected Streams to the Biological Diversity of Watersheds: a case study in the St. Regis River subbasin, Montana

Basic Information

Title:	The Importance of Ecologically Connected Streams to the Biological Diversity of Watersheds: a case study in the St. Regis River subbasin, Montana
Project Number:	2008MT165B
Start Date:	3/1/2008
End Date:	2/28/2010
Funding Source:	104B
Congressional District:	At-Large
Research Category:	Biological Sciences
Focus Category:	Conservation, Management and Planning, Ecology
Descriptors:	
Principal Investigators:	Winsor Lowe

Publications

There are no publications.

**THE IMPORTANCE OF ECOLOGICALLY CONNECTED STREAMS TO THE BIOLOGICAL DIVERSITY
OF WATERSHEDS: A CASE STUDY IN THE ST. REGIS RIVER SUBBASIN, MONTANA**

Final Report
prepared by

Winsor H. Lowe
Adam J. Sepulveda
Lindy B. Mullen

University of Montana

Executive summary: We assessed the importance of healthy and connected headwater stream networks to Idaho Giant salamander (*Dicamptodon aterrimus*; IGS) distribution, abundance, and persistence in headwater streams of the St. Regis River subbasin of western Montana. The IGS is listed as a state species of concern, but little is known about its natural history and ecology because there have only been five recorded observations in Montana prior to our research. In our research, we (1) identified variables that influence patterns of IGS distribution and abundance, (2) used genetics (microsatellite DNA markers) and mark-capture-recapture (MCR) to assess the importance of connected stream networks to IGS population persistence and (3) determined the effect of human disturbance on stream connectivity. Funding from this grant has already resulted in the publication of two manuscripts (Sepulveda and Lowe 2009; Mullen et al. 2009), a manuscript that is in review, and a manuscript that is being prepared for submission.

Objective 1: To identify variables that influence patterns of IGS distribution and abundance

Overview.— We divided this objective into two separate, but complementary studies. In Section 1, we used data from field surveys to compare support for local and landscape-scale models that explain *D. aterrimus* occurrence and density in streams distributed throughout the St. Regis River subbasin, MT and Lochsa River subbasin, Idaho. Local-scale models included covariates that reflect habitat quality. Landscape-scale models included variables that reflect predictions from metapopulation theory about the importance of habitat size, connectivity, and fragmentation. Our results suggest that landscape-scale processes are important controls on *D. aterrimus* occurrence and that this species has broad habitat requirements within streams. Specifically, we found that probability of *D. aterrimus* occurrence was highest in roadless drainages and lowest in spatially isolated streams and in drainages with high old-growth forest

density. Surprisingly, we found that *D. aterrimus* density was greatest in streams with a high proportion of embedded substrate and fine sediment. The positive association with embedded substrate may reflect adaptation to a high frequency of natural disturbances, such as landslides and fires, in our study areas. We suggest that management and conservation efforts for this species focus on protecting roadless areas and restoring stream connectivity in human-impacted areas, rather than on only improving habitat quality within streams.

In Section 2, we used first principles of fluvial geomorphology to more directly assess the influence of stream substrate on patterns of IGS distribution and abundance. Stream substrate disturbance is an important driver of community composition. Substrate moves when the driving forces of water on the stream bed exceed the resisting forces holding the substrate. Channel morphology can mitigate disturbance by shifting the balance between driving and resisting forces. We assessed the importance of high flow disturbance and channel morphology on IGS occurrence and density in 30 streams in the St. Regis basin of Montana. We compared support for models that describe *D. aterrimus* occurrence and density as a function of channel confinement (bankfull width: valley width) and the ratio of bankfull flow competence (τ^*) to the shear stress required to set a particle into motion (τ_c^*). These models were compared to the top-ranked models that described salamander occupancy and density as functions of habitat quality, connectivity, and fragmentation in a previous study (Sepulveda and Lowe, 2009). We hypothesized that channel geomorphology influences *D. aterrimus* occupancy and density during high flow and predicted that streams with low confinement and low $\tau^* : \tau_c^*$ would have greater occupancy and density. Support for channel confinement's influence on salamander occupancy and density was plausible, but had less support than models from the previous study. Probability of occurrence and density increased as channel confinement decreased, but $\tau^* : \tau_c^*$ had little effect. Results suggest that salamanders are (1) resistant to high flow disturbance and/or that (2) that disturbance has low intensity because high flows do not mobilize the entire stream bed. Experimental studies are needed to better understand how channel morphology and high flows interact to affect stream organisms.

Section 1: Local and landscape-scale models that explain *D. aterrimus* occurrence and density

Introduction.— The size, quality, and configuration of patches are landscape-scale variables known to affect local population persistence and occurrence across taxa (Dunham 1980, Dunning et al. 1992, Fahrig and Merriam 1994). In amphibians, population persistence is correlated with patch size and connectivity and negatively correlated with habitat fragmentation and habitat alteration (reviewed in Cushman 2006). Large patches often have greater resistance and resilience to disturbance because populations are larger (Marsh and Pearman 1997), there is a broader diversity of habitat conditions and resources within patches (Schlosser 1995), and the scale of a given disturbance relative to the size of the patch is smaller (Stoddard and Hayes 2005). Patch connectivity decreases extinction risk by increasing demographic and genetic input

from immigrants, by increasing the chance of recolonization after extinction and by increasing opportunities for resource supplementation and complementation among patches (reviewed in Dunning et al. 1992, Hastings and Harrison 1994). Finally, habitat fragmentation and alteration of the intervening habitats can effectively increase patch isolation by reducing rates of movement among patches (reviewed in Saunders et al. 1991). Greater understanding of how patch size, patch connectivity, and fragmentation and alteration of intervening habitat affect stream amphibians will help in developing effective conservation strategies.

We used model selection to identify an effective spatial scale to manage a stream salamander species, *Dicamptodon aterrimus* (Idaho Giant salamander), which is listed as a species of concern in the northern Rocky Mountains. Little is known about *D. aterrimus*, but available information suggests that its distribution is patchy across and within stream drainages (Carstens et al. 2005). In the region where *D. aterrimus* occurs, many stream drainages have undergone timber harvest and road building, anthropogenic disturbances that can reduce habitat quality within streams and reduce population connectivity among streams (Fagan 2002, Rodgers et al. 2007). Additionally, these drainages experience natural disturbances such as fire, floods, and landslides, which can create local extinctions of stream organisms in suitable habitat patches (e.g., Rieman and Dunham 2000, Pilliod et al. 2003, e.g., Davic and Welsh Jr 2004). We used data from field surveys to compare support for local and landscape-scale models that describe *D. aterrimus* occurrence in 55 streams in the St. Regis River basin of Montana and the Lochsa River basin of Idaho. To increase knowledge of *D. aterrimus* natural history, we also compared support for local-scale models explaining variation in *D. aterrimus* density within streams. Local-scale models include covariates that reflect patch quality, whereas landscape-scale models include covariates that reflect predictions from metapopulation and landscape ecology theory about the importance of patch size, connectivity, and fragmentation. We had three objectives: (1) to identify an effective spatial scale to manage *D. aterrimus*; (2) to identify *D. aterrimus* habitat associations at each spatial scale; and (3) to explore important correlates of *D. aterrimus* density at the local scale.

Methods.—*Dicamptodon aterrimus* is a large salamander (up to 220 mm snout-vent length) found in or near streams and rivers in the Rocky Mountains of northern and central Idaho and extreme western Montana (Stebbins 2003). This species exhibits facultative paedomorphosis, a polymorphism that results in the coexistence of gilled and fully aquatic paedomorphic adults and terrestrial metamorphic adults in the same populations. No studies have addressed the natural history and habitat associations of *D. aterrimus*, but its similarity to the Pacific Giant salamander (*D. tenebrosus*) would suggest that *D. aterrimus* has narrow physiological tolerances and requires specific local habitat conditions. Past studies indicate that aquatic individuals of *D. tenebrosus* occur in cold-shaded headwater streams with unembedded cobble substrate (Bury et

al. 1991, Roni 2002) and terrestrial adults inhabit moist coniferous forests (Nussbaum et al. 1983).

Fires and landslides are common disturbances in this region. Fire regimes are mixed: infrequent, patchy stand-replacement fire dominates in upper-elevation forests and frequent, lower-severity, surface fires dominate at lower elevations (Brown et al. 1994). The combination of fire-affected soils, weathering granitic rocks, steep slopes, and rain-on-snow events (defined as rain that falls on existing snow cover; MacDonald and Hoffman 1995) has produced landslides throughout the basin. As a result, total sediment volume in streams can exceed water quality standards for salmonids, even in the roadless Selway-Bitterroot Wilderness Area (McClelland et al. 1997, Munday et al. 2001).

A goal of this research was to identify local and landscape-scale variables that predict the occurrence and density of *D. aterrimus* within patches of potentially suitable habitat. We assumed that individual headwater stream drainages satisfied the Hanksi and Gilpin (1997) definition of a patch: a continuous area of space with all necessary resources for the persistence of a local population. We have found *D. aterrimus* in larger streams, but preliminary surveys and discussions with freshwater managers in the region suggested that occurrence and local densities are higher in headwater streams (J. Sauder, Idaho Fish & Game, personal communication; B.A. Maxell, Montana Natural Heritage Program, personal communication). Previous research on *D. tenebrosus* supports this assumption: both occurrence and density of *D. tenebrosus* are higher in 1st- and 2nd-order streams than in larger streams and rivers (e.g., Grialou et al. 2000, Johnston and Frid 2002, Roni 2002), and telemetry data suggest that most individuals move less than 30 m along streams over a season (Johnston and Frid 2002). The headwater streams we sampled were fed by drainages of 1 – 30 km², and multiple drainages were aggregated within catchments of 25 – 200 km².

Within each catchment, we randomly selected 2-3 headwater drainages and sampled the main stream in each drainage. Within each stream, we surveyed two 50-m reaches separated by 200 m for *D. aterrimus* occurrence and density. The lower reach began 25 m upstream of the confluence with a similar or higher-order stream. We used a backpack electrofisher (Smith & Root, LR 24, pulsed DC with 400-520 volts) to search for salamanders within the stream. Comparisons with light-touch surveys in five of my sampled streams suggest that electroshocking is an effective tool for assessing *D. aterrimus* occurrence and density. We found > 10 *D. aterrimus* per stream when using an electroshocker and found 0 - 2 *D. aterrimus* in these same plots when using light-touch surveys. We did not survey for *D. aterrimus* terrestrial adults in the riparian area because they are extremely cryptic and believed to be rare (J. Sauder, Idaho Fish & Game, personal communication); therefore, our inferences pertain to the occurrence and density of aquatic *D. aterrimus*. All reaches were surveyed three times within one season and we recorded the number of salamanders captured during each survey and noted the presence of

stream fishes. We had very high detection probability: 54 of 55 study reaches had *D. aterrimus* always present or always absent in all three surveys. Consequently, we assumed a detection probability of 1.0 for all sites. We used *D. aterrimus* occurrence (presence/absence) and density within a stream as response variables. We calculated density for each headwater stream as the mean number of salamanders per m² captured in the lower and upper stream reaches over the three surveys.

We measured only local abiotic and biotic variables that have been shown to be important for stream salamanders, particularly *Dicamptodon* species. Abiotic variables included mesohabitat type (e.g., pool, riffle, or cascade; Welsh and Lind, 2002), substrate size and composition (Parker 1991, Davic and Welsh Jr 2004), stream width (Stoddard and Hayes 2005), canopy cover (Davic and Welsh Jr 2004) and aspect (Stoddard and Hayes 2005). Biotic variables included fish presence (Sih et al. 1992). We recognize that other local variables can influence stream salamander occurrence and density; however, predictive models with a large number of variables are difficult for managers to embrace (Stoddard and Hayes 2005) and have reduced statistical power in studies like ours, when sample size is logistically constrained (White and Burnham 1999).

We assessed local variables within each stream reach. I recorded mesohabitat as percent occurrence of pools, riffles, and cascades over each 50-m reach (Hawkins et al. 1993). We measured substrate composition and stream width at four random, 1-m wide transects that extended between bank-full channel edges within each reach. At six random points along each transect, we recorded the proportion of substrate in four categories (Lane et al. 1947): boulder-bedrock (>256.0 mm), cobble (64.0 - 256.0 mm), gravel-pebble (2.0 – 64 mm), and fines (< 2.0 mm). We also recorded the proportion of substrate that was embedded, defined as having visible vertical surfaces buried in either silt or sand (Lowe and Bolger 2002, Davic and Welsh Jr 2004). Stream reach aspect (0 – 360°) was measured at the most downstream transect of each reach. Abiotic variables were averaged across the two study reaches within each headwater stream. Occurrence of salmonid fishes was recorded as presence or absence within each headwater stream.

We derived indices of patch size, patch connectivity, habitat fragmentation, and habitat alteration within each drainage using the most recent GIS coverages. We defined patch size using two covariates: total stream distance in the drainage and link magnitude (number of headwater streams in the drainage; (number of headwater streams in the drainage; Rich Jr et al. 2003) . We defined patch connectivity as the distance to the nearest stream in a neighboring headwater drainage, but logistical constraints did not allow us to determine the occupancy status of these nearest neighbor streams. In our model, patch connectivity can potentially represent: (1) a metapopulation effect of colonization/recolonization (Hanski and Gilpin 1997), (2) source-sink dynamics (Dunning et al. 1992), (3) a “Moran effect” that described correlated environments,

and, (4) habitat complementation or neighborhood effects that describes resource use and availability (Dunning et al. 1992). The occupancy status of the nearest neighbor stream is not critical to our test of landscape v. local-scale predictors of *D. aterrimus* occurrence because patch occupancy and patch suitability are expected to change over time in a dynamic landscape that has a high frequency of natural disturbance, such as the Lochsa River and St. Regis River basins. Unoccupied patches with suitable habitat are generally predicted to be critical to species persistence in metapopulation models (Hanski and Gilpin 1997).

Because *D. aterrimus* can move within the stream channel or overland, we measured distance to the nearest stream along the channel network (i.e., minimum distance along the stream corridor from the mouth of the sampled headwater drainage to the mouth of the nearest headwater drainage) and by the Euclidean distance to this nearest stream (i.e., straight-line topographic distance from any stream segment within a sampled headwater drainage to any stream segment within a neighboring headwater drainage; (Dunham 1980, Gresswell et al. 2006). We characterized habitat fragmentation and alteration by road density and forest structure. Roads can lead to direct mortality of stream amphibians (Trombulak and Frissell 2000), act as barriers to dispersal (Demaynadier and Hunter Jr 1998), and increase sedimentation within streams (Davic and Welsh Jr 2004). We quantified road density as length of roads standardized by headwater drainage area (km of road per km²). We described forest structure by the density of old-growth trees based on the northern Idaho old growth standards (Smith and Green 2005), which takes into account tree age and size. Previous studies have found that occurrence of stream amphibians is related to conditions in surrounding forests, including density, age and size of forests (Davic and Welsh Jr 2004, Stoddard and Hayes 2005).

We used model selection to identify the most plausible statistical models for predicting *D. aterrimus* probability of occurrence and density when present. Prior to this analysis, we identified highly correlated pairs of variables (those with $r \geq 0.7$; Davic and Welsh Jr 2004) and used principal components analysis (PCA) to reduce collinearity among these variables. We then used combinations of these variables to predict (1) *D. aterrimus* occurrence as a function of local- or landscape-scale variables and (2) *D. aterrimus* density as a function of local-scale variables. With the exception of a global model, we did not include models that mixed local and landscape-scale variables because my primary objective was to determine which of the two spatial scales better describes patterns of *D. aterrimus* occurrence. Finally, we used Akaike's Information Criterion (AIC) based methods to select the best models of *D. aterrimus* occurrence and density from sets of candidate models (White and Burnham 1999). We used log, square-root, and arcsine square-root transformations on predictor variables where necessary.

Four categories of variables defined local-scale conditions: mesohabitat type, substrate composition, aspect, and fish presence (Table 1). Proportions of riffles and cascades were positively correlated with the proportion of gravel-pebble, cobble, and boulder-bedrock

substrate. We used PCA to produce one axis that accounted for 58% of the variation in these measures (coefficients of the first eigenvector: riffles = -0.53, cascades = 0.52, gravel-pebble = 0.20, cobble = -0.47, boulder-bedrock = 0.43). Therefore, high values reflect streams dominated by cascades, gravel-pebble, and boulder-bedrock substrate. Proportions of embedded and fine substrate were positively correlated, so we used PCA to produce one axis that accounted for 75% of this variation (coefficients of the first eigenvector: embedded substrate = 0.71, proportion of fines substrate = 0.71). These procedures yielded six local variables: (1) proportion of stream with cascades and gravel-pebble/boulder-bedrock substrate, (2) proportion of pools per stream, (3) proportion of fine-embedded substrate per stream, (4) stream width, (5) aspect, and (6) fish presence. These local-scale variables were not correlated with any of the landscape-scale variables.

Four categories of variables defined landscape-scale conditions: stream size (total stream length and link magnitude), stream isolation (minimum distance along the stream channel and Euclidean distance to the stream), and habitat fragmentation and alteration (road density and old-growth tree density; Table 1). Total stream length and link magnitude were correlated, so they were subjected to PCA to produce a single axis that accounted for 86% of the variation (coefficients of the first eigenvector: total stream length = 0.71, link magnitude = 0.71). Therefore, high values reflect longer streams with many links. Minimum stream channel distance and Euclidean distance were correlated, so they were subjected to PCA to produce a single axis that accounted for 98% of the variation (coefficients of the first eigenvector: minimum stream channel distance = 0.71, Euclidean distance = 0.71). Therefore, high values reflect increasing isolation (low connectivity). Road density and old-growth density were not correlated. We considered linear models with all possible combinations of these variables, which yielded 16 possible landscape models, including the landscape core model that included all landscape variables.

To predict *D. atterimus* occurrence, we compared the relative likelihood of the global model (all local and landscape-scale variables), the 56 local models, the 16 landscape models, one landscape-core model (all four landscape variables), one local-core model (all six local variables), and one local-abiotic model that included all five abiotic variables. Logistic regression was used to determine the relative likelihood of each candidate model given the data. We evaluated the strength of support for alternative models using AIC_c , a bias-corrected version of AIC for small sample size (White and Burnham 1999).

To predict *D. atterimus* density, we compared the relative likelihood of the global model (all six local variables), the 56 local models, and one local-abiotic model that included all five abiotic variables. We used multiple linear regression to determine the relative likelihood of each candidate model given the data. We evaluated the strength of support for alternative models using AIC_c .

We determined strength of support for the model using ΔAIC_c values, AIC_c weights (ω), and evidence ratios (White and Burnham 1999). Models with $\Delta\text{AIC}_c \leq 4$ for small sample size ($n/K < 40$; where n = sample size and K = number of parameters) have empirical support as being plausible (White and Burnham 1999). We only present models with $\Delta\text{AIC}_c \leq 4$ because $n/K < 40$ for all models. To assess the importance of individual parameters within the presented models, we calculated importance weights by summing ω values of all models in which the parameter occurs (White and Burnham 1999). Parameters with importance weights > 0.20 are considered to be significant (Stoddard and Hayes 2005). Finally, coefficients (β) of local and landscape habitat covariates for *D. aterrimus* occurrence and relative density were obtained by averaging across all models weighted by ω (i.e., model averaging; White and Burnham 1999). Odds ratios were calculated from *D. aterrimus* occurrence coefficient estimates as $\exp(\beta)$. An odds ratio of 1.0 indicates no difference between the proportion of sample points with or without salamanders, while odds ratios close to zero or substantially >1.0 indicates a large difference. Odds ratios less than 1.0 indicate a negative effect while ratios greater than 1.0 indicate a positive effect (Keating and Cherry 2004). All statistical analyses were performed in JMP 7.0 (SAS Institute 2007).

Results.– We found *D. aterrimus* presence in 22 of 55 sampled headwater streams, with densities ranging from 0.01 – 0.24 individuals per m^2 . Detection probability of *D. aterrimus* was extremely high. Capture history of 21 of the 22 streams with *D. aterrimus* present was 1-1-1, while one stream had a capture history of 0-1-1. Capture history of the 23 streams with *D. aterrimus* absence was always 0-0-0.

Support for landscape-scale influences on *D. aterrimus* occurrence was greater than support for local-scale influences (Table 2). The most plausible model for *D. aterrimus* occurrence included roads, patch isolation, and old-growth tree density; its evidence ratio was six times greater than the most supported local model. Probability of *D. aterrimus* occurrence was highest in headwater stream drainages with low road and old-growth tree density and low patch isolation. Road density and patch isolation had the highest importance weights and had odds ratios < 1.0 , which indicate that increases in these variables had a negative effect on probability of *D. aterrimus* occurrence (Table 3). The odds ratio for old-growth tree density was extremely low because of the large standard error. The only local-scale model with $\Delta\text{AIC}_c < 4$ included aspect. *Dicamptodon aterrimus* occurrence was associated with a western ($200 - 300^\circ$) patch aspect. There was little evidence for other local-scale influences on *D. aterrimus* occurrence.

The most plausible model of *D. aterrimus* density included only embedded substrate, and all models with a $\Delta\text{AIC}_c < 4$ included this variable (Table 4). Parameter importance weights indicated that embedded substrate was the best predictor of *D. aterrimus* density (Table 5). Surprisingly, *D. aterrimus* density was greatest in patches with a high proportion of embedded substrate. Less plausible models suggest that *D. aterrimus* relative density was greatest in western aspects ($200 - 300^\circ$) and fishless patches.

Discussion.— To identify an effective scale of management for *D. aterrimus*, we compared model support for local and landscape-scale predictors of *D. aterrimus* occurrence in 55 headwater streams. Our results suggest that management and conservation efforts for this species would be more effective at the landscape scale than at the local scale. The five most supported models of *D. aterrimus* occurrence were composed of only landscape-scale predictors, and the importance weights of all landscape-scale predictors were greater than local-scale predictors. Specifically, we found that *D. aterrimus* occurrence was highest in unfragmented headwater drainages with few roads, lowest in spatially isolated streams, and insensitive to patch size and local-scale variables that influence stream habitat quality. Our research suggests that patch spatial structure in the surrounding landscape influences *D. aterrimus* occurrence, and that developing effective forest management rules that minimize road establishment and habitat fragmentation are essential for protecting populations of this stream amphibian.

Our results provide greater support for the rejection of the focus on local processes, but we cannot readily assume that *D. aterrimus* has a metapopulation structure. The significance of road density may affect the movement of individuals between patches to make use of non-substitutable and substitutable resources (Dunning et al. 1992), rather than affecting dispersal, colonization, recolonization, and rescue dynamics. Similarly, patch connectivity may be correlated with environmental and geographic attributes such that a site near an occupied site may tend to have similar characteristics to those of an occupied site (Bradford et al. 2003). Discrimination between metapopulation dynamics and landscape physiognomy and composition is necessary to understand mechanistically the role of patch spatial structure on *D. aterrimus* occurrence.

The importance of road density and spatial connectivity in predicting *D. aterrimus* occurrence could be related to the ability of *D. aterrimus* individuals to rescue and recolonize declining or locally extinct populations. Roads may impede salamander movement between streams by altering the intervening terrestrial habitat, or they may impede movement along streams with the presence of road crossings and culverts. Previous studies have shown that roads limit overland movement because of salamander physiological restrictions and predator-avoidance behavior (Marsh et al. 2005, Semlitsch et al. 2007). Road crossings of streams and the associated culverts may also limit movements of organisms within the stream channel because of excessive water velocity and insufficient water depth (Warren Jr and Pardew 1998). Within federal lands in the northern Rocky Mountains, there are 1.3 culverts per road kilometer (FEMAT 1993). Relative to fish, stream salamanders are poor swimmers, suggesting that culverts may significantly limit *D. aterrimus* movement along streams significantly (Sagar 2004). Culverts may also create predation hotspots that affect salamanders directly through increased mortality from large fish that accumulate in culvert outlets, or indirectly through predator avoidance behavior. However, these mechanisms remain speculative because we do not

know the spatial extent, frequency, and pathways of movement in *D. aterrimus*. Future research is needed that addresses specifically the influence of culverts and roads on stream salamander movement.

The high importance weights of road density and stream connectivity in our occurrence models may relate to a reduced ability of *D. aterrimus* to recolonize suitable streams after natural disturbances in human-altered stream drainages. Natural disturbances, such as floods and debris flows, have been linked to impaired habitat quality and lower densities of *D. tenebrosus* and stream fishes (e.g., *Cottus* sp.) in Oregon streams (Harvey 1987, Swanson et al. 1998). Furthermore, land use activities in the surrounding drainage, such as road construction and timber harvest, are believed to exacerbate the impact of natural disturbance on the recolonization of biotic communities (Gregory et al. 1991, Swanson et al. 1998). The St. Regis River and Lochsa River basins have a high frequency of natural disturbance that includes fire, rain on snow floods, and landslides (Munday et al. 2001). These disturbances are often confined to local stream reaches and are spatially heterogeneous within and across stream networks. For example, 49% of the Lochsa River basin has burned since 1910 and there is an average of 57 fire starts per year (Brown et al. 1994), but most fire starts burn less than 1 km². The combination of fire-damaged soils and rain-on-snow floods results in frequent landslide mass wasting events and debris flows that affect stream channels. In 1996-1997, there were 907 landslides in this region; however, streams adjacent to roads and timber harvest may be more vulnerable to landslides, as 60% of the 1996-97 landslides were related to cut and fill slopes along roads and 12% were associated with timber harvest (Munday et al. 2001). All streams in our study area seem to be vulnerable to natural disturbance, but streams in drainages with roads may have an elevated extinction risk.

The negative relationship we observed between *D. aterrimus* occurrence and old-growth tree density may reflect a habitat condition that we did not measure, such as standing stock of primary production and invertebrate biomass. Previous studies on stream salamanders in the Pacific Northwest have shown increased occurrence and abundance of *Dicamptodon* species in streams running through clearcut and second-growth timber stands relative to streams in old-growth stands (Hawkins et al. 1983, Steele et al. 2003, Trakhtenbrot et al. 2005). These increases are thought to be linked to increases in primary production and invertebrate biomass due to greater light penetration and warmer temperatures of streams with removed riparian canopy cover (e.g., Hawkins et al. 1982). We are reluctant to make inferences about the influence of timber harvest on *D. aterrimus* and stream community dynamics because the covariate of old-growth density had a lower importance weight than road density and stream isolation. In addition, we believe that my metric of old growth forest (northern Idaho old growth standards) failed to discern effects of timber harvest from effects of fire on stand structure. In our study area, fires have consumed old growth trees in areas with and without roads so most stands are

mixed aged, similar to harvested areas. The occurrence of fire may explain why road density is not correlated with forest stand structure.

We found that the *D. aterrimus* density was greatest in streams with a high proportion of fine-embedded substrate. For most stream amphibians, fine-embedded substrate is negatively correlated with occurrence and abundance because interstitial spaces between substrate provide egg-laying sites (Bruce 1978), important refuge from natural disturbances (e.g., high-flow events) and predation (Sih et al. 1992), and are linked to increases in stream invertebrate richness and abundance (Flecker and Allan 1984). A simple hypothesis to explain the observed relationship between *D. aterrimus* density and fine-embedded substrate is that sampling efficiency of *D. aterrimus* is greater when substrates are more embedded. We can reject this hypothesis because probability of recapture was not correlated with embedded substrate or any other local-scale variables. Rather, the positive association with fine-embedded substrate may reflect adaptation to natural disturbances such as fires and landslides that add sediment to streams (Lytle and Poff 2004). Streams in the Selway-Bitterroot Wilderness Area, where only natural disturbances occur, have greater stream sediment volumes than streams in the adjacent national forest land, where roads and timber harvest also occur (Munday et al. 2001). Having evolved with high stream sediment loads in the Lochsa River basin, *D. aterrimus* may be able to burrow through the fine sediment to seek refugia, or they may use microhabitat sites that our surveys did not record, such as undercut banks. It is interesting to note that this species may not need refugia from fish predation: models of *D. aterrimus* occurrence and density had weak support for the covariate of fish presence.

Conclusion.—We found that landscape-scale models were the best predictors of *D. aterrimus* occurrence. Specifically, we found that probability of *D. aterrimus* occurrence was greatest in roadless drainages and lowest in isolated stream drainages. In addition, we found that the relative density of *D. aterrimus* was greatest in streams with a high proportion of embedded substrate and fine sediment. These results suggest that *D. aterrimus* patches are spatially structured across stream networks, and that *D. aterrimus* is tolerant of a wide range of local conditions within streams. Further research is needed on *D. aterrimus* natural history for a mechanistic understanding of local habitat associations. We suggest that management efforts focus on protecting roadless areas and restoring stream and overland connectivity in human-impacted areas, rather than on only improving habitat quality within a stream.

Our analysis of models relating *D. aterrimus* occurrence and density to local and landscape factors is a useful starting point for understanding the spatial ecology and habitat associations of this stream salamander species. Our results support findings of other studies of amphibians and stream fishes in the Pacific Northwest and Northern Rocky Mountains that show the importance

of roadless areas and stream connectivity to population persistence (e.g., Dunham 1980, Rieman and Dunham 2000, Davic and Welsh Jr 2004). We also found that *D. aterrimus* had broad habitat requirements and was positively associated with embedded substrate. These results conflict with data on other stream amphibian species about local habitat associations and question the broad application of amphibian occurrence and abundance as ecosystem indicators of human land-use. We caution that our management recommendations are based on limited information about *D. aterrimus* occurrence and density patterns. Our understanding of the conservation biology of this and other stream amphibians would be strengthened with future research using direct (i.e., mark-capture-recapture and radio-telemetry) and indirect (i.e., genetics) methods to determine the spatial structure of populations, the frequency of dispersal between populations, and dispersal pathways.

REFERENCES

- Alford, R. A., and S. J. Richards. 1999. Global amphibian declines: a problem in applied ecology. *Annual Review of Ecology and Systematics* **30**:133-165.
- Bailey, L. L., T. R. Simons, and K. H. Pollock. 2004. Estimating site occupancy and species detection probability parameters for terrestrial salamanders. *Ecological Applications* **14**:692-702.
- Benda, L., N. L. Poff, D. Miller, T. Dunne, G. Reeves, G. Pess, and M. Pollock. 2004. The network dynamics hypothesis: how channel networks structure riverine habitats. *BioScience* **54**:413-427.
- Bradford, D. F., A. C. Neale, M. S. Nash, D. W. Sada, and J. R. Jaeger. 2003. Habitat patch occupancy by toads (*Bufo punctatus*) in a naturally fragmented desert landscape. *Ecology* **84**:1012-1023.
- Brown, J. H., and A. Kodric-Brown. 1977. Turnover rates in insular biogeography: effect of immigration on extinction. *Ecology* **58**:445-449.
- Brown, J. K., S. F. Arno, S. W. Barrett, and J. P. Menakis. 1994. Comparing the prescribed natural fire program with presettlement fires in the Selway-Bitterroot Wilderness. *International Journal of Wildland Fire* **4**:157-168.
- Bruce, R. C. 1978. Life-history patterns of the salamander *Gyrinophilus porphyriticus* in the Cowee Mountains, North Carolina. *Herpetologica* **34**:53-64.

- Bury, R. B., P. S. Corn, K. B. Aubry, F. F. Gilbert, and L. L. C. Jones. 1991. Aquatic amphibian communities in Oregon and Washington. USDA Forest Service general technical report PNW-GTR-Pacific Northwest Research Station (USA).
- Carstens, B. C., J. D. Degenhardt, A. L. Stevenson, and J. Sullivan. 2005. Accounting for coalescent stochasticity in testing phylogeographical hypotheses: modelling Pleistocene population structure in the Idaho giant salamander *Dicamptodon aterrimus*. *Molecular Ecology* **14**:255-265.
- Cushman, S. A. 2006. Effects of habitat loss and fragmentation on amphibians: a review and prospectus. *Biological Conservation* **128**:231-240.
- Davic, R. D., and H. H. Welsh Jr. 2004. On the ecological roles of salamanders. *Annu. Rev. Ecol. Evol. Syst* **35**:405-434.
- Demaynadier, P. G., and M. L. Hunter Jr. 1998. Effects of silvicultural edges on the distribution and abundance of amphibians in Maine. *Conservation Biology* **12**:340-352.
- Dunham, A. E. 1980. An experimental study of interspecific competition between the iguanid lizards *Sceloporus merriami* and *Urosaurus ornatus*. *Ecological Monographs* **50**:309-330.
- Dunning, J. B., B. J. Danielson, and H. R. Pulliam. 1992. Ecological processes that affect populations in complex landscapes. *Oikos* **65**:169-175.
- Fagan, W. F. 2002. Connectivity, fragmentation, and extinction risk in dendritic metapopulations. *Ecology* **83**:3243-3249.
- Fahrig, L., and G. Merriam. 1994. Conservation of fragmented populations. *Conservation Biology* **8**:50-59.
- FEMAT. 1993. Forest Ecosystem Management: An ecological, economic, and social assessment, Portland, OR. Report of Forest Ecosystem Management Assessment Team (FEMAT), Government Printing Office, Washington, DC.
- Flecker, A. S., and J. D. Allan. 1984. The importance of predation, substrate and spatial refugia in determining lotic insect distributions. *Oecologia* **64**:306-313.

- Gregory, S. V., F. J. Swanson, W. A. McKee, and K. W. Cummins. 1991. An ecosystem perspective of riparian zones. *BioScience* **41**:540-551.
- Gresswell, R. E., C. E. Torgersen, D. S. Bateman, T. J. Guy, S. R. Hendricks, J. E. B. Wofford, R. H. Hughes, L. Wang, and P. W. Seelbach. 2006. A spatially explicit approach for evaluating relationships among coastal cutthroat trout, habitat, and disturbance in small Oregon streams. Pages 457-471 *in*. American Fisheries Society, 5410 Grosvenor Ln. Ste. 110 Bethesda MD 20814-2199 USA.
- Grialou, J. A., S. D. West, and R. N. Wilkins. 2000. The effects of forest clearcut harvesting and thinning on terrestrial salamanders. *The Journal of Wildlife Management* **64**:105-113.
- Gulve, P. S. 1994. Distribution and extinction patterns within a northern metapopulation of the pool frog, *Rana lessonae*. *Ecology* **75**:1357-1367.
- Hairton Sr, N. G. 1987. Community ecology and salamander guilds. Cambridge University Press, New York, NY (USA).
- Hanski, I., and M. E. Gilpin. 1997. Metapopulation Biology: Ecology, Genetics, and Evolution. Academic Press, London.
- Hanski, I., and M. E. Gilpin. 1998. Metapopulation dynamics. *Nature* **396**:41-49.
- Harvey, B. C. 1987. Susceptibility of young-of-the-year fishes to downstream displacement by flooding. *Transactions of the American Fisheries Society* **116**:851-855.
- Hastings, A., and S. Harrison. 1994. Metapopulation dynamics and genetics. *Annual Review of Ecology and Systematics* **25**:167-188.
- Hawkins, C. P., J. L. Kershner, P. A. Bisson, M. D. Bryant, L. M. Decker, S. V. Gregory, D. A. McCullough, C. K. Overton, G. H. Reeves, and R. J. Steedman. 1993. A hierarchical approach to classifying stream habitat features. *Fisheries* **18**:3-12.
- Hawkins, C. P., M. L. Murphy, and N. H. Anderson. 1982. Effects of canopy, substrate composition, and gradient on the structure of macroinvertebrate communities in Cascade Range streams of Oregon. *Ecology* **63**:1840-1856.

- Hawkins, C. P., M. L. Murphy, N. H. Anderson, and M. A. Wilzbach. 1983. Density of fish and salamanders in relation to riparian canopy and physical habitat in streams of the northwestern United States. *Canadian Journal of Fisheries and Aquatic Sciences* **40**:1173-1185.
- Johnston, B., and L. Frid. 2002. Clearcut logging restricts the movements of terrestrial Pacific giant salamanders (*Dicamptodon tenebrosus*). *Canadian Journal of Zoology* **80**:2170-2177.
- Keating, K. A., and S. Cherry. 2004. Use and interpretation of logistic regression in habitat-selection studies. *The Journal of Wildlife Management* **68**:774-789.
- Knapp, R. A., K. R. Matthews, H. K. Preisler, and R. Jellison. 2003. Developing probabilistic models to predict amphibian site occupancy in a patchy landscape. *Ecological Applications* **13**:1069-1082.
- Lane, E. W., C. Brown, G. C. Gibson, C. S. Howard, W. C. Krumbein, G. H. Matthes, W. W. Rubey, A. C. Trowbridge, and L. G. Straub. 1947. Report of the subcommittee on sediment terminology. *Transactions of the American Geophysical Union* **28**:936-938.
- Lawton, J. H. 1999. Are there general laws in ecology? *Oikos*:177-192.
- Levins, R. 1968. *Evolution in changing environments*. Princeton University Press.
- Lowe, W. H., and D. T. Bolger. 2002. Local and landscape-scale predictors of salamander abundance in New Hampshire headwater streams. *Conservation Biology* **16**:183-193.
- Lytle, D. A., and N. L. R. Poff. 2004. Adaptation to natural flow regimes. *Trends in Ecology & Evolution* **19**:94-100.
- MacArthur, R., and R. Levins. 1964. Competition, habitat selection, and character displacement in a patchy environment. *Proceedings of the National Academy of Sciences* **51**:1207.
- MacDonald, L. H., and J. A. Hoffman. 1995. Causes of peak flows in northwestern Montana and northeastern Idaho. *Water Resources Bulletin* **31**:79-95.
- Mackenzie, D. I., and J. A. Royle. 2005. Designing efficient occupancy studies: general advice and tips on allocation of survey effort. *Journal of Applied Ecology* **42**:1105-1114.

- Marsh, D. M., G. S. Milam, N. P. Gorham, and N. G. Beckman. 2005. Forest roads as partial barriers to terrestrial salamander movement. *Conservation Biology* **19**:2004-2008.
- Marsh, D. M., and P. B. Pearman. 1997. Effects of habitat fragmentation on the abundance of two species of Leptodactylid frogs in an Andean montane forest. *Conservation Biology*:1323-1328.
- Marsh, D. M., and P. C. Trenham. 2001. Metapopulation dynamics and amphibian conservation. *Conservation Biology*:40-49.
- McClelland, D. E., R. B. Foltz, W. D. Wilson, T. W. Cundy, R. Heinemann, J. A. Saurbier, and R. L. Schuster. 1997. Assessment of the 1995 and 1996 Floods and Landslides on the Clearwater National Forest, Part I: Landslide Assessment. A Report to the Regional Forester, Northern Region, US Forest Service **52**.
- Munday, P. L., G. P. Jones, and M. J. Caley. 2001. Interspecific competition and coexistence in a guild of coral-dwelling fishes. *Ecology* **82**:2177-2189.
- Novinger, D. C., and F. J. Rahel. 2003. Isolation management with artificial barriers as a conservation strategy for cutthroat trout in headwater streams. *Conservation Biology* **17**:772-781.
- Nussbaum, R. A., E. D. Brodie, and R. M. Storm. 1983. Amphibians and reptiles of the Pacific Northwest. Idaho Research Foundation.
- Parker, M. S. 1991. Relationship between cover availability and larval Pacific giant salamander density. *Journal of Herpetology* **25**:355-357.
- Peterman, W. E., J. A. Crawford, and R. D. Semlitsch. 2008. Productivity and significance of headwater streams: population structure and biomass of the black-bellied salamander (*Desmognathus quadramaculatus*). *Freshwater Biology* **53**:347-357.
- Petranka, J. W. 1983. Fish predation: a factor affecting the spatial distribution of a stream-breeding salamander. *Copeia* **1983**:624-628.
- Pilliod, D. S., R. B. Bury, E. J. Hyde, C. A. Pearl, and P. S. Corn. 2003. Fire and amphibians in North America. *Forest Ecology and Management* **178**:163-181.

- Rich Jr, C. F., T. E. McMahon, B. E. Rieman, and W. L. Thompson. 2003. Local-habitat, watershed, and biotic features associated with bull trout occurrence in Montana streams. *Transactions of the American Fisheries Society* **132**:1053-1064.
- Ricklefs, R. E. 1987. Community diversity: relative roles of local and regional processes. *Science* **235**:167.
- Rieman, B. E., and J. B. Dunham. 2000. Metapopulations and salmonids: a synthesis of life history patterns and empirical observations. *Ecology of Freshwater Fish* **9**:51-64.
- Rodgers, A. R., A. P. Carr, H. L. Beyer, L. Smith, and J. G. Kie. 2007. HRT: Home Range Tools for ArcGIS. Version 1.1. Ontario Ministry of Natural Resources, Centre for Northern Forest Ecosystem Research, Thunder Bay, Ontario, Canada.
- Roni, P. 2002. Habitat use by fishes and Pacific giant salamanders in small western Oregon and Washington streams. *Transactions of the American Fisheries Society* **131**:743-761.
- Sagar, J. P. 2004. Movement and demography of larval coastal giant salamanders (*Dicamptodon tenebrosus*) in streams with culverts in the Oregon Coast Range. *in*. Oregon State University, Corvallis.
- SAS, I. 2007. JMP Software: Release 7.0. 1. SAS Institute Inc., Cary, NC.
- Saunders, D. A., R. J. Hobbs, and C. R. Margules. 1991. Biological consequences of ecosystem fragmentation: a review. *Conservation Biology*:18-32.
- Schlosser, I. J. 1995. Dispersal, boundary processes, and trophic-level interactions in streams adjacent to beaver ponds. *Ecology* **76**:908-925.
- Semlitsch, R. D., T. J. Ryan, K. Hamed, M. Chatfield, B. Drehman, N. Pekarek, M. Spath, and A. Watland. 2007. Salamander abundance along road edges and within abandoned logging roads in Appalachian forests. *Conservation Biology* **21**:159-167.
- Shurin, J. B., and E. G. Allen. 2001. Effects of competition, predation, and dispersal on species richness at local and regional scales. *The American Naturalist* **158**:624-637.

- Sih, A., L. B. Kats, and R. D. Moore. 1992. Effects of predatory sunfish on the density, drift, and refuge use of stream salamander larvae. *Ecology* **73**:1418-1430.
- Smith, M. A., and D. M. Green. 2005. Dispersal and the metapopulation paradigm in amphibian ecology and conservation: are all amphibian populations metapopulations? *Ecography* **28**:110.
- Stebbins, R. C. 2003. A field guide to western reptiles and amphibians. Houghton Mifflin Harcourt (HMH).
- Steele, C. A., E. D. Brodie Jr, and J. G. MacCracken. 2003. Relationships between abundance of cascade torrent salamanders and forest age. *The Journal of Wildlife Management* **67**:447-453.
- Stoddard, M. A., and J. P. Hayes. 2005. The influence of forest management on headwater stream amphibians at multiple spatial scales. *Ecological Applications* **15**:811-823.
- Storfer, A., and A. Sih. 1998. Gene flow and ineffective antipredator behavior in a stream-breeding salamander. *Evolution* **52**:558-565.
- Stuart, S. N., J. S. Chanson, N. A. Cox, B. E. Young, A. S. L. Rodrigues, D. L. Fischman, and R. W. Waller. 2004. Status and trends of amphibian declines and extinctions worldwide. *Science* **306**:1783.
- Swanson, F. J., S. L. Johnson, S. V. Gregory, and S. A. Acker. 1998. Flood disturbance in a forested mountain landscape. *BioScience* **48**:681-689.
- Trakhtenbrot, A., R. Nathan, G. Perry, and D. M. Richardson. 2005. The importance of long-distance dispersal in biodiversity conservation. *Diversity & Distributions* **11**:173-181.
- Trenham, P. C., W. D. Koenig, and H. B. Shaffer. 2001. Spatially autocorrelated demography and interpond dispersal in the salamander *Ambystoma californiense*. *Ecology* **82**:3519-3530.
- Trombulak, S. C., and C. A. Frissell. 2000. Review of ecological effects of roads on terrestrial and aquatic communities. *Conservation Biology*:18-30.
- Van Buskirk, J. 2005. Local and landscape influence on amphibian occurrence and abundance. *Ecology* **86**:1936-1947.

Warren Jr, M. L., and M. G. Pardew. 1998. Road crossings as barriers to small-stream fish movement. Transactions of the American Fisheries Society **127**:637-644.

White, G. C., and K. P. Burnham. 1999. Program MARK: survival estimation from populations of marked animals. Bird Study **46**:120-138.

Wiens, J. A. 1989. Spatial scaling in ecology. Functional ecology:385-397.

Table 1. Abbreviations and definitions of local and landscape -scale variables used in competing models to predict *Dicamptodon aterrimus* occupancy and density.

Variable	Abbreviation	Definition
<i>Local</i>		
Pools	P	Average proportion of pools per stream
Embedded Substrate	ES	First axis from a PCA of average proportions of fine substrate and embedded substrate
Stream Type	ST	First axis from a PCA on average proportion of gravel-pebble, cobble, boulder-bedrock substrate and average proportion of cascades and riffles per stream
Aspect	A	Downstream orientation of the stream, 0 – 360°
Stream Width	SW	Average width (m) of bank-full channel edges at high-flow conditions
Fish Presence	FP	Occupancy (presence/absence) of salmonid fish
<i>Landscape</i>		
Patch Connectivity	PC	First axis from a PCA on distance (km) along the stream corridor to the nearest drainage and Euclidean distances (km).
Patch Size	PS	First axis from a PCA on stream length (km) and link magnitude
Road Density	RD	Length of roads (km) per drainage km ²
Old Growth Density	OG	Mean number of old growth trees per 0.004 km ²

Table 2. Model selection results (AIC values corrected for small sample size) for the occupancy of *Dicamptodon aterrimus*. K refers to the number of parameters in each model, including the intercept. Boldface type indicates the best model and all those with an Akaike weight (w) > 0.1. The evidence ratio ($w_j:w_i$) indicates the multiplicative probability by which the best model (w_j) is more likely than competing models (w_i), given the set of candidate models and the data. Covariate abbreviations are listed in Table 1.

Model Name	Log-Likelihood	K	ΔAIC_c	w	Evidence Ratio
Landscape: PC, RD, OG	-19.65	4	0.00	0.23	1.00
Landscape: RD	-23.44	2	2.04	0.08	2.88
Landscape: PC, RD	-22.07	3	2.04	0.08	2.88
Landscape: PC, PS, RD, OG	-19.57	5	2.48	0.07	3.29
Landscape: RD, OG	-22.52	3	2.83	0.06	3.83
Local: A	-24.23	2	3.33	0.04	5.75
Landscape: PC	-24.55	2	3.84	0.03	7.67
Global: all local + landscape	-17.86	11	18.88	0.00	--
Landscape Core: PC, PS, RD, OG	-19.57	5	2.48	0.07	3.29
Local Core: P, ES, ST, A, SW, FP	-24.09	7	16.35	0.00	--

Table 3. Importance weights, coefficients (range), 95% confidence intervals and odds ratios of local and landscape habitat covariates predicting *Dicamptodon aterrimus* occupancy obtained by averaging across all models weighted by the Akaike weights (Burnham and Anderson 2002). The intercept is not shown. Boldface indicates estimates for which the 95% confidence intervals did not overlap zero.

Scale	Importance Weight	Coefficient Estimate	95% C.I.	Odds Ratio
<i>Local</i>				
P	0.07	-0.03 (-0.04 – - 0.03)	0.06	0.93
ES	0.08	-0.08 (-0.20 – 0.00)	0.05	0.92
ST	0.07	-0.04 (-0.07 – 0.24)	0.12	1.04
A	0.16	0.03 (0.02 – 0.11)	0.07	1.03
SW	0.07	-0.09 (-0.80 – -0.02)	0.54	0.91
FP	0.07	-0.01 (-0.02 – 0.00)	0.18	1.01
<i>Landscape</i>				
PI	0.46	-0.55 (-0.41 – -0.07)	0.26	0.58
PS	0.17	-0.04 (-0.09 – -0.02)	0.04	0.96
RD	0.60	-0.40 (-0.52 – -0.34)	0.14	0.67
OG	0.42	-70.54 (-38.47 – -81.12)	26.30	2.32E-31

Table 4. Model selection results (AIC values corrected for small sample size) for the relative density of *Dicamptodon aterrimus*. K refers to the number of parameters in each model, including the intercept. Boldface type indicates the best model and all those with an Akaike weight (w) > 0.1. The evidence ratio ($w_j:w_i$) indicates the multiplicative probability by which the best model (w_j) is more likely than competing models (w_i), given the set of candidate models and the data. Covariate abbreviations are listed in Table 1.

Scale	Importance Weight	Coefficient Estimate	95% C.I.
P	0.22	0.09 (0.02 – 0.80)	0.16
ES	0.79	0.03 (0.02 – 0.04)	0.00
ST	0.20	0.01 (0.00 – 0.02)	0.01
A	0.26	-0.14 (-0.24 – 0.07)	0.13
SW	0.23	-0.08 (-0.19 – 0.01)	0.08
FP	0.28	-0.04 (-0.11 – 0.02)	0.03

Table 5. Importance weights, coefficients (range), and 95% confidence intervals of local habitat covariates predicting *Dicamptodon aterrimus* density, obtained by averaging across all models weighted by the Akaike weights (Burnham and Anderson 2002). The intercept is not shown. Boldface indicates estimates for which the 95% confidence intervals did not overlap zero.

Model Name	Log-Likelihood	K	ΔAIC_c	w	Evidence Ratio
Density					
ES	-51.31	2	0.00	0.21	1
ES, FP	-51.97	3	1.67	0.09	2.33
ES, SW	-51.75	3	2.10	0.07	3.00
ES, A	-51.66	3	2.28	0.07	3.00
ES, ST	-51.66	3	2.29	0.07	3.00
ES, P	-51.53	3	2.54	0.06	3.50
ES, P, FP	-52.62	4	3.86	0.03	7.00
Global: P, ES, ST, A, SW, FP	-53.15	7	17.90	0.00	--

Section 2: To assess the influence of stream substrate on patterns of IGS distribution and abundance.

Introduction.— Floods influence the abundance and diversity of stream organisms by disturbing stream substrate that provides refuge and food (Resh et al. 1988). At high flows, substrate is mobilized and transported and the benthic stream organisms can be flushed downstream. Flood frequency and duration are determined by regional variables, such as climate, but the intensity of substrate disturbance is mediated by the stream's geomorphology at the reach-scale (Poff et al. 1997, Knighton 1998). Intensity can be described as the hydraulic shear stress (τ), which is the force applied by water on the stream bed surface (Matthaei et al. 1999). As τ increases, the potential to mobilize and transport sediment increases. For substrate to move, the driving forces of water on the stream bed (e.g., τ) must exceed the resisting forces holding the substrate in place (e.g., gravity, grain resistance, and hydraulic roughness) .

Flow depth and channel slope drive increases in τ 's magnitude. Therefore reaches with a wide floodplain should have more stable substrate than confined channels of similar gradient and sediment size because shear stress increases linearly only until bankfull flow, when the energy of further discharge increases is dispersed over the floodplain (Leopold et al. 1964). Understanding how channel geomorphology interacts with disturbance to influence the distribution and abundance of stream biota is a major goal for stream ecologists. This need to improve understanding is underscored by the increase in flood frequency and magnitude due to climate change.

To improve understanding, we assessed the importance of substrate disturbance by high flows to the occurrence and density of a stream salamander, *Dicamptodon aterrimus* (Idaho Giant salamander) in the St. Regis River and Lochsa River basins. *Dicamptodon aterrimus* use stream substrate as a food source and as refuge from predators and high flows. Because these organisms are poor colonizers (Sepulveda and Lowe, 2009), stream reaches with stable substrate are predicted to have a greater probability of occurrence and higher densities than streams with a higher frequency of disturbance. Floods in the Lochsa and St. Regis basins are a dominant disturbance force because of frequent rain on snow events, but the variability in stream geomorphology within stream networks may mitigate the disturbance intensity and allow for

greater habitat stability. Little is known about the natural history and ecology of *D. aterrimus*, but previous research found that *D. aterrimus* occurrence was highest in unfragmented headwater drainages with few roads, lowest in spatially isolated streams, and insensitive to habitat size (e.g., link magnitude) and local-scale variables (e.g., large wood density, fish presence, and canopy cover) that influence stream habitat quality (Sepulveda and Lowe 2009). In addition, *D. aterrimus* density was greatest in streams with a high proportion of fine-embedded substrate. The low predictive power of these models ($r^2 < 30\%$) suggest that there are other controls on *D. aterrimus* occurrence and density that were not considered previously.

Here, we used data from field surveys to compare support for models that describe *D. aterrimus* occupancy and density as a function of channel confinement and the ratio of bankfull flow competence (τ^*) to the shear stress required to set a particle into motion (τ_c^*) in 55 streams across the St. Regis River and Lochsa River basin. These models were then compared to the top-ranked models that described *D. aterrimus* occupancy and density as functions of habitat quality, connectivity, and fragmentation in a previous analysis (Sepulveda and Lowe 2009). We hypothesized that channel geomorphology influences patterns of *D. aterrimus* occupancy and density and predicted that streams with low confinement and low $\tau^* : \tau_c^*$ would have greater occupancy and density.

Methods.— In 2006 and 2007, we surveyed 55 headwater streams in the Lochsa River and St. Regis River basins. Within each stream, we surveyed two 50-m reaches separated by 200 m for *D. aterrimus* occurrence and density. The lower reach began 25 m upstream of the confluence with a similar or higher-order stream. We used a backpack electrofisher to search for salamanders within the stream. To determine detection probability, all reaches were surveyed three times within one season. We used *D. aterrimus* occurrence (presence/absence) and density within a stream as response variables. *Dicamptodon aterrimus* were declared present in a headwater stream if they were detected in at least one 50-m reach in at least one of the three surveys. We calculated density for each headwater stream as the mean number of salamanders per m^2 captured in the lower and upper stream reaches over the three surveys.

We used channel confinement and the ratio of bankfull flow competence (τ^*) to the shear stress required to set a particle into motion (τ_c^*) as predictor variables (Table 1). Channel confinement was calculated as the ratio of valley width to channel width such that high values describe low confinement. Competence is a dimension-free measure of the shear stress exerted by the flow on the bed and was calculated as

$$\tau^* = \frac{\rho g d S}{g(\rho_s - \rho)D},$$

where ρ_s and ρ are the sediment and fluid densities, respectively; g is the acceleration of gravity, d is maximum flow depth, and D is the median particle size (Church 2006). Because τ_c^* values range from 0.03 to 0.06 in most streams, we set $\tau_c^* = 0.045$ for all stream reaches.

To estimate channel confinement and $\tau^*:\tau_c^*$, we measured valley width using USGS digital elevation maps. In the field, we measured bankfull width at four random, 1-m wide transects that extended between bank-full channel edges within each reach. At six random points along each transect, we recorded stream depth and substrate particle diameter. Stream slope was estimated as the difference in elevation between the upstream and downstream ends of each plot divided by the distance between these points. Abiotic variables were averaged across the two study reaches within each headwater stream.

We also estimated variables associated with the top-ranked models from Sepulveda and Lowe (2009). The top-ranked occupancy model included habitat connectivity, fragmentation, and alteration and the top-ranked density model included the proportion of fine and embedded substrate (Table 1). We measured habitat connectivity as the minimum distance along the stream corridor from the mouth of the sampled headwater drainage to the mouth of the nearest headwater drainage. We characterized habitat fragmentation and alteration by road density and forest structure. We quantified road density as length of roads standardized by headwater drainage area (km of road per km²). We described forest structure as the density of old-growth trees (trees per km²). We also recorded the proportion of fine substrate (< 2 mm) and substrate that was embedded, defined as having visible vertical surfaces buried in either silt or sand (Welsh et al., 1997) at 6 points along each transect within each study reach. Proportions of embedded and fine substrate were positively correlated, so we used principle components

analysis (PCA) to produce one axis that accounted for 75% of this variation (coefficients of the first eigenvector: embedded substrate = 0.71, proportion of fines substrate = 0.71).

To identify predictors of *D. aterrimus* occupancy, we compared two sets of models: (1) all possible combinations of the three channel geomorphology variables and, (2) the top-ranked model from Sepulveda and Lowe (2009), which included habitat connectivity, fragmentation, and alteration. To identify predictors of *D. aterrimus* density, we compared two sets of models: (1) all possible combinations of the three channel geomorphology variables and, (2) the top-ranked model from Sepulveda and Lowe (2009), which included the proportion of fine-embedded substrate. We then used model selection to identify the most plausible statistical models for predicting *D. aterrimus* and probability of occurrence and density when present. Prior to this analysis, we tested for highly correlated pairs of variables (those with $r \geq 0.7$) and used PCA to reduce collinearity among these variables. Logistic regression was used to determine the relative likelihood of each candidate occupancy model and multiple linear regression was used to determine the relative likelihood of each candidate density model. Finally, we used Akaike's Information Criterion for small samples (AIC_c) based methods to select the best models of occurrence and density from sets of candidate models (Burnham and Anderson, 2002).

We determined strength of support for the model using ΔAIC_c values and AIC_c weights (ω). Models with $\Delta AIC_c \leq 4$ for small sample size ($n/K < 40$; where n = sample size and K = number of parameters) have empirical support as being plausible (Burnham and Anderson, 2002). To assess the importance of individual parameters within the presented models, we calculated importance weights by summing ω values of all models in which the parameter occurs (Burnham and Anderson, 2002). Parameters with importance weights > 0.20 are considered to be significant (Stoddard and Hayes, 2005). Finally, coefficients (β) of local and landscape habitat covariates for *D. aterrimus* occurrence and relative density were obtained by averaging across all models weighted by ω (we.e., model averaging; Burnham and Anderson, 2002). Odds ratios were calculated from *D. aterrimus* occurrence coefficient estimates as $\exp(\beta)$. An odds ratio of 1.0 indicates no difference between the proportion of sample points with or without salamanders, while odds ratios close to zero or substantially >1.0 indicates a large difference. Odds ratios less

than 1.0 indicate a negative effect while ratios greater than 1.0 indicate a positive effect (Keating and Cherry, 2004).

Results.— Support for channel confinement's influence on salamander occupancy and density was plausible, but had less support than models from the previous study. All models of *D. aterrimus* occupancy had empirical support as being plausible because ΔAIC_c values < 4 (Table 2). Habitat connectivity, road density, and old growth density had the highest importance weights, while $\tau^*:\tau_c^*$ had the lowest importance weight (Table 3). The coefficient estimates and odds ratios indicate that patch connectivity was positively associated with *D. aterrimus* occupancy, but that high road densities and old growth forest densities were negatively associated with occupancy (Table 3). Probability of occurrence increased as channel confinement decreased (Fig. 1), but $\tau^*:\tau_c^*$ had little effect.

Models of *D. aterrimus* density that included the proportion of fine-embedded substrate and channel confinement had the most support (Table 2). However, the importance weight of the proportion of fine-embedded substrate was much greater than channel confinement (Table 3). Coefficient estimates and odds ratios indicated that habitats with embedded substrate and less confined channels were associated with higher *D. aterrimus* densities, but that excess shear stress was not associated with density.

Discussion.— To identify the effect of high flow on *D. aterrimus* occurrence and density, we compared model support for channel geomorphology predictors of high flow disturbance against predictors of habitat quality, connectivity, and fragmentation tested in a previous analysis. The most supported model of *D. aterrimus* occurrence was composed of variables that described habitat connectivity, fragmentation and alteration, while the most supported models of *D. aterrimus* density were composed of variables that described habitat quality. Specifically, we found that *D. aterrimus* occurrence was highest in unfragmented headwater drainages with few roads and low densities of old growth trees, and lowest in spatially isolated streams. Density was greatest in streams with a high proportion of embedded-fine substrate. Occurrence and density models that contained channel geomorphology variables were also plausible, but they had lower

support. Our results suggest that high flow disturbance has minimal effect on *D. aterrimus*, especially in unconfined channels.

Disturbance influences community composition across ecosystems by ameliorating habitat (Connell 1978). However, disturbance is patchy in space and seldom destroys all available habitats. In this study, we investigated the potential of substrate disturbance during bankfull flow events and found that excess shear stress was a poor predictor of salamander occurrence and density patterns. We suggest that excess shear stress was a poor predictor because it only described potential for partial transport of substrate rather than mobilization of the entire stream bed (e.g., Wilcock 1998, Wilcock 2004, Church 2006). If only partial transport occurs, salamanders are able to use rocks that have not been mobilized. In addition, the equation for excess shear stress assumes a nearly homogenous particle size and wide stream bed. In our study streams, there was great substrate size heterogeneity and most streams were narrow (< 2 m). Thus, it is possible that there was size-selective transport of smaller substrate and that substrate near the banks was more stable than substrate in the thalweg because the banks have greater hydraulic roughness and friction resistance (Leopold et al. 1964, Dietrich and Whiting 1989). In narrow streams, a large proportion of substrate has contact with the bank. The positive association of salamanders with fine-embedded substrate may also reflect association with stream substrate that is more resistant to mobilization and transport. Finally, large wood in our study streams was abundant and is known to increase hydraulic roughness and lower competence (τ^*) (Buffington and Montgomery 1999). Our estimate of excess shear stress did not account for wood. However, models with large wood density were not supported in our previous analysis (Sepulveda and Lowe 2009).

We found that channel confinement was weakly associated with *D. aterrimus* occupancy and density. Less confined streams had a greater probability of salamander occupancy and had greater densities. We predicted that less confined channels would have lower shear stress than confined channels because shear stress increases linearly only until bankfull flow, when the energy of further increases in discharge is dispersed over the floodplain (Leopold et al. 1964). However, channel confinement was not correlated with excess shear stress ($\tau^*:\tau_c^*$) in our study streams. Therefore, it is likely that channel confinement was spuriously correlated with stream

salamander occurrence and density. Confined streams were often location in bedrock channels, while unconfined streams were frequently plane-bed channels with greater habitat complexity (Montgomery and Buffington 1997).

To test the interaction of channel geomorphology and high flow disturbance on salamander occurrence and density, we made several assumptions. First, we used cross-section data collected at minimum flow to make inferences about channel geomorphology during bankfull flow. Maximum depth at low flow was used as a variable in the shear stress equations rather than the hydraulic radius. Second, we used digital elevation maps to estimate valley width so observation error was high. Third, we assumed a $\tau_c^* = 0.045$. Finally, we assumed steady-uniform flow during spring run-off, when flow changes rapidly with time. Violation of these assumption would alter results. Validation of our minimum-flow estimates of channel geomorphology against data collected during bankfull flow is needed to assess precision and accuracy.

Conclusion.— Our results suggest that *D. aterrimus* are resistant to high flow disturbance. The St. Regis River and Lochsa River basins have a high frequency of natural disturbance that includes fire, rain on snow floods, and landslides (Jones, 1999). The positive association with fine-embedded substrate may reflect adaptation to natural disturbances such as fires and landslides that add sediment to streams (Lytle and Poff, 2004). Having evolved with high stream sediment loads, *D. aterrimus* may be able to burrow through the fine sediment to seek refugia during high flows. Alternatively, *D. aterrimus* may have little need to adapt to stochastic and seasonal flow pulses because high flow may not mobilize the entire stream bed. Experimental studies are needed to better understand how channel confinement, bank resistance, particle size heterogeneity, and substrate embeddedness interact with high flows to affect stream organisms.

REFERENCES

Buffington, J. M., and D. R. Montgomery. 1999a. Effects of hydraulic roughness on surface textures of gravel-bed rivers. *Water Resources Research* 35:3507-3521.

- Burnham, K. and D. Anderson. 2002. Model selection and multimodel inference: a practical information-theoretic approach. Springer Science: New York.
- Church, M. 2006. Bed material transport and the morphology of alluvial river channels. *Annual Review of Earth and Planetary Sciences* 34: 325-354.
- Connell, J. 1978. Diversity in tropical rain forests and coral reefs. *Science* 199:1302-1310.
- Dietrich, W., and P. Whiting. 1989. Boundary shear stress and sediment transport in river meanders of sand and gravel. *River Meandering*, American Geophysical Union Water Resources Monograph 12:1-50.
- Green, P., J. Joy, D. Sirucek, W. Hann, A. Zack, and B. Naumann, 1992. Old-growth forest types of the northern region. Northern Region, R-1 SES 4/92. Missoula, MT.
- Keating, K., and S. Cherry. 2004. Use and interpretation of logistic regression in habitat-selection studies. *The Journal of Wildlife Management*:774-789.
- Knighton, D. 1998. *Fluvial forms and processes*. Arnold London.
- Leopold, Luna B., Wolman, M.G., and Miller, J.P., 1964, *Fluvial Processes in Geomorphology*, San Francisco, W.H. Freeman and Co., 522p.
- Lowe, W., and D. Bolger. 2002. Local and Landscape-Scale Predictors of Salamander Abundance in New Hampshire Headwater Streams. *Conservation Biology* 16:183.
- Matthaei, C.D., K.A. Peacock, and C.R. Townsend. 1999. Patchy surface stone movement during disturbance in a New Zealand stream and its potential significance for the fauna. *Limnology and Oceanography* 44(4): 1091-1102.
- Montgomery, D.R. and J.M. Buffington. 1997. Channel reach morphology in mountain drainage basins. *GSA Bulletin* 109: 596-611.
- Poff, N., J. Allan, M. Bain, J. Karr, K. Prestegard, B. Richter, et al. 1997. The natural flow regime. *BioScience*:769-784.

- Resh, V.H., A.V. Brown, A.P. Covich, et al. 1988. The role of disturbance in stream ecology. *Journal of North American Benthological Society* 7(4): 433-455.
- Sepulveda, A. and W. Lowe. *In press*. Local and landscape-scale influences on the occurrence and density of *Dicamptodon aterrimus*, the Idaho Giant Salamander. *Journal of Herpetology*.
- Stoddard, M., and J. Hayes. 2005. The influence of forest management on headwater stream amphibians at multiple spatial scales. *Ecological Applications* 15:811-823.
- Welsh Jr, H., L. Ollivier, and D. Hankin. 1997. A habitat-based design for sampling and monitoring stream amphibians with an illustration from Redwood National Park. *Northwestern Naturalist*:1-16.
- Wilcock, P.R. 1998. "Two-fraction model of initial sediment motion in gravel-bed rivers". *Science*. 280: 410 - 412.
- Wilcock, P.R. 2004. Sediment Transport in the Restoration of Gravel-bed Rivers, Invited paper, *Proceedings*, ASCE Environmental and Water Resources Institute Annual Congress, Salt Lake City.

TABLE 1. Abbreviations and definitions of variables used in competing models to predict *Dicamptodon aterrimus* occupancy and density.

Variable	Abbreviation	Definition
<i>Channel</i>		
Channel confinement	CC	Bank width : Valley width
Excess shear stress	τ^*/τ_c^*	A dimension-free measure of excess shear stress required to set a particle into motion
<i>Previous models</i>		
Habitat Connectivity	PC	First axis from a PCA on distance (km) along the stream corridor to the nearest drainage and Euclidean distances (km)
Road Density	RD	Length of roads (km) per drainage km ²
Old Growth Density	OG	Mean number of old growth trees per 0.004 km ²
Embedded Substrate	ES	First axis from a PCA of average proportions of fine substrate and embedded substrate

TABLE 2. Model selection results (AIC values corrected for small sample size) for the (A) occupancy and (B) relative density of *Dicamptodon aterrimus*. K refers to the number of parameters in each model, including the intercept. The evidence ratio ($w_j:w_i$) indicates the multiplicative probability by which the best model (w_j) is more likely than competing models (w_i), given the set of candidate models and the data. Covariate abbreviations are listed in Table 1.

Model Name	K	ΔAIC_c	W	Evidence Ratio
A) Occupancy				
PC, RD, OG	4	0.00	0.41	1.00
CC	2	0.93	0.26	1.59
GLOBAL	6	1.19	0.23	1.82
CC, τ^*/τ_c^*	3	2.89	0.10	4.24
τ^*/τ_c^*	2	7.39	0.01	40.25
B) Density				
GLOBAL	4	0.00	0.48	1
ES	2	0.58	0.36	1.34
CC	2	3.45	0.09	5.61
τ^*/τ_c^*	1	4.67	0.05	10.33
CC, τ^*/τ_c^*	3	5.56	0.03	16.12

TABLE 3. Importance weights, coefficients, 95% confidence intervals (C.I.), and odds ratios of local and landscape habitat covariates predicting *Dicamptodon aterrimus* (A) occupancy and (B) density, obtained by averaging across all models weighted by the Akaike weights (Burnham and Anderson 2002). The intercept is not shown. Boldface indicates estimates for which the 95% confidence intervals did not overlap zero.

Variable	Importance Weight	Coefficients	± 95 % C.I.	Odds Ratio
A)				
PC	0.96	-0.55	0.26	0.58
RD	0.96	-0.40	0.14	0.67
OG	0.96	-70.54	26.30	2.32E-31
CC	0.58	-4.70	2.34	0.01
τ^*/τ_c^*	0.33	-0.20	0.20	0.82
B) Density				
ES	0.84	0.02	0.01	1.03
CC	0.59	0.06	0.05	1.06
τ^*/τ_c^*	0.56	-0.01	0.01	1.00

Obj. 2: To use genetics (microsatellite DNA markers) to assess the importance of connected stream networks to IGS population persistence.

Introduction.— We explored the effects of both network architecture and spatial scale on population genetic structure of the Idaho Giant salamander, *Dicamptodon aterrimus*. *D. aterrimus* is facultatively paedomorphic, and has the potential to disperse by stream and overland pathways. We examined genetic variation of microsatellite loci to investigate the genetic structure of *D. aterrimus* populations in river networks of Idaho and Montana, USA. Using microsatellite data, we tested Meffe and Vrijenhoek's (1988) and Finn *et al.*'s (2007) models of population structure by (1) examining hierarchical partitioning of genetic variation at multiple spatial scales in stream networks, and (2) testing for isolation by distance to assess the relative influence of within-stream and overland gene flow on population genetic structure.

Methods.— *Dicamptodon aterrimus* occurs in mesic forests of northern Idaho and western Montana, USA. This species was isolated from other *Dicamptodon* between 2-5 million years ago due to the xerification of the Columbia river basin following the orogeny of the Cascade Mountains (Carstens *et al.* 2005a). Mitochondrial DNA analysis supports a single refugial population in the south fork of the Salmon River of Idaho during the last glacial maximum (Carstens *et al.* 2005b), with range expansion and colonization of habitats most likely occurring northward as glaciers receded. The current distribution extends from the south fork of the Salmon River in Idaho to the northernmost peripheral populations in the St. Regis drainage of Montana. While its current distribution is patchy (Carstens *et al.* 2005b), we know occurrence of *D. aterrimus* is influenced by landscape-scale factors, including roads, stream isolation, and old growth forest density (Sepulveda & Lowe 2009).

D. aterrimus is facultatively paedomorphic: larvae develop in streams and reach maturation after several years as either terrestrial or aquatic forms (Nussbaum *et al.* 1983). Our observations in the field suggest that *D. aterrimus* are present in headwater and higher-order reaches. While no data on overland dispersal exists for *D. aterrimus*, Richardson and Neill (1998) showed that its facultatively paedomorphic sister species, *D. tenebrosus*, can move several hundred meters overland in a few days. Direct measures of in-stream dispersal by *D. aterrimus* show that short-distance movements (5-50 m) are common, but movements > 100 m

are rare. However, we lack information on the frequency and scale of dispersal beyond individual streams, and on the relative importance of movements along stream corridors versus overland pathways. Testing for support of models of genetic structure may provide insight into both the importance of overland v. in-stream gene flow, and how stream network architecture influences population structure.

To examine the spatial extent of gene flow and population structure in *D. aterrimus*, we applied a consistent sampling design that encompassed three hierarchical scales: streams, catchments, and basins. We sampled individuals in 1st-order streams which were nested within catchments of confluent streams draining into a mainstem river. Catchments were nested within basins of three major rivers: the Lochsa (four catchments), the St. Joe (two catchments) and the St. Regis (two catchments) (Fig. 1). We collected 15 *D. aterrimus* adults (both aquatic and terrestrial) and juveniles from three 1st-order streams within each catchment. Catchments were selected in basins so that they were separated by a common ridge running approximately perpendicular to the mainstem river. This orientation allowed us to test for in-stream and overland gene flow within and among adjacent catchments.

In each stream, we used an LR-20 backpack electrofisher (Smith-Root Inc., Vancouver, WA) to collect salamanders from stream reaches beginning at least 25 m upstream of the confluence with a higher-order stream. Survey reaches ranged from 125-391 m in length (mean survey length \pm 1 SD: 220 m \pm 72.7). Longer survey reaches were required to capture the minimum number of individuals used for analyses. In two streams we sampled three 30 m reaches separated by approximately 15 m (LWWF and LPEF).

A small section of tail tissue was clipped from captured salamanders and stored it in 95% ethanol. Both juvenile and adult salamanders were sampled. Snout-vent lengths of sampled animals ranged from 22 -160 mm and weights ranged from < 1 - 130 g. All sampling took place in July – October of 2008, except for five samples from one stream that were collected in July of 2007 (LSSP).

Fifteen salamanders from each stream were genotyped at 14 microsatellite loci developed for *Dicamptodon tenebrosus* and *D. copei* (Curtis & Taylor 2000; Steele *et al.* 2008). To extract

DNA, we digested tissues with protease in a detergent based cell lysis buffer, then precipitated proteins with an ammonium acetate solution and DNA with isopropyl alcohol. Isolated DNA was re-suspended in 100 μ L TE buffer and diluted 1:10 for polymerase chain reaction (PCR) amplification in a PTC-100 thermocycler (MJ Research Inc., Waltham, MA) with a total volume of 10 μ L. Multiplex reactions were setup with QIAGEN multimix, following the QIAGEN microsatellite protocol (QIAGEN Inc., Valencia, CA). We used a single PCR touchdown profile for multiplexed markers, primer annealing started at 67°C and dropped 0.5°C for 20 cycles, followed by 25 cycles with a 57°C annealing temperature. Microsatellite markers *Dte5*, *D04*, *D24*, and *D18* were PCR amplified individually following QIAGEN microsatellite protocols with separate PCR annealing temperatures. Following individual PCRs, these markers were pooled with multiplexed markers for fragment analysis. PCR products were visualized on an ABI3130xl Genetic Analyzer (Applied Biosystems Inc., Foster City, CA) in the Murdock DNA Sequencing Facility at the University of Montana, Missoula, MT. Allele sizes were determined using the ABI GS600LIZ ladder (Applied Biosystems Inc.) and alleles were called with GeneMapper version 3.7 and verified manually (Applied Biosystems Inc.).

We tested for significant departures from Hardy-Weinberg (HW) proportions and for non-random association of pairs of loci across populations (gametic disequilibrium) using exact tests implemented in GENEPOP version 4.0 (Raymond & Rousset 1995). Loci that deviated from HW proportions in each population were removed from further analyses. Genetic diversity within streams was calculated as allelic richness (A_S), the number of alleles observed in populations (N_A), and expected and observed heterozygosity (H_E and H_O). We then calculated genetic differentiation among streams with pairwise F_{ST} using Arlequin version 3.1 (Excoffier *et al.* 2005). The inbreeding coefficient, F_{IS} , was calculated for each locus in streams to detect significant heterozygote deficit or excess in streams (GENEPOP; Raymond & Rousset 1995).

We examined pairwise F_{ST} values to assess levels of divergence occurring among streams. To partition genetic variance within and among hierarchical scales, we used a hierarchical analysis of genetic variation (AMOVA implemented in the hierfstat package in R v 2.8.1; Goudet 1995). Specifically, we tested for structure at four levels: among basins, among catchments within basins, among streams within catchments, and within streams. To test for

influence of local genetic structure on overall patterns, we performed two additional AMOVAs: (1) within the Lochsa river basin, and (2) within and between the adjacent St. Joe and St. Regis river basins. These two additional AMOVAs were chosen because of the proximity of the basins; we had no samples from a basin adjacent to the Lochsa river basin, but the St. Regis and St. Joe river basins are adjacent and share boundaries. The AMOVAs generated hierarchical F -statistics (Yang 1998) in which F_{BT} was divergence among basins, F_{CB} was divergence among catchments within basins, F_{SC} was divergence among streams within catchments, F_{IS} was the inbreeding coefficient of streams, and F_{ST} was the global divergence among streams. To understand how levels of genetic divergence were influenced by effective population sizes (N_e), we used the linkage disequilibrium method (Bartley *et al.* 1992) to estimate N_e of each stream we sampled with N_e Estimator (Peel *et al.* 2004).

Genetic structure was also visually interpreted using principal components analysis (PCA) which reduces dimensions in a multivariate dataset such that the first principal component (PC1) explains as much of the variance in allele frequencies as possible (Reich *et al.* 2008). To maintain quasi-independence of the data set, we removed the highest frequency allele of each locus and performed the PCA on remaining allele frequencies (Leary *et al.* 1993). Plots of PC1 against PC2 and of PC1 against PC3 were examined to assess the similarity of allele frequencies among streams within catchments, among catchments within basins, and among basins.

We used partial Bayesian individual assignment tests (Rannala & Mountain 1997) to classify individuals to populations based on the expected frequency of an individual's multilocus genotype in each population (basins, catchments, and streams; GENECLASS2; Piry *et al.* 2004). Those individuals most likely to originate from a population other than their sampling origin were examined with a partial Bayesian exclusion test for a measure of confidence associated with assignment (Paetkau *et al.* 2004). Individuals with lower than 95% probability of originating in the sampled population were also tested with exclusion methods.

Leaving the individual to be assigned out, distributions of genotypic likelihoods that would occur in sampled populations were approximated with 10,000 Monte Carlo simulations. The likelihoods calculated for genotypes of sampled individuals were then compared to the

distribution of genotype likelihoods, and if the genotype likelihood was below the $\alpha = 0.01$ threshold, the population was excluded as an origin (Cornuet *et al.* 1999; Paetkau *et al.* 2004; Piry *et al.* 2004). Assignments of individuals to populations other than their collection location were interpreted as migration events when genotypes were unlikely to occur from a random combination of alleles ($P \geq 0.95$). Identification of migrants using this method has been possible especially when genetic differentiation is substantial and many loci are used (Berry *et al.* 2004; Paetkau *et al.* 2004). We performed three assignment tests with the above standards: (1) assignment of individuals to basins with basins as reference populations, (2) assignment of individuals to catchments with catchments as reference populations, and (3) assignment of individuals to streams with streams as reference populations.

To understand the role of gene flow by in-stream versus overland pathways, we tested alternative hypotheses of *D. aterrimus* gene flow resulting in isolation by distance (IBD). IBD is detected by testing for correlations among matrices of genetic distance (F_{ST}) and geographic distance with Mantel tests that correct for non-independence of pairwise points (Mantel 1967). We used two measures of pairwise distance between midpoints of survey reaches to test alternate pathways of gene flow with FSTAT version 2.9.3.2 (Goudet 1995).

To test the hypothesis that *D. aterrimus* gene flow occurs primarily along stream corridors (isolation by stream distance [IBSD]), we estimated the correlation between F_{ST} and stream distance in each basin. Stream distance was the shortest pathway along streams connecting two points (ArcMap 9.2, ESRI, Redlands, CA). Second, we tested the hypothesis that gene flow in *D. aterrimus* occurs primarily overland (isolation by Euclidean distance [IBED]) by estimating the correlation between F_{ST} and surface distance in each basin. Surface distance was the Euclidean distance connecting two points that corrects for changes in elevation along the path (ArcMap 9.2). Significance of correlations in all Mantel tests were assessed with 10,000 matrix randomizations. Basins were tested separately for IBSD and IBED to detect regional differences in the scale and strength of IBD due to in-stream versus overland gene flow. Pairwise stream and surface distances were significantly correlated ($r = 0.88$, $P < 0.001$). Therefore, the strengths of correlations of genetic distance with stream distance versus surface distance were used to assess the relative importance of in-stream versus overland gene flow. Plots of pairwise

F_{ST} and stream distance were analyzed to detect shifts in the relationship due to hierarchical scale.

Results.— We genotyped 361 individuals from 24 streams at 14 microsatellite loci (Table S2). Four microsatellite loci were monomorphic (*Dte4*, *Dte5*, *Dte8*, and *Dte14*) and were therefore discarded. Another locus, *Dte11*, deviated significantly from HW proportions in three of the six streams exhibiting polymorphism before correction for multiple significance tests. Moreover, the inbreeding coefficient for *Dte11* indicated a deficit of heterozygotes and suggested the presence of a null allele. Because *Dte11* was not highly polymorphic and did not conform to HW expectations, it was removed from further analyses. No other locus had significant departures from HW proportions in more than three streams after correcting for multiple significance tests with sequential Bonferroni corrections (Rice 1989). Two of 24 streams deviated from HW proportions with only a single locus out of HW proportions (Table S3). After sequential Bonferroni correction, no populations deviated significantly from HW proportions. Of the 707 tests for linkage disequilibrium, 5.1% were significant ($P < 0.05$), just slightly more than expected by chance with multiple tests. No pairs of loci were non-randomly associated in more than four of the 24 streams, and no comparisons were significant after Bonferroni correction.

Overall, genetic variation was low (A_S mean: 2.54, range: 2.11 – 3.44; H_E mean: 0.359, range: 0.187 - 0.508) and in most streams at least one locus was fixed for a particular allele. There were no significant correlations between genetic diversity (A_S , N_A , H_E) and either date or stream survey length ($P > 0.05$). Six F_{IS} values were significantly different from zero before correcting for multiple tests, none were significant after sequential Bonferroni correction, and no population had more than two loci showing either heterozygote excess or deficit. Pairwise genetic distances (F_{ST}) among streams exhibited a wide range of values with the lowest divergence occurring between streams within catchments. Overall, divergence among streams tended to be high (median $F_{ST} = 0.39$). Five pairwise F_{ST} values were not significantly different from zero and all non-significant tests corresponded to pairs of streams in the same catchment.

The global AMOVA indicated significant structure at all levels (Table 1). Most genetic variation (58.2%) occurred among individuals within streams, and the greatest proportion of structural genetic variation (23.1%) was due to differences among catchments within basins. While there was significant variation due to differences among streams within catchments, this level explained a small proportion of variation in the data (5.6%). The within-Lochsa river basin AMOVA resulted in the same patterns as the global AMOVA. Conversely, the St. Joe-St. Regis river basins AMOVA indicated that variation due to differences among basins was not significant, accounting for only 0.8% of total genetic variation. However, variation among catchments in the St. Joe-St. Regis complex was highly significant, accounting for 29.5% of total genetic variation (Table 1). Our estimates of N_e (Table 2) show that the N_e of streams is variable, with large 95% confidence intervals around these estimates. Confidence intervals around N_e estimates using the linkage disequilibrium method often include infinity (e.g., Bartley *et al.* 1992; Fraser *et al.* 2007).

Principal components analysis showed concordant patterns of genetic divergence across hierarchical network scales. PC1 accounted for 30% of the variance in allele frequencies and separated catchments into three groups consisting of (1) St. Regis and St. Joe catchments, (2) Pappoose Cr. and Wendover Cr. catchments in the Lochsa, and (3) Badger Cr. and Squaw Cr. catchments in the Lochsa (Fig. 2). PC2 accounted for an additional 18% of the variation in allele frequencies, and PC3 accounted for an additional 14% of the variation. PC2 and PC3 separated catchments in the St. Regis and St. Joe river basins but did not group catchments from basins together.

Individual assignment tests supported patterns of genetic structure shown in AMOVA and PCA. The majority of individuals were assigned to the basin (99.4%) and catchment (98.9%) where they were sampled. However, assignment of individuals to the stream where they were sampled was much lower (67.1%). Individuals most likely to originate from a population other than their sampling origin ($n = 119$) and those assigned to their sampling origin with $p < 0.95$ ($n = 147$) were evaluated with exclusion methods for a measure of confidence associated with assignment (Paetkau *et al.* 2004).

The partially Bayesian exclusion test identified no potential migrants among basins, one potential migrant among catchments in the Lochsa river basin, and five potential migrants among streams within catchments in the Lochsa and St. Regis river basins. Exclusion tests identified 156 individuals that had the highest likelihood of occurring in another stream. Two of those were excluded from all sampled streams ($P < 0.01$). Six had the highest likelihood of originating in a stream from a neighboring catchment in the Lochsa river basin ($P > 0.90$ for two individuals, $P > 0.70$ for four individuals). The remaining 148 individuals had the highest likelihood of occurring in another stream within their catchment. Although only five were considered potential migrants ($P \geq 0.95$), 67 individuals had a high likelihood of originating from another stream within the catchment ($P > 0.7$); five of these were terrestrial adults. These individuals may be descendants of immigrants from previous generations. Collectively, individual assignments identified more migrants among streams within catchments than among catchments or among basins.

There was a significant, positive correlation between stream distance and F_{ST} (IBSD) in the Lochsa river basin (Mantel; $r = 0.63$, $P < 0.001$), in the St. Regis river basin ($r = 0.93$, $P < 0.001$), and in the St. Joe river basin ($r = 0.83$, $P < 0.001$). There were significant but weaker positive correlations between surface distance and F_{ST} (IBED) in the Lochsa river basin ($r = 0.42$, $P < 0.001$), in the St. Regis river basin ($r = 0.80$, $P < 0.001$), and in the St. Joe river basin ($r = 0.72$, $P < 0.01$). All Mantel tests were significant after sequential Bonferroni adjustment.

The hierarchical analysis of genetic variation (AMOVA) identified subdivision due to restricted gene flow across catchment boundaries. This pattern suggests that genetic exchange is more frequent within than between catchments, and that if gene flow is limited by geographic distance, isolation by distance should be apparent within catchments but not between catchments of a particular basin. Mantel tests indicate that correlations F_{ST} and geographic distance were higher for stream distance than surface distance. Plots of pairwise genetic and geographic distances in basins showed a positive relationship between F_{ST} and distance among pairs of streams within catchments (Fig. 3). However, no relationship was apparent for pairs of streams that were not in the same catchment. This change in the relationship between F_{ST} and geographic distance suggests a major shift in the relative influences of gene flow and drift due to

hierarchical scale and catchment boundaries. Because of the limited number of streams sampled within catchments, we could not test correlations within individual catchments.

Discussion.— Differences in hierarchical scales at the among-stream, among-catchment, and among-basin levels all contributed to the genetic structure of *D. aterrimus*, but structure was clearly dominated by two patterns: isolation and high divergence between adjacent catchments in a basin, and lower divergence among streams within catchments. These data suggest that among-catchment structure is driven by genetic drift, which is consistent with the death valley model of population structure (Meffe & Vrijenhoek 1988). They also suggest that within-catchment structure is driven by a different force, which is gene flow among streams, supporting the stream hierarchy model (Meffe & Vrijenhoek 1988).

Divergence among catchments due to genetic drift had a large effect on *D. aterrimus* population structure (global $F_{CB} = 0.27$). There was also evidence for significant divergence among streams (global $F_{SC} = 0.09$), but to a much lower degree than among catchments. While gene flow can explain the moderate divergence among streams, both contemporary and historical patterns influence genetic structure, and distinguishing between current and historical gene flow is difficult (Peakall *et al.* 2003). Two lines of evidence point to contemporary gene flow as the cause of this pattern, including (1) field observations that suggest small population sizes, (2) small N_e estimates, and (3) the identification of potential migrants with individual assignment tests.

Up to two hours of shock time (10-12 hours surveying) was required to collect just 15 individuals from many sites. Because effective population sizes (N_e) are often only 10% of census population sizes (N_c) in wildlife populations (Frankham 1995), and estimates of N_e are generally lower than N_c for salamanders (Gill 1978; Jehle *et al.* 2005), these survey results suggest N_e of *D. aterrimus* was small. Our estimates of N_e using the linkage disequilibrium method (Bartley *et al.* 1992) also provide evidence for small and variable N_e in streams (Table 2). Divergence among populations is a function of N_e and time (t) according to the following

equation: $F_{ST} = 1 - \left(1 - \frac{1}{2(N_e)}\right)^t$. Therefore, F_{ST} increases rapidly over short periods of time when

N_e is small (Wright 1969; Nei & Chakravarti 1977). In the absence of migration, the observed variation among streams in N_e (Table 2) should also increase genetic divergence (Whitlock 1992). In light of our field observations and N_e estimates, it appears likely that migration was important in minimizing divergence among streams within catchments. Individual assignment tests provide further support for contemporary migration among streams, identifying few potential migrants among basins and catchments, but many among streams within catchments.

Levels of genetic divergence of *D. aterrimus* at the among catchment level are high compared to those seen in terrestrial mammals (e.g., Schwartz *et al.* 2002; F_{ST} 0.00 – 0.07), some populations of pond-breeding amphibians (e.g., Spear *et al.* 2005; F_{ST} 0.010 – 0.479) and stream associated frogs (e.g., Spear & Storfer 2008; F_{ST} 0.00 – 0.38), but are similar to estimates for some freshwater fish (e.g., Whiteley *et al.* 2004; F_{ST} = 0.304). Bulltrout (*Salvelinus confluentus*) have high levels of genetic divergence due to small N_e , habitat fragmentation, and other ecological and life-history related factors (Whiteley *et al.* 2004). Similarly, the high levels of genetic divergence at among-catchment and among-basin levels in *D. aterrimus* appear to be driven by genetic drift due to small N_e , and limited dispersal at these larger hierarchical scales.

During the most recent glacial maximum (18,000 ybp), the Cordilleran ice sheet extended into northern Idaho (Richmond *et al.* 1965), forcing organisms into southern refugia that provided climatic insulation (Daubenmire 1975). Carstens *et al.*'s (2005a) coalescent simulations suggest that a single refugial population of *D. aterrimus* subsisted in the south fork of the Salmon River, Idaho during this period. This putative refuge is situated at the southern end of *D. aterrimus*' current range, suggesting that the population expanded northward as glaciers receded. Northward expansion appears to have left a signature in our data as well: PC1 identified more divergence in allele frequencies among catchments in the Lochsa river basin compared to the St. Joe and the St. Regis river basins (Fig. 2). These results are consistent with Good's model in Slatkin (1993), which predicts that stepwise range expansion from a single refugial population will result in greater genetic divergence among earlier founded populations than among more recently founded populations, regardless of geographic distances among populations.

This pattern of historical range expansion was also apparent in the AMOVA (Table 1). Divergence among basins was significant in the global test (among St. Regis, St. Joe, and Lochsa river basins), but not between the St. Regis and St. Joe river basins. Because the Lochsa river basin was likely colonized first, greater genetic divergence has accumulated between the Lochsa river basin and the St. Regis and St. Joe river basins. Conversely, basins separated by minimal distances (i.e., St. Regis and St. Joe), with shorter divergence time, were not structured at the among-basin level. Rather, the structure imposed by differences among catchments in the St. Regis and St. Joe river basins was so strong that the relative effect of basin structure was minimal.

Genetic divergence (F_{ST}) and in-stream distance were strongly correlated (Fig. 3) among pairs of streams in each basin, consistent with increased likelihood of genetic exchange among nearby populations and divergence among more distant populations due to drift (Wright 1945; Hutchison & Templeton 1999). However, plots of F_{ST} and in-stream distance show a major shift in the relative influences of gene flow vs. drift that was not due to geographical distance. Instead, this shift occurred because of hierarchical catchment boundaries and scale dependency in patterns of gene flow. IBD was apparent only among streams within catchments, signifying that gene flow is more important within catchments than between catchments, and that drift overrules gene flow among catchments.

Studies of other species of *Dicamptodon* in Washington state suggest that genetic structure is strongly affected by life history (Steele *et al.* 2009). *D. copei* has a primarily aquatic life-history (non-metamorphosing) and a pattern of isolation by stream distance (IBSD), whereas *D. tenebrosus* is a facultative paedomorph (metamorphosing) with no apparent isolation by stream or Euclidean distances among sites separated by a maximum of 20 km. Steele *et al.* (2009) concluded that overland dispersal by terrestrial *D. tenebrosus* adults was an important influence on genetic structure. Although *D. aterrimus* can metamorphose, F_{ST} was more strongly correlated with stream distance than with surface distance, suggesting that gene flow occurs primarily along stream corridors. High divergence between adjacent catchments (Table 1) is further evidence of limited overland gene flow, but because the two measures of distance were themselves correlated we cannot rule it out. Consistent with the stream hierarchy model (Meffe

& Vrijenhoek 1988), *D. aterrimus* appears to use catchment mainstems as corridors for dispersal and potentially as habitat as well, suggesting that it is not an ecologically isolated headwater specialist (Nussbaum & Clothier 1973).

This study highlights the importance of stream network structure in controlling population processes of freshwater organisms. While populations of *D. aterrimus* are structured by dispersal along stream channels at the within catchment hierarchical scale, the among-catchment scale shows isolation, resulting in high divergence over small geographic scales. Long-term persistence of *D. aterrimus* will depend in part on the maintenance of genetic variation within catchments via dispersal among streams, enabling adaptation in response to shifting environmental conditions. However, our data also suggest that recolonization of catchments would be very slow, making this species especially vulnerable to disturbances that affect entire catchments, such as road networks, wildfires, and environmental impacts of climate change.

References

- Bartley D, Bagley M, Gall G, Bentley B (1992) Use of linkage disequilibrium data to estimate effective size of hatchery and natural fish populations. *Conservation Biology*, **6**, 365-375.
- Bartley D, Bagley M, Gall G, Bentley B (1992) Use of linkage disequilibrium data to estimate effective size of hatchery and natural fish populations. *Conservation Biology*, **6**, 365-375.
- Berry O, Tocher MD, Sarre SD (2004) Can assignment tests measure dispersal? *Molecular Ecology*, **13**, 551-561.
- Carstens BC, Brunfeldt SJ, Demboski JR, Good JM, Sullivan J (2005a) Investigating the evolutionary history of the Pacific Northwest mesic forest ecosystem: hypothesis testing within a comparative phylogeographic framework. *Evolution*, **59**, 1639-1652.
- Carstens BC, Degenhardt JD, Stevenson AL, Sullivan J (2005b) Accounting for coalescent stochasticity in testing phylogeographical hypotheses: modeling Pleistocene population structure in the Idaho giant salamander *Dicamptodon aterrimus*. *Molecular Ecology*, **14**, 255-265.
- Cornuet J, Piry S, Luikart G, Estoup A, Solignac M (1999) New methods employing multilocus genotypes to select or exclude populations as origins of individuals. *Genetics*, **153**, 1989-2000.

- Curtis JM, Taylor EB (2000) Isolation and characterization of microsatellite loci in the Pacific Giant salamander *Dicamptodon tenebrosus*. *Molecular Ecology*, **9**, 116-118.
- Daubenmire R (1975) *Floristic Plant Geography of Eastern Washington and Northern Idaho*. Brigham Young University Press, Provo, UT.
- Excoffier L, Laval G, Schneider S (2005) An integrated software package for population genetics data analysis. *Evolutionary Bioinformatics Online*, **1**, 47-50.
- Fausch KD, Torgersen CE, Baxter CV, Li HW (2002) Landscapes to riverscapes: bridging the gap between research and conservation of stream fishes. *BioScience*, **52**, 485-498.
- Finn DS, Blouin MS, Lytle DA (2007) Population genetic structure reveals terrestrial affinities for a headwater stream insect. *Freshwater Biology*, **52**, 1881-1897.
- Finn DS, Theobald DM, Black WC, Poff L (2006) Spatial population genetic structure and limited dispersal in a Rocky Mountain alpine stream insect. *Molecular Ecology*, **15**, 3553-3566.
- Frankham R (1995) Conservation Genetics. *Annual Review of Genetics*, **29**, 305-327.
- Fraser DJ, Hansen MM, Ostergaard S, *et al.* (2007) Comparative estimation of effective population sizes and temporal gene flow in two contrasting population systems. *Molecular Ecology*, **16**, 3866-3889.
- Funk CW, Blouin MS, Corn PS, *et al.* (2005) Population structure of Columbia spotted frogs (*Rana luteiventris*) is strongly affected by the landscape. *Molecular Ecology*, **14**, 483-496.
- Gill DE (1978) Effective population size and interdemic migration rates in a metapopulation of the Red-Spotted Newt, *Notophthalmus viridescens* (Rafinesque). *Evolution*, **32**, 839-849.
- Goudet J (1995) FSTAT Version 1.2: a computer program to calculate F-statistics. *Journal of Heredity*, **86**, 485-486.
- Grant EHC, Green LE, Lowe WH (2009) Salamander occupancy in headwater stream networks. *Freshwater Biology*, **54**, 1370-1378.
- Grant EHC, Lowe WH, Fagan WF (2007) Living in the branches: population dynamics and ecological processes in dendritic networks. *Ecology Letters*, **10**, 165-175.
- Halley JM, Hartley S, Kallimanis AS, *et al.* (2004) Uses and abuses of fractal methodology in ecology. *Ecology Letters*, **7**, 254-271.
- Hanski I, Gilpin ME (eds.) (1997) *Metapopulation biology: ecology, genetics, and evolution*. Academic Press, San Diego, CA.
- Horton RE (1945) Erosional of streams and their drainage basin: hydrophysical approach to quantitative morphology. *Geological Society of America Bulletin*, **56**, 255-370.

- Hughes JM, Schmidt DJ, Finn DS (2009) Genes in streams: using DNA to understand the movement of freshwater fauna and their riverine habitat. *BioScience*, **59**, 573-583.
- Hutchison DW, Templeton AR (1999) Correlation of pairwise genetic and geographic distance measures: inferring the relative influences of gene flow and drift on the distribution of genetic variability. *Evolution*, **53**, 1898-1914.
- Jehle R, Wilson GA, Arntzen JW, Burke T (2005) Contemporary gene flow and the spatio-temporal genetic structure of subdivided newt populations (*Triturus cristatus*, *T. marmoratus*). *Journal of Evolutionary Biology*, **18**, 619-628.
- Keyghobadi N, Roland J, Strobeck C (1999) Influence of landscape on the population genetic structure of the alpine butterfly *Parnassius smintheus* (Papilionidae). *Molecular Ecology*, **8**, 1481-1495.
- Leary RF, Allendorf FW, Forbes SH (1993) Conservation genetics of bull trout in the Columbia and Klamath River drainages. *Conservation Biology*, **7**, 856-865.
- Levin SA (1992) The problem of pattern and scale in ecology. *Ecology*, **73**, 1943-1967.
- Lowe WH, Likens GE, Power ME (2006) Linking scales in stream ecology. *BioScience*, **56**, 591-597.
- MacArthur RH, Wilson EO (1967) *The theory of island biogeography*. Princeton University Press, Princeton, NJ.
- Manel S, Schwartz MK, Luikart G, Taberlet P (2003) Landscape genetics: combining landscape ecology and population genetics. *Trends in Ecology and Evolution*, **18**, 189-197.
- Mantel N (1967) The detection of disease clustering and a generalized regression approach. *Cancer Research*, **27**, 209-220.
- Meffe GK, Vrijenhoek RC (1988) Conservation genetics in the management of desert fishes. *Conservation Biology*, **2**, 157-169.
- Muneepeerakul R, Bertuzzo E, Lynch HJ, *et al.* (2008) Neutral metacommunity models predict fish diversity patterns in Mississippi-Missouri basin. *Nature*, **453**, 220-U229.
- Nei M, Chakravarti A (1977) Drift variances of FST and GST statistics obtained from a finite number of isolated populations. *Theoretical Population Biology*, **11**, 307-325.
- Nussbaum RA, Clothier GW (1973) Population structure, growth, and size of larval *Dicamptodon ensatus* (Eschscholtz). *Northwest Science*, **47**, 218-227.
- Nussbaum RA, Jr. EDB, Storm RM (1983) *Amphibians & Reptiles of the Pacific Northwest*. University of Idaho Press, Moscow, ID.

- Paetkau D, Slade R, Burdens M, Estoup A (2004) Genetic assignment methods for the direct, real-time estimation of migration rate: a simulation-based exploration of accuracy and power. *Molecular Ecology*, **13**, 55-65.
- Peakall R, Ruibal M, Lindenmayer DB (2003) Spatial autocorrelation analysis offers new insights into gene flow in the Australian Bush Rat, *Rattus fuscipes*. *Evolution*, **57**, 1182-1195.
- Peel D, Ovenden JR, Peel SL (2004) NeEstimator: software for estimating effective population size, Version 1.3. Queensland Government, Department of Primary Industries and Fisheries, Queensland, AU.
- Piry S, Alapetite A, Cornuet J, *et al.* (2004) GENECLASS2: A software for genetic assignment and first-generation migrant detection. *Journal of Heredity*, **95**, 536-539.
- Piry S, Alapetite A, Cornuet JM, *et al.* (2004) GENECLASS2: A software for genetic assignment and first-generation migrant detection. *Journal of Heredity*, **95**, 536-539.
- Preziosi RF, Fairbairn DJ (1992) Genetic population structure and levels of gene flow in the stream dwelling waterstrider, *Aquarius (=Gerris) remigis* (Hemiptera: Gerridae). *Evolution*, **46**, 430-444.
- Rannala B, Mountain JL (1997) Detecting immigration by using multilocus genotypes. *Proceedings of the National Academy of Sciences USA*, **94**, 9197-9201.
- Raymond M, Rousset F (1995) GENEPOP (version 1.2): population genetics software for exact tests and ecumenicism. *Journal of Heredity*, **86**, 248-249.
- Reich D, Price AL, Patterson N (2008) Principal component analysis of genetic data. *Nature Genetics*, **40**.
- Rice WR (1989) Analyzing tables of statistical tests. *Evolution*, **43**, 223-225.
- Richardson JS, Neill WE (1998) Headwater amphibians and forestry in British Columbia: Pacific giant salamanders and tailed frogs. *Northwest Science*, **72**, 122-123.
- Richmond GM, Fryxell R, Neff GE, Weis PL (1965) The Cordilleran ice sheet of the northern Rocky Mountains and related Quaternary history. In: *The Quaternary of the United States*, (eds. Wright HJ, Frey D), pp. 231-242. Princeton University Press, Princeton, NJ.
- Schneider DC (2001) The rise of the concept of scale in ecology. *Bioscience*, **51**, 545-553.
- Schwartz MK, Mills LS, McKelvey KS, Ruggiero LF, Allendorf FW (2002) DNA reveals high dispersal synchronizing the population dynamics of Canada lynx. *Nature*, **415**, 520-522.
- Sepulveda AJ, Lowe WH (2009) Local and landscape-scale influences on the occurrence and density of *Dicamptodon aterrimus*, the Idaho Giant Salamander. *Journal of Herpetology*, **43**, 469-484.

- Slatkin M (1993) Isolation by distance in equilibrium and non-equilibrium populations. *Evolution*, **47**, 264 - 279.
- Spear SF, Peterson CR, Matocq MD, Storfer A (2005) Landscape genetics of the blotched tiger salamander (*Ambystoma tigrinum melanostictum*). *Molecular Ecology*, **14**, 2553-2564.
- Spear SF, Storfer A (2008) Landscape genetic structure of coastal tailed frogs (*Ascaphus truei*) in protected vs. managed forests. *Molecular Ecology*, **17**, 4642-4656.
- Steele C, Baumsteiger J, Storfer A (2009) Influence of life-history variation on the genetic structure of two sympatric salamander taxa. *Molecular Ecology*, **18**, 1629-1639.
- Steele CA, Baumsteiger J, Storfer A (2008) Polymorphic tetranucleotide microsatellites for Cope's giant salamander (*Dicamptodon copei*) and Pacific giant salamander (*Dicamptodon tenebrosus*). *Molecular Ecology*, **8**, 1071-1073.
- Wang IJ, Savage WK, Shaffer HB (2009) Landscape genetics and least-cost path analysis reveal unexpected dispersal routes in the California tiger salamander (*Ambystoma californiense*). *Molecular Ecology*, **18**, 1365-1374.
- Whiteley AR, Spruell P, Allendorf FW (2004) Ecological and life history characteristics predict population genetic divergence of two salmonids in the same landscape. *Molecular Ecology*, **13**, 3675-3688.
- Whitlock MC (1992) Nonequilibrium population structure in forked fungus beetles: extinction, colonization and the genetic variance among populations. *The American Naturalist*, **139**, 952-970.
- Wishart MJ, Hughes JM (2003) Genetic population structure of the net-winged midge, *Elporia barnardi* (Diptera : Blephariceridae) in streams of the south-western Cape, South Africa: implications for dispersal. *Freshwater Biology*, **48**, 28-38.
- Wright S (1945) Isolation by distance. *Genetics*, **28**, 114-138.
- Wright S (1951) The genetical structure of natural populations. *Annals of Eugenics*, **15**, 323-354.
- Wright S (1969) The theory of gene frequencies. In: *Evolution and the Genetics of Populations*. University of Chicago Press, Chicago.
- Yang RC (1998) Estimating hierarchical F-statistics. *Evolution*, **52**, 950-956.

Figure Legends

Figure 1. Map of sampling streams in the St. Regis, St. Joe, and Lochsa river basins of Idaho and Montana in northwestern USA. Center points of stream survey reaches are marked with stars, and four letter stream codes are indicated. Four catchments were sampled from the Lochsa river basin: Squaw Ck. (streams: LSDO, LSSP, LSU1), Badger Ck. (streams: LBU1, LBU2, LBU3), Wendover Ck. (streams: LWEF, LWWF, LWU1), and Papoose Ck. (streams: LPTW, LPTE, LPEF). Two catchments were sampled from the St. Regis river basin: Big Ck. (streams: RBMC, RBU1, RBU2), and Deer Ck. (streams: RDTU, RDUU, RDU1). Two catchments were sampled from the St. Joe river basin: Quartz Ck. (streams: JQU1, JQUE, JQU3), and Gold Ck. (streams: JGPR, JGU1, JGU2).

Figure 2. Plots of the first three principal component scores of allele frequencies of nine microsatellite loci among streams sampled from basins and catchments in Idaho and Montana. Points corresponding to streams within catchments are circled and catchments are labeled. Streams sampled in the Lochsa river basin are circles, streams from the St. Joe river basin are squares, and streams from the St. Regis river basin are triangles.

Figure 3. Scatter plot of F_{ST} and stream distance for pairs of streams within the same basin. Pairs in the St. Joe river basin are squares, in the St. Regis river basin are triangles, in the Lochsa river basin are circles. Pairs of streams that are located within the same catchment (solid) are distinguished from those that are not within the same catchment (open).

Table 1. Results of hierarchical analysis of molecular variance: (A) Global AMOVA, (B) Within Lochsa AMOVA, (C) St. Joe - St. Regis AMOVA. Significant *P* values are in bold.

Source of Variation	<i>df</i>	Variance components	Percentage of variation	<i>F</i> statistics	<i>P</i>
A					
Among basins	1	0.725	13.0	$F_{BT} = 0.130$	0.0022
Among catchments within basins	2	1.285	23.1	$F_{CB} = 0.266$	<0.001
Among streams within catchments	5	0.310	5.6	$F_{SC} = 0.087$	<0.001
Within streams	353	3.236	58.2	$F_{IS} = -0.024$	
Total	361	5.556		$F_{ST} = 0.418$	
B					
Among catchments within basins	1	1.117	24.3	$F_{CB} = 0.243$	<0.001
Among streams within catchments	3	0.335	7.3	$F_{SC} = 0.096$	<0.001
Within streams	176	3.147	68.4	$F_{IS} = -0.012$	
Total	180	4.599		$F_{ST} = 0.316$	
C					
Among basins	1	0.044	0.8	$F_{BT} = 0.009$	0.1685
Among catchments within basins	1	1.533	29.6	$F_{CB} = 0.298$	0.0039
Among streams within catchments	2	0.285	5.5	$F_{SC} = 0.079$	<0.001
Within streams	177	3.324	64.1	$F_{IS} = -0.035$	
Total	181	5.187		$F_{ST} = 0.359$	

Table 2. Estimates of effective population size and 95% confidence intervals.

Basin	Catchment	Stream	N_e	95% CI	
St. Regis	Big	RBMC	∞	38.4	∞
		RBU1	163.3	21.4	∞
		RBU2	66.7	16.6	∞
	Deer	RDTU	8.8	4.8	20.9
		RDU1	16.1	7.3	103.1
		RDUU	∞	12.3	∞
St. Joe	Gold	JGPR	16.4	9.2	42.4
		JGU1	25.8	10.9	∞
		JGU2	11.4	6.3	28.6
	Quartz	JQU1	53.0	19.4	∞
		JQU3	17.2	7.3	249.0
		JQUE	20.9	9.7	153.3
Lochsa	Badger	LBU1	∞	29.1	∞
		LBU2	∞	38.1	∞
		LBU3	29.8	11.7	∞
	Papoose	LPEF	37.4	13.8	∞
		LPTE	14.9	7.7	48.4
		LPTW	33.6	12.7	∞
	Squaw	LSDO	∞	30.7	∞
		LSSP	11.4	7.0	22.4
		LSU1	17.1	7.6	145.9
	Wendover	LWEF	22.0	7.8	∞
		LWU1	688.3	12.9	∞
		LWWF	2.3	1.7	3.0

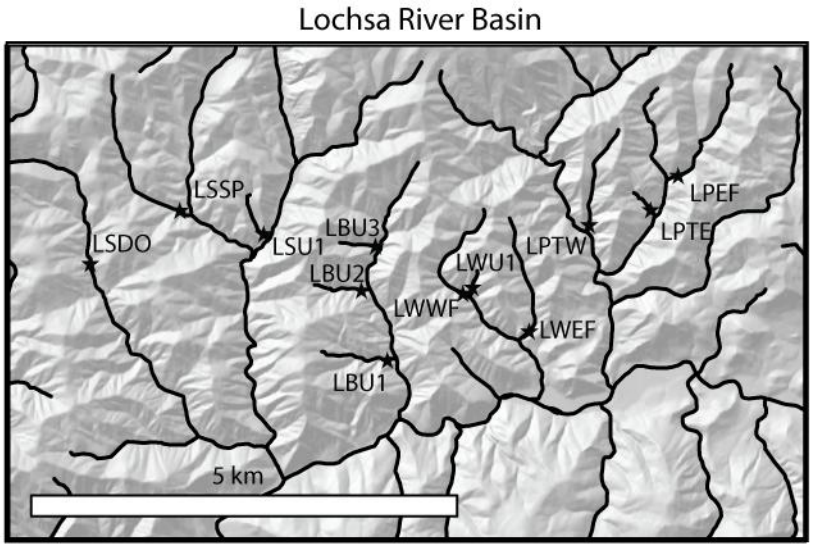
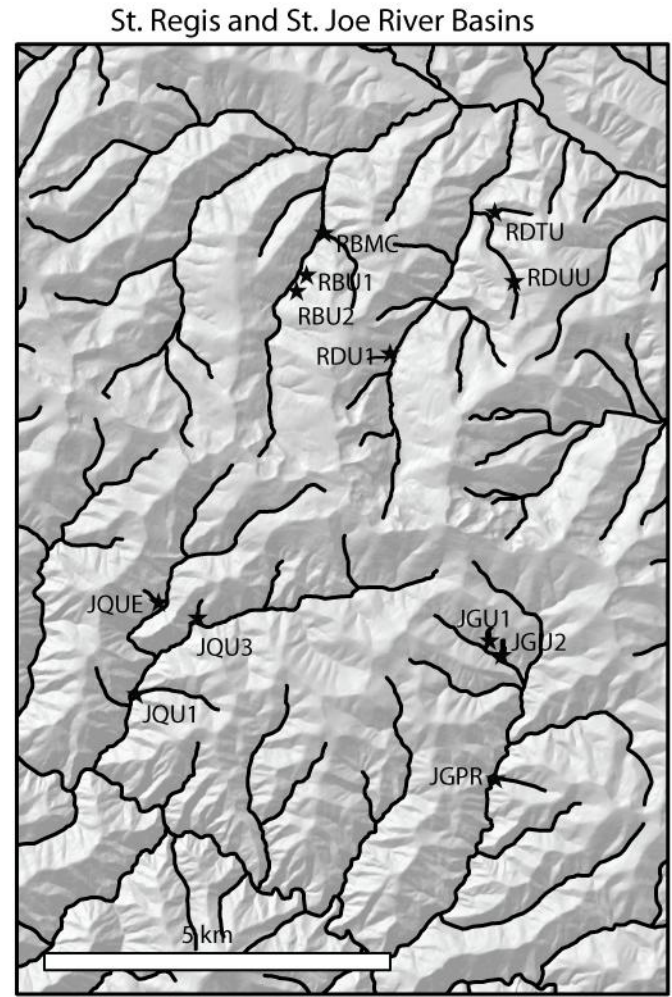
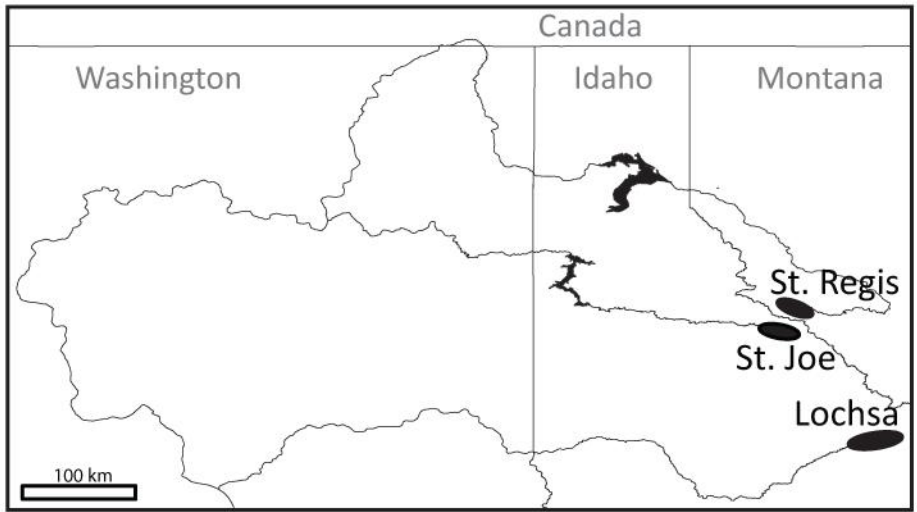


Fig. 1

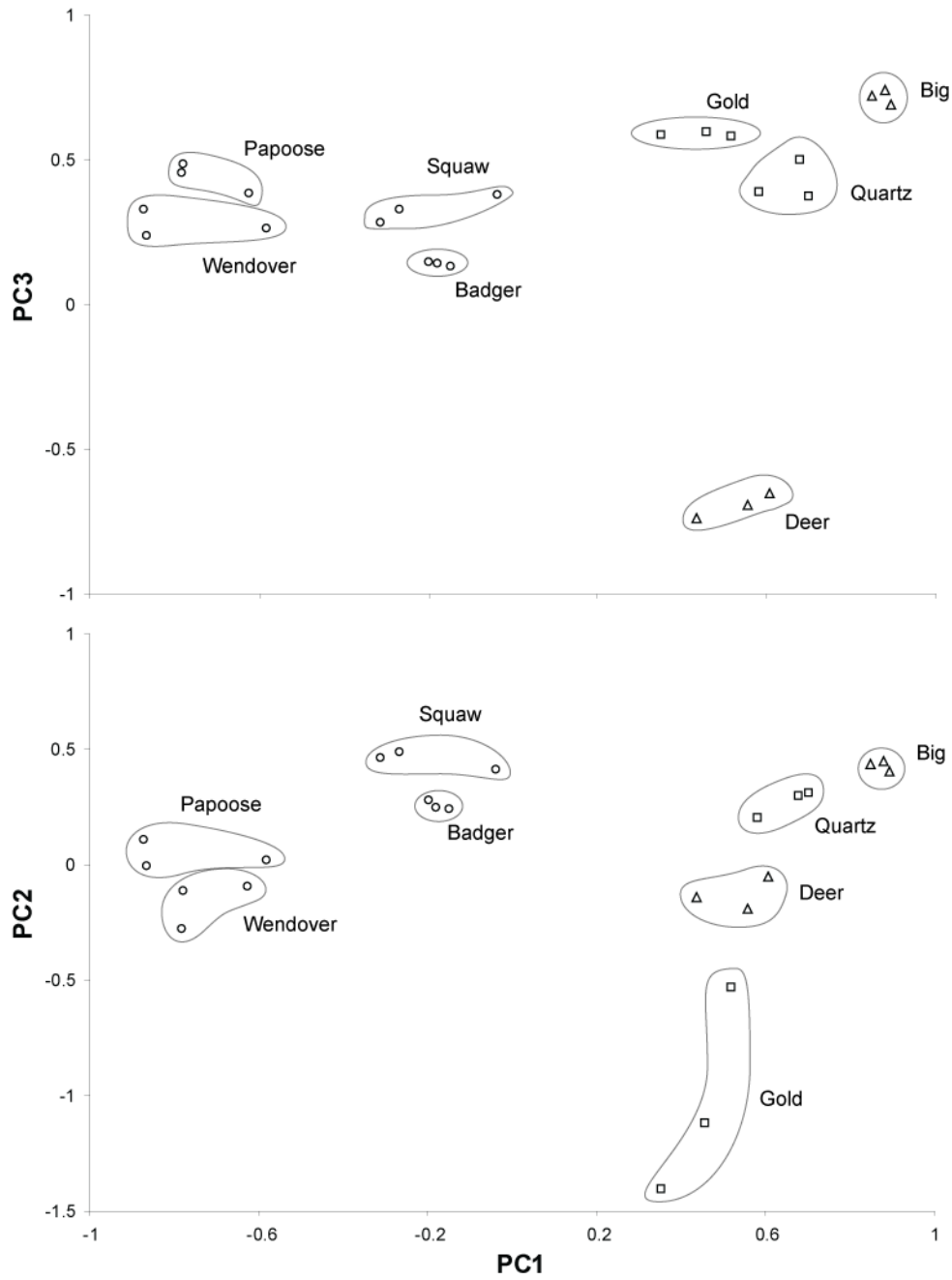


Fig. 2

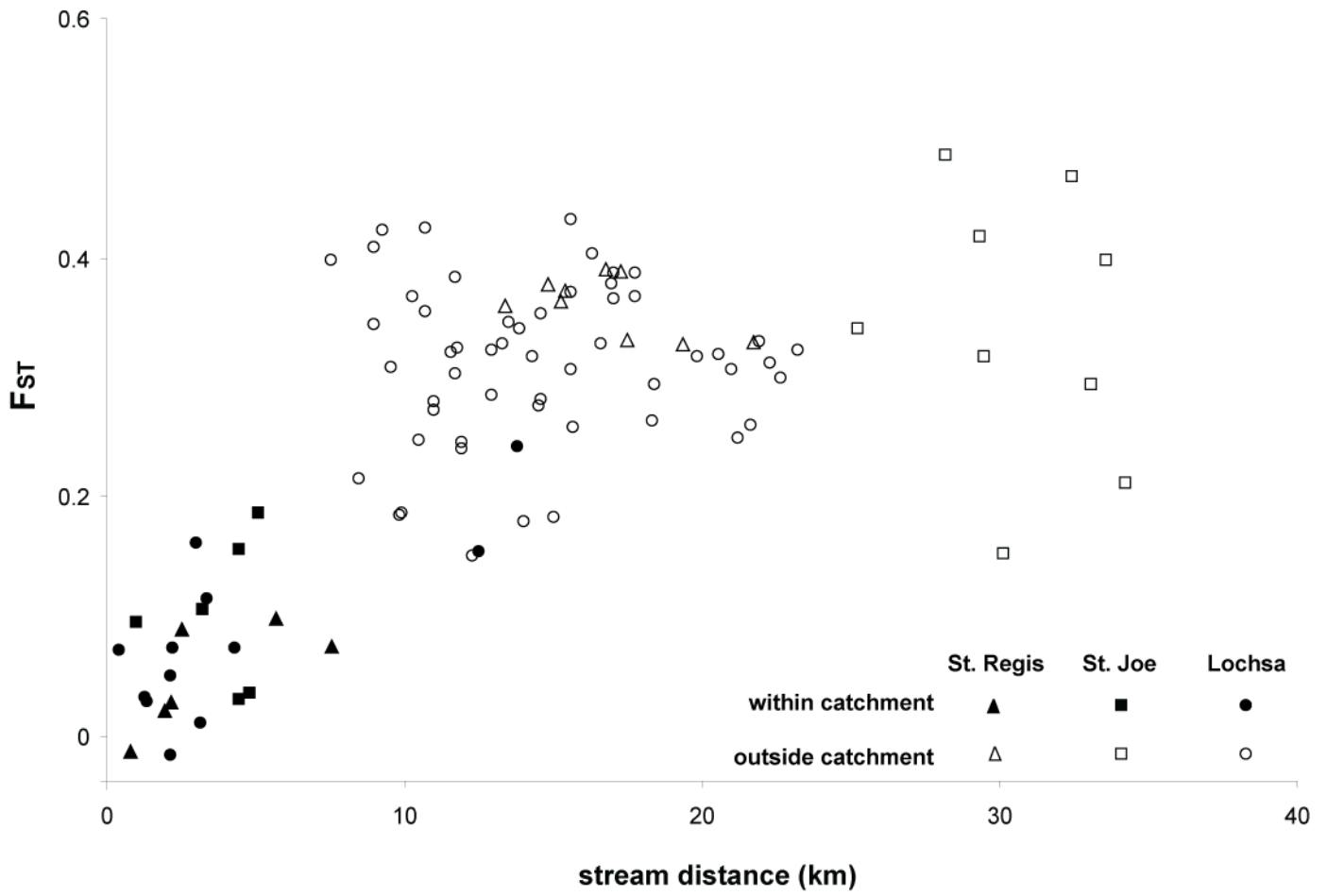


Fig. 3

Evolution of channel morphology and aquatic habitat in the Middle Clark Fork River following removal of Milltown Dam

Basic Information

Title:	Evolution of channel morphology and aquatic habitat in the Middle Clark Fork River following removal of Milltown Dam
Project Number:	2008MT168B
Start Date:	3/1/2008
End Date:	2/28/2010
Funding Source:	104B
Congressional District:	At-Large
Research Category:	Water Quality
Focus Category:	Geomorphological Processes, Sediments, Water Quality
Descriptors:	
Principal Investigators:	Andrew Wilcox

Publication

1. Wilcox, A. C., D. Brinkerhoff, C. Woelfle-Erskine. 2008. Initial geomorphic responses to removal of Milltown Dam, Clark Fork River, Montana, USA. EOS Trans. AGU. 89(53) Fall Meet. Suppl. Abstract H41I-07.

UPSTREAM GEOMORPHIC RESPONSE TO DAM REMOVAL:
THE BLACKFOOT RIVER, MONTANA

By

JOSHUA AARON EPSTEIN

B.A. University of California, Los Angeles, 2001

Thesis

Presented in partial fulfillment of the requirements
for the degree of

Master of Science
in Environmental Studies

The University of Montana
Missoula, MT

Summer 2009

Approved by:

Dr. Perry Brown, Dean
Graduate School

Dr. Andrew Wilcox, Chair
Department of Geosciences

Dr. Vicki Watson
Department of Environmental Studies

Dr. Johnnie Moore
Department of Geosciences

Epstein, Joshua A., M.S., Summer 2009

Environmental Studies

Upstream Geomorphic Response to Dam Removal: The Blackfoot River, Montana

Committee Chair: Dr. Andrew Wilcox

As dam removal is increasingly used as a tool to restore rivers, developing a conceptual and field-based understanding of the upstream fluvial response is critical. Using empirical data and modeling, I investigated the spatial and temporal pattern of reservoir sediment erosion and upstream channel evolution of the Blackfoot River, MT, following the 8 m base level reduction caused by the removal of Milltown Dam. Field data collected include surveys of channel bed topography and water surface elevation profiles which were integrated into a flow modeling approach. Headward erosion extended 4.5 km upstream of the dam site during the first five months following the dam removal. In the lower 1.8 km of the reservoir, up to 3 m of highly mobile silt and sand was evacuated. Upstream, the river incised into a coarse deltaic sediment deposit (D_{50} 70mm) in the upper reservoir. The analysis of erosion through the hydrograph shows that the channel incised up to 2 m in some locations and maximum volumetric erosion of $260,000 \text{ m}^3$ was reached several days after the flood peak ($286 \text{ m}^3/\text{s}$, 3.5 year return interval). Net erosion following the dam removal, accounting for both scour and deposition, was $150,000 \text{ m}^3$ across the 5 km study reach. The modeling-based water surface elevation analysis revealed the intra-hydrograph pattern of erosion that otherwise would have been missed by comparing pre- and post-removal cross section topography. The post-removal evolution of the lower Blackfoot was heavily influenced by confinement of the channel and the above average discharge. Widening was associated with areas of local aggradation, whereas narrowing was associated with degradation—a finding similar to those from previous flume experiments.

Key words: Dam removal, reservoir sediment erosion, upstream geomorphic response, base level, large woody debris.

Acknowledgements

I am indebted to various individuals and organizations for their financial, field and intellectual support of my thesis research. First of all, I thank my advisor, Andrew Wilcox, for helping to elevate my technical and analytical skills necessary to complete this work. The valuable discussions and initial field site visits with Andrew Wilcox and Leonard Sklar helped develop critical elements of this research. I would also like to thank committee members Johnnie Moore and Vicki Watson whose contributions positively influenced this work. The data necessary to complete this study would not have been collected and processed without the assistance of Doug Brinkerhoff, Cleo Woelfle-Erskine, Aaron Deskins, Ben Horan, Tim Gilbert, James Johnsen, Lorri Eberle, Michael Morris, Diane Whited, Deana DeWire and Dave Granger often-times in the rain and snow commonly found in Montana's Spring and Fall seasons. Financial support for this work was provided by various awards and grants including NSF EPS-0701906, NSF EAR-0809082, Bryon D. and Bernice Dawson Memorial Fund, UM Watershed Health Clinic, EVST Linduska Opportunity Fund, and a Montana Water Research / USGS 104(b) Seed Grant.

TABLE OF CONTENTS

Abstract		ii
List of Figures		v
List of Tables		vi
I.	Introduction	1
	Fluvial Sediment Dynamics and Base level.....	2
	Conceptual Model of Erosion and Channel Evolution....	4
II.	The Problem	7
III.	Study Site	9
IV.	Methods	13
	WSE Analysis.....	16
	HEC-RAS Modeling.....	16
	Exponential Decay.....	19
V.	Results	20
	Sediment Surface Texture and Mobility.....	20
	Net Morphological change analysis.....	25
	Δ WSE Analysis.....	29
	Exponential Decay.....	32
VI.	Sensitivity Analysis	34
VII.	Discussion	37
	Net Morphological Change vs. WSE Analysis.....	37
	Erosion Predictions vs. Observations.....	39
	Sediment Texture and Mobility.....	40
	Exponential Decay.....	41
	Widening vs. Erosional Narrowing.....	42
	Knickpoint.....	43
	Monitoring and Management Implications.....	45
	2006 Reservoir Drawdown and Stimson Dam Removal.	46
	Challenges.....	47
	Comparison to Other Dam Removals.....	47
	Implications for Other Systems.....	53
VIII.	Conclusion	55
	Future Directions.....	56
References Cited		57
Appendix I: Cross Section Plots		61
Appendix II: GPS Data		67
Appendix III: Exponential Decay Derivation		69

FIGURES

1. Idealized Diagram of Base Level	3
2. Channel Evolution Model	6
3. Four Knickpoint Migration Patterns (Stewart 2006)	7
4. Overview Map: Upper Columbia	11
5. Aerial Photo of Study Area	11
6. Photo: Wood in BFR From the 1908 Flood	12
7. Stimson Dam Photos	12
8. Conceptual Diagram of Headward Erosion of 2 reservoir sediment Deposits	13
9. 2004 NAIP Aerial Photo Showing Cross Section Locations	15
10. 2008 Hydrograph and Survey Dates	15
11. Pre-erosion Cross Section I	17
12. Air Photos Lower 2km	21
13. Grain Size Distribution: Lower Reservoir	22
14. Grain Size Distribution: Upper Reservoir	22
15. Grain Size Distribution 4.4 km Upstream	23
16. Percent Change in D50	23
17. Change in D50	24
18. Critical Discharge Needed to Mobilize Spring 2008 Bed	24
19. Spring-Fall 2008 Change in Area	26
20. Longitudinal Bed Profile	26
21. Spring vs. Fall 08 XS VII	27
22. Changes in Width	27
23. Air Photos 2-3 km Upstream	28
24. Δ WSE Through the 2008 Hydrograph	30
25. Mean Δ WSE, Volumetric Erosion Through the 2008 Hydrograph	31
26. Water Surface Profiles 2003- Fall 2008	32
27. Exponential Decay and Erosion Estimates	33
28. Sensitivity Analysis Plots.	35
29. Δ WSE Incorporating Sensitivity Analysis Results (A) 6/27, (B) 9/5	36
30. Hysteresis in Pattern of Erosion	39
31. Repeat Photography at Stimson Dam Site	44
32. Idealized Diagram of Sediment Filling a Reservoir	50
33. Proportion of Reservoir Sediment Eroded – Comparison	50
34. Lower BFR Wood	54

TABLES

1. Manning's n Values for HEC-RAS	18
2. Discharge Modeled in HEC-RAS	19
3. Exponential Decay	33
4. Recent Dam Removals	51

I. INTRODUCTION

Caught at the crossroads of declining ecosystem services, decaying infrastructure, and increasing interest in ecological restoration, the U.S. has entered into an era of dam removal (Doyle et al. 2008). Dam removal is perhaps the largest of available options to restore rivers, but in many cases has a significant potential to restore or enhance ecosystem services valued by society (Graf 2002, Pizzuto 2002). Despite decades of dam removal practice, there are few detailed studies performed before and after such projects are completed to enhance our understanding of river response (Doyle et al. 2002). From planning stages to execution, perhaps the most critical element to dam removal projects is the fate of sediment stored behind a given dam (Shuman 1995, Cui and Wilcox 2008). The fate of reservoir sediment can be the costliest and least certain component of a dam removal, and is therefore of interest to scientists and policy-makers (Cui and Wilcox 2008). Reservoir sediments may be a source of contamination, interact with certain life history stages of aquatic organisms, or affect adjacent communities. Furthermore, the questions surrounding the evacuation of reservoir sediment is coupled with the how a channel upstream of a given dam will evolve.

This study will focus on the upstream sediment dynamics including erosion of reservoir sediment and the evolution of the newly reclaimed Blackfoot River above Milltown Dam. The Milltown Dam removal is part of the larger > \$100 million dollar multi-year Superfund remediation effort. While significant resources were allocated to feasibility studies to prepare for the dam removal and mechanical excavation of contaminated sediments, significant questions surrounding the fate of reservoir sediment and the upstream response of rivers remain for scientists and policy-makers to consider in future dam removals. For example, in the first spring runoff following the removal of the dam, 180,000 m³ of contaminated sediments eroded from the upper portion of the Clark Fork arm of Milltown reservoir (Wilcox et al. 2008). The 180,000 m³ is equivalent to ~4500% of the volume predicted to be eroded from the upper reservoir area by the pre-removal modeling efforts (Envirocon 2004). The spatial component of the upstream response was not captured by the modeling efforts applied to the problem of predicting reservoir sediment erosion to manage contamination.

Fluvial Sediment Dynamics and Base Level

Building a dam creates a reservoir where sediment transport capacity is greatly reduced. Annual sediment loads supplied from upstream hill-slope and fluvial processes are trapped by the low velocity slack-water behind a dam, filling the reservoir with sediment over time (Graf 1999, Graf 2002). When a dam is removed, the sediment balance tips in the opposite direction: the system's capacity to transport sediment is increased while having a large supply in the reservoir sediment deposit. Dam removal reactivates sediment supply to downstream river reaches in a sediment pulse (or series of several pulses) as the reservoir deposit erodes. The post-removal sediment pulse may be orders of magnitude higher than typical seasonal sediment flux in a given river system, because of the potentially large reservoir sediment deposit and the unique geomorphic context which can lead to flux of large volumes at high transport rates (Major et al. 2008).

The concept of base level is useful in placing upstream geomorphic response to dam removal into a theoretical context. Given upland watershed processes and climate operating within normal levels of variability, rivers tend toward an equilibrium base level, defined as the level below which a river cannot down-cut (Leopold and Bull 1979). Base level is considered to be a downstream control on rivers, a reduction of which will cause upstream degradation or incision (Knighton 1998). Base level changes can occur over geologic time scales through tectonically driven uplift which may create landscapes in a transient state (Crosby and Whipple 2006, Bishop 2005). The rapid decrease in water surface elevation caused by dam removal can be considered as a change in local base level (Doyle et al. 2002). Such a case may constrain the upstream fluvial response to a shorter time scale than in other physiographic settings, such as in bedrock systems. For example, a study of upstream migrating incision into networks of bedrock channels found climate-driven base level fall propagated knickpoints upstream over 18,000 years (Crosby and Whipple 2006).

Base level may change due to naturally occurring processes at the confluence of two rivers through altered climate and discharge (Leopold and Bull 1979) or changes in incision rates at the main-stem river (Crosby and Whipple 2006). Base level for streams

flowing into lakes can be set by long-term fluctuations in lake level driven by climatic variations (Galay 1983, Figure 1).

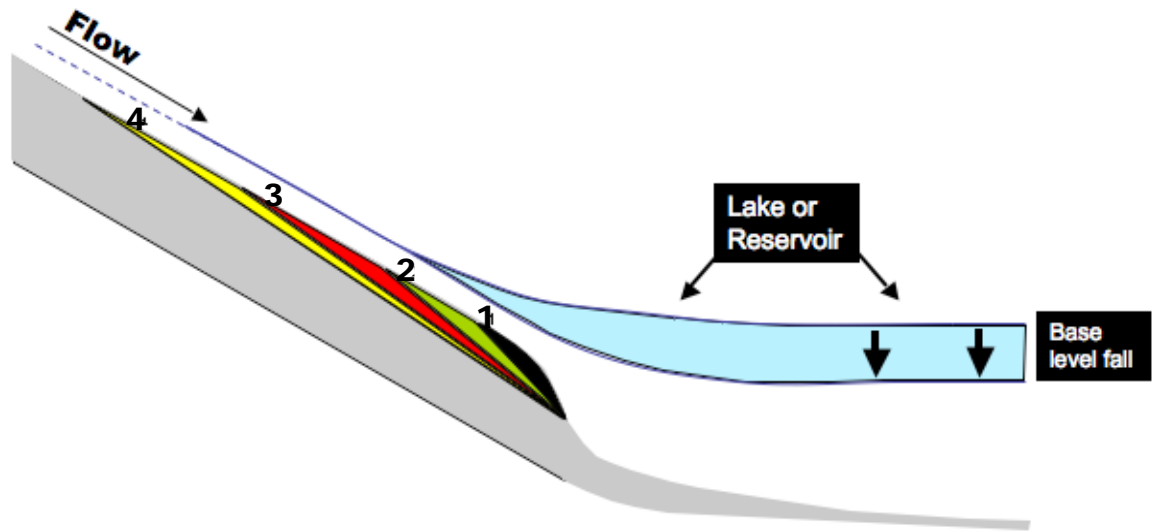


Figure 1. Idealized diagram of base level fall from a reduction in lake or reservoir elevation. Progression of upstream erosion through time ($t = 1$ through 4). Adapted from Galay 1983.

Furthermore, changes in sea level and anthropogenic disturbances such as water diversion, dam construction, reservoir regulation and dam removal are additional drivers of base level change. In the case of dam removal, the base-level drop reduces the downstream control on the stored reservoir sediment (Doyle et al. 2002) and will initiate upstream geomorphic response such as incision and headward migrating knickpoints (Larue 2008). Other potential responses include changes in slope, surface sediment textures, roughness, sinuosity or lateral channel migration resulting in altered aquatic and associated riparian habitats (Leopold and Bull 1979). Furthermore, the literature has been summarized to predict that the effect of base level fall will be most pronounced when it occurs rapidly and the upstream channel is confined (Knighton 1998).

Conceptual Model of Reservoir Sediment Erosion and Channel Evolution

Channel evolution following base level reduction has been explored both in the field and laboratory by several authors (Begin 1981, Schumm 1984, Simon and Hupp 1987, Begin 1988, Doyle et al. 2002, Doyle et al. 2003, Cantelli et al. 2004). Channel evolution models (CEMs) that originate in empirical studies of incised sand-bed channels have been applied to dam removal (Doyle et al. 2002, See Figure 2). Accordingly, headward migrating channel degradation increases bank height above a lowering bed surface, leading to channel widening driven by bank failure (which is controlled by bank angle, height, and sediment cohesion properties). Sediment contributed to the channel from widening (bank failure) can mitigate the effects of degradation, or where critical discharge for downstream transport of bank material is reached, greatly increase the total amount of sediment evacuated from a given stream reach (Doyle et al. 2002). Flume experiments on dam removal found erosional narrowing to occur during the initial incision into the reservoir deposit (Cantelli et al. 2004, Cantelli et al. 2007). As the flume channel rapidly incised into the reservoir sediment deposit, the channel actually narrows before widening.

Following perturbation of the system through base level change, it would be expected that fluvial response would lead to some state of equilibrium. One field study described upstream channel response to base level rise approaching a new equilibrium state with a similar slope to the pre-perturbation channel. The development of an upstream sediment wedge resulting from dam construction extended 1.5 km upstream after 25 years and adjusted to 83% of the initial slope (Van Haveren et al. 1987, Knighton 1998). In the case of dam removal, it may be possible that post-removal channel equilibrium would reach a slope similar to pre-dam conditions at a different mean bed elevation following degradation.

It has also been shown that in some sand-bed systems, upstream channel evolution following base-level fall is governed by the migration rate of a knickpoint (Doyle et al. 2002). A knickpoint is a point of dramatic slope increase in the longitudinal profile of a stream inclusive of small rapids through the spectrum to a vertical waterfall (Brush and Wolman 1960, Crosby and Whipple 2006). Knickpoints migrate upstream over a variety of timescales depending on the individual case, and are often formed by

base level fall. A knickpoint may maintain its shape and move upstream as a stepped knickpoint. Alternatively, it may get longer and less steep if the top of the knickpoint erodes faster than the base, creating a rotating knickpoint (Stewart 2006). Flume experiments investigating “blow and go” removal of a dam with results up-scaled to gravel-bed rivers support the rotating knickpoint phenomena (Cantelli et al. 2004). Field observations of low-head dam removals in sand bed, low gradient systems in the mid-west found both stepped and rotating knickpoints migrating upstream through reservoir sediment deposits (Doyle et al. 2003, Cheng and Granata 2007, Evans 2007, Major et al. 2008). Furthermore, knickpoint form is also controlled by how the sediment eroded from the face moves downstream. Stewart (2006) proposed that knickpoints may evolve in four possible modes following dam removal: 1. rotating with diffusion, 2. rotating with dispersion, 3. stepped with diffusion, or 4. stepped with dispersion (Figure 3). As the literature covering fluvial response of fine-bed channels to base level reduction is more developed, there is some disagreement on what form a knickpoint will take in gravel bed rivers. Furthermore, it is possible for erosion of reservoir sediment to occur without the formation of a knickpoint. In the removal of Saeltzer Dam on Clear Creek, California, headcutting was not observed in the coarse sediment exposed to high discharge (Cui and Wilcox 2008).

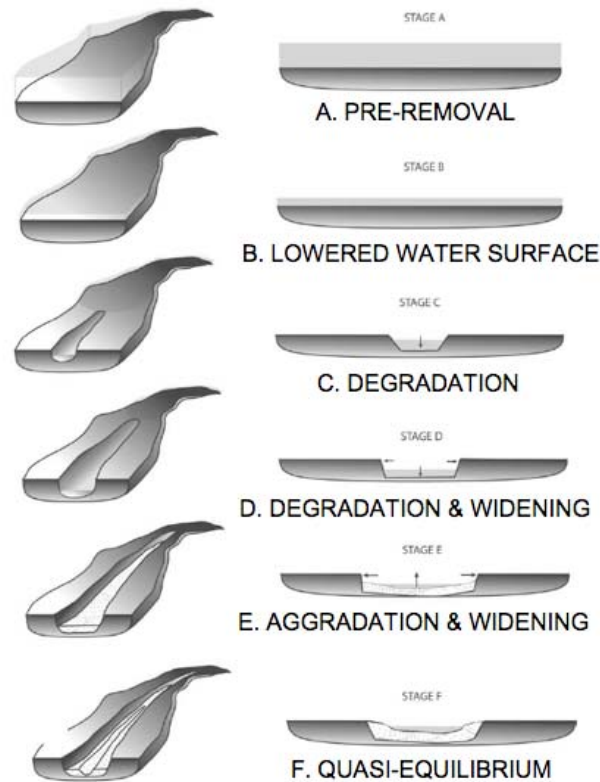


Figure 2. Channel evolution model for upstream response to dam removal from Doyle et al. 2003, based on incising channels. Modifications for larger reservoir and mixed sediment composition of reservoir deposit may be needed for this study.

Studies applying a diffusion model showed that base-level reduction may cause degradation along the length of the channel equal to the amount of base level fall, maintaining a stream with the same slope (Begin 1988, Knighton 1998). Application of these results to the Blackfoot this would predict degradation on the order of 8 m (Begin 1988). It was noted that heterogeneous sediment and armoring could produce different results. The BFR has both heterogeneous sediment, and complications of variable roughness (bedrock, large woody debris, rip-rap banks, and bridge piers). Additionally, the diffusion model results may be inappropriate for application to large unconfined alluvial rivers that can alter sinuosity and roughness preventing the signal of base level fall from migrating far upstream (Knighton 1998), but perhaps more applicable to the constrained BFR channel.

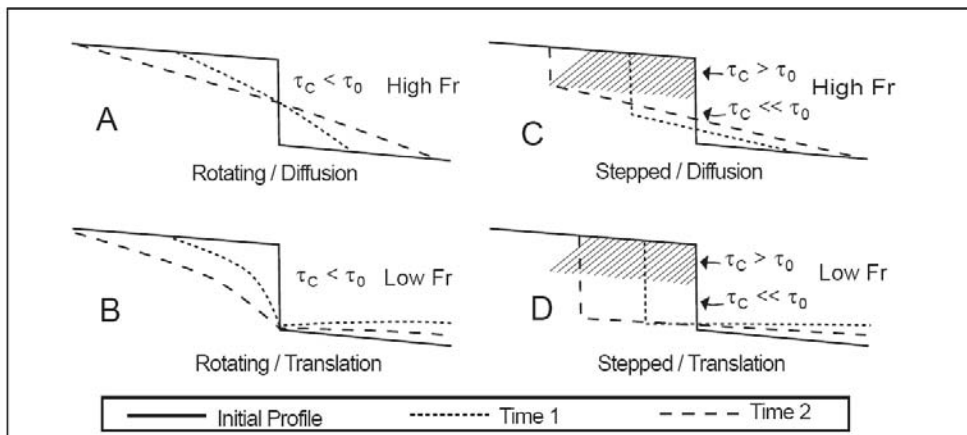


Figure 3. Four potential knickpoint migration patterns proposed by Stewart (2006). Sediment transported downstream is predicted to move via diffusion at high Froude (Fr), and translation at low Fr (from Stewart 2006).

Recent studies of dam removal have centered on low gradient sand-bed, with the exception of the removal of Marmot Dam from the Sandy River in Oregon. Marmot Dam was removed from the Sandy River, a tributary to the Columbia River, on October 19, 2007. Of the 730,000 m³ of sand and gravel stored behind the dam, 100,000 m³ eroded within 48 hours of the dam breaching through a combination of headward and lateral erosion of the unconsolidated banks of the newly incised channel (Major et al. 2008). A knickpoint formed at the coffer-dam, which migrated 500 meters in the 48 hour time period. The combination of a steep channel (0.006 - 0.009 m/m) and a discharge of 30% above the mean annual discharge allowed for rapid incision of the channel into the reservoir sediment deposit.

II. THE PROBLEM

The primary objectives of this study are to better understand (1) the spatial and temporal pattern of reservoir sediment erosion, (2) how a gravel-bed river channel evolves upstream of a dam removal. In light of the literature reviewed, I would like to explore the applicability of channel evolution models to a confined, mountain gravel-bed channel. The Blackfoot is a confined, gravel-bed mountain river which flowed into the reservoir behind Milltown Dam from 1907 to 2008. In the Blackfoot arm of Milltown

Reservoir, a fine (silt-sand) deposit accumulated in the lower portion and a coarse deltaic deposit pro-graded downstream in the upper end of the reservoir (additional study site information is detailed in the following section).

I hypothesize that two distinct phenomena will be seen in the upper and lower Blackfoot reservoir reflecting erosion of two bed sediment types. The fine sediment deposit in the lower reservoir will erode rapidly during the rising limb of the first hydrograph these sediments are exposed to. Investigation of the processes initiated by dam removal in mountain gravel bed rivers may enhance our understanding of how rivers respond to such actions. In the case of dam removal leading to a rapid increase in sediment transport capacity with a large sediment supply, I hypothesize that cross sectional area (A) is the dominant variable changing through the first hydrograph expected to erode reservoir sediments. The comparison of observed water surface elevations (WSE_{obs}) to modeled elevations (WSE_{model}) will be used to reveal the process of reservoir sediment erosion through the 2008 hydrograph.

Furthermore, I would like to explore whether reservoir sediment erosion following dam removal can be described by an exponential decay function, where erosion is a function of time and a decay constant (α). Furthermore, roughness and grain size are the key factors that will control the decay constant (α) in the case of the BFR due to the limited lateral migration potential and existence of features that will contribute to roughness (large woody debris, bedrock, etc.). The data set gathered in this study provides the opportunity to test the ability of an exponential decay function to describe reservoir sediment erosion.

Three different approaches were devised to elucidate the surface textural response and the pattern of reservoir sediment erosion in the BFR following the removal of Milltown Dam: (1) a surface sediment texture analysis, (2) a net morphological change analysis, and (3) an analysis of the upstream response through the 2008 spring runoff. A combined flow modeling and field measurement approach was devised to understand the intra-hydrograph patterns of erosion patterns following the breaching of Milltown Dam. By exploring this method, I hoped to achieve a higher temporal resolution to fill in the gap between the two base flow topographic surveys.

III. STUDY SITE

The Blackfoot River (BFR), MT, is a tributary to the Clark Fork River (CFR) and drains an area of 5,931 km² (Figure 4, Rothrock et al. 1998). The BFR flows through glaciated meadows in the upper watershed, moving downstream through conifer forest and wetlands, open ranch and timbered areas, then between steep forested slopes with some narrow canyon sections in the lower river before it meets the CFR (Figure 5). The lower BFR is naturally confined to a narrow active zone bounded by steep mountains and canyon walls on either side of the channel. Adjacent development and road projects have further confined the river in some reaches.

Milltown Dam was constructed in 1907 at the confluence of the Blackfoot and Clark Fork Rivers. One hundred years later, in March of 2008, the dam was breached allowing the BFR and CFR to flow freely, exposing more than 100 years of accumulated reservoir sediment in the BFR to river erosion. The Milltown project is unprecedented in size and complexity. The 20 m high, 200 m long dam stored approximately 4.6×10^6 m³ of sediment in the reservoir, which filled during a 300-500 year flood in 1908. Mine tailings were transported downstream by the 1908 flood largely filling Milltown reservoir with sediment. Decades later, Milltown Reservoir became the nation's largest EPA Superfund site (EPA 2004). The removal of Milltown Dam has garnered substantial attention because of the presence of contaminated sediments in the Clark Fork arm of Milltown Reservoir, but river erosion of uncontaminated sediments from the Blackfoot arm has provided an opportunity to examine upstream geomorphic response.

In addition to Milltown Dam, a second and smaller dam influenced the lower BFR. The Stimson Dam, 2 km upstream of Milltown Dam was constructed in 1884 to supply power to the adjacent lumber mill, and to catch harvested timber floated down the Blackfoot during log drives (Figures 6, 7). The two dams created distinct backwater effects. The Stimson Dam converted the lower BFR into a reservoir-tailwater reach. Approximately 20 years later the creation of Milltown reservoir flooded the Stimson reservoir (Milltown water surface elevation surpassed the elevation of the Stimson reservoir at high discharge). The net result after 1907 was an increase in the base level at the mouth of the BFR, altering local geomorphology, hydrology and ecology in ways

typically associated with dam construction (e.g., Dynesius and Nilsson 1994, Graf 1999, Ward and Stanford 1995). Furthermore, the human-induced recruitment of large woody debris to the channel from logging operations upstream left a legacy of > 10,000 individual logs in the lower 3 km of the BFR (Figure 6). At the time of the dam removal, the large woody debris was located on the bed and buried in the coarse reservoir sediment deposit in the upper reservoir.

The BFR reservoir provides a unique case as it has two spatially distinct sediment deposits: silt and sand up to 3 m deep in the lower 2000 m of the reservoir (Envirocon 2004), and a coarse gravel-cobble deltaic deposit at the upstream end of the reservoir prograding downstream (typical form of reservoir deltaic sediment deposits, Figure 8). The lower 2500 m of the reservoir is the most confined, with maximum confinement in a 500 m section where a rip-rap bank narrows the channel against a bedrock wall. The staged removal of Milltown dam has lowered the reservoir water surface elevation, and base level controlling the upstream channels, from 2006-2008. In 2006, the reservoir was drawn down by 4m to begin the mechanical removal of contaminated sediment from the CFR arm of the reservoir. The March 2008 breaching of Milltown dam lowered the local base level by an additional 5 m. Studies commissioned by the EPA and state agencies estimated 150,000 – 229,000 m³ of reservoir sediment accumulated in the BFR over the life of the dam (Envirocon 2005).

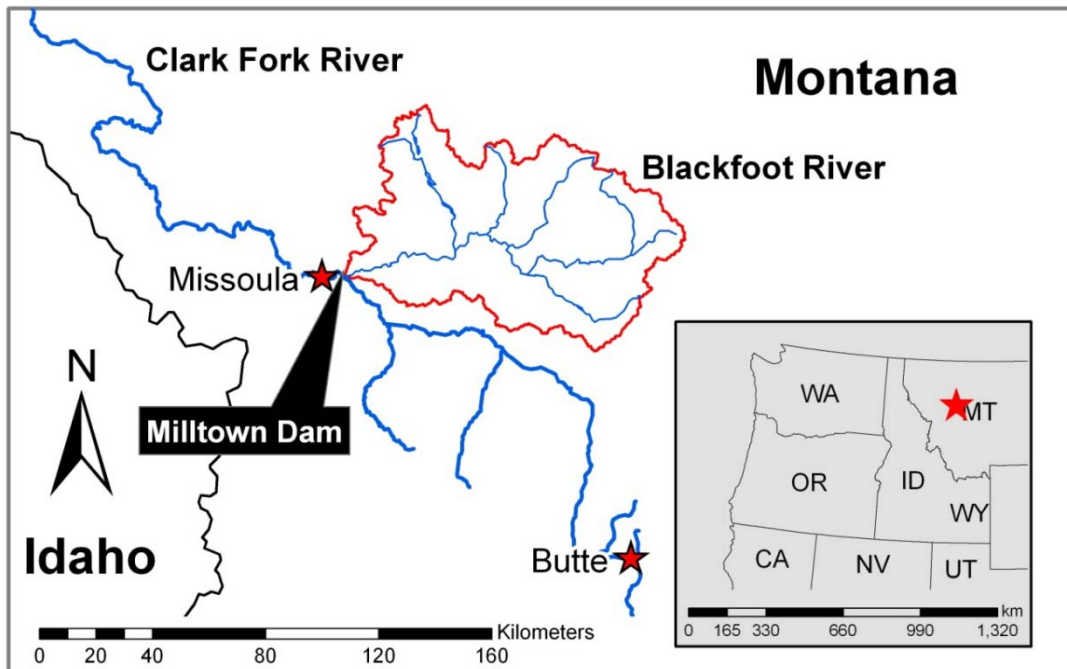


Figure 4. Overview map of the upper Columbia River basin in Western Montana. The Blackfoot watershed is outlined in red and meets the Clark Fork River West of Missoula and immediately upstream of the former site of Milltown Dam.

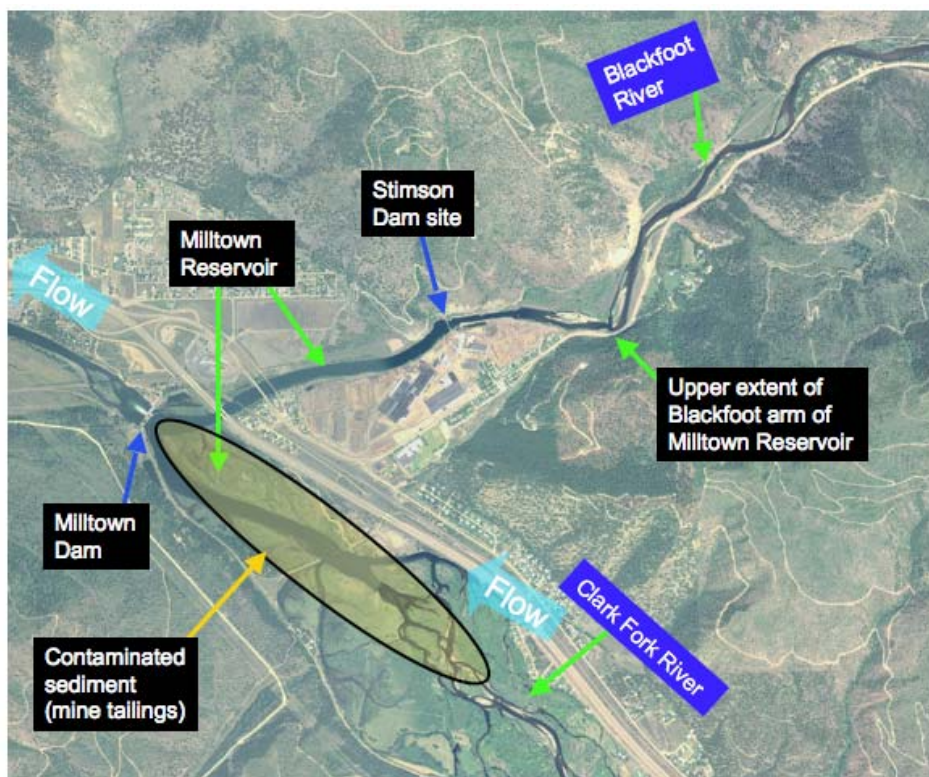


Figure 5. Aerial photo of the Milltown Dam area. Locations of Milltown and Stimson Dams indicated, in addition to location of contaminated sediment removed as a part of superfund remediation program in the Clark Fork arm of Milltown Reservoir. NAIP 2004.



Figure 6. River of wood: cut timber fully covering the Blackfoot River in Bonner adjacent to the Stimson Mill following the 1908 flood (The Montana Collection, Mansfield Library, The University of Montana).

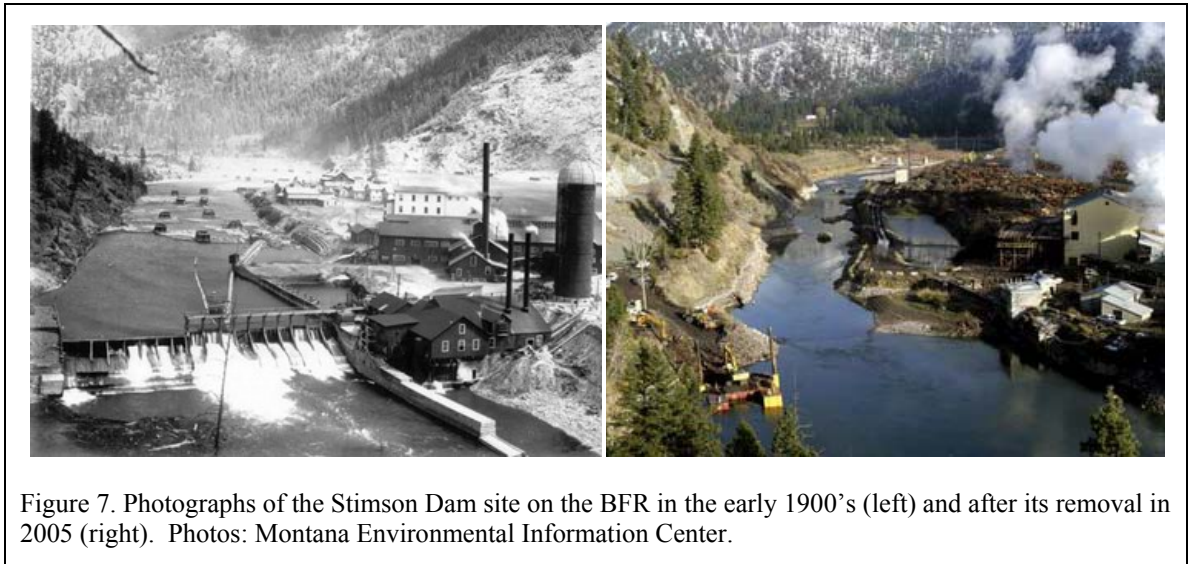


Figure 7. Photographs of the Stimson Dam site on the BFR in the early 1900's (left) and after its removal in 2005 (right). Photos: Montana Environmental Information Center.

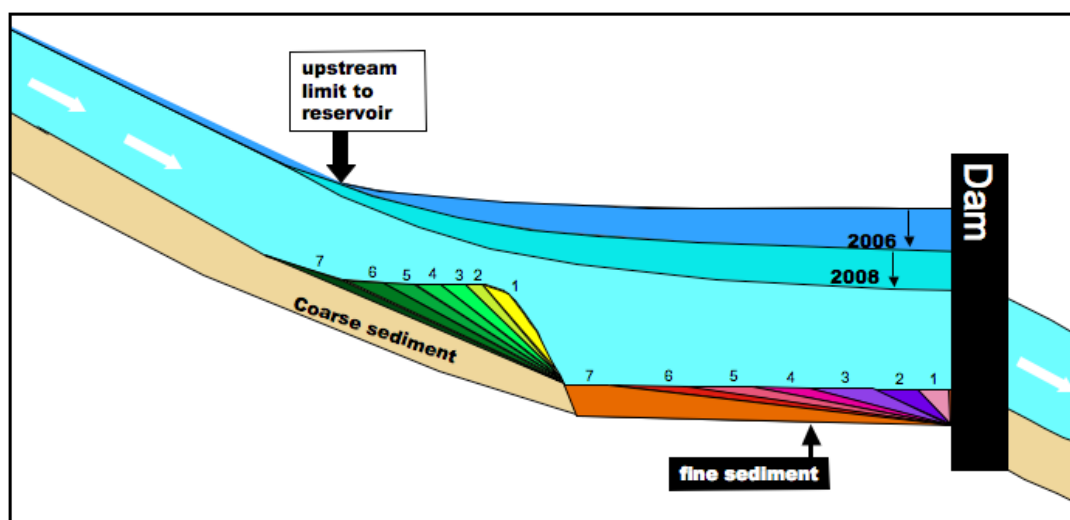


Figure 8. Conceptual diagram of headward erosion of the two distinct reservoir sediment deposits and evolution of water surface elevation from 2004 through the Milltown Dam breach in 2008.

IV. METHODS

To investigate the upstream response of the BFR following the removal of Milltown Dam, three approaches were used: (1) a surface sediment texture analysis, (2) a Spring –Fall 2008 net morphological change analysis, and (3) an analysis of erosion through the 2008 spring runoff. To achieve a higher temporal resolution that fills in the gap between the two base flow topographic surveys, a combined flow modeling and field measurement approach was devised to analyze the pattern of reservoir sediment erosion.

In order to evaluate morphological changes, I measured cross sections throughout the study reach. The BFR-CFR confluence is located in the middle of the Superfund remediation and dam removal site with active construction equipment and crews working at the time this study was done. This made some of the lower river inaccessible for field data collection. The study reach for this project began 900 m upstream of the dam site and extended to 5 km upstream of the dam. Approximately 6 km upstream of the dam, the BFR changes from a gravel-cobble, alternating pool riffle channel to a plane-bed channel with cobbles and boulders. Focusing field efforts on the lower 5km of the BFR was logical given this distinct change in channel type above 6 km and limited time to survey in the Spring of 2008. Cross sections were established in areas that could be surveyed at base-flow ($Q < 17 \text{ m}^3/\text{s}$).

Conventional cross section surveying techniques (total station, survey-grade GPS) were used. Cross sections were surveyed using a Leica Total Station TPS300 and Trimble Real Time Kinematic (RTK) GPS units (R7, 5800 receivers) with maximum horizontal and vertical precision of GPS data of 0.003 – 0.03 m. Seven cross sections were established within the area influenced by Milltown Reservoir in addition to six cross sections upstream (Figure 9). Wade-able cross sections were surveyed in riffles and tail-outs of pools. Boat-based surveys were done in areas that were too deep to wade and had suitable surfaces for setting static line anchors. Cross section data were used to develop longitudinal thalweg profiles.

The response of surface sediment to the change in base level was evaluated using pebble counts or soil cores done in the Spring and Fall of 2008. Wolman 100-particle counts (Wolman 1964) were used where surface texture was $> 2\text{mm}$, and a soil corer in the fine deposit in the lower reservoir where individual grains were smaller than 2 mm (mean D_{50} of 0.2 mm). Bed sediment from the fine reservoir deposit was sieved and the $< .5\text{ mm}$ fraction was analyzed using a laser diffractometer (Malvern Mastersizer particle size analyzer). Grain size data were used to assess changes in bed surface texture and grain mobility throughout the study reach at a variety of discharges. Grain mobility was calculated for the two reservoir deposits: the fine deposit in the lower 1.8 km, and the coarse deposit in the upper reservoir. The 2003 Wilcock and Crowe sediment transport function in the Bedload Assessment in Gravel-bedded Streams (BAGS) software was used (Pitlick et al. 2007). I used BAGS to assess grain mobility throughout the study reach, to develop an understanding of where and when particles started moving. BAGS calculates sediment transport rates and incipient motion using six substrate and surface-based transport models. The Wilcock and Crowe 2003 surface-based equation was selected due to its ability to model transport of both fine ($< 2\text{mm}$) and coarse sediment. Among the six models in BAGS, Wilcock and Crowe 2003 best represents the influence of sand on gravel transport (Wilcock et al. 2001, Wilcock and Crowe 2003). Reach-average grain size data were combined by averaging percent-finer-than intervals from individual grain size distributions.

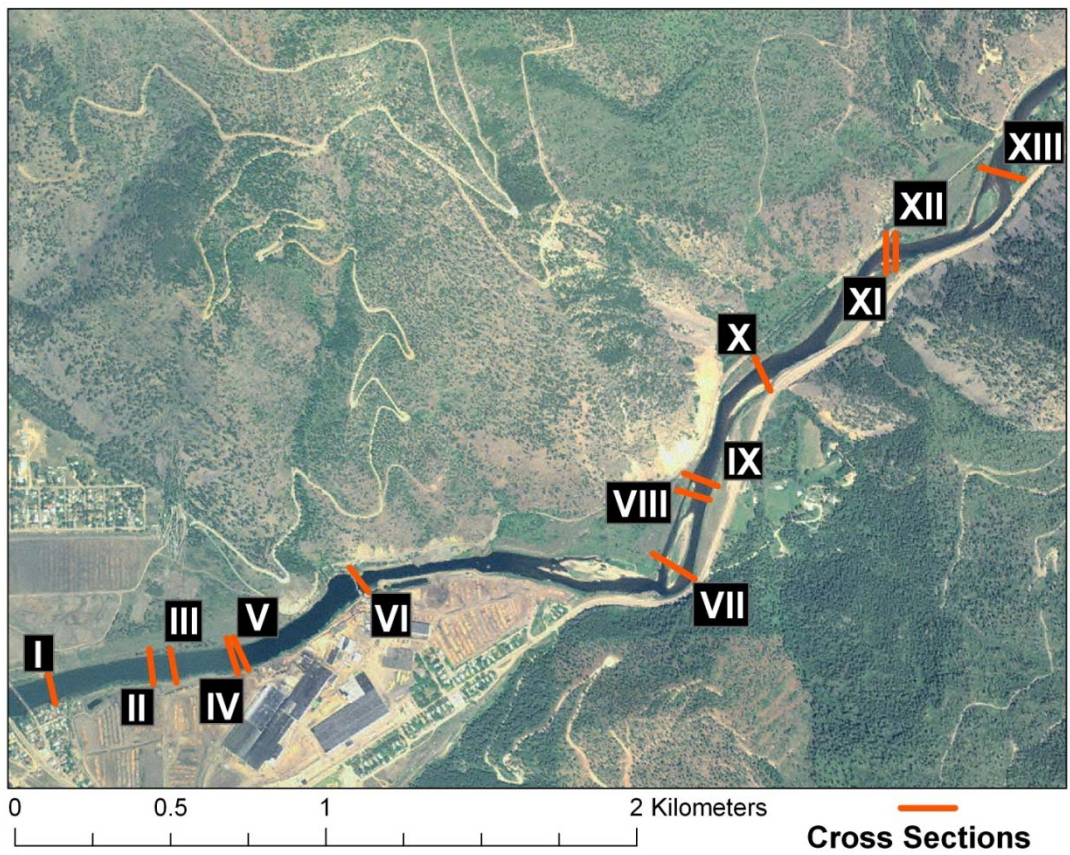


Figure 9. 2004 USDA NAIP aerial photo of the study area. Cross section locations denoted respectively by red lines.

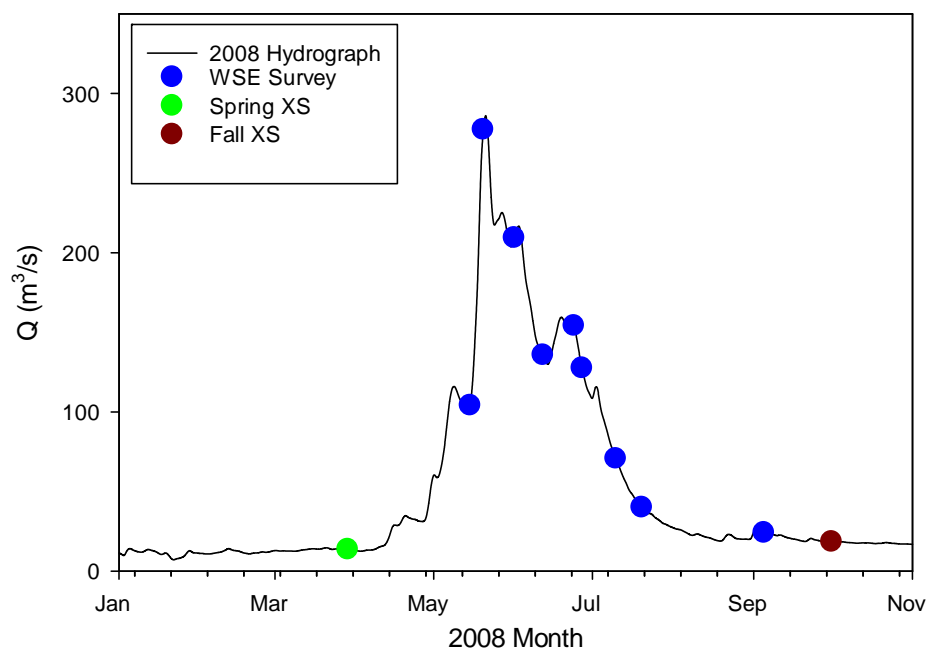


Figure 10. 2008 hydrograph for the Blackfoot River. Closed points show water surface elevation (WSE) survey dates, and open dots show repeat cross section survey dates at base flow.

Water Surface Elevation (WSE) Analysis

In order to evaluate spatial and temporal patterns of reservoir sediment erosion, an approach using flow modeling and water surface profile surveys was used. Water surface profiles were surveyed in the lower 4 km of the BFR throughout the 2008 Spring runoff. RTK-GPS units were used to survey water surface profiles at both left and right wetted edges of the channel when possible (Figure 10). This analysis was performed to supplement the morphological change analysis from Spring 2008 to Fall 2008. The proxy for erosion using this approach is the deviation of a modeled water surface elevation from the observed elevation, from which local scour or deposition can be calculated (Figure 11).

In order for the analysis based on observed water surface elevations to be applied to erosion, I reviewed the relationship between channel height and other physical parameters for a given channel. I used the discharge form of the Manning equation:

$$Q = \frac{Ah^{2/3}S^{1/2}}{n} \quad (1)$$

where Q is discharge (m^3/s), and is a function of flow area, A (m^2); average depth, h (m); slope, S (m/m); and roughness, Manning's n , (dimensionless). By rearranging equation (1), h can be solved for:

$$h = \left[\frac{Qn}{AS^{1/2}} \right]^{3/2} \quad (2)$$

Channel height (h in relation to a datum or WSE) can fluctuate due to changes in discharge, slope, roughness, and area. Based on equation 2, three potentially dynamic variables, n , A , and S control h . In order for changes in WSE from the modeled WSE to be used in analyzing the pattern of erosion the primary dynamic variable would have to be A . Changes in WSE in a reach where erosion of reservoir sediments is expected, and confinement of the channel would prevent widening, degradation would conceivably cause an increase in A and a lowering of WSE.

HEC-RAS Modeling

HEC-RAS is used for 1-dimensional hydraulic modeling of natural and altered systems (HEC 2008). The purpose of using HEC-RAS in this study was to evaluate the

temporal and spatial patterns of erosion in the BFR. The HEC-RAS Steady Flow Analysis tool was employed to model steady flow through input channel geometry and boundary conditions at a variety of discharges in the 2008 hydrograph taken from the USGS station Blackfoot River near Bonner MT (Gauge #1234000, Table 1). A calibration process using both known water surface elevations at pre-erosion discharges, and an analysis of results as a percentage of mean flow depth was done before using output water surface elevations for analysis. These modeled data were then compared to observed WSE through the 2008 hydrograph. The subsequent analyses of the deviations of observed WSE from the modeled WSE ($\Delta WSE = WSE_{obs} - WSE_{model}$) through space and time was performed to reveal the process of sediment erosion from Spring 2008 to Fall 2008.

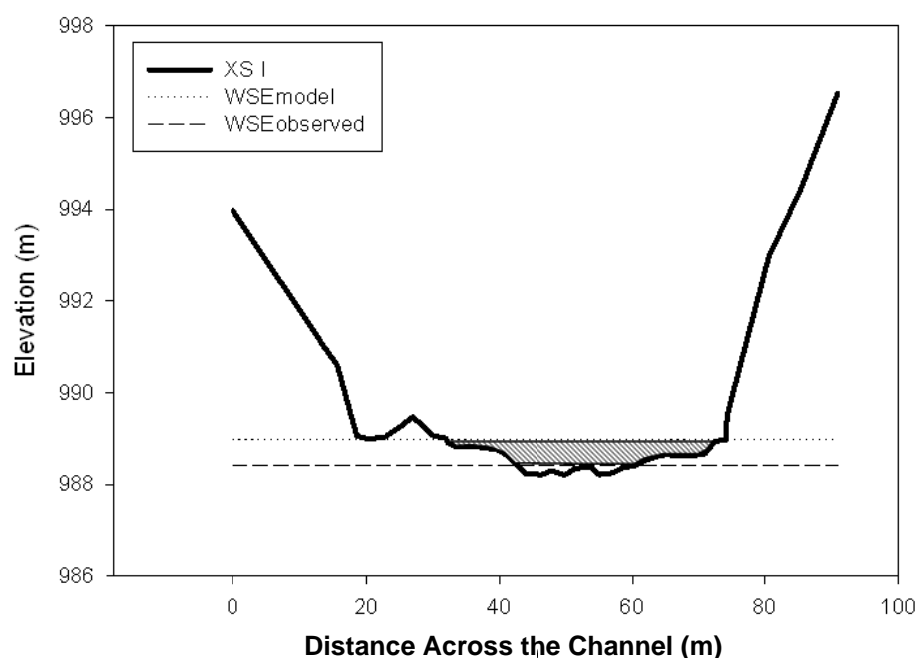


Figure 11. Pre-erosion cross sectional topography for Cross Section I. Dotted line is WSE_{model} , dashed line is WSE_{obs} . Erosion of the shaded cross sectional area between the two lines is the hypothesized mechanism causing a deviation between the observed and modeled water surface elevations.

ΔWSE was later used to calculate change in area (ΔA , or net erosion at a cross section) and then used in the spatial and temporal analyses of reservoir sediment erosion through the hydrograph.

The model river network was set up using the HEC GeoRAS 4.1.1 add-in for ArcGIS 9.3 and split into two separate reaches, cross section I to VI and cross section VII to X. Cross sections XI to XIII were upstream of the extent of repeat water surface

elevation surveys, and therefore not used in the HEC-RAS analysis. The model river network represents the lower 3.8 km of the BFR. From Arc, the model network was exported and brought into the HEC-RAS interface. Expansion and contraction coefficients were set to recommended values of 0.1 and 0.3 respectively (HEC 2008). The model was calibrated to measured pre-erosion WSEs at base-flow when the Spring 2008 survey was done using n values within the range expected for gravel-bed rivers (Table 1). Flows ranging from 12 – 277 m³/s were routed through the network using the steady flow analysis tool in order to model WSE at each cross section. Downstream boundary conditions were set to known pre-erosion WSEs at Spring 2008 base-flow.

To evaluate changes in channel width, HEC-RAS was used to model a 1.5 year return interval flow (187 m³/s) through both Spring and Fall 2008 model networks. Channel widening is of interest as the literature depicts widening as a common theoretical and observed upstream response to dam removal.

Model Parameters		
<i>Cross Section</i>	<i>Distance Upstream of Milltown Dam (m)</i>	HEC-RAS <i>n</i>
*XIII	4877	
*XII	4389	
*XI	4359	
X	3784	0.026
IX	3367	0.03
VIII	3320	0.04
VII	3076	0.06
VI	2014	0.065
V	1554	0.02
IV	1528	0.02
III	1330	0.03
II	1260	0.02
I	935	0.035

Table 1. Cross sections and distances upstream of Milltown Dam. Manning's n values input into HEC-RAS modeling framework.

*Cross section upstream of water surface elevation analysis reach.

Date	Q (m ³ /s)
3/11/2008	13
3/17/2008	14
3/23/2008	14
3/29/2008	14
3/31/2008	13
4/1/2008	13
4/9/2008	14
4/12/2008	16
5/15/2008	104
5/20/2008	277
6/1/2008	209
6/12/2008	136
6/24/2008	154
6/27/2008	127
7/10/2008	71
7/20/2008	40
9/5/2008	24

Table 2. Discharges modeled through the Spring 2008 topography from USGS Blackfoot River near Bonner Station (#12340000).

Exponential Decay

Estimates of the temporal pattern of reservoir sediment erosion were used to test the applicability of an exponential decay function. Exponential decay functions are used to describe decay of a substance or material at a rate proportional to the initial quantity, based on time, and a decay constant. In the case of modeling sediment release following dam removal, the rate of decay of an initial quantity of reservoir sediment (or erosion) is hypothesized to follow an exponential decay as a function of a decay constant (α); time (t); and the initial volume of sediment (V_i). Analyzing the reservoir sediment erosion and fitting it to an exponential decay function may help address some key questions. For example, it is unknown what influences the decay constant (α): grain size, roughness, or channel geometry.

At any given time, t , the change in the volume of sediment ($\partial V/\partial t$) is a function of α , a decay constant and V_i , the initial volume of sediment such that (Q_s , the flux of sediment out of the reach, m^3/t , at a given time, t):

$$Q_s = \frac{\partial V}{\partial t} = -\alpha V = -\alpha V_i e^{-\alpha t} \quad (3)$$

The decay constant, α , can also be viewed as a sediment transport constant, as the decay in this case is erosion (m^3).

V. RESULTS

In the first spring runoff following the removal of Milltown Dam, the fine sediment accumulated in the lower 1.8 km of the BFR was largely evacuated. The river incised into the coarse sediment deposit and transported gravel and cobbles to the lower reservoir and out of the study reach once the critical discharge was reached. In the lower reservoir area, gravel deposited as the BFR flushed out fines and re-established its channel while being supplied with coarse material. This reach developed alternating point bars with a series of mid channel bars (Figure 12).

Sediment Surface Texture and Mobility

Surface sediment texture coarsened by two orders of magnitude in the lower 1.8 km of the reservoir, and generally became finer upstream (Figure 13-17). The largest changes in grain size occurred in the lower reservoir, where median grain size increased by 10 to > 10,000 percent (Figure 16). Gravel and cobble (D_{50} 13-60 mm) deposited after the silt and sand deposit was evacuated from the lower reservoir area. Furthermore, sediment patches sampled at ≥ 4 km upstream showed little change from Spring to Fall 2008 (Figure 15).

The grain mobility analysis performed in BAGS shows that the silt-sand deposit was mobile at virtually all discharges. The fine deposit was likely scoured out of the study reach well before the peak discharge on May 20. Upstream, the coarse bed was mobilized at discharges ranging from 32 - 369 m^3/s (Figure 18).

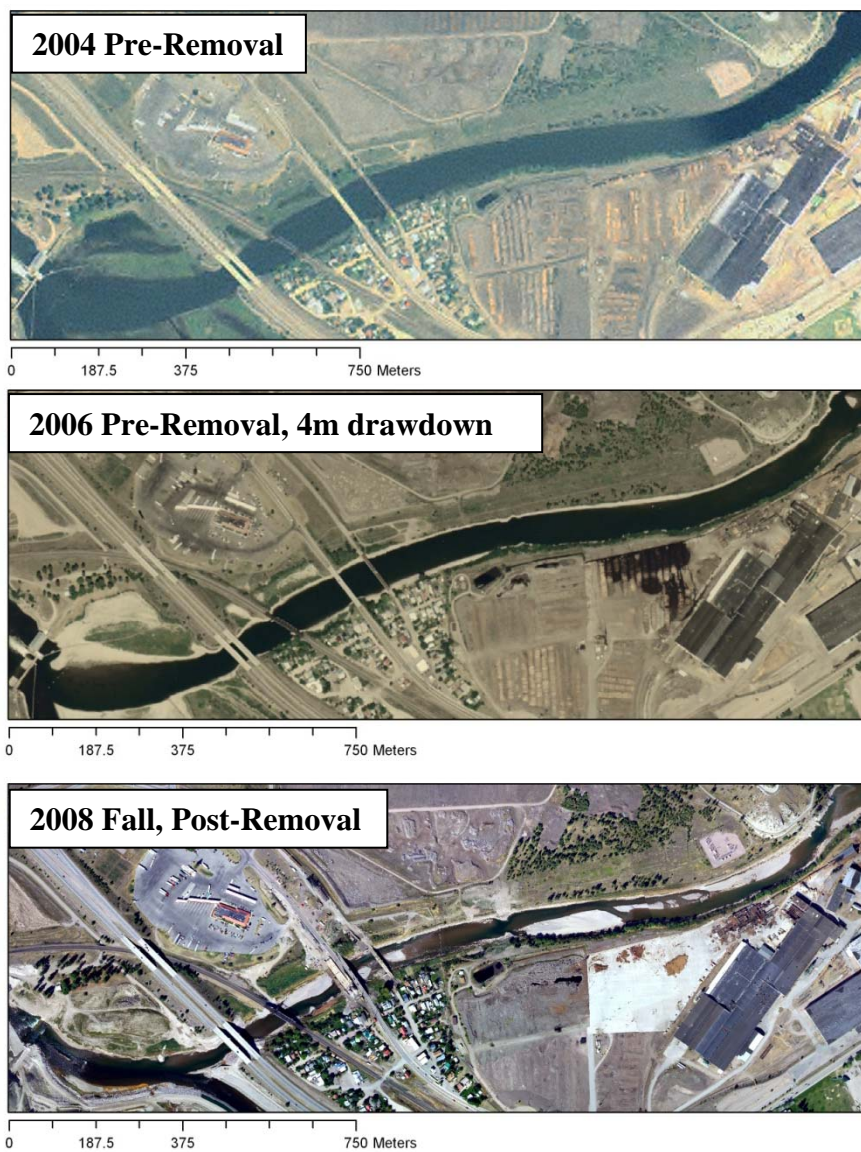


Figure 12. The lower 2 km of BFR in 2004, 2006 and 2008. The Milltown Dam site is located in the lower left of the image. NAIP 2004, 2006. Flow is from right to left.

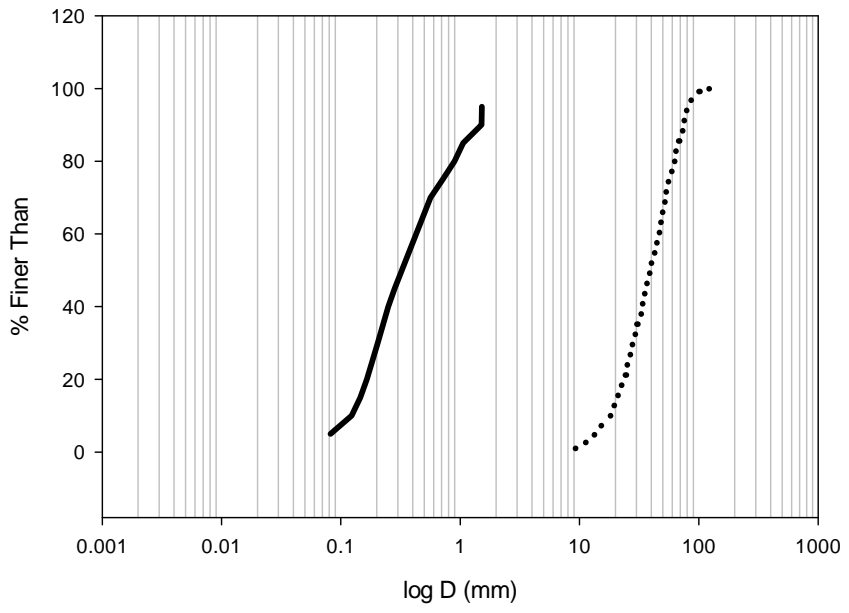


Figure 13. Mean surface textures for Spring 2008 (solid line) and Fall 2008 (dotted line) for the fine sediment reservoir deposit in the lower 1.8 km (XS I – V) of the study reach composed of silt and sand.

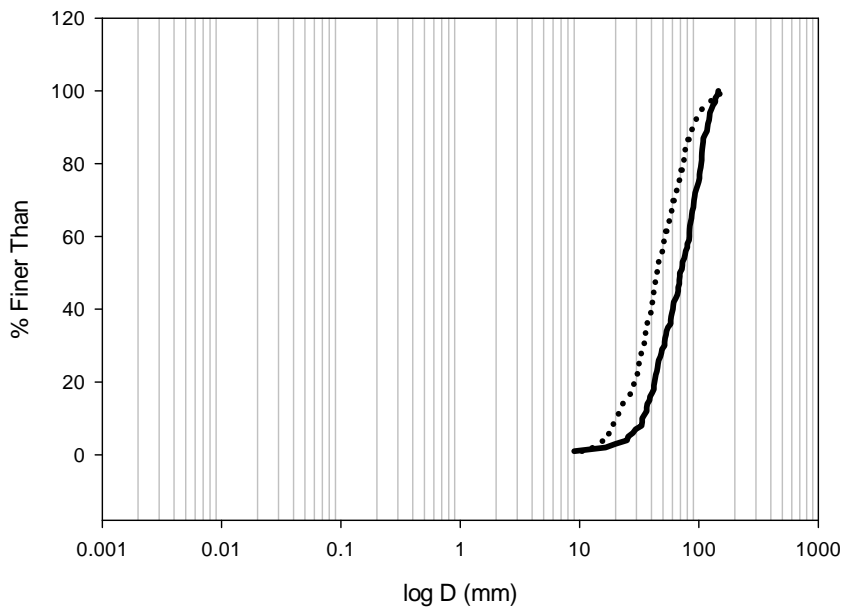


Figure 14. Mean surface textures for Spring 2008 (solid line) and Fall 2008 (dotted line) in a zone of local upstream fining (cross sections VII and VIII, 3.0- 3.8 km upstream of Milltown Dam).

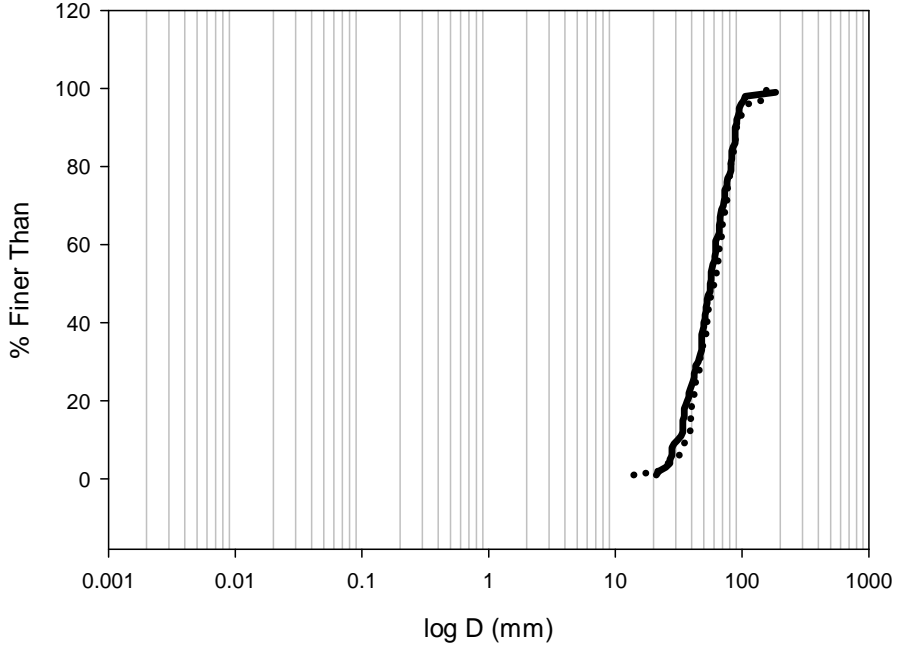


Figure 15. Mean surface textures for Spring 2008 (solid line) and Fall 2008 (dotted line) 4.4 km (XS XII) upstream of the dam site, where surface texture showed little response.

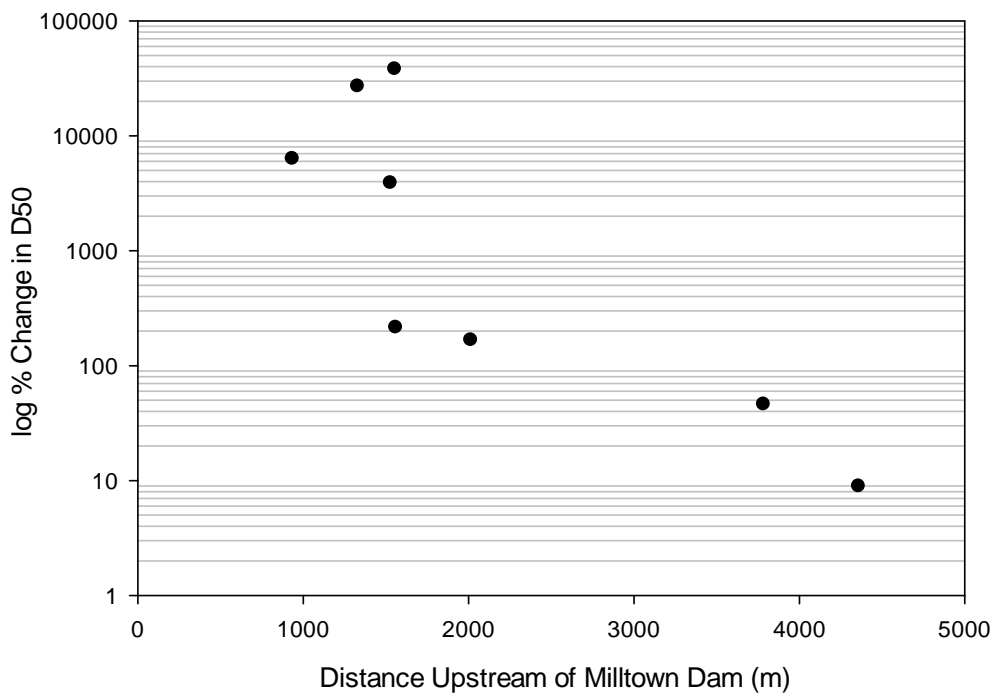


Figure 16. Percent change in the median grain size illustrating the coarsening of the bed in the lower reservoir. Fining (negative values) not depicted in this log-scale figure.

Net Morphological Change Analysis

Although no knickpoint was observed, the comparisons of pre- and post-removal cross section data show that an incisional pulse extended 4.5 km upstream of the Milltown Dam site (and 2 km above of the upper extent of the reservoir, Figure 19, 20). It is possible that a knickpoint did develop, but was not detected by the methods employed in this study. Bed lowering was found from the lower reservoir 4.5km upstream, with the exception of local net aggradation at 1.5 km where a pool filled. The maximum bed lowering occurred at cross section VII (3 km) where a vegetated bar was eroded, the channel incised and the main channel thalweg migrated 80 m across the active zone (Figures 21, 23). Due to the confined nature of the lower BFR, minimal channel widening occurred based on the analysis of channel widths at a 1.5 year flood discharge. Alternatively, the mean change in channel width observed was narrowing by 3.1 m. Maximum narrowing of 16.8 m occurred at cross section VII, 3 km upstream of the dam site (Figure 22). The comparison of pre-erosion (Spring 2008) and Fall 2008 cross sectional topography reveals the net change in cross sectional area. Based on the spring and Fall 2008 topographic surveys, I estimated that net volumetric erosion from the 2008 runoff was 150,000 m³.

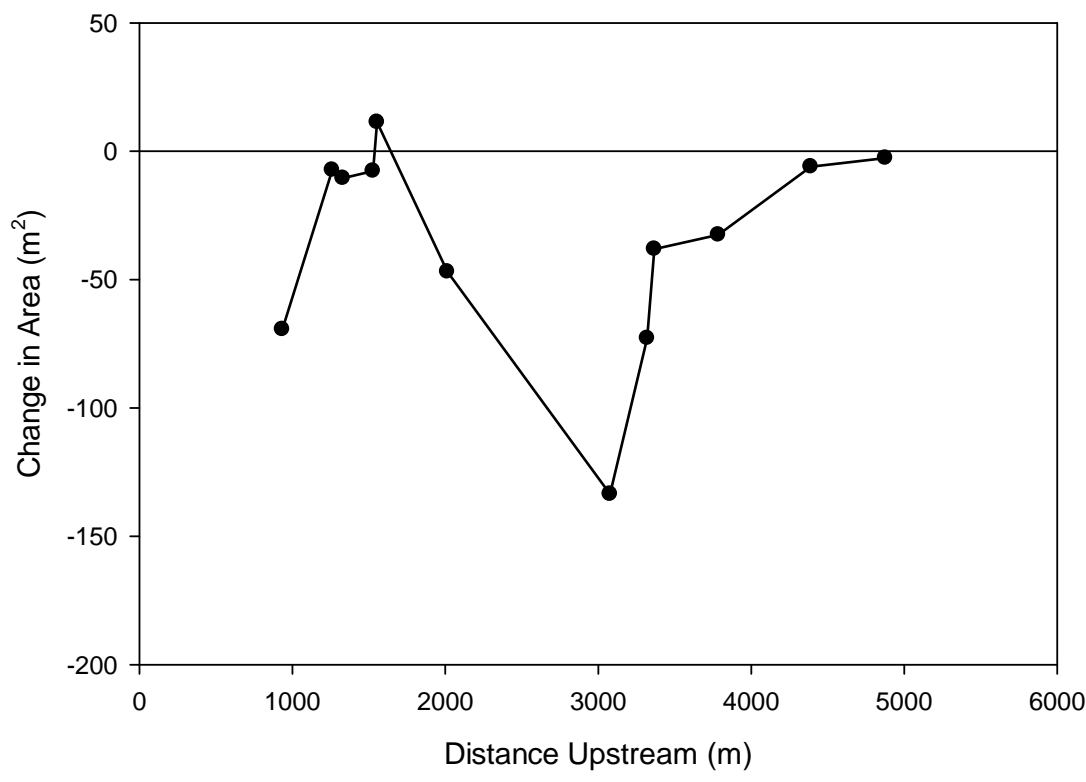


Figure 19. Spring-Fall 2008 change in cross sectional area (based on repeat cross section surveys) shown versus distance upstream of Milltown Dam (x). Negative and positive changes in cross sectional area show local scour (-) and deposition (+). The geomorphic response extended 5 km upstream of the dam, and 2 km beyond the upstream limit to the reservoir.

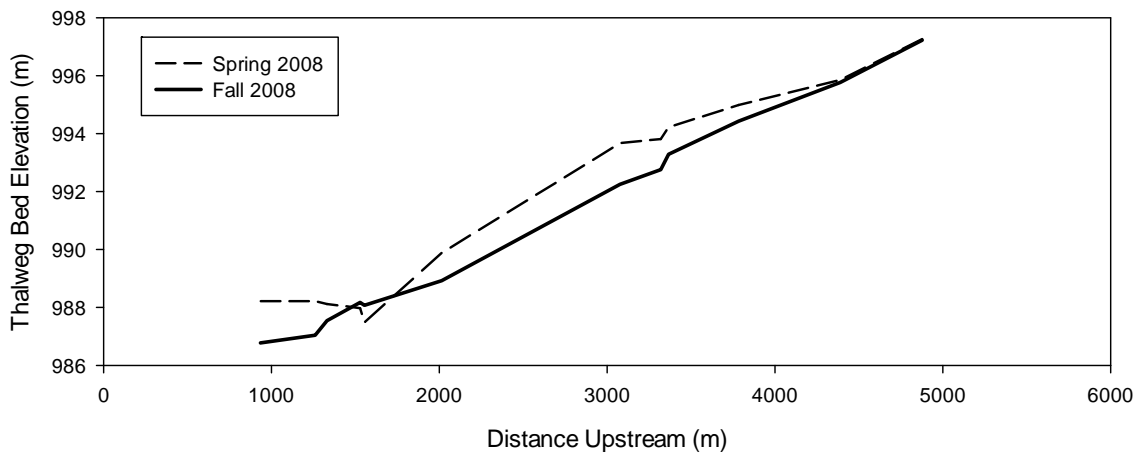


Figure 20. Longitudinal profile showing Spring and Fall 2008 bed elevations based on repeat cross section surveys. Headward erosion extended 4.5 km upstream.

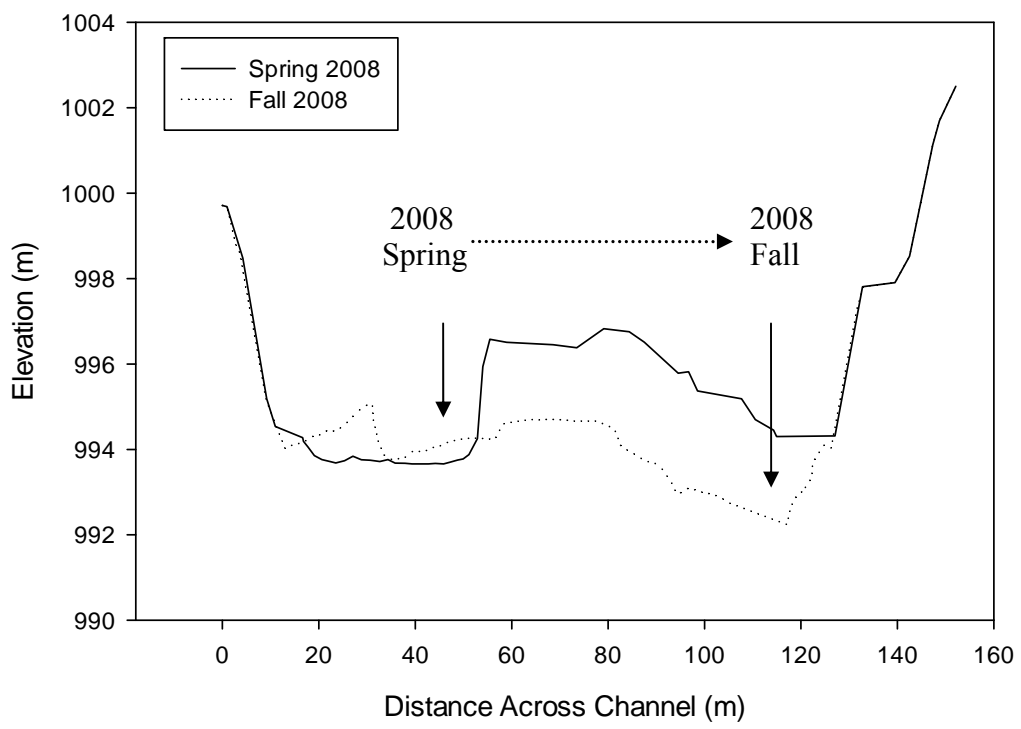


Figure 21. Spring 2008 (solid line) and Fall 2008 (dotted line) cross sections shown for Cross section VII. At this site, 3 km upstream of the dam, bed lowering of up to 2m was observed. The thalweg migrated 80 m across the active channel.

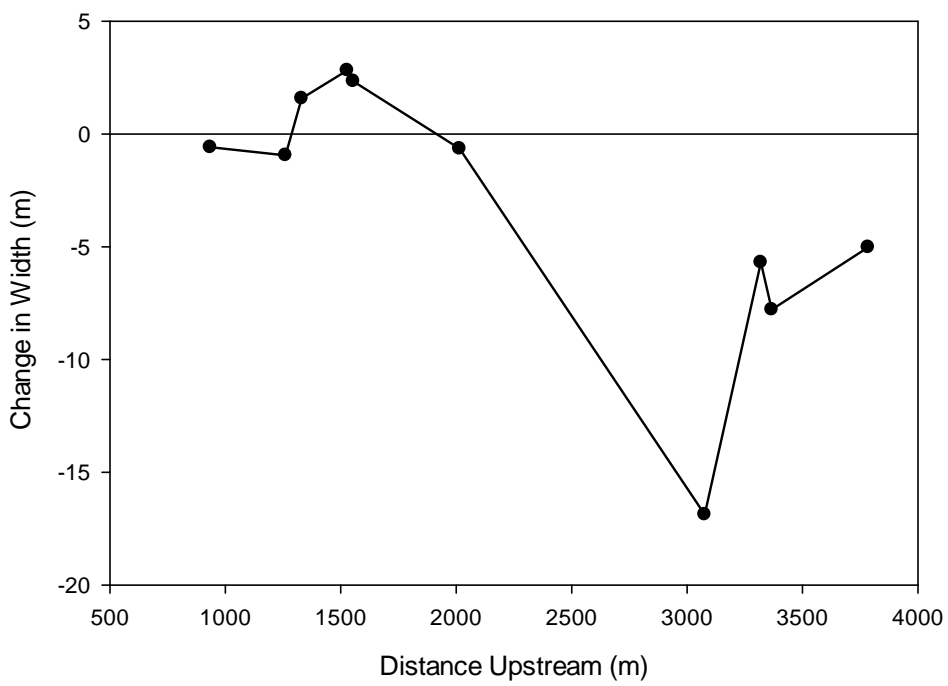


Figure 22. Distance upstream of Milltown Dam plotted against change in channel width from Spring to Fall 2008 at 1.5 year return interval flow ($187 \text{ m}^3/\text{s}$).

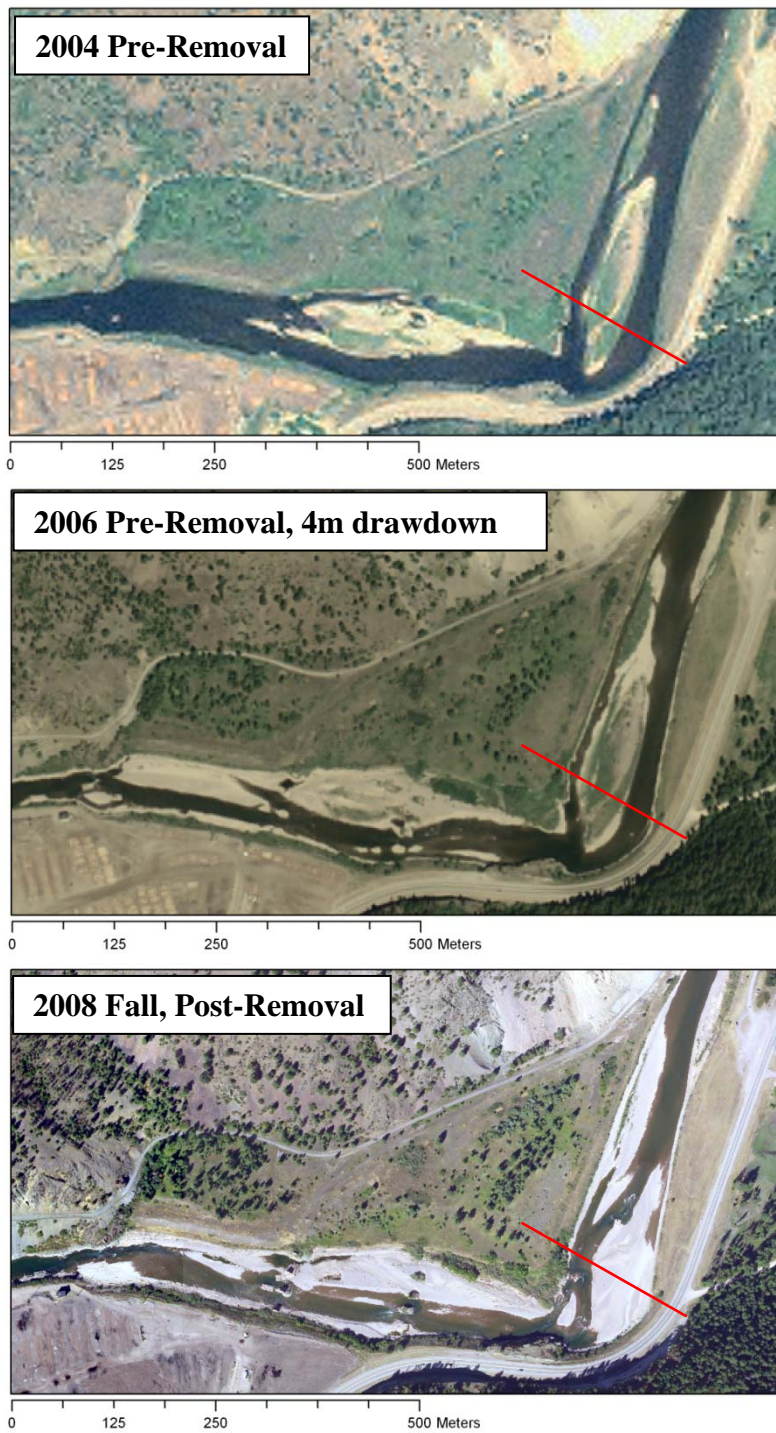


Figure 23. Time series aerial photography of the reach located 2 – 3.5km upstream of Milltown Dam. NAIP 2004, 2006. Red line is cross section VII—downstream end of the vegetated bar that was eroded in the Spring 2008 runoff. Flow is from top right to bottom left.

Δ WSE Analysis

Figure 24 shows the spatial and temporal patterns of reservoir sediment erosion using the flow modeling method. The pre-erosion condition was effectively modeled and shown using the WSE analysis. The Δ WSE approach shows that the entire modeled 3.7 km reach eroded at some point. It appears that both erosion and deposition happened concurrently at different locations in time and space. Figure 25 shows that modeled volumetric erosion occurred rapidly during the rising limb of the hydrograph, peaking close to June 11. This point of maximum modeled bed lowering occurred just after the peak of the 2008 hydrograph. The flow modeling approach developed to quantify reservoir sediment erosion throughout the 2008 hydrograph showed a similar spatial pattern of erosion seen in the pre-erosion (Spring) and Fall base-flow morphological comparison (Figure 19, 24). At the log jam complex 1.5 km upstream, the Δ WSE failed to capture the net aggradation, as the increase in roughness caused by the log jams was not modeled in HEC-RAS. The temporal pattern of erosion shows that significantly more erosion may have occurred than can be captured by the net volumetric change. The HEC-RAS results indicate that the maximum erosion occurred on June 1, eleven days after the peak in the hydrograph, by which time a total of 260,000 m³ had been eroded from the lower 4.5 km of the BFR (Table 2, Figure 25). After the BFR returned to base-flow in the fall, the net volumetric change was 72,000 m³ as of 9/5/08 (Q= 24 m³/s). Based on the flow modeling approach, the peak erosion of 260,000 m³ on June 1 represents 115% - 174% of the initial volume of reservoir sediment stored in the BFR arm of Milltown Reservoir (Envirocon 2005). Longitudinal profiles derived from water surface profiles surveyed are shown in Figure 26, for comparison with the pre-removal reservoir WSE.

The 8 m base level reduction is evident in the evolution of the water surface through the 2008 hydrograph.

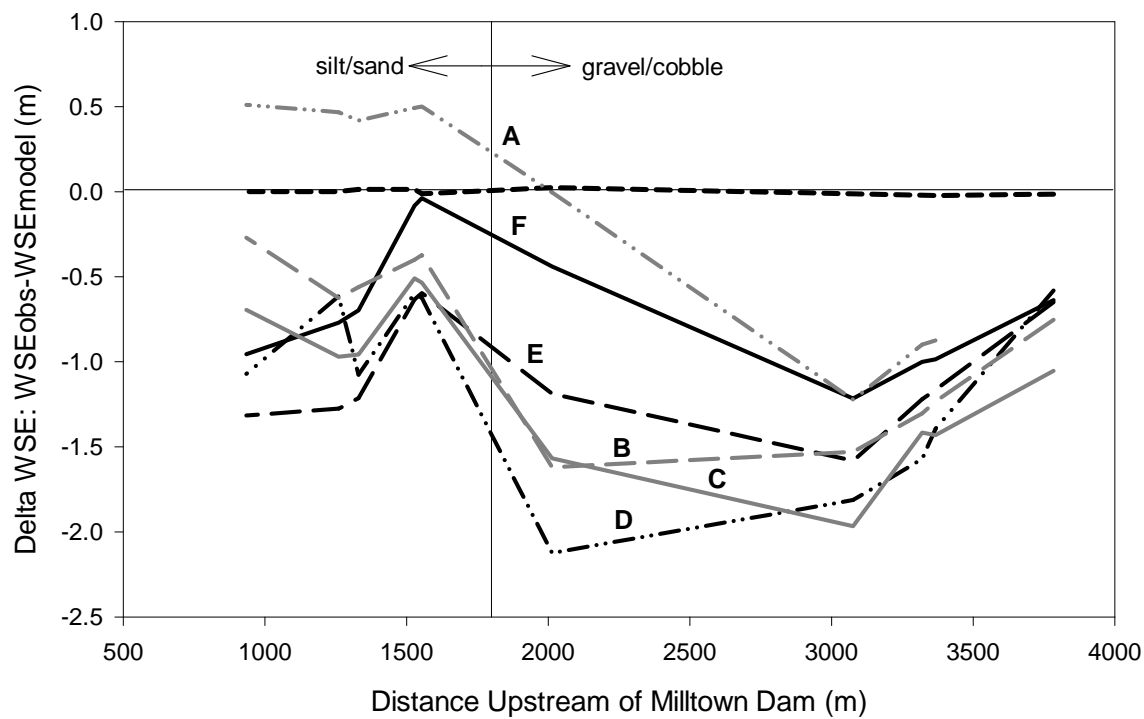


Figure 24. ΔWSE curves throughout the hydrograph plotted against distance upstream. The bold dashed calibration line shows WSE_{model} fits the WSE_{obs} at Spring 2008 baseflow. A, the gray dash-dotted line, is the earliest date and associated discharge modeled. F, the solid black line, is the latest discharge modeled, from 9/5/08. Note the vertical line representing the gravel-sand transition in the Spring of 2008.

Date, Q (m ³ /s)	
---	Calibration
F	9/5/08, 24.1
E	7/10/08, 70.8
D	6/27/08, 127.4
C	6/1/08, 209.3
B	5/20/08, 277.2
A	5/15/08, 103.9

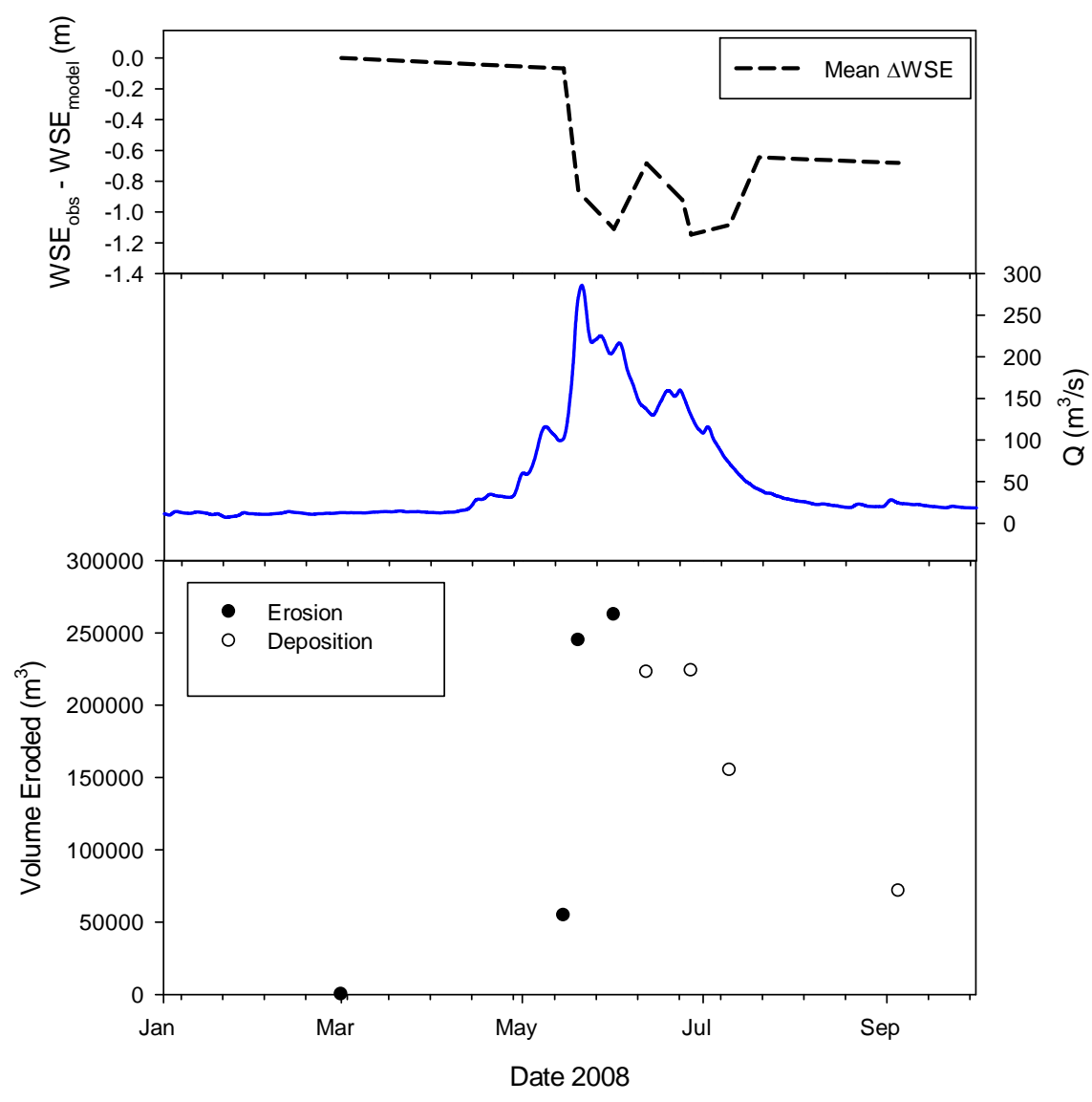


Figure 25. Mean ΔWSE , 2008 hydrograph and volumetric erosion through the hydrograph. Solid points show increasing erosion, and white points show sediment deposition during the falling limb of the hydrograph.

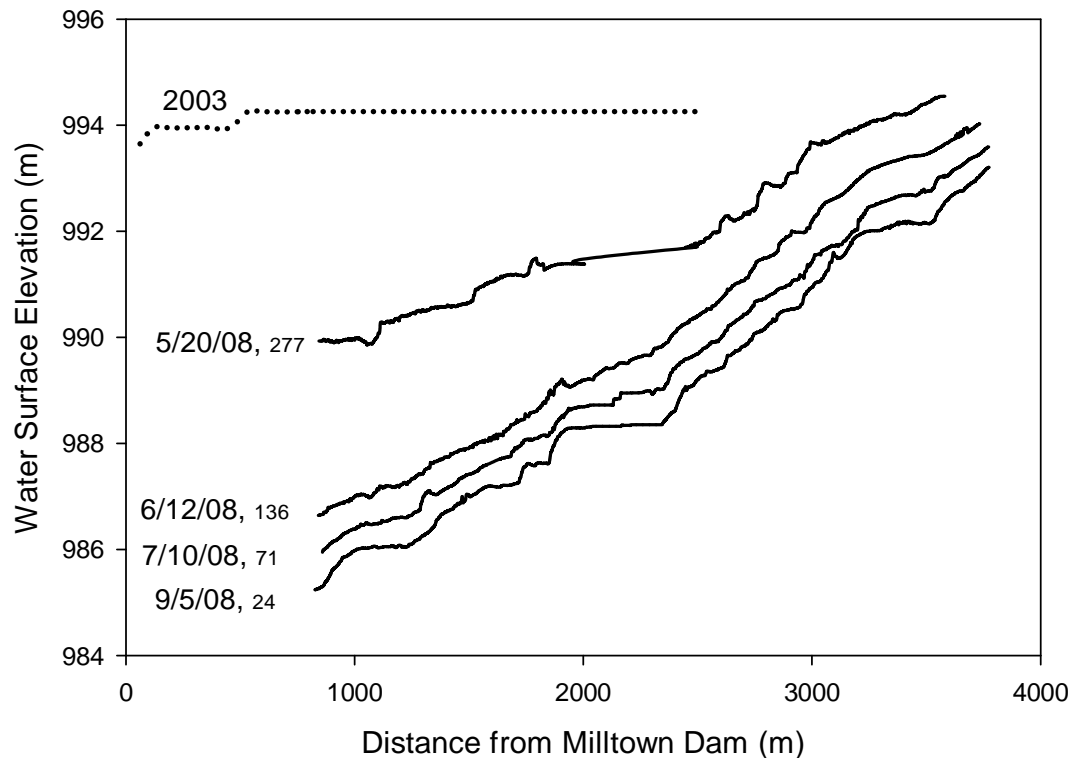


Figure 26. Water surface profiles throughout the 2008 hydrograph shown with the 2003 reservoir water surface. Dates for water surface profiles surveyed in 2008 listed with discharge (m^3/s).

Exponential Decay

The exponential decay hypothesis was tested by fitting two exponential decay functions to match volumetric erosion estimates. Decay curves that fit ΔWSE and net morphological change analysis erosion estimates had α values of 0.06 and 0.0058 respectively (Figure 27). First, to show the peak erosion of 260,000 m^3 as of June 11, 2008, an exponential decay curve was fit to the modeled data (before deposition occurred) using an α value of 0.06. This is a rapid rate of decay in comparison to the more gradual erosion shown by the curve fitted to the net morphological change of 150,000 m^3 . Fitting the decay functions to these data shows a range of predictions for the full evacuation of the stored reservoir sediment in the BFR: 2 - 17 months.

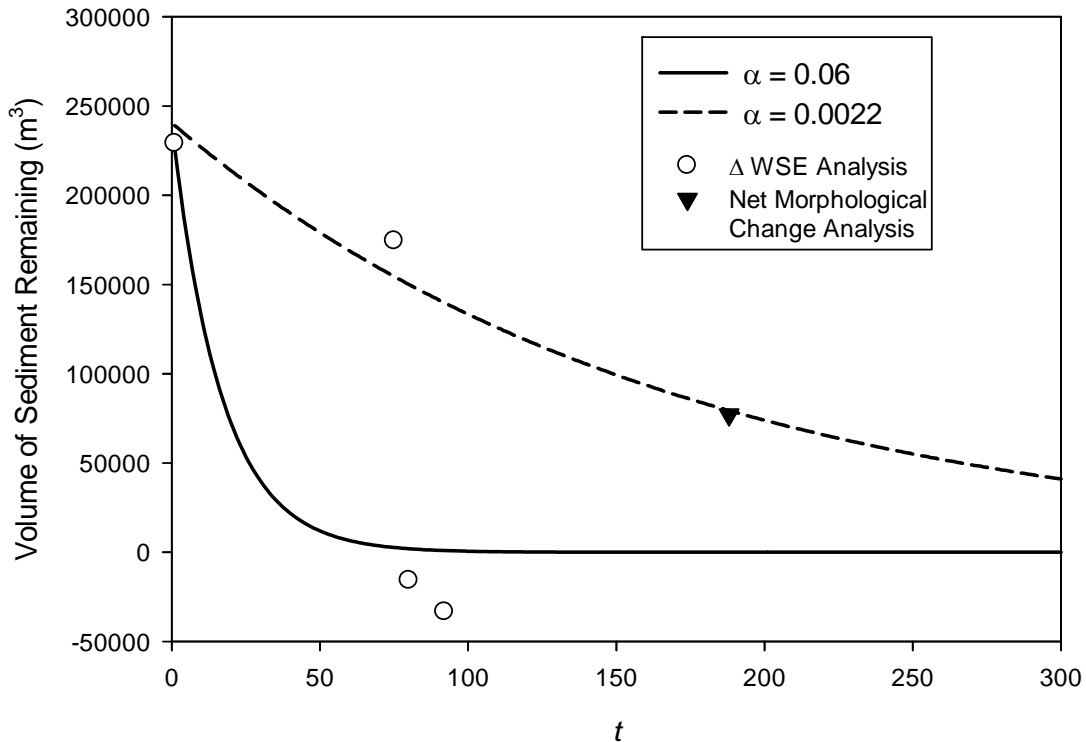


Figure 27. Exponential decay functions fit through the Δ WSE and net morphological change estimates of volumetric erosion. The pattern of erosion in the time period examined does not appear to exponential. However, subsequent years may prove that erosion may show an exponential decay pattern.

Decay Constant α	% Eroded (t, days)	
	50%	95%
0.0059	118	518
0.06	12	65

Table 3. Estimated time (t , days) for the reservoir sediment deposit to decay using three different values for α , ranging from < 3 months to several years.

VI. SENSITIVITY ANALYSIS

In order to evaluate the appropriateness of using a Δ WSE analysis to detect local scour or aggradation, a sensitivity analysis was performed to evaluate the potential contribution of changes in Manning's n and S (slope) to the Δ WSE calculations. The main purpose of the sensitivity test was to determine how much of Δ WSE could be accounted for by changes in S and n without eroding or depositing sediment to drive changes in cross sectional area (A). For assessing the sensitivity of WSE to slope, repeat calculations were performed using equation (2), holding all other variables fixed. To test WSE sensitivity to roughness, repeat runs of the Steady Flow Analysis in HEC-RAS was done. The parameters S and n were incrementally varied from 2%-100%, and the resulting change in h was calculated as a percentage of Δ WSE for a given cross section.

The sensitivity analysis shows that WSE is not sensitive to changes in roughness, and slightly more sensitive to changes in slope. A doubling of slope contributed 20% Δ WSE for most stations evaluated, and up to 50% for only a few (Figure 28). Doubling n could only account for a maximum of ~10% Δ WSE. Although the sensitivity test results illustrate the complexity of using WSE changes to assess bed sediment dynamics, they indicate that changes in S and n cannot solely explain the fluctuations in WSE.

As changes in roughness is shown to have a minimal effect on the WSE analysis results, the potential dilution of the results by changes in slope were computed at two discharges (24 and 127 m³/s) in order to express the accuracy of the Δ WSE. Figure 29 illustrates the potential contribution of a 100% increase in slope to the Δ WSE analysis. Generally, a doubling of slope could only explain a fraction of the total deviation

between observed and modeled WSE. However, at cross section IV, a 100% increase in slope actually overwhelms the effect. Repeat topographic surveys showed that the channel aggraded at cross section IV.

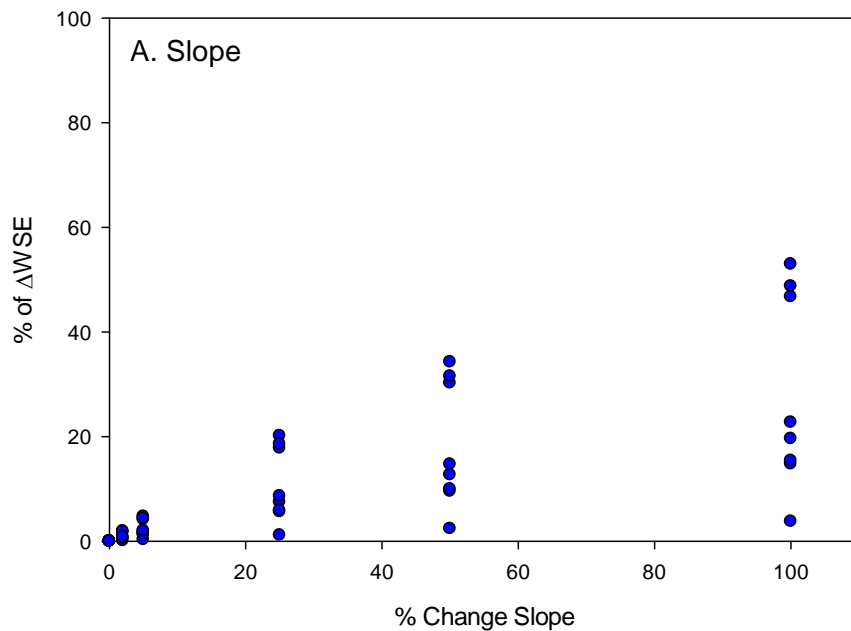
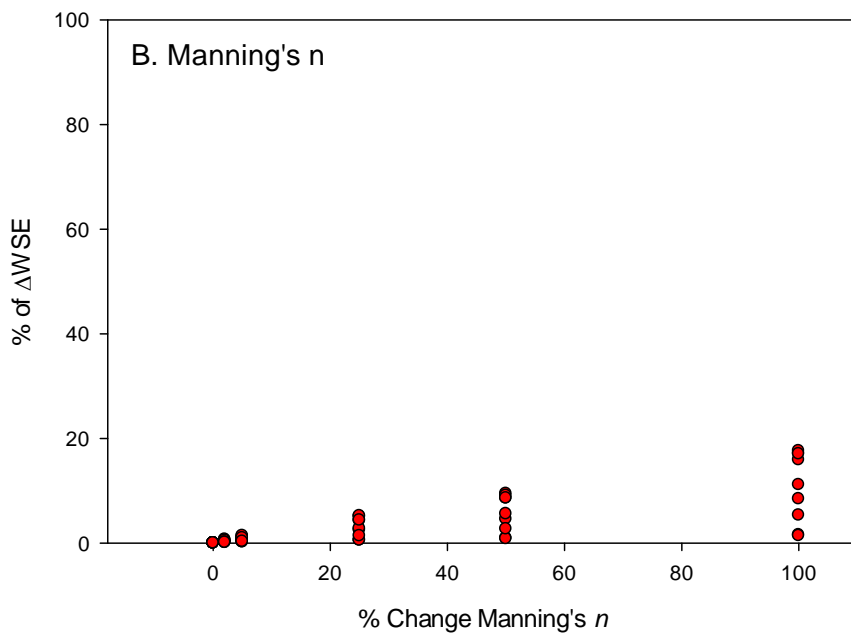


Figure 28. Sensitivity analysis of h to changes in A. Slope, and B. Manning's n . A 100% increase in Manning's n could account for ~10% of Δ WSE, while a 25% change in slope may account for 20% of Δ WSE.



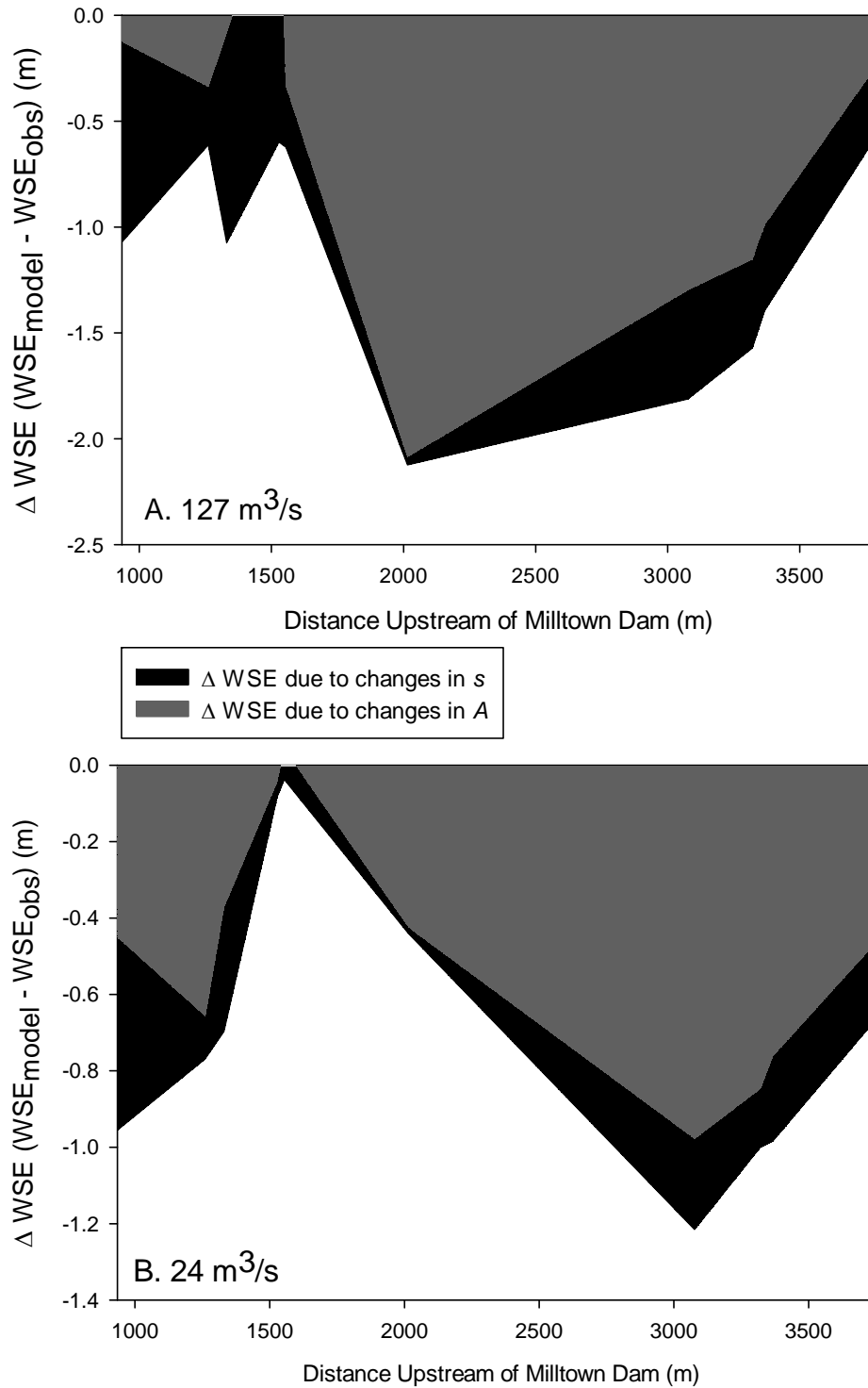


Figure 29. ΔWSE with sensitivity analysis results incorporated for (A) 6/27/08 ($Q = 127 \text{ m}^3/\text{s}$) and (B) 9/5/08 ($Q = 24 \text{ m}^3/\text{s}$). The potential maximum dilutive effects of a 100% change in slope is illustrated by these two ΔWSE analyses. The black area represents the proportion of ΔWSE that can be explained by a 100% change in slope. The black and grey areas added together represent the total ΔWSE .

VII. DISCUSSION

Net Morphological Change vs. WSE Analysis

The Δ WSE and flow modeling approach to tracking the process of reservoir sediment erosion through the 2008 hydrograph generated a similar pattern to that observed in the morphological comparison derived from spring and fall topographic surveys. The modeling approach reveals more information about how much erosion may have happened between the spring and fall topographic survey dates. Headward erosion lowered the bed and was followed by aggradation during the falling limb of the hydrograph. The final base-flow erosion estimate from the modeling approach under-predicts volumetric erosion in comparison with the estimate derived from the topographic surveys (72,000 m³ vs. 150,000 m³). Quantifying changes in fluvial bedforms from observed water surface elevations is somewhat of a simplification of complex interacting variables (n , S , A). Furthermore, it is possible that the modeling-based approach behaves differently at different points in the hydrograph. During the Spring 2008 flood peak (286 m³/s on 5/21/2008), the Δ WSE analysis could lead to over-prediction of volumetric erosion, while at low discharge (i.e. 24 m³/s on 9/5/08) the volumetric erosion may be under-predicted. Perhaps the resulting temporal analysis should be used more as a range in volumetric erosion, rather than a single estimate. Furthermore, the sensitivity analysis results show that where Δ WSE is small or near zero, a doubling in slope overwhelms any signal that can be extracted from the WSE analysis. The above average discharge and significant erosion throughout the reach made changes in cross sectional area the largest driver of Δ WSE.

Furthermore, the WSE method may have missed some of the erosion in the lower reservoir due to the potential rapid changes in slope and roughness in the fine sediment reservoir deposit. The calculated changes in cross sectional area can only be estimates in cases where the WSE_{obs} was lower than the original minimum bed surface. Computing ΔA for such cases becomes more of a low-bound estimate rather than an exact calculation. This is a potential explanation for the deviation between the Fall 2008 base-flow volumetric erosion estimate (based on WSE) and the calculation from repeat cross section surveys, 72,000 and 150,000 m^3 respectively. The model-based calculation represents a lower bound, as the ΔWSE may represents other geomorphological changes in addition to a potential increase of cross sectional area (scour).

The volumetric erosion estimates based on the net morphological change and the ΔWSE approach are consistent with those derived from observed bedload measurements. Bedload was sampled at the bottom of the study reach on two days before the peak (5/17, 5/18/2008) and two after the peak (5/26, 5/27/2008). Transport rates ranged from 41 – 1500 m^3/day . A rating curve based on the bedload samples taken during the 2008 hydrograph suggest evacuation of 150,000 to 300,000 m^3 using bedload : washload ratios of 1:5 and 1:10 respectively (Johnsen 2009).

The total volumetric change calculated through the hydrograph reaches its peak during the falling limb (Figure 25). This is consistent with hysteresis found in sediment transport, where transport rates are higher on the falling limb due to a lag time in the creation and destruction of bed roughness elements (Figure 30, Lee et al 2004, Kuhnle 2006). Hysteresis seen in the BFR is likely due to the time taken for material eroded from the coarse sediment deposit to transport out of the reach. The maximum volumetric

change, as seen on June 1 (Figure 25), would only reflect the evacuation of the coarse material once it was flushed out of the study reach.

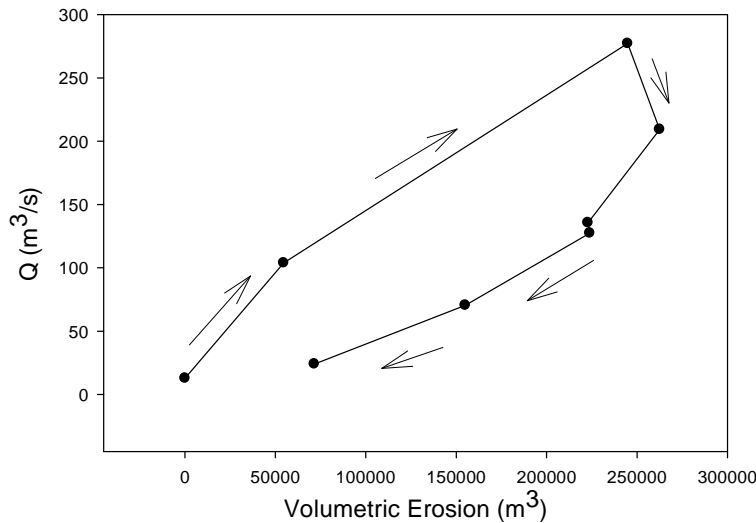


Figure 30. Hysteresis seen in volumetric erosion plotted against discharge (Q). This finding is consistent with sediment transport studies documenting similar patterns of hysteresis in sediment transport (Kuhnle 2006).

Erosion Predictions vs. Observations

During the Milltown Superfund Remediation initial stages, a subcontracted engineering firm modeled erosion using HEC-6 (USACE 1993). Although HEC-6 is a 1-dimensional modeling framework which cannot model channel widening, it likely was an appropriate model for application to the confined lower BFR where the potential for channel widening is small. In feasibility studies, the reservoir deposit was estimated to be 150,000 - 229,000 m³. A variety of bed and flow conditions were run in HEC-6 which produced a range of sediment transport estimates using the Ackers-White equation (Ackers and White 1974). The HEC-6 results were used to make predictions of total sediment transport over a four-year period, starting with the initial reservoir draw-down through the full removal of Milltown Dam. The peak erosion derived from the WSE analysis exceeds the range predicted by pre-dam removal studies done for Milltown. The 260,000 m³ of erosion I estimated from the period of March – September 2008 accounts

for 115% to 140% of the total HEC-6 erosion predicted to occur over a period of 4 years following the dam removal (Envirocon 2004).

Sediment: Texture and Mobility

Upstream, fining occurred in three out of four sites sampled. At cross section VII, this can be explained by the erosion of a high vegetated bar, reducing the variation in bed elevation (see Figure 22). Coarsening was expected at cross sections I and II resulting from incision however fining was observed. This may be because the patches re-sampled may not best represent the new cross section morphologies at these sites. Furthermore, it is important to consider how much the above average peak discharge—flood peak return interval of 3.5 years—may have contributed to the sediment transport versus the dam removal. It has been shown that because of the unique geomorphic context of dam removal and headward erosion, high rates of transport can occur at moderate discharge (Major et al. 2008). However, when discharge is high (~ bankfull discharge, $Q > 1.5 - 2$ year return interval) does more erosion occur, or just more sediment delivered from upstream?

Grain mobility assessed using the Wilcock and Crowe model in BAGS show that bed sediment in the upper reservoir was not likely mobilized below ($< 100 \text{ m}^3/\text{s}$, Figure 18). Alternatively, the fine material in the lower reservoir was mobile at all discharges which indicates that much of the sand and silt deposit likely was transported early in the 2008 hydrograph. This would suggest that during the rising limb of the hydrograph, below $100 \text{ m}^3/\text{s}$, large particles were not mobilized and supplied to the lower reservoir area. Conceptually, as larger particles are delivered to the lower reservoir, changes in

local shear stress (in this generally less steep reach) could cause such particles to fall out of transport and armor the fine bed. It is likely that the time lag between incipient motion of coarse material, and its eventual delivery to the lower 1.8 km of the reservoir, would have been large enough to allow for even more time for erosion of the fine sediment deposit.

Exponential Decay

Although the pattern of erosion observed in the BFR did not follow an exponential decay, testing the applicability of exponential decay to reservoir sediment erosion revealed some interesting questions and limitations. How should an exponential decay function (which by nature is decaying an initial volume) be used to model a complex process that involves both erosion and deposition? Ignoring sediment deposition, we could say that 95% of the reservoir deposit had been eroded 65 days following the dam removal (Table 3, Figure 26). However, this overlooks the complexity of a longer-term adjustment and erosion of coarse sediment from the upper reservoir, and from upstream reaches as headward erosion progresses. Should an exponential decay model be used to describe total export of sediment, or to approximate volumetric changes (i.e. erosion and deposition)? I did not contemplate how deposition would confuse the erosion signal and more generally how deposition of sediment is a process that cannot be predicted by a mathematical function that only decays (erodes). As shown in the HEC/WSE analysis results, deposition during the falling limb of the hydrograph strongly influenced the signal. Deposition of sediment in the study reach will be an integral part of the upstream response as the BFR nears a new equilibrium state.

My observations of the erosion in the BFR are limited to one spring runoff cycle. This is both a challenge within the year, and in a multi-year time frame. Erosion is not occurring during the greater part of a given year. Although it is possible that an exponential decay may summarize erosion over one year, it will show that erosion continues to happen when, in reality, discharge is not sufficient to mobilize bed sediment. This alone may indicate that exponential decay is inappropriate for this application. Tracking the erosion over a longer period of time (i.e. 2 - 5 years) may ultimately follow an exponential decay. However, the data showing erosion and deposition dynamics from Spring – Fall 2008 do not show a pattern of exponential decay.

Widening vs. Erosional Narrowing

It appears that in a confined channel, bed degradation may lead to channel narrowing, while zones of aggradation can drive widening. In the BFR, local degradation was observed to further entrench the channel, causing the width to decrease (evaluated at a 1.5 year flood discharge). The location of maximum bed degradation corresponds with maximum channel narrowing (cross section VII , 3 km upstream). The absence of widening in the analysis of channel width pre- and post-removal at a 1.5 year flood should be treated differently than widening as a mechanism of reservoir sediment erosion. I observed failing vertical or near-vertical, unconsolidated banks on the rising limb of the 2008 hydrograph (Figure 28). Widening certainly acted as a mechanism to erode reservoir sediment, as noted in other studies (see Figure 17, Doyle et al. 2003, Cantelli et al. 2004, Evans et al. 2007). Although the analysis of channel widths at a 1.5 year return interval (RI) did not show that significant widening had occurred in the study

reach, the observations in the BFR do support the Doyle et al. 2003 proposed conceptual model for channel evolution following dam removal. Although the confined nature of the BFR set a boundary on potential lateral response, widening was one of the processes observed to evacuate reservoir sediment.

Furthermore, channel narrowing seen in locations with the greatest degree of bed lowering may support the Cantelli flume experiment results. As the data collected in this study do not match the spatial and temporal resolution of the collected in a flume environment, it is impossible to verify whether the accompanying numerical model is a good fit for the response of the BFR (Cantelli et al. 2007).

Knickpoint

Although no knickpoint was detected, it is clear that a pulse of erosion migrated upstream through the two distinct reservoir deposits. It is possible that two different and concurrent knickpoints may have formed at the downstream end of the two reservoir deposits and met as the lower knickpoint reached the upper. At the time of the dam breaching in March of 2008, a knickpoint was observed moving through the coffer dam and upstream to the confluence of the BFR and CFR. It is difficult to say exactly what happened when it hit the split of the two channels. The CFR side of the confluence led to a rip-rap bypass channel with an immobile bed. If a knickpoint did continue up the BFR, then it would have immediately run into a series of highway, railroad, and pedestrian bridges. These structures could have dissipated a knickpoint. The data do not show the existence of a knickpoint moving through either sediment deposit.

It is unclear which of the four knickpoints may have been present, if at all, in the BFR (see Figure 3). Given the presence of coarse material and abandoned bridge piers which stabilized certain parts of the bed, it is unlikely that a stepped knickpoint could have moved through the reach. It is possible that a rotating knickpoint with diffusion could have marched upstream, stopping 4.5 km upstream of the dam. Further data analysis may be possible to explore this possibility.

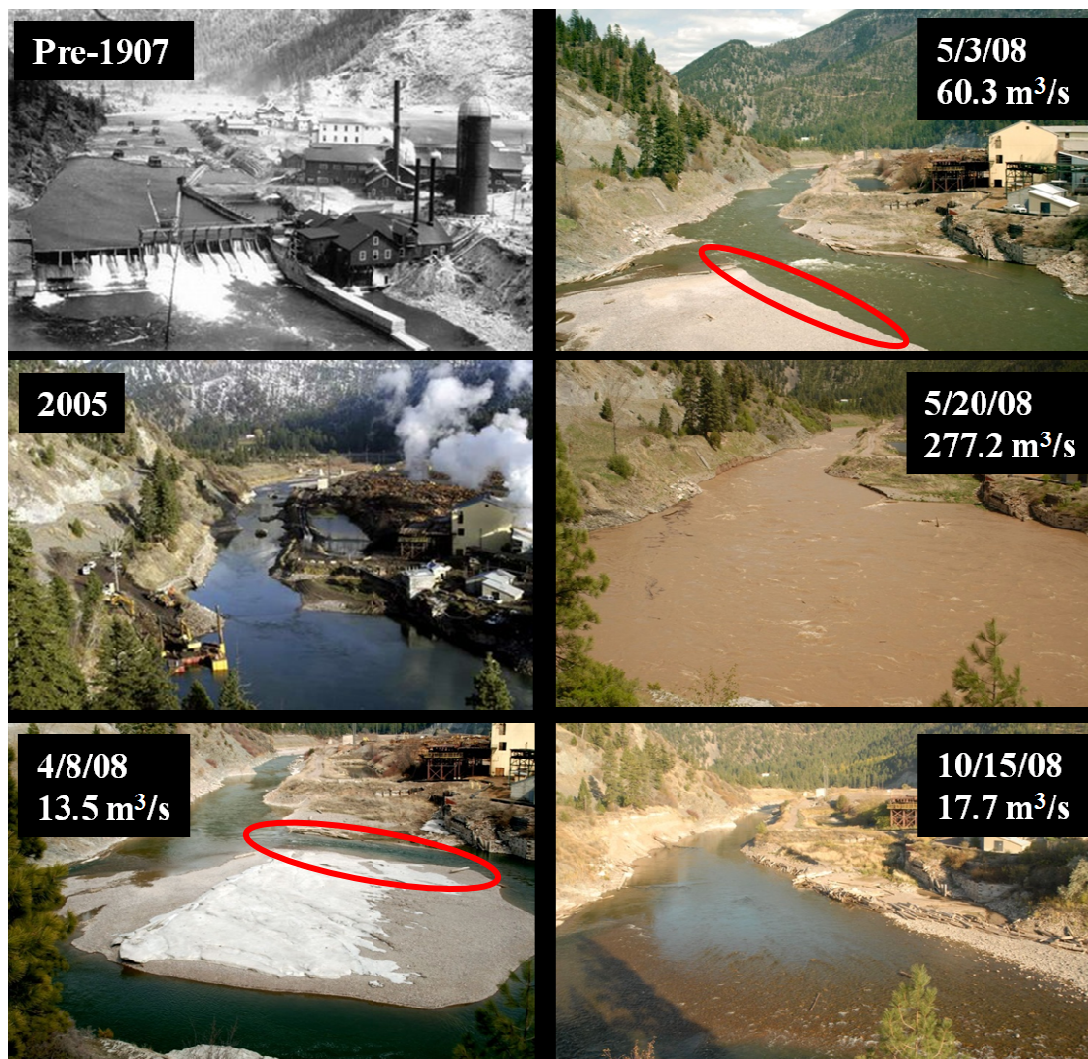


Figure 31. Repeat photography at the Stimson Dam site (2 km upstream of Milltown dam), where a large mid channel bar formed in the 2006-2008 period, and eroded in the 2008 runoff peak. The progression of 5/3/08 to 5/20/08 shows how the channel widened through the mid-channel bar. The vertical bank (indicated by the red oval) made of unconsolidated coarse material contributed sediment to the channel for downstream transport.

Monitoring and Future Restoration

Tracking the adjustment of the BFR to the new base level condition should be a multi-year endeavor. The BFR will continue to be in a transient state over several years until it reaches a new equilibrium. Perhaps the most dramatic period of response will be the Fall 2008 - Fall 2009 period depending on the size of the spring flood peak. During the Fall of 2008, contractors hired by the Montana Department of Natural Resource Conservation removed individual logs and several old bridge piers. These objects had partitioned shear stress away from grains on the bed. As these elements of roughness are removed from the channel, more shear stress will act upon the bed sediments allowing the river to more efficiently transport sediment downstream.

The lower BFR is a naturally and anthropogenically constrained channel. Following the removal of Milltown Dam and the subsequent erosion of reservoir sediment, the bed has lowered and the river is entrenched to a greater degree. From a flood management perspective, this is a good thing as the possibility for a large spring runoff to overflow the banks and affect adjacent property is very low. However, longer-term restoration of the lower portion of the watershed could include giving back some adjacent property to the river corridor. The most dramatically altered section is adjacent to the Stimson Lumber Mill property where the channel has been pushed against a bedrock and scree slope by a steep rip-rap bank. This is also the location of polychlorinated biphenyl (PCB) contamination on the industrial property. After the remediation of the contaminated site, giving back some of the Stimson property to the river corridor would continue river restoration efforts started by the removal of Milltown Dam. The lower BFR is comprised of a sequence of riffles and pools. The 500 m stretch

along the Stimson property is a narrow, high velocity section that is an anomaly in comparison to less impacted adjacent reaches. The bankfull channel width in the narrowed reach is ~18 to 30 m, compared to ~30 to 105 m in the 2km reach upstream. Furthermore, in the lower 1.8 km, vertical banks from 0.5 to 3 m tall remain on the northwest side of the channel. These banks could be viewed as a hazard to recreational users of the river. It is possible that some active management or restoration of those banks could be appropriate including bank setbacks and re-vegetation.

2006 Reservoir Drawdown and the Stimson Dam Removal

The upstream response of the BFR to the removal of Milltown Dam began before the March 2008 breach. The removal of Stimson Dam in 2005 followed by the 2006 3.4 m reservoir drawdown created the conditions to initiate the upstream response and the erosion of coarse reservoir sediment. As approximately 2 km of the BFR was still a part of Milltown reservoir from 2006 -March 2008, the fine sediment deposit remained intact in the reservoir reach. Although the BFR did begin its adjustment before I collected any data, I feel that my field efforts from Spring – Fall 2008 captured the majority of the response as the majority of the sediment remained in the study reach until after March

2008 with the additional 4.6 base level reduction (8 m total base level change from 2006 –March 2008). Any coarse sediment mobilized from the upper end of the reservoir (the portion of the river that began flowing after the 2006 drawdown) before 2008 could not have been transported below ~2 km above the dam. A 13 m deep scour hole below the Stimson Dam was filled with gravel and cobbles during the 2005-2008 period, as evidenced by field observations and comparisons with bathymetry data from

2003 (Envirocon 2004). It is possible that some incision into the reservoir sediment occurred, however monitoring of the BFR during this time period was not performed by Milltown contractors or others. The majority of sediment mobilized from the study reach during the 2005-2008 period can be viewed as a transfer within the reach.

Challenges

The analysis of erosion through the hydrograph was complicated by the challenge presented by surveying river bed topography at moderate-to-high discharges in medium-sized alluvial systems. Typical survey techniques are limited to flows at which cross sections can be waded or measured using a static line from which a small boat can be fixed. Boat based surveying techniques typically employed in large river systems were not well suited to the BFR. Without the installation of fixed cableways (such as at USGS gauging stations), other infrastructure, or specialized equipment, surveying at high flows is not possible. Furthermore, river hazards created by several thousand logs and other debris (mill saw blades, metal debris, bridge piers, and a submerged vehicle) made using motorized boat surveying techniques impractical at high discharges. Given such restrictions to surveying at high flows, only topographic data collected at base-flow conditions was available for analyzing the upstream response.

Comparison to other Dam Removals

In relation to recent dam removals documented by various investigators, the sediment release from the BFR following the removal of Milltown Dam presents a distinct case study. My results show that a large proportion of the reservoir sediment that

accumulated in the lower BFR was evacuated in the first 5 months following the removal of Milltown Dam. Depending on the variety of estimates for both the amount of sediment stored, and my erosion estimates, 75% - 175% of the reservoir deposit eroded during the 5 month time frame of this study. Given that the BFR is still several years away from reaching a new equilibrium and will likely evacuate a significant volume of sediment during the 2009 Spring runoff period, the total volumetric export may greatly exceed the initial reservoir sediment deposit size.

Compared to published studies of dam removals in recent years, this represents one of the more rapid rates (if not the most rapid rate) of reservoir sediment flushing (Table 4, Figure 33). The studies summarized in Table 3 reported 4 – 14% of reservoir sediment flushed following the removal of dams from low gradient, fine sediment systems, with the exception of Marmot Dam which flushed a larger proportion of the coarse reservoir deposit (43% in 3 months). This comparison is not exhaustive given the variety of physiographic settings each dam removal was performed within. In order to enhance this comparison, it would be useful to explicitly account for discharge, grain size, slope, the initial volume of sediment at the time of dam removal, and the morphology of the reservoir sediment deposit at each of these dam removals.

Marmot Dam The removal of Marmot Dam from the Sandy River, OR, presents the most appropriate comparison given the similarity of the two systems: confined gravel-bed rivers. As described earlier, 100,000 m³ of reservoir sediment was eroded following the breaching of Marmot Dam in 48 hours at moderate discharge ($Q \sim 50 \text{ m}^3/\text{s}$, which is 30% above the mean annual flow of 38 m³/s). A comparable discharge on the BFR would be 57 m³/s (mean annual flow is 44 m³/s). Peak discharge of 287 m³/s was reached on

May 21, 2008, exposing the reservoir sediments to much higher discharge in comparison to the 48 hour period following the Marmot Dam removal.

The hydrology of the Sandy and BFR differ significantly. The Sandy's hydrograph is determined by large rain events and snowmelt from the Cascades. The Sandy River near Marmot, Oregon (USGS station # 14137000) typically shows a flashy pattern from Fall through June or July, spiking with rain events throughout that time. Peak discharge may occur in Fall, Winter or Spring due to the influence of both rain events and snowmelt. Alternatively, the BFR is a typical snowmelt driven river system with peak discharge typically occurring in May or June.

Two primary factors differentiate the conditions and response on the Sandy and Blackfoot Rivers: channel slope and the morphology of the reservoir sediment deposit. The Sandy River at Marmot Dam is a high gradient, confined channel (slope 0.06 - 0.09) and the sediment deposit extended up to the dam itself (Figure 32). Alternately, the lower BFR near Milltown Dam had a lower gradient (slope = 0.001-0.005) and an elongated reservoir sediment deposit with spatially distinct zones of fine and coarse sediment (see Figure 8). The less compact sediment deposit and the lower slope in the BFR made the response more dependent on high flows, whereas results from the Marmot Dam removal show that moderate discharge mobilized a large volume of sediment. The grain mobility analysis for the BFR shows that much of the coarse sediment would not have been mobile at $57 \text{ m}^3/\text{s}$, which is equivalent to the 30% of mean annual discharge that eroded 15% of the Marmot Dam sediment in only 48 hours. Furthermore, a knickpoint developed at the Marmot coffer dam site moved 500 meters upstream in the first 48 hours (Major et al. 2008). The morphology of the sand and gravel deposit included a steep

slope at the downstream face of the coffer dam presented the conditions to initiate a knickpoint.

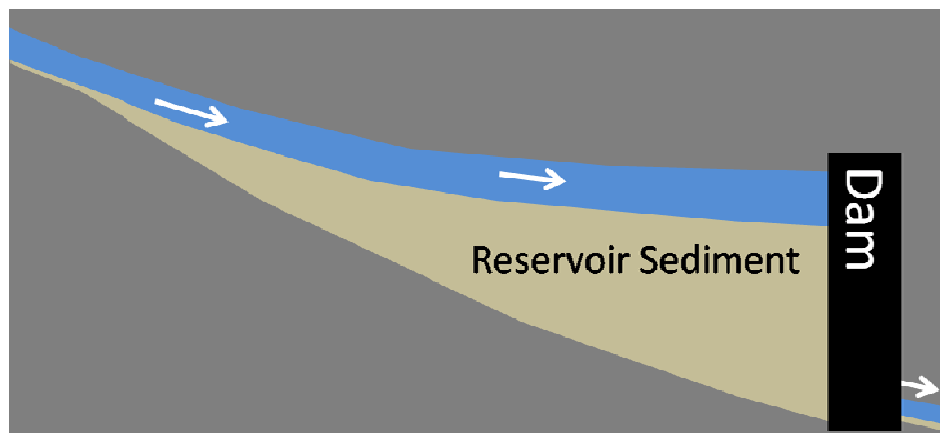


Figure 32. Idealized diagram of a coarse reservoir sediment deposit that extends up to a dam, tapering off upstream. This diagram shows the morphology of the deposit in the Marmot Dam on the Sandy River, for comparison to that found in the BFR (Figure 8).

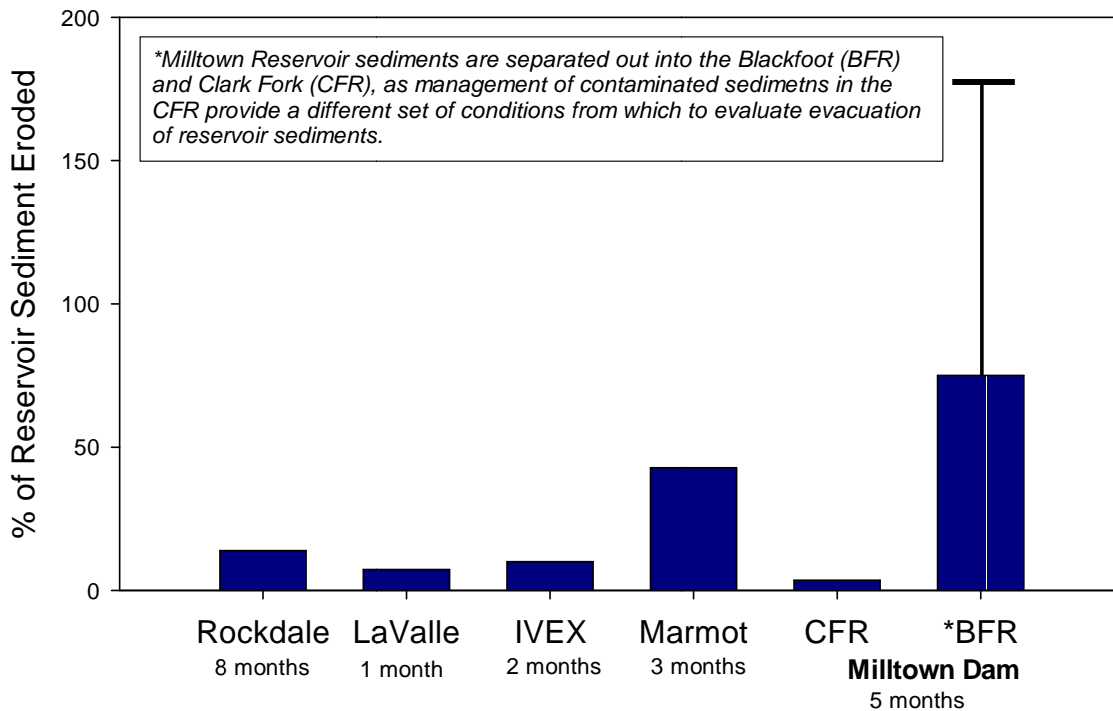


Figure 33. Proportion of reservoir sediment eroded following removal of the four respective dams from published studies documenting fluvial response (See Table 4). Range of estimates for total reservoir sediment (175,000 – 229,000 m³) and erosion (150,000 – 260,000 m³) for Milltown shown. Note: time period of observed sediment release shown for each dam.

Dam	River	Drainage Area (km ²)	Dam Height (m)	Reservoir Sediment	Reservoir Sediment Storage (m ³)	Sediment Evacuated (m ³ /time)	Slope (m/m)	Observed Upstream Response	Knickpoint
¹ Rockdale Dam	Koshkonong (WI)	360	3.3	silt-sand	287,000	40,000 m ³ / ~8 months	0.0007	Headcutting	YES
¹ LaValle Dam	Baraboo (WI)	575	2	silt-sand	140,100	10,200 m ³ / ~1 month	0.0005	Incision into reservoir deposit, bed lowering	NO
² St. Johns Dam	Sandusky (OH)	3637	2.2	Sand-gravel	200,000	N/A	.0001	Decrease in slope after sand filled pools, zones of erosion and deposition upstream of dam	NO
³ Saeltzer Dam	Clear Creek (CA)	720	4.6	Gravel-cobble	N/A	N/A	N/A	Incision, lateral erosion	NO
⁴ IVEX Dam	Chagrin (OH)	692	7.4	Fine sediment	236,000	23,700-31,300 m ³ / 2 months	N/A	Incision, widening, Modified Doyle 2003 CEM	YES
⁵ Marmot Dam	Sandy (OR)	1300	14	sand-gravel	730,000	100,000 m ³ /48 hrs, 300,000 m ³ / 3 months	0.006 - 0.009	Headward and lateral erosion, bank failures, widening through reservoir deposit, Q ~50 m ³ /s	YES
^{6,7} Milltown Dam (CFR)	Clark Fork River	9430	20	Silt-sand	> 5,000,000	180,000 5 months	0.0012 - 0.0028	Widening, channel migration across historic floodplain, headward erosion 2.6 – 2.8 km upstream of the dam site	NO
Milltown Dam (BFR)*	Blackfoot (MT)	5931	20	silt-sand, gravel-cobble	175,000 - 229,000	150,000 - 260,000 m ³ / 5 months,	0.0012 - 0.005	Narrowing, headward erosion 4.5 km upstream of the dam in first 5 months, 3.5 year RI peak (287 m ³ /s)	NO

*Excluding sediments accumulated in the Clark Fork Arm of Milltown Reservoir

Table 4. Review of detailed dam removal studies from around the U.S. Adapted from ¹Doyle et al. 2003, ²Cheng and Granata 2007, ³Ferry and Miller 2003, ⁴Evans 2007, ⁵Major et al. 2008, ⁶Wilcox et al. 2008, ⁷Brinkerhoff 2009. IVEX was a dam failure that has been compared to “blow and go” dam removal. NOTE: although a knickpoint developed in the coffer dam at the time of the breaching of Milltown Dam, it is unclear what happened to it as it moved upstream and reached the complex of bridges in the lower BFR, and the entrance to the rip-rap bypass channel in the Clark Fork River.

Clark Fork Arm of Milltown Dam Intensive management of the contaminated sediments in the Clark Fork arm of Milltown reservoir prevented the CFR from responding naturally to the base level lowering. However, there are differences between the BFR and CFR that warrant some exploration and comparison of how each of these two rivers have responded. Unlike the confined BFR, the CFR is a broad, complex floodplain reach. Based on historical documents and hand-drawn maps, it has been shown that the ~5 km reach immediately upstream of Milltown Dam had a complex multiple channel plan-form with islands and bars (Woelfle-Erskine 2008). Furthermore, the reservoir sediment in the CFR is largely composed of the fine sediment that originated upstream and filled the reservoir following the 1908 flood.

In the months leading up to the breach of Milltown Dam, the CFR was diverted into a rip-rap bypass channel to keep the channel away from ongoing mechanical removal of contaminated sediments. Although much of the contaminated sediments in the CFR were protected by immobile banks and grade control, 180,000 m³ of contaminated sediment was eroded from the upper portion of the reservoir as the channel migrated across the broad floodplain (Wilcox et al. 2008). Field observations show that some banks migrated more than 200 m in the first spring runoff following the dam removal. The unconfined alluvial valley that the CFR occupies illustrates how rivers will adjust their plan-form via channel migration given a new base level condition. Alternatively, in systems like the BFR or the Sandy River, the confinement of the channel forces the primary modes of adjustment to be slope and grain size.

The 180,000 m³ that eroded in 2008 is a small proportion of the total reservoir sediment stored in the CFR (3-4 %). Due to the contamination of the CFR sediments,

approximately one-third of the $> 5,000,000 \text{ m}^3$ of reservoir sediment was mechanically excavated and was not available for river erosion. It is also possible that the wide alluvial valley setting would contribute to a slower rate (in comparison to the BFR) of reservoir sediment evacuation upstream of a removed dam. If a channel is unconfined and able to migrate, the migration rate of the channel would determine the rate at which the reservoir sediment would be eroded.

Implications for Other Systems

The results of this study should be considered in the context of the following controls on the upstream response:

- Slope (S)
- Discharge following the dam breach (Q)
- Grain size (D)
- Roughness (n)
- Initial volume of sediment (V_0)
- Confinement of the channel
- Morphology of the reservoir sediment deposit

Perhaps the most efficient way to encourage the evacuation of sediment behind a dam is to do so in a confined channel with sufficient slope and discharge. The comparison of the Marmot and Milltown Dam removals illustrates that a compact sediment deposit in a steeper channel required only moderate flows to flush sediment quickly. The shape of the sediment deposit was critical for providing the conditions to propagate a knickpoint upstream and evacuate sediment rapidly. Alternatively, the spread-out reservoir sediment deposit in the BFR lacked the steep slope and likely did not result in a headward migrating knickpoint. However, the BFR had sufficient discharge to achieve a rapid rate of reservoir sediment evacuation.

Roughness was a strongly interacting variable in controlling the geomorphic response of the BFR to the removal of Milltown Dam. In the lower reservoir, channel morphology, deposition, and surface texture response were strongly linked to the roughness (shear stress partitioning) caused by log jams that organized in the lower reservoir (Figure 31). The roughness in the channel is thought to have slowed the downstream transport of reservoir sediment from the lower reservoir area and increased habitat heterogeneity in the newly reclaimed BFR. The integration of natural or constructed logjams in an evolving reservoir after a dam removal could provide a useful tool to manage the ensuing sediment pulse, foster channel complexity, and increase habitat heterogeneity for aquatic organisms.



Figure 34. Lower BFR flowing for the first time since 1907 conversion to reservoir. Distinct sediment and vegetation banding shows phased reduction in base level, starting in 2006, and recently completed by the coffer dam breaching on March 28, 2008 (Photo taken 4/8/2008)

VIII. CONCLUSION

The observations and processes described in this study may be useful in other dam removals and human induced or natural reductions of base level in river systems. Observed water surface elevations can be used to approximate the erosion and elucidate patterns (spatial, temporal) through a known pre-disturbance topography. However, a more robust integration of changes in slope and roughness could help improve a flow modeling approach's ability to provide specific estimates in place of what I consider to be a range of estimates produced in this study. Furthermore, it appears that in a confined mountain channel, headward migrating erosion may drive channel narrowing, where bed lowering further entrenches the channel into the confined active zone. Narrowing was most pronounced at cross sections with the largest magnitude of incision or bed lowering. Alternatively, local sediment deposition may be a mechanism causing some widening in such systems.

In summary, following the removal of Milltown Dam, I observed the following response of the Blackfoot River:

- Headward erosion extended 4.5 km upstream of the dam site in the first 5 months following the removal of Milltown Dam.
- A large proportion of BFR reservoir sediment was evacuated in the first 5 months (a range of 75%-175% of estimated reservoir sediment deposit).
- Δ WSE analysis show that entire initial volume of reservoir sediment (V_0) eroded in the first 100 days following the dam breach.
- Response was influenced by confinement of the channel, shear stress partitioning by LWD, and above-average discharge (287 m³/s, 3.5 year RI).
- The flow modeling WSE analysis seems to be a reasonable approach and provided insight into the pattern of erosion through the 2008 hydrograph.

Future Directions

A quantitative assessment of the effects of large woody debris on the BFR would help develop the important role of roughness in the geomorphic response. This could be done using the high resolution air photos acquired in the Fall of 2008, in combination with some existing methods to account for flow resistance from wood in channels (Wilcox et al. 2006). Furthermore, some of the water surface profile data could be further explored in an attempt to locate a knickpoint signal. Also, because the channel will likely continue adjusting over the next few years, repeating cross section surveys and acquisition of aerial photography will help show how BFR continues to evolve and reach a new state of equilibrium. Furthermore, acoustic backscatter or Laser In-Situ Scattering and Transmissometry sensors could be installed to measure suspended sediment exiting the lower BFR (Gray et al. 2003), for comparison with data sets from the USGS gauging station upstream (1234000), and the station downstream on the CFR (12340500).

REFERENCES CITED

- Ackers, P. and White, W., 1975. Sediment Transport - New Approach and Analysis. JOURNAL OF THE HYDRAULICS DIVISION-ASCE, 101(NHY5): 621-625.
- Begin, Z.B., 1988. Application of a Diffusion-Erosion Model to Alluvial Channels Which Degrade Due To Base-Level Lowering. EARTH SURFACE PROCESSES AND LANDFORMS, 13(6): 487-500.
- Bishop, P., Hoey, T., Jansen, J. and Artza, I., 2005. Knickpoint Recession Rate and Catchment Area: The Case of Uplifted Rivers in Eastern Scotland. EARTH SURFACE PROCESSES AND LANDFORMS, 30(6): 767-778.
- Brinkerhoff, D. 2009. Personal Communication.
- Brush, L.M., Wolman, M.G., 1960. Knickpoint Behavior in Non-Cohesive Material: A Laboratory Study. BULLETIN OF THE GEOLOGICAL SOCIETY OF AMERICA. 71: 59-74.
- Buffington, J. and Montgomery, D., 1999. Effects of Hydraulic Roughness on Surface Textures of Gravel-Bed Rivers. WATER RESOURCES RESEARCH, 35(11): 3507-3521.
- Cantelli, A., Paola, C. and Parker, G., 2004. Experiments on Upstream-Migrating Erosional Narrowing and Widening of an Incisional Channel Caused by Dam Removal. WATER RESOURCES RESEARCH, 40(3).
- Cantelli, A., Wong, M., Parker, G. and Paola, C., 2007. Numerical Model Linking Bed and Bank Evolution of Incisional Channel Created by Dam Removal. WATER RESOURCES RESEARCH, 43(7).
- Cheng, F. and Granata, T., 2007. Sediment Transport and Channel Adjustments Associated With Dam Removal: Field Observations. WATER RESOURCES RESEARCH, 43(3).
- Clark Fork River Technical Assistance Committee. August 2008.
<http://www.cfrtac.org/sitehistory.php>
- Crosby, B. and Whipple, K., 2006. Knickpoint Initiation and Distribution Within Fluvial Networks: 236 Waterfalls in the Waipaoa River, North Island, New Zealand. GEOMORPHOLOGY, 82(1-2): 16-38.
- Cui, Y., A. Wilcox. 2008. Development and Application of Numerical Modeling of Sediment Transport Associated with Dam Removal. In: M.H. Garcia, Ed.

Sedimentation Engineering. ASCE Manual 110. Reston, VA: American Society of Civil Engineers.

- Doyle, M., Stanley, E. and Harbor, J., 2002. Geomorphic analogies for assessing probable channel response to dam removal. *JOURNAL OF THE AMERICAN WATER RESOURCES ASSOCIATION*, 38(6): 1567-1579.
- Doyle, M., Stanley, E. and Harbor, J., 2003. Channel adjustments following two dam removals in Wisconsin. *WATER RESOURCES RESEARCH*, 39(1).
- Doyle, M., Stanley, E., Havlick, D., Kaiser, M., Steinbach, G., Graf, W., Galloway, G., Riggsbee, J., 2008. Environmental Science - Aging Infrastructure and Ecosystem Restoration. *SCIENCE*, 319(5861): 286-287.
- Dynesius, M., Nilsson, C., 1994. Fragmentation and Flow of River Systems in the Northern 3rd of the World. *SCIENCE*, 266(5186): 753-762.
- Envirocon. *Milltown Reservoir Scour Evaluation Addendum 2 – Evaluation of Potential Infrastructure Impacts Associated with Dam-Removal Induced Scour and Effectiveness of Possible Countermeasures.* April 28, 2005.
- Envirocon. *Milltown Reservoir Dry Removal Scour Evaluation, Addendum 1, Proposed Plan Updated Scour Evaluation.* October 7, 2004.
- Envirocon. Remedial Design Data Summary Report #1, Milltown Reservoir Sediments Site. June 8, 2004.
- EPA. *Biological Assessment of the Milltown Reservoir Sediments Operable Unit, Revised Proposed Plan and of the Surrender Application for the Milltown Hydroelectric Project (FERC No. 2543).* August 2004.
- Evans, J., 2007. Sediment Impacts of the 1994 Failure of IVEX Dam (Chagrin river, NE Ohio): A test of Channel Evolution Models. *JOURNAL OF GREAT LAKES RESEARCH*, 33: 90-102.
- Ferry, M., Miller, P., 2003, The Removal of Saeltzer Dam on Clear Creek : An Update. Water Resources Center Archives, The University of California.
- Graf, W., 1999. Dam nation: A geographic census of American dams and their large-scale hydrologic impacts. *WATER RESOURCES RESEARCH*, 35(4): 1305-1311.
- Graf, W., (Ed.) 2002. *Dam Removal Research: Status and Prospects*, H. John Heinz II Center for Science, Economics and the Environment., Washington, D.C.
- Gray, J.R., Melis, T., Patino, E., Larsen, C., Topping, D., Rasmussen, P., Figueroa-Alamo, C., 2003. U.S. Geological Survey Research on Surrogate Measurements for

Suspended Sediment. Proceedings, Interagency Conference on Research in the Watersheds.

HEC-RAS 4.0. 2008. User's Manual. Hydrologic Engineering Center, US Army Corps of Engineers.

Johnsen, J. 2009. Personal Communication.

Knighton, D. 1998. "Fluvial Forms and Processes: A New Perspective." Oxford University Press, New York, NY.

Lane, E.W. 1955. The Importance of Fluvial Morphology in Hydraulic Engineering. American Society of Civil Engineers Proceedings, 81, 1-17. Physical Monograph Series, Vol. 89, edited by J.E. Costa et al.

Larue, J., 2008. Effects of Tectonics and Lithology on Long Profiles of 16 Rivers of the Southern Central Massif Border Between the Aude and the Orb (France). GEOMORPHOLOGY, 93(3-4): 343-367.

Lee, K., Liu, Y. and Cheng, K., 2004. Experimental Investigation of Bedload Transport Processes Under Unsteady Flow Conditions. HYDROLOGICAL PROCESSES, 18(13): 2439-2454.

Leopold, L., and Bull, W., 1979. Base Level, Aggradation and Grade. PROCEEDINGS OF THE AMERICAN PHILOSOPHICAL SOCIETY, 123(3): 168-202.

Major, J. J., J. E. O'Connor, G. E. Grant, K. R. Spicer, H. M. Bragg, A. Rhode, D. Q. Tanner, C. W. Anderson, and J. R. Wallick (2008), Initial Fluvial Response to the Removal of Oregon's Marmot Dam, EOS TRANSACTIONS. AGU, 89(27), doi:10.1029/2008EO270001.

Pitlick, J., P.R. Wilcock, J.P. Potyondy, P. Bakke, Y. Cui. 2007. Bedload Assessment in Gravel-bedded Streams. Stream Systems Technology Center, United States Forest Service, Department of Agriculture.

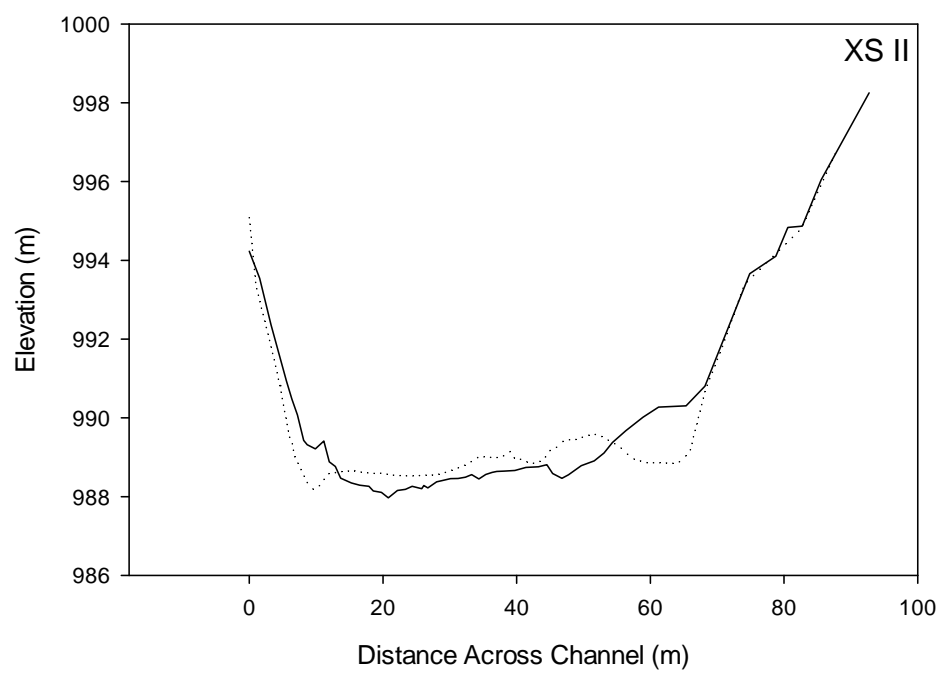
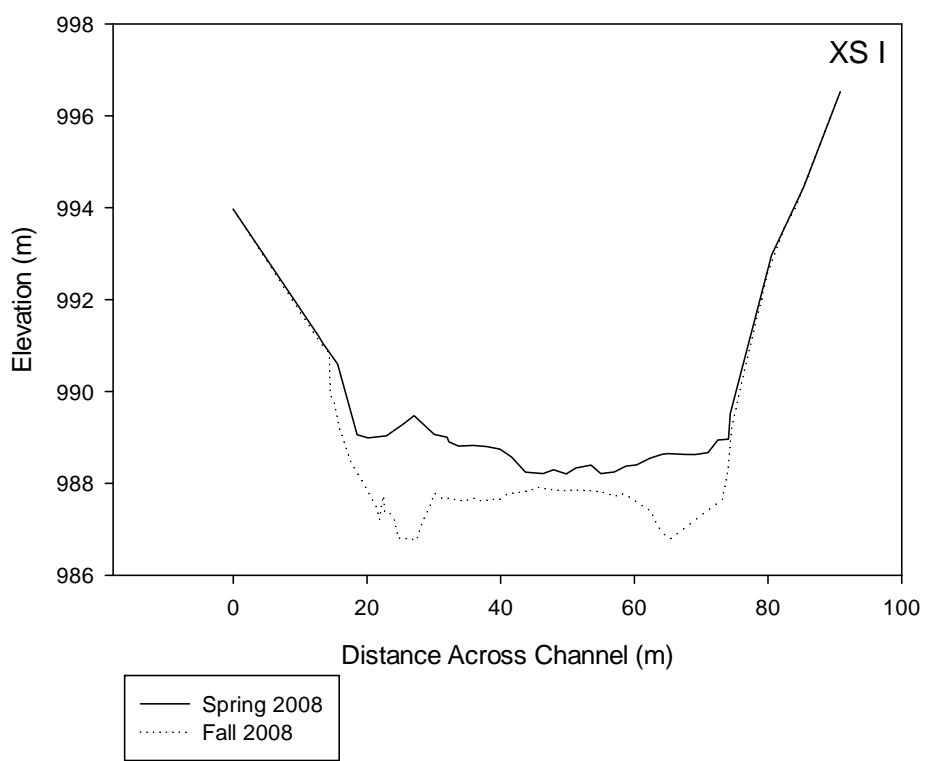
Pizzuto, J., 1994. Channel Adjustments to Changing Discharges, Powder River, Montana. GEOLOGICAL SOCIETY OF AMERICA BULLETIN, 106(11): 1494-1501.

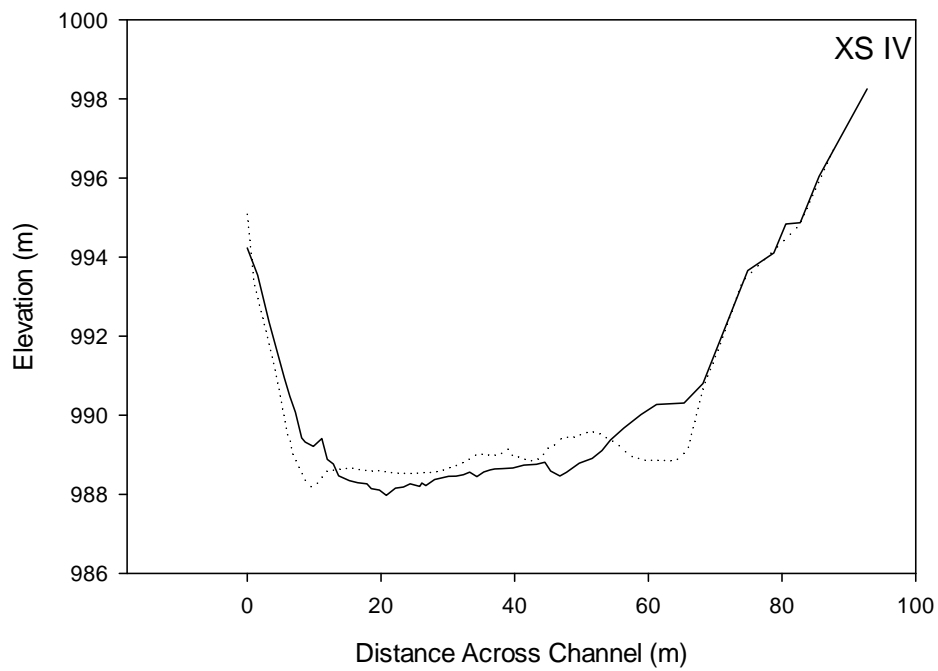
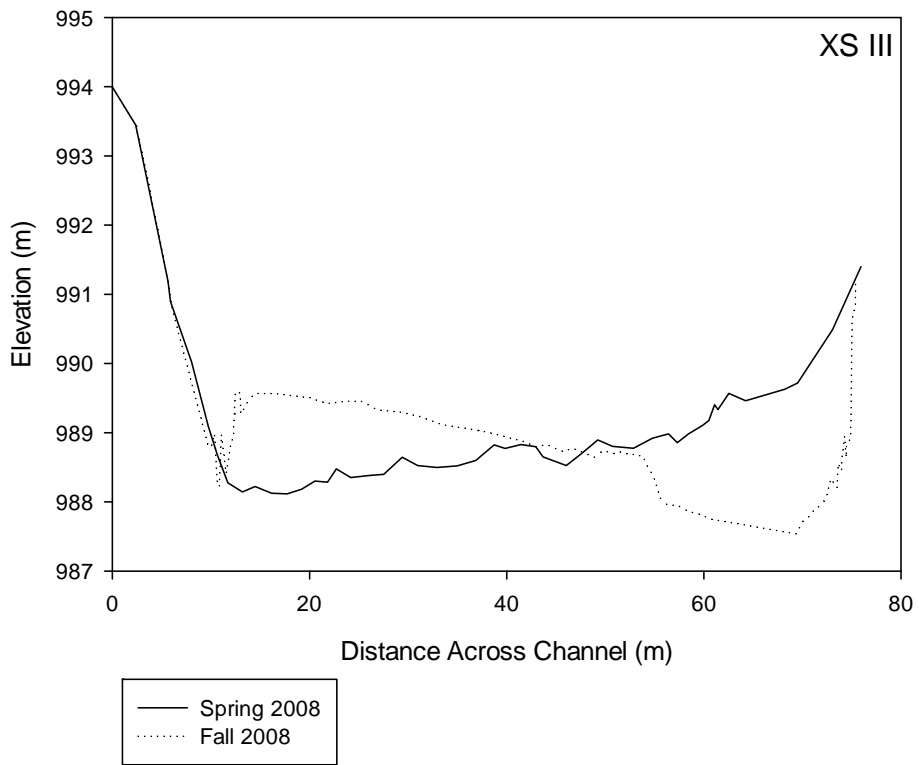
Pizzuto, J. 2002. Effects of Dam Removal on River Form and Process. BIOSCIENCE. 52(8): 683-691.

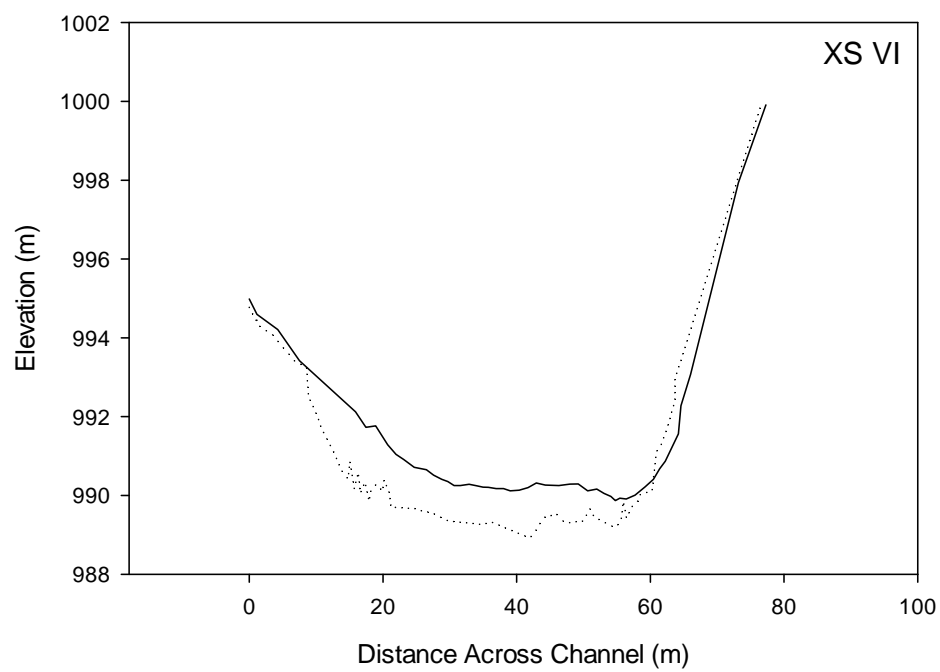
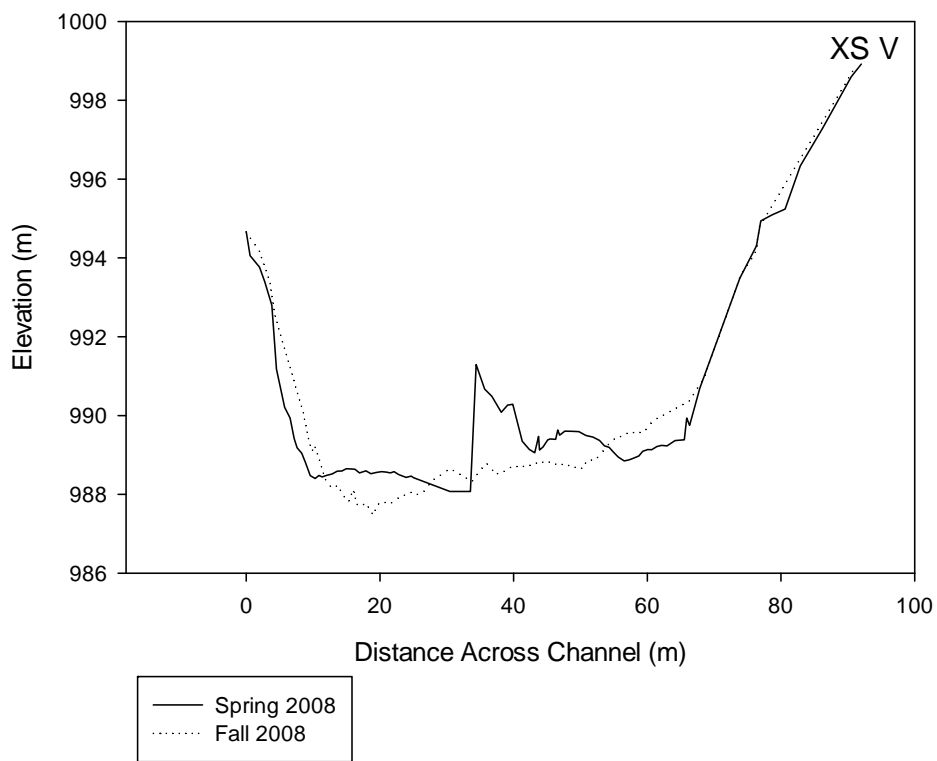
Rothrock, J., Barten, P. and Ingman, G., 1998. Land Use and Aquatic Biointegrity in the Blackfoot River Watershed, Montana. JOURNAL OF THE AMERICAN WATER RESOURCES ASSOCIATION, 34(3): 565-581.

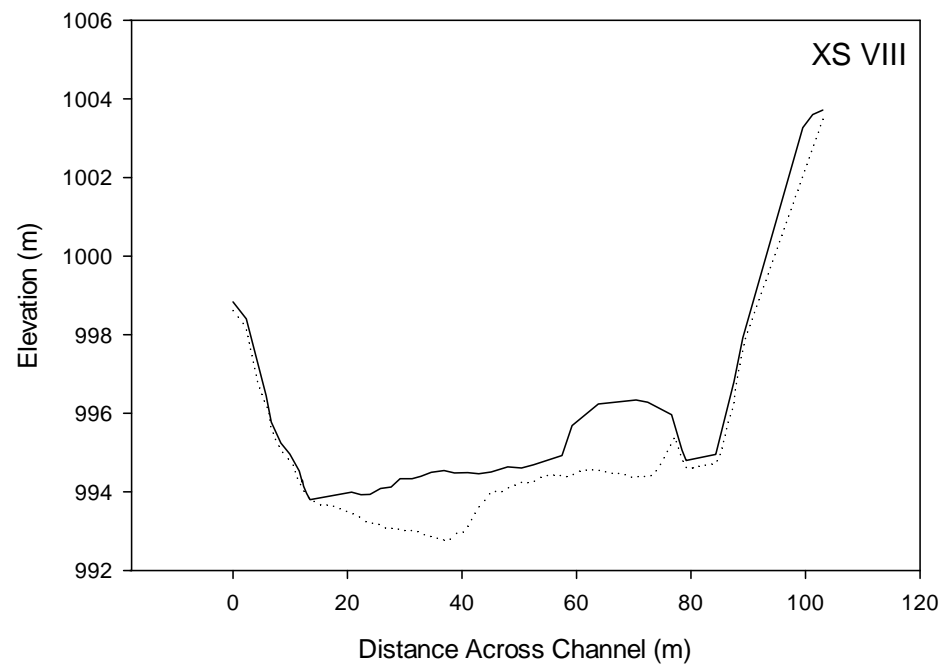
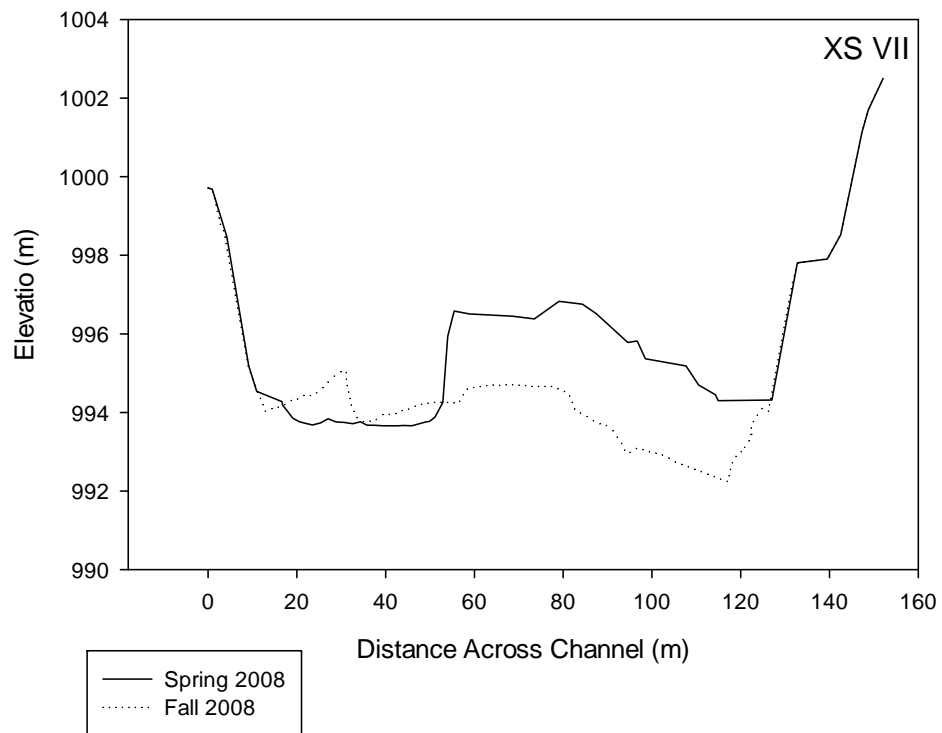
- Shuman, J., 1995. Environmental Considerations for Assessing Dam Removal Alternatives for River Restoration. *REGULATED RIVERS-RESEARCH & MANAGEMENT*, 11(3-4): 249-261.
- Stewart, G.B. 2006. Patterns and Processes of Sediment Transport following Sediment-filled Dam Removal in Gravel Bed Rivers. Dissertation. Oregon State University.
- Van Haveren, B.P., W.L. Jackson, G.C. Lusby. 1987. Sediment Deposition Behind Sheep Creek Barrier Dam, Southern Utah. *JOURNAL OF HYDROLOGY (New Zealand)* 26:185-196.
- Ward, J. and Stanford, J., 1995. Ecological Connectivity in Alluvial River Systems and its Disruption by Flow Regulation. *REGULATED RIVERS-RESEARCH & MANAGEMENT*, 11(1): 105-119.
- Wilcock, P.R., Kenworthy, S.T. and Crowe, J.C., 2001. Experimental Study of the Transport of Mixed Sand and Gravel. *WATER RESOURCES RESEARCH*, 37(12): 3349-3358.
- Wilcock, P.R. and Crowe, J.C., 2003. Surface-Based Transport Model for Mixed-Size Sediment. *JOURNAL OF HYDRAULIC ENGINEERING-ASCE*, 129(2): 120-128.
- Wilcox, A., Nelson, J. and Wohl, E., 2006. Flow Resistance Dynamics in Step-Pool Channels: 2. Partitioning Between Grain, Spill, and Woody Debris Resistance. *WATER RESOURCES RESEARCH*, 42(5).
- Wilcox, A. C., Brinkerhoff, D., Woelfle-Erskine, C., 2008. Initial geomorphic responses to removal of Milltown Dam, Clark Fork River, Montana, USA. *EOS Trans. AGU*. 89(53) Fall Meet. Suppl. Abstract H41I-07.
- Woelfle-Erskine, C. 2009. History and uncertainty in post-Milltown dam removal restoration on the Clark Fork River, Montana. Honors Thesis, Department of Geosciences, The University of Montana.
- Wolman, M.G., 1954. A Method of Sampling Coarse Bed Material. American Geophysical Union, *TRANSACTIONS*, 35: 951-956.

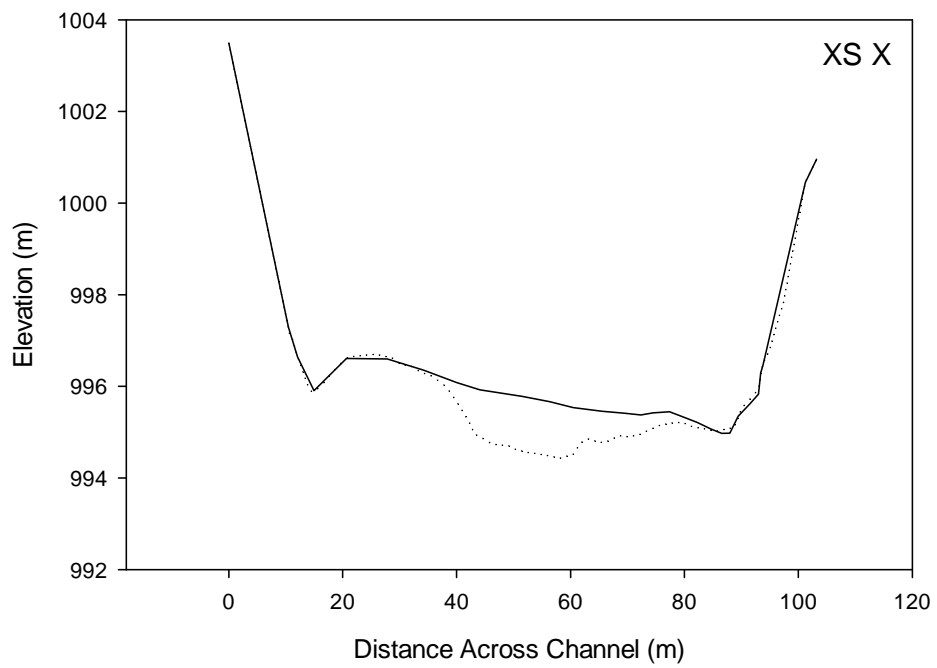
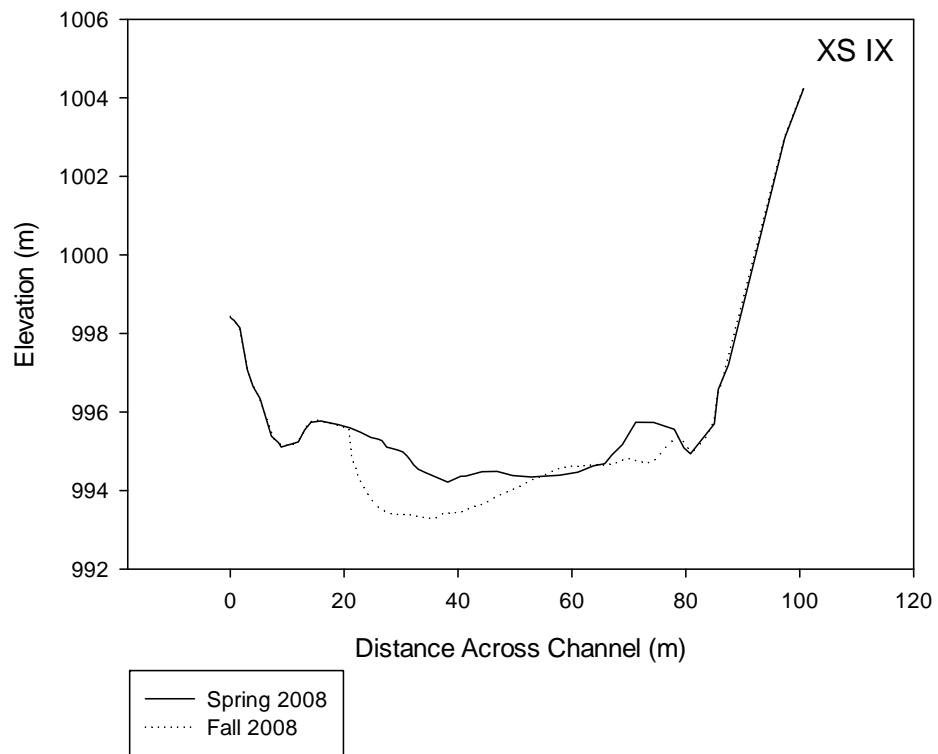
APPENDIX I: CROSS SECTIONS

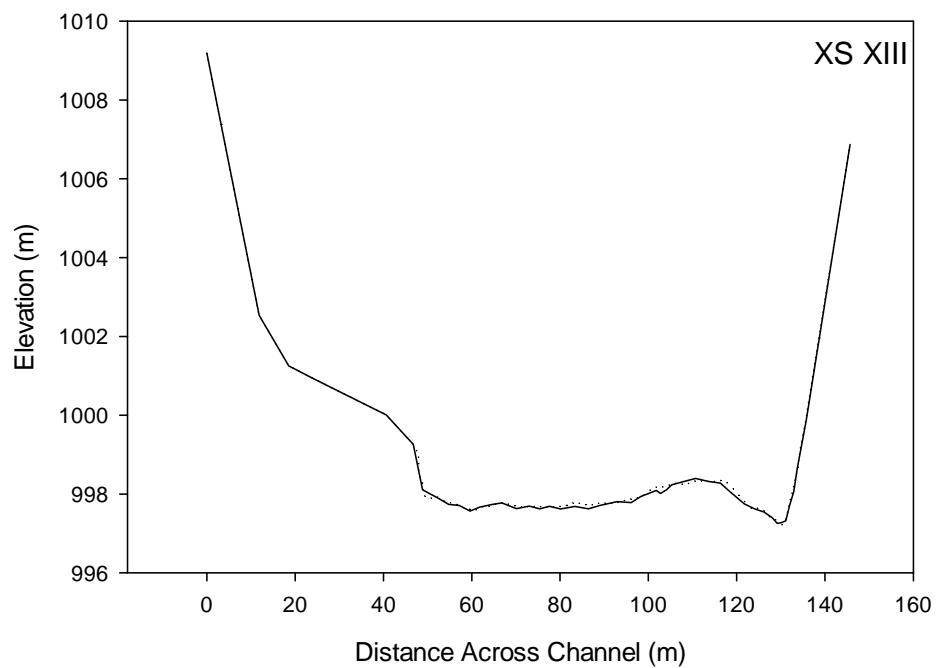
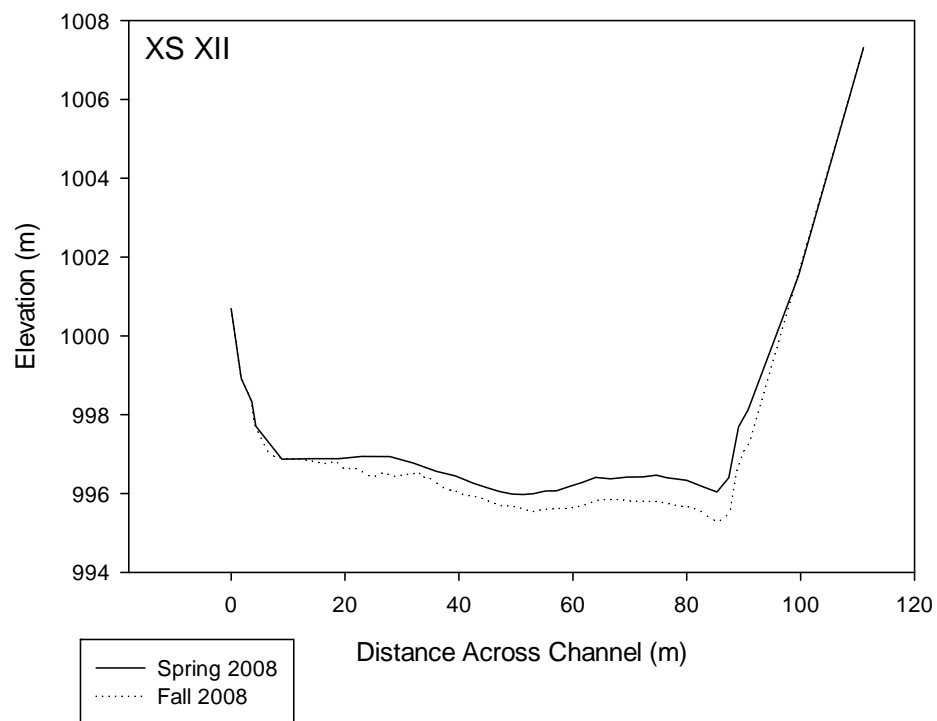












APPENDIX II: GPS DATA

Cross Section Endpoints

XS	LEFT, RIGHT BANK	NORTHING (m)	EASTING (m)	ELEVATION (m)
I	LB	5195178.190	280412.059	996.528
	RB	5195089.003	280428.991	993.973
II	LB	5195220.775	280739.838	997.488
	RB	5195134.691	280745.823	993.728
III	LB	5195212.319	280809.260	993.038
	RB	5195132.641	280817.565	994.004
IV	LB	5195239.652	280998.052	998.257
	RB	5195149.244	281018.633	994.240
V	LB	5195241.480	281016.129	996.419
	RB	5195155.819	281046.419	992.313
VI	LB	5195437.388	281406.577	997.563
	RB	5195374.575	281451.592	992.636
VII	LB	5195415.850	282378.782	1000.150
	RB	5195330.015	282504.381	997.364
VIII	LB	5195609.324	282473.540	1001.366
	RB	5195575.822	282570.991	996.487
IX	LB	5195657.152	282498.946	1001.888
	RB	5195615.008	282590.356	996.058
X	LB	5196008.978	282755.632	998.610
	RB	5195911.458	282789.424	1001.142
XII	LB	5196381.472	283202.879	1004.966
	RB	5196270.827	283193.439	998.336
XIII	LB	5196379.322	283232.525	1001.861
	RB	5196271.265	283224.812	1001.244
XIV	LB	5196565.467	283526.208	1004.525
	RB	5196517.933	283663.921	1006.835

All data are in UTM 12 North, North American Datum 1983, using the GEOID Model 2003.

Sediment Sampling Locations

XS	NORTHING (m)	EASTING (m)	ELEVATION (m)	NOTES
XIII	5196535.959	283560.075	996.052	pc
XII	5196308.905	283227.209	994.195	pc
XI	5196289.973	283178.348	994.703	pc
X	5195940.170	282774.567	994.076	pc
IX	5195652.475	282564.543	992.465	pc
XIII	5195588.640	282540.567	992.068	pc
XII	5195316.176	282437.679	991.540	pc
XI	5195393.505	281384.146		pc
V.A	5195207.180	281067.338	999.360	pc
V.B	5195196.594	281081.780	999.378	pc
V	5195207.481	281032.549		sc
IV	5195198.906	281006.162		sc
III	5195193.115	280808.284	986.894	sc10
II	5195170.450	280744.040	986.712	sc7
II	5195181.237	280743.167	986.643	sc8
II	5195199.788	280743.287	987.041	sc9
I	5195161.152	280415.343	986.434	sc1
I	5195160.886	280414.741	986.561	sc2
I	5195161.078	280413.844	986.569	sc3

All data are in UTM 12 North, North American Datum 1983, using the GEOID Model 2003. SC = soil core, PC = pebble count.

Appendix III: Exponential Decay Derivation

Q_s flux of sediment out of the reservoir reach, m^3 /day
 V_o initial volume of sediment, m^3
 α decay constant, dimensionless
 t , time, days

$$\frac{\partial V}{\partial t} = -\alpha V \quad (3)$$

Rearranging equation 3:

$$\frac{\partial V}{V} = -\alpha dt \quad (4)$$

And taking the natural logarithm of V we show that

$$\ln V = -\alpha t + c \quad (5)$$

$$V(t) = e^{-\alpha t} e^c \quad (6)$$

At time zero,

$$V = V_o = e^c \quad (7)$$

Therefore,

$$Q_s = \frac{\partial V}{\partial t} = -\alpha V = -\alpha V_o e^{-\alpha t} \quad (8)$$

Tracking Human-Derived Nitrogen through Stream Food Webs in a Rapidly Developing Mountain Watershed

Basic Information

Title:	Tracking Human-Derived Nitrogen through Stream Food Webs in a Rapidly Developing Mountain Watershed
Project Number:	2009MT189B
Start Date:	3/1/2009
End Date:	2/28/2011
Funding Source:	104B
Congressional District:	At-Large
Research Category:	Biological Sciences
Focus Category:	Ecology, Nutrients, Acid Deposition
Descriptors:	
Principal Investigators:	Geoffrey Poole, Brian Leonard McGlynn

Publications

There are no publications.

Abstract

For this research effort, we are looking at the effects of human development and associated nutrient loading on stream food webs in the West Fork of the Gallatin River watershed. To date, we have completed two month-long field campaigns, covering the range of conditions, both natural and human-driven, seen within this system during two different seasons. Preliminary results indicate that human-derived nutrients, specifically nitrogen in wastewater, are having significant impacts on the characteristics of stream food webs. In particular, reaches with greater development influence have higher epilithic biomass, which in turn has higher nutrient content. The isotopic signatures of nitrogen in the epilithon (as well as those of streamwater and benthic macroinvertebrates) indicate that wastewater is an important source of nutrients for food webs at these sites. Future work in this area will quantify the effects that such changes in food web characteristics can have on nutrient uptake dynamics. The results of this research will increase our understanding of how human activities can affect stream systems and their associated ecosystem functions at both local and regional scales.

Progress to date

To date, two month-long field campaigns have been completed on this project – one in August 2009 and one in February/March 2010. These campaigns were designed to address the two specific objectives of the proposal. As outlined in the first objective, we wanted to quantify the spatial and temporal variability of food web utilization of human-derived nitrogen (N) within the West Fork of the Gallatin River. To address the spatial component of this question, 31 reaches were selected from across the stream network, covering broad ranges in elevation, stream order, subwatershed size, and development influence. Samples of streamwater, epilithon, and benthic macroinvertebrates were collected at each reach. Each sample type was analyzed for N concentrations and isotopic composition, as well as carbon (C) and phosphorus (P) concentrations. Measurements of biomass and chlorophyll a content were made for epilithon samples. Macroinvertebrates were identified to family prior to elemental analysis to facilitate estimates of the effects of nutrient loading on biodiversity – part of our approach to the second objective. Fish, which were included in the original proposal, were removed from the sampling campaign to enable more detailed examination of lower trophic positions across a greater area within this highly variable watershed.

The timing of our field campaigns were designed to capture two different portions of the hydrograph in this area – summer baseflow (August 2009) and winter baseflow (February/March 2010). The differences in temperature and light levels between these two times are important for food web dynamics in any ecosystem, as growth rates tend to be accelerated in warmer and lighter periods. In the West Fork in particular, these two times are also associated with different patterns of N loading, as treated wastewater effluent (the major human-derived source for this system) is stored over the winter and then used to irrigate the Big Sky public golf course during the summer months. We might therefore expect a higher utilization of human-derived N by food webs in summer due to its increased availability, as well as due to increased biotic demand for nutrients during this warmer season.

Preliminary results

At this point, samples from the August 2009 field campaign have been analyzed, so no information regarding temporal variability is included in this interim report. Based on the summer data alone, however, we are seeing marked spatial variability in stream food web characteristics associated with the variability of human-derived N loading in this system. These variations are particularly pronounced at the base of the food web, as represented by the epilithon (i.e., living and non-living algal-microbial mixture on the stream bed). Reaches with increased development in their subwatersheds had significantly higher epilithic biomass, as expected due to the higher dissolved N concentrations (higher nutrient availability) measured in streamwater at these sites. This increased availability of N within the water column at more heavily influenced sites also leads to reduced carbon to nutrient ratios (i.e., C:N) within the epilithon, due to increased incorporation of N into each unit of biomass produced at the base of the food web.

Epilithon with lower C:N ratios are in turn better food resources for macroinvertebrate consumers, as there are more nutrients contained in each unit of food consumed. As a result, we would expect to see increased biomass of these consumers at sites with higher nutrient loading and availability. Based on qualitative observations during the field campaigns, this trend also holds for the West Fork. We did not, however, see any significant shifts in macroinvertebrate community structure associated with changes in nutrient loading, as has been reported for other human-impacted ecosystems. However, detailed taxonomic analyses have not been conducted.

Isotopic evidence, from both dissolved N and the N contained within the epilithon and invertebrates, suggests that these increased N levels are primarily due to human sources. Wastewater N has a much higher $\delta^{15}\text{N}$ value (+10 to +12‰) than that of N derived from precipitation (-2 to +2‰). As a result, sites with greater wastewater influence should have correspondingly higher $\delta^{15}\text{N}$ values, and we see this trend within the West Fork watershed, at least during summer baseflow.

Planned work for the next year

Based on the data available so far, there are significant shifts in both the biomass and elemental composition of epilithon as a result of development and associated nutrient loading, primarily from wastewater inflow. These changes likely have major consequences for reach-scale nutrient uptake, and subsequently on nutrient availability and food web dynamics at sites located further downstream. To address these effects of nutrient loading on stream ecosystems at a larger scale, we will be conducting a series of experiments in August 2010 to quantify nutrient uptake and cycling. The data collected during the August 2009 field campaign will be used to select a subset of sites that represent paired stream reaches with respect to elevation, stream order, and subwatershed size, but with different epilithic C:N:P. At each site, we will use a method recently developed at MSU (McGlynn's laboratory) to quantify uptake of nitrogen and phosphorus under summer baseflow conditions. The results of these experiments will provide insight into how changes at the base of the food web, in this case due to human influence, can affect a larger-scale ecosystem process such as nutrient uptake dynamics. These data should be of high utility for understanding how changes in the West Fork watershed may lead to enrichment of downstream ecosystems, including the Gallatin River.

In addition to these experiments, the summer of 2010 will be spent primarily on laboratory work to analyze the samples collected during the February/March 2010 sampling campaign. The rest of the grant period will then be devoted to data analysis and interpretation, and to the writing of a master's thesis and related manuscripts for scientific publication. A full final report will also be completed for submission to USGS.

Organic Wastewater Chemicals in Ground Water and Blacktail Creek, Summit Valley, Montana

Basic Information

Title:	Organic Wastewater Chemicals in Ground Water and Blacktail Creek, Summit Valley, Montana
Project Number:	2009MT190B
Start Date:	3/1/2009
End Date:	2/28/2011
Funding Source:	104B
Congressional District:	At-Large
Research Category:	Water Quality
Focus Category:	Groundwater, Water Quality, Water Supply
Descriptors:	
Principal Investigators:	Gary Icopini, Stephen Parker

Publications

There are no publications.

Title: Organic Wastewater Chemicals in Ground Water and Blacktail Creek, Summit Valley, Montana

Start Date: March 1, 2009

End Date: February 28, 2011

Principal Investigator: Dr. Gary Icopini, Montana Bureau of Mines and Geology, Montana Tech, Butte, MT 59701; 406-496-4841; 406-496-4451(fax); gicopini@mtech.edu

Co-Principal Investigator: Dr. Stephen Parker, Dept. of Chem. & Geochem., Montana Tech, Butte, MT 59701; 406-496-4185(office); 406-496-4135(fax); sparker@mtech.edu

Abstract

The primary objective of this project is to assess Summit Valley groundwater for presence of organic wastewater chemicals (OWC) contamination by sampling water-supply wells that were previously sampled for inorganic constituents, particularly nitrate. In addition to the ground-water analysis, two surface-water samples from Blacktail Creek will also be collected to assess potential OWC contamination of creek. This project will provide an initial assessment of the presence of OWCs in groundwater of the Summit Valley and provide preliminary data for further studies of the fate and transport of OWCs in ground-water systems.

Commercially available enzyme-linked immunosorbent assays (ELISA) are being used to quantify OWCs in these waters. One type of ELISA kit requires a pre-concentration step using solid phase extraction (SPE) media. The pre-concentration step is often the greatest source of error in these analyses. There are currently no standard methods for the pre-concentration step used in conjunction with ELISA OWC analysis. A comparison between our existing method and a recently published U.S. EPA method was conducted to identify the best OWC pre-concentration procedure for ELISA analysis as a first step in our project. As part of this comparison, one domestic well was sampled with one sample collected at the well head (untreated water) and one sample collected after passing through the home's water treatment system. Unfortunately, the comparison data for both pre-concentration methods were compromised. Indications of compromised data included non-reproducibility and blank concentrations that nearly exceeded the linear range of the ELISA method. The MBMG has used our established ELISA procedure to measure the concentrations of these analytes in over 150 samples in the past and these analytical problems have not been previously observed. We are currently working to eliminate the analytical problems with the ELISA method and plan to complete all aspects of the project this summer.

Project Progress Report:

Revised Timeline:

This project forms the basis for a Master's of Science thesis by Jacqueline Timmer at Montana Tech in Geochemistry. Timmer is currently employed with the Organics Laboratory of Montana Bureau of Mines and Geology. During the summer of 2009 the normal work load of the MBMG Organics Laboratory more than quadrupled unexpectedly. This additional work load

has since abated; however, the additional work load caused a delay of approximately six months in starting this project. An additional delay arose from the moving of the MBMG Organics Laboratory to a new building and the analytical difficulties encountered with the comparison analysis. We feel that our prior experience with ELISA will allow us to identify the analytical difficulties and eliminate them quickly. We plan to complete the sampling portion of this project within the next three months under the following revised timeline.

	2009	2010				2011
	Oct - Dec	Jan - Mar	Apr - Jun	Jul - Sep	Oct - Dec	Jan - Mar
Method Development	X	X				
Field Sampling			X	X		
Sample Analysis			X	X		
Results presentation					X	
Publication work					X	X

Project Modifications:

Aside from the timeline, the only project modification that has been made was to substitute progesterone for 17 α -ethinylestradiol as one of the four OWC analytes. This substitution was made because progesterone was detected more frequently than 17 α -ethinylestradiol during a recent study of OWCs in Gallatin County. Progesterone may also be more abundant than 17 α -ethinylestradiol since progesterone is a natural hormone and 17 α -ethinylestradiol is a synthetic hormone. We do not anticipate other modifications to the proposed work at this time.

Method Comparison:

We devised a strategy to compare the U.S EPA pre-concentration method (U.S. EPA, 2008) with our existing pre-concentration method to see which method was best suited to ELISA analysis. The strategy consisted of processing the same fluids with each method. The first solution was reagent water (blank) spiked with progesterone and sulfamethoxazole at four different concentrations including one blank with no spike. The second solution was an untreated groundwater sample that was processed both raw and with aliquots containing spikes of progesterone and sulfamethoxazole at three concentrations. The third solution was treated groundwater from the same well as the untreated groundwater sample and the treated sample was processed the same as the untreated sample for the comparison analysis. The treatment was from an on-site home filtration system. All of the solutions were extracted in triplicate, so that a quantitative assessment could be made concerning the extraction efficiencies of the two different methods.

The results for the comparison test were similar both pre-concentration methods. Unfortunately, none of the data was deemed acceptable due high predicted concentrations in the

blanks and non-reproducible data for most of the solutions. For example, the progesterone concentrations in a reagent water (blank) using our existing extraction method ranged from non-detect to 1040 ng/L in the same triplicate set, while the progesterone concentrations in the same blank extracted with the EPA method ranged from 73 to 500 ng/L. Similar results were observed for both pre-concentration methods when using the sulfamethoxazole ELISA kit. The MBMG has used our established ELISA procedure to measure the concentrations of these analytes in over 150 samples in the past and these analytical problems have not been previously observed.

We are currently working to eliminate the analytical problems with the ELISA method. One possible explanation of these data is that the ELISA kits were in some way compromised or damaged. Both kits were ordered at the same time and it is possible that they may have been damaged in shipping or at the factory prior to receipt by MBMG personnel. Another possibility is that eluent solvent was not sufficiently removed prior to analysis via the ELISA kit. The OWCs are eluted off the SPE column with either methylene chloride (our method) or methanol (EPA method) and then evaporated to near dryness before being resuspended in 10% methanol. During this analysis it was discovered that methylene chloride reacts with the plastic ELISA containers and causes visual changes, which interferes with the optical properties of the material and compromises the analysis. The reaction of methylene chloride with the ELISA containers is a factor we will take into consideration in the overall assessment of the two methods. Since the analytical problems were observed for both pre-concentration methods, it would not be prudent to proceed with the analysis of groundwater and surface-water samples until these analytical problems have been eliminated. That said we feel confident that we can resolve the technical issues associated with the ELISA analysis in a timely fashion and complete this project within the revised timeline above.

U.S. EPA, 2007, Method 1694: Pharmaceuticals and Personal Care Products in Water, Soil, Sediment, and Biosolids by HPLC/MS/MS, U.S. Environmental Protection Agency, EPA-821-R-08-002, 77 pp.

Quantification of Coal-Aquifer Baseflow in Montana Rivers Using Carbon Isotopes

Basic Information

Title:	Quantification of Coal-Aquifer Baseflow in Montana Rivers Using Carbon Isotopes
Project Number:	2009MT191B
Start Date:	3/1/2009
End Date:	2/28/2011
Funding Source:	104B
Congressional District:	At-Large
Research Category:	Ground-water Flow and Transport
Focus Category:	Hydrogeochemistry, Methods, Water Quantity
Descriptors:	
Principal Investigators:	Elizabeth Meredith

Publications

There are no publications.

Title: Quantification of Coal-Aquifer Baseflow in Montana Rivers Using Carbon Isotopes

Principal Investigator: Dr. Elizabeth Brinck Meredith, Assistant Research Professor
Montana Tech and Montana Bureau of Mines and Geology
1300 N 27th Street, Billings, Montana
Phone: 406-657-2929, Fax: 406-657-2633,
Email:EMeredith@mtech.edu

Interim Report May 12, 2010

Abstract of work to date:

The objective of this project is to quantify the amount of groundwater contributed by the Knobloch coal aquifer to the Tongue River, Powder River, Rosebud Creek and Otter Creek, in the Powder River Basin of southeastern Montana. Quantification will be accomplished through isotope mixing models based on naturally-occurring, stable isotopes of carbon. Carbon isotopes (in dissolved inorganic carbon form) effectively fingerprint water associated with coalbed methane production in Wyoming because isotope fractionation in water associated with methane generation can be very different from surface water.

Surface water samples and groundwater samples were to be collected at baseflow; however a quick drop in temperature in October (to -35 C) caused some of the surface water sample sites to freeze before sampling could take place. Three wells completed in the Knobloch were sampled in November 2009. The published literature states that coal aquifers with methanogenesis should have carbon isotope ratios that range from +12 to +22 ‰, however the results from the three Knobloch coal wells sampled in Montana were -13.2, -13.9 and -1.0. The dominant cations and anions in these samples were sodium-bicarbonate, sodium-sulfate, and sodium-bicarbonate, respectively. Methanogenesis is only associated with water that is dominated by sodium-bicarbonate water chemistry. Among the three measured samples, there is no correlation between carbon isotope ratio and water chemistry associated with methanogenesis.

Surface water samples from three rivers were collected in March 2010, after the ice had broken-up along most of the rivers, but before the snow pack had started to melt significantly. To check for the presence of recent snow melt, oxygen and hydrogen isotope samples were collected at the same time (results not yet available). Depth and width composite samples were collected above and below the Knobloch outcrop on Rosebud Creek, Otter Creek, and the Tongue River. Carbon isotope ratios for the paired samples on the streams were very close, within or near the measurement error of 0.1‰.

Because carbon isotopes are mutable and subject to fractionation in the natural environment, a second isotope ratio, $^{87}\text{Sr}/^{86}\text{Sr}$, was chosen as a check on the carbon isotope system. Strontium isotopes are not fractionated during natural processes and, frequently, can effectively fingerprint water from distinct sources. The strontium isotope analysis for these samples was sponsored by a matching program, not this grant, but may prove useful in evaluating the effectiveness of carbon isotopes in groundwater/surface water mixing studies. Strontium isotope ratios are not yet available.

Future work will focus on Otter Creek, which has shown the most promise for successfully identifying baseflow.

Preliminary Results

Nine samples have been collected to date and have been sent for carbon isotope, strontium isotope, and major and minor constituent analyses. As a part of the minor constituent analysis, the concentration of dissolved inorganic carbon and strontium are measured. Additionally, 6 samples will be analyzed for oxygen and hydrogen isotope ratios (Table 1). Major and minor constituent analyses have been received for the three Knobloch coal wells (Appendix A). Two of the samples were dominated by sodium and bicarbonate, which is the chemical composition that would be expected of a coal that has methanogenesis, and one sample is dominated by sodium and sulfate, which indicates that this coal is not likely to have methane. However, there was no correlation between carbon isotope ratio and major ion chemistry.

River samples in Table 1 are arranged such that the upgradient samples (before the Knobloch outcrop) precede the down-gradient samples (after the Knobloch outcrop). The strontium isotope ratios measured for the Knobloch coal samples are fairly consistent (low 0.708), however the concentrations varied greatly from 0.249 to 7.631 mg/L. The Otter Creek and Rosebud Creek samples may show the influence of the Knobloch coal strontium isotope ratio, however because the strontium concentrations from the coal aquifer vary greatly, no reliable calculation of baseflow rate can be made at this time.

Table 1. Preliminary sample results (empty cells are pending unless otherwise marked)

	Date	Sample	d13C (UofA)	DIC (Mtech)	Water Chemistry (Mtech)	Sr Isotope ratio (UNC)	%STD error	dO [Sr]	dH (U.Wyo)	dH (U.Wyo)
								UNC		
River Samples	3/11/2010	O.C. @ Taylor	-8.6			0.709638	0.0008	1.97		
	3/11/2010	O.C. @ 10 mile	-8.4			0.709576	0.0008	1.86		
	3/10/2010	R.C. @ Taylor	-8.8			0.710365	0.0008	0.731		
	3/10/2010	R.C. @ N.C.	-8.9			0.710184	0.0007	0.799		
	3/10/2010	T.R. @ Birney	-6.3			0.709490	0.0008	0.599		
	3/10/2010	T.R. @ B.D.	-6.4			0.709517	0.0008	0.546		
								MTECH		
Knobloch Coal Samples	11/4/2009	203697 CBM02-8KC	-13.2	208	Na HCO3	0.708382	0.0009	0.249	n/a	n/a
	11/3/2009	251797 GC09-KC	-13.9	139	Na SO4	0.708473	0.0007	7.631	n/a	n/a
	11/3/2009	207099 WL-2	-1.0	289	Na HCO3	0.708258	0.0008	0.356	n/a	n/a

Future Work

Results from this preliminary sampling effort have changed the focus of the project from a broad survey of four rivers to a detailed look at one. The wide range of carbon isotope ratios and the highly variable strontium concentrations from Knobloch coal wells indicates that, for an accurate mixing analysis, the Knobloch coal water samples used as the end-member in the mixing equation need to be collected from wells that are very close to the coal outcrop that may be providing baseflow to the creeks. Wells completed in the Knobloch coal are very close to outcrop only along Otter Creek. At fall baseflow (October 2010), several samples will be taken along Otter Creek from the headwaters, above the Knobloch coal outcrop, and below the coal outcrop. The nearby Knobloch coal wells will be sampled at that same time. These samples will be analyzed for carbon isotope ratios, strontium isotope ratios, and major and minor constituents. Where samples are collected, a flow rate measurement will also be made.

Appendix A
Water Quality Reports

Ground-Water Information Center Water Quality Report

Site Name: MBMG MONITORING WELL CBM02-8KC

Report Date: 5/4/2010

[Compare to Water Quality Standards](#)

Location Information

Sample Id/Site Id: 2010Q0472 / 203697	Sample Date: 11/4/2009 1:00:00 PM
Location (TRS): 05S 42E 28 DDAC	Agency/Sampler: MBMG / ELM
Latitude/Longitude: 45° 22' 8" N 106° 32' 50" W	Field Number: 203697
Datum: WGS84	Lab Date: 2/1/2010
Altitude: 3262.3	Lab/Analyst: MBMG / SM
County/State: ROSEBUD / MT	Sample Method/Handling: BAILER / 4230
Site Type: WELL	Procedure Type: DISSOLVED
Geology: 125KNCB, 125TGRV, 125FRUN	Total Depth (ft): 208
USGS 7.5' Quad: BIRNEY	SWL-MP (ft): NR
PWS Id:	Depth Water Enters (ft): 190
Project: CBMPRBMON	

Major Ion Results

	mg/L	meq/L		mg/L	meq/L
Calcium (Ca)	6.950	0.347	Bicarbonate (HCO3)	1,126.500	18.463
Magnesium (Mg)	4.970	0.409	Carbonate (CO3)	14.400	0.774
Sodium (Na)	459.000	19.967	Chloride (Cl)	10.400	0.293
Potassium (K)	3.550	0.091	Sulfate (SO4)	<25.0	0.000
Iron (Fe)	8.900	0.478	Nitrate (as N)	<0.5 P	0.000
Manganese (Mn)	0.280	0.010	Fluoride (F)	13.280	0.699
Silica (SiO2)	42.500		Orthophosphate (as P)	<0.5	0.000
Total Cations		22.282	Total Anions		20.229

Trace Element Results (µg/L)

Aluminum (Al):	8,432.000	Cesium (Cs):	0.713	Molybdenum (Mo):	2.000	Strontium (Sr):	249.000
Antimony (Sb):	<0.8	Chromium (Cr):	14.900	Nickel (Ni):	7.440	Thallium (Tl):	<0.5
Arsenic (As):	1.740	Cobalt (Co):	2.630	Niobium (Nb):	<1.3	Thorium (Th):	5.270
Barium (Ba):	316.000	Copper (Cu):	<5.1	Neodymium (Nd):	8.140	Tin (Sn):	<0.6
Beryllium (Be):	<1.1	Gallium (Ga):	2.590	Palladium (Pd):	<0.9	Titanium (Ti):	32.900
Boron (B):	387.000	Lanthanum (La):	9.400	Praseodymium (Pr):	2.170	Tungsten (W):	<1.3
Bromide (Br):	<500	Lead (Pb):	10.400	Rubidium (Rb):	9.610	Uranium (U):	1.140
Cadmium (Cd):	<1.4	Lithium (Li):	44.300	Silver (Ag):	<0.7	Vanadium (V):	11.900
Cerium (Ce):	19.600	Mercury (Hg):	NR	Selenium (Se):	<1.6	Zinc (Zn):	44.800
						Zirconium (Zr):	5.160

Field Chemistry and Other Analytical Results

**Total Dissolved Solids (mg/L):	1,127.570	Field Hardness as CaCO3 (mg/L):	NR	Ammonia (mg/L):	NR
**Sum of Diss. Constituents (mg/L):	1,699.400	Hardness as CaCO3:	37.810	T.P. Hydrocarbons (µg/L):	NR
Field Conductivity (µmhos):	NR	Field Alkalinity as CaCO3 (mg/L):	NR	PCP (µg/L):	NR
Lab Conductivity (µmhos):	1720	Alkalinity as CaCO3 (mg/L):	947.68	Phosphate, TD (mg/L as P):	0.442
Field pH:	NR	Ryznar Stability Index:	6.993	Field Nitrate (mg/L):	NR
Lab pH:	8.37	Sodium Adsorption Ratio:	32.480	Field Dissolved O2 (mg/L):	NR
Water Temp (°C):	NR	Langlier Saturation Index:	0.689	Field Chloride (mg/L):	NR
Air Temp (°C):	NR	Nitrite (mg/L as N):	NR	Field Redox (mV):	NR
		Hydroxide (mg/L as OH):	NR		

Sample Condition:

Field Remarks:

Lab Remarks: DIC=208

Notes

Explanation: mg/L = milligrams per Liter; µg/L = micrograms per Liter; ft = feet; NR = No Reading in GWIC

Qualifiers: A = Hydride atomic absorption; E = Estimated due to interference; H = Exceeded holding time; K = Na+K combined; N = Spiked sample recovery not within control limits; P = Preserved sample; S = Method of standard additions; * = Duplicate analysis not within control limits; ** = Sum of Dissolved Constituents is the sum of major cations (Na, Ca, K, Mg, Mn, Fe) and anions (HCO3, CO3, SO4, Cl, SiO2, NO3, F) in mg/L. Total Dissolved Solids is reported as equivalent weight of evaporation residue.

Disclaimer

These data represent the contents of the GWIC databases at the Montana Bureau of Mines and Geology at the time and date of the retrieval. The information is considered unpublished and is subject to correction and review on a daily basis. The Bureau warrants the accurate transmission of the data to the original end user. Retransmission of the data to other users is discouraged and the Bureau claims no responsibility if the material is retransmitted.

Ground-Water Information Center Water Quality Report

Report Date: 5/4/2010

Site Name: MBMG MONITORING WELL GC09-KC

[Compare to Water Quality Standards](#)

Location Information

Sample Id/Site Id: 2010Q0471 / 251797	Sample Date: 11/3/2009 1:14:00 PM
Location (TRS): 05S 43E 02 BAB	Agency/Sampler: MBMG / ELM
Latitude/Longitude: 45° 26' 15" N 106° 23' 30" W	Field Number: 251797
Datum: NAD83	Lab Date: 2/1/2010
Altitude:	Lab/Analyst: MBMG / SM
County/State: ROSEBUD / MT	Sample Method/Handling: BAILER / 4230
Site Type: WELL	Procedure Type: DISSOLVED
Geology: 125KNCB, 125FRUN	Total Depth (ft): NR
USGS 7.5' Quad:	SWL-MP (ft): NR
PWS Id:	Depth Water Enters (ft): NR
Project: CBMPRBMON	

Major Ion Results

	mg/L	meq/L		mg/L	meq/L
Calcium (Ca)	194.000	9.681	Bicarbonate (HCO3)	660.200	10.821
Magnesium (Mg)	197.000	16.211	Carbonate (CO3)	0.000	0.000
Sodium (Na)	700.000	30.450	Chloride (Cl)	<25.0	0.000
Potassium (K)	15.100	0.386	Sulfate (SO4)	2,229.000	46.430
Iron (Fe)	<0.292	0.000	Nitrate (as N)	<0.5 P	0.000
Manganese (Mn)	0.420	0.015	Fluoride (F)	<2.5	0.000
Silica (SiO2)	14.900		Orthophosphate (as P)	<2.5	0.000
Total Cations		56.952	Total Anions		57.251

Trace Element Results (µg/L)

Aluminum (Al):	<435.0	Cesium (Cs):	<1.1	Molybdenum (Mo):	<1.4	Strontium (Sr):	7,631.000
Antimony (Sb):	<1.6	Chromium (Cr):	<1.1	Nickel (Ni):	<3.9	Thallium (Tl):	<1.0
Arsenic (As):	<2.3	Cobalt (Co):	1.940	Niobium (Nb):	<2.7	Thorium (Th):	<0.6
Barium (Ba):	44.100	Copper (Cu):	<10.1	Neodymium (Nd):	<1.5	Tin (Sn):	<1.1
Beryllium (Be):	<2.1	Gallium (Ga):	<1.5	Palladium (Pd):	2.340	Titanium (Ti):	29.000
Boron (B):	360.000	Lanthanum (La):	<1.3	Praseodymium (Pr):	<1.0	Tungsten (W):	<2.6
Bromide (Br):	<2500	Lead (Pb):	<2.6	Rubidium (Rb):	17.200	Uranium (U):	3.880
Cadmium (Cd):	<2.9	Lithium (Li):	181.000	Silver (Ag):	<1.4	Vanadium (V):	<0.9
Cerium (Ce):	<1.4	Mercury (Hg):	NR	Selenium (Se):	<3.2	Zinc (Zn):	33.200
						Zirconium (Zr):	<1.0

Field Chemistry and Other Analytical Results

**Total Dissolved Solids (mg/L):	3,675.160	Field Hardness as CaCO3 (mg/L):	NR	Ammonia (mg/L):	NR
**Sum of Diss. Constituents (mg/L):	4,010.030	Hardness as CaCO3:	1,295.270	T.P. Hydrocarbons (µg/L):	NR
Field Conductivity (µmhos):	4323	Field Alkalinity as CaCO3 (mg/L):	NR	PCP (µg/L):	NR
Lab Conductivity (µmhos):	4460	Alkalinity as CaCO3 (mg/L):	541.31	Phosphate, TD (mg/L as P):	<0.611
Field pH:	7.5	Ryznar Stability Index:	5.058	Field Nitrate (mg/L):	NR
Lab pH:	7.9	Sodium Adsorption Ratio:	8.463	Field Dissolved O2 (mg/L):	NR
Water Temp (°C):	12	Langlier Saturation Index:	1.421	Field Chloride (mg/L):	NR
Air Temp (°C):	NR	Nitrite (mg/L as N):	NR	Field Redox (mV):	130
		Hydroxide (mg/L as OH):	NR		

Sample Condition:

Field Remarks:

Lab Remarks: DIC=139

Notes

Explanation: mg/L = milligrams per Liter; µg/L = micrograms per Liter; ft = feet; NR = No Reading in GWIC

Qualifiers: A = Hydride atomic absorption; E = Estimated due to interference; H = Exceeded holding time; K = Na+K combined; N = Spiked sample recovery not within control limits; P = Preserved sample; S = Method of standard additions; * = Duplicate analysis not within control limits; ** = Sum of Dissolved Constituents is the sum of major cations (Na, Ca, K, Mg, Mn, Fe) and anions (HCO3, CO3, SO4, Cl, SiO2, NO3, F) in mg/L. Total Dissolved Solids is reported as equivalent weight of evaporation residue.

Disclaimer

These data represent the contents of the GWIC databases at the Montana Bureau of Mines and Geology at the time and date of the retrieval. The information is considered unpublished and is subject to correction and review on a daily basis. The Bureau warrants the accurate transmission of the data to the original end user. Retransmission of the data to other users is discouraged and the Bureau claims no responsibility if the material is retransmitted.

Ground-Water Information Center Water Quality Report

Site Name: MBMG MONITORING WELL WL-2

Report Date: 5/4/2010

[Compare to Water Quality Standards](#)

Location Information

Sample Id/Site Id: 2010Q0473 / 207099	Sample Date: 11/3/2009
Location (TRS): 05S 43E 21 BBDC	Agency/Sampler: MBMG / ELM
Latitude/Longitude: 45° 23' 30" N 106° 26' 8" W	Field Number: 207099
Datum: NAD27	Lab Date: 2/1/2010
Altitude: 3187.6	Lab/Analyst: MBMG / SM
County/State: ROSEBUD / MT	Sample Method/Handling: / 4230
Site Type: WELL	Procedure Type: DISSOLVED
Geology: 125KNCB, 125TGRV, 125FRUN	Total Depth (ft): 199
USGS 7.5' Quad:	SWL-MP (ft): NR
PWS Id:	Depth Water Enters (ft): 191
Project: CBMPRBMON	

Major Ion Results

	mg/L	meq/L		mg/L	meq/L
Calcium (Ca)	3.550	0.177	Bicarbonate (HCO3)	1,527.400	25.034
Magnesium (Mg)	1.710	0.141	Carbonate (CO3)	0.000	0.000
Sodium (Na)	672.000	29.232	Chloride (Cl)	64.990	1.833
Potassium (K)	4.420	0.113	Sulfate (SO4)	<25.0	0.000
Iron (Fe)	0.090	0.005	Nitrate (as N)	<0.5 P	0.000
Manganese (Mn)	0.014	0.001	Fluoride (F)	4.560	0.240
Silica (SiO2)	12.400		Orthophosphate (as P)	<0.5	0.000
Total Cations		29.706	Total Anions		27.107

Trace Element Results (µg/L)

Aluminum (Al):	<43.0	Cesium (Cs):	<0.6	Molybdenum (Mo):	1.480	Strontium (Sr):	356.000
Antimony (Sb):	<0.8	Chromium (Cr):	3.280	Nickel (Ni):	<2.0	Thallium (Tl):	<0.5
Arsenic (As):	2.490	Cobalt (Co):	<0.8	Niobium (Nb):	<1.3	Thorium (Th):	<0.3
Barium (Ba):	328.000	Copper (Cu):	<5.1	Neodymium (Nd):	<0.7	Tin (Sn):	<0.6
Beryllium (Be):	<1.1	Gallium (Ga):	<0.7	Palladium (Pd):	<0.9	Titanium (Ti):	<1.4
Boron (B):	320.000	Lanthanum (La):	<0.6	Praseodymium (Pr):	<0.5	Tungsten (W):	<1.3
Bromide (Br):	<500	Lead (Pb):	<1.3	Rubidium (Rb):	4.860	Uranium (U):	<0.5
Cadmium (Cd):	<1.4	Lithium (Li):	60.300	Silver (Ag):	<0.7	Vanadium (V):	<0.4
Cerium (Ce):	<0.7	Mercury (Hg):	NR	Selenium (Se):	<1.6	Zinc (Zn):	<10.1
						Zirconium (Zr):	1.190

Field Chemistry and Other Analytical Results

**Total Dissolved Solids (mg/L):	1,515.480	Field Hardness as CaCO3 (mg/L):	NR	Ammonia (mg/L):	NR
**Sum of Diss. Constituents (mg/L):	2,290.260	Hardness as CaCO3:	15.900	T.P. Hydrocarbons (µg/L):	NR
Field Conductivity (µmhos):	NR	Field Alkalinity as CaCO3 (mg/L):	NR	PCP (µg/L):	NR
Lab Conductivity (µmhos):	2510	Alkalinity as CaCO3 (mg/L):	1252.4	Phosphate, TD (mg/L as P):	0.093
Field pH:	NR	Ryznar Stability Index:	7.514	Field Nitrate (mg/L):	NR
Lab pH:	8.19	Sodium Adsorption Ratio:	73.325	Field Dissolved O2 (mg/L):	NR
Water Temp (°C):	NR	Langlier Saturation Index:	0.338	Field Chloride (mg/L):	NR
Air Temp (°C):	NR	Nitrite (mg/L as N):	NR	Field Redox (mV):	NR
		Hydroxide (mg/L as OH):	NR		

Sample Condition:

Field Remarks:

Lab Remarks: DIC=289

Notes

Explanation: mg/L = milligrams per Liter; µg/L = micrograms per Liter; ft = feet; NR = No Reading in GWIC

Qualifiers: A = Hydride atomic absorption; E = Estimated due to interference; H = Exceeded holding time; K = Na+K combined; N = Spiked sample recovery not within control limits; P = Preserved sample; S = Method of standard additions; * = Duplicate analysis not within control limits; ** = Sum of Dissolved Constituents is the sum of major cations (Na, Ca, K, Mg, Mn, Fe) and anions (HCO3, CO3, SO4, Cl, SiO2, NO3, F) in mg/L. Total Dissolved Solids is reported as equivalent weight of evaporation residue.

Disclaimer

These data represent the contents of the GWIC databases at the Montana Bureau of Mines and Geology at the time and date of the retrieval. The information is considered unpublished and is subject to correction and review on a daily basis. The Bureau warrants the accurate transmission of the data to the original end user. Retransmission of the data to other users is discouraged and the Bureau claims no responsibility if the material is retransmitted.

Student Fellowship: Variability in the Characteristics of Wildfire Ash: Implications for Post-Fire Runoff, Erosion, and Water Quality

Basic Information

Title:	Student Fellowship: Variability in the Characteristics of Wildfire Ash: Implications for Post-Fire Runoff, Erosion, and Water Quality
Project Number:	2009MT192B
Start Date:	3/1/2009
End Date:	12/31/2009
Funding Source:	104B
Congressional District:	At-Large
Research Category:	Water Quality
Focus Category:	Water Quality, None, None
Descriptors:	
Principal Investigators:	Victoria Balfour

Publications

There are no publications.

Summary of Studies & Fellowship Work

I have recently finished the second year of my PhD program, where upon I have completed my required course work and made ample progress on my research goals. Due to the unpredictable nature of wildfires, field work and ash sampling over the past year have been limited however I have been able to improvise and slightly alter my research objectives to still address the effects of wildfire ash on runoff and erosion.

I am currently in the process of writing the first paper to be included in my dissertation, which will be submitted for peer review in the beginning of 2010. The research for this paper addresses the physical and chemical alterations of wildfire ash following hydration as well as the hydraulic properties that are linked to these alterations (such as hydraulic conductivity and pore size). The study consists of both laboratory and wildfire ash samples, and the implications of this research are the first building blocks to understanding how and why ash may alter post-fire runoff and erosion. Next year I propose to continue addressing the evolution of ash crusts by conducting rainfall simulation experiments and quantifying infiltration and erosion rates in the laboratory as well as the field.

The following are some highlights from my past year of research:

- The opportunity to help conduct post-fire erosion experiments with Dr. Peter Robichaud and his USFS fire research team based out of Moscow, Idaho. This experience granted me access to numerous fires shortly after containment and resulted in collection of wildfire ash samples from British Columbia, California and western Montana. These samples will be incorporated into the next portion of my research. Working with this USFS team also allowed me the opportunity to determine how my research could best be utilized to aid in the mitigation of post-fire hazards. The USFS also provided me with a field spectrometer, which allowed me to collect spectral signatures of ash samples taken from the field. I plan to link these signatures to ash properties in order to aid in the remote assessment of post-fire hazards such as areas prone to high erosion or runoff events as well as possible debris flows.
- Presenting my research in the Fire Effects special session of the Geomorphology conference in Melbourne, Australia. This was an extraordinary opportunity, as it allowed me to discuss my research with renowned scientists in the field (Deborah Martin (USA), Dr. Artemi Cerda (University of Valencia, Spain) and Dr. Jorge Mataix-Solera (University Miguel Hernandez, Alicante Spain) and many more), as well as gain insightful information regarding fires in Australian ecosystems.
- My original PhD proposal included a semester of research in Europe, however due to limited funding I was unable to incorporate this aspect. I did however spend a month at the University of Swansea, Wales working with Dr. Stefan Doerr. Within this time I was able to learn a new analysis technique, Thermo-Gravimetric Analysis (TGA), as well as interact with scientists working on similar issues but in a very different environment to the western United States. My current findings were further supported by my TGA analysis conducted at Swansea and will be incorporated into the aforementioned paper. My visit also overlapped with a fellow PhD student, Mercedes Bodi, who is working under Dr. Artemi Cerda in Spain and also addressing the effects of ash on runoff and erosion. Mercedes and I were able to discuss our research as well as collaborate on a possible joint publication for 2010. I was also able to obtain ash sample from field sites in the Mediterranean, allowing me to further assess the variability (through differing ecosystems) on the characteristics of wildfire ash. Furthermore, during my time at Swansea I was able to present my research to the Department of Environment and Society, which allowed very insightful feedback.

The funds from the Montana Water Center have greatly enhanced my research and PhD experience. Thank you for your support and I look forward to presenting my research at next year's Water Center conference. Please contact me if any further details or clarification are needed regarding my research or current development.

Sincerely,

Victoria Balfour

Student Fellowship: A More Efficient Micro-hydro that Utilizes a Tesla Turbine Technology

Basic Information

Title:	Student Fellowship: A More Efficient Micro-hydro that Utilizes a Tesla Turbine Technology
Project Number:	2009MT195B
Start Date:	3/1/2009
End Date:	12/31/2009
Funding Source:	104B
Congressional District:	At-Large
Research Category:	Engineering
Focus Category:	Models, None, None
Descriptors:	
Principal Investigators:	Alaina Garcia

Publications

There are no publications.

Summary of “Building a Tesla Turbine”: Alaina Garcia, Mechanical Engineering, MSU

The present Tesla turbine prototype is not a copy of the original Tesla unit, but uses the same principals, spins on compressed air and probably would produce more torque on steam versus water. This is one of the biggest learning concepts of the project thus far. Yet one of the great things about the Tesla turbine is its simplicity. To make the turbine run, high-pressure fluid enters the nozzle at the outer chamber stator inlet. The fluid passes parallel between the rotor disks and causes the rotor to spin using boundary-layer adhesion from the fluid's viscosity. Eventually, the fluid exits through the exhaust ports in the center of the turbine and two aluminum cuffs hold the disks in position on the shaft. As the disks will be (come spring semester) keyed to the shaft, their rotation is transferred directly to the shaft. The rotor assembly is housed within a cast acrylic stator and the axis is the only moving part. The prototype has 8 disks (computer hard drives), 4 inches in diameter, spaced at .004 inches, and develops speeds of 4,000 RPM (measured using a tachometer in Norm's physics machine shop at MSU) using compressed air from a machine shop. One of the design changes for the next semester will allow the shaft to have a lower coefficient of friction and higher rpm by aluminum lining the aluminum axis shaft so it is not spinning on cast acrylic.

In Tesla's final attempt to commercialize his invention in 1910, he persuaded the Allis-Chalmers Manufacturing Company in Milwaukee to build three turbines. Two had 20 disks, 18 inches in diameter, and developed speeds of 12,000 and 10,000 rpm respectively. The third had 15 disks, 60 inches in diameter and was designed to operate at 3,600 rpm; generating 675 horsepower. Tesla's original design called for two inlets, which allowed the turbine to run either clockwise or counterclockwise. During the tests, engineers from Allis-Chalmers grew concerned about the mechanical efficiency of the turbines, as well as their ability to endure prolonged use. They found the disks distorted to a great extent and concluded the turbine would have eventually failed. This, more than anything, prevented the Tesla turbine from becoming widely used. Nowadays, composites such as carbon-fiber, titanium-impregnated plastic and Kevlar-reinforced disks could prove to be more qualified materials.

Spring research will continue to vary the size and number of the disks. Tesla's patent paperwork doesn't define a specific number, but uses a more general description, stating the rotor should contain a "plurality" of disks with a "suitable diameter and spacing." Tesla-type turbomachinery probably cannot prove competitive as an application in which more conventional machines have adequate efficiency and performance. Tesla turbine applications are for small shaft power, or the use of very viscous fluids, or of non-Newtonian fluids. For that reason they should be further investigated for applications to produce power from geothermal steam and particle-laden industrial gas flows. There is considerable evidence that multiple disk turbomachinery can operate quieter and to resist fluid cavitation that is specifically avoided in the design of machines such as turbines or propellers.

Finally, I would like to say “Thanks!” to the Montana Water Center and Robb Larson for the opportunity to do the research and design of a Tesla turbine! It has been a very interesting learning experience. With the assistance of the Undergraduate Scholars Program, I will continue work on a prototype that will spin (speed is yet to be determined) with water from a stream and function as a micro-hydro unit with the assistance of an alternator.

Student Fellowship: Bayesian Uncertainty and Sensitivity Analysis for Complex Environmental Models, with Applications in Watershed Management

Basic Information

Title:	Student Fellowship: Bayesian Uncertainty and Sensitivity Analysis for Complex Environmental Models, with Applications in Watershed Management
Project Number:	2009MT199B
Start Date:	3/1/2009
End Date:	12/31/2009
Funding Source:	104B
Congressional District:	At-Large
Research Category:	Water Quality
Focus Category:	Non Point Pollution, Agriculture, Surface Water
Descriptors:	
Principal Investigators:	Able Mashamba

Publications

There are no publications.

Summary of Montana Water Center Fellowship Report

A comprehensive Soil and Water Assessment Toolkit (SWAT) ground-phase hydrologic model was built, calibrated, validated and used to study the effects of targeted watershed conservation policies on channel discharge and on sediment, nitrogen and phosphorus concentrations and loadings in the case study watershed. Online and Montana State University Extension Services field data for the Buffalo Rapids irrigation district in Eastern Montana, Lower Yellowstone River watershed was used. The main findings of the simulation experiments were that: (1) Irrigation systems that deliver smaller amounts of water more frequently counter-intuitively results in lower flow rates than less frequent application of larger amounts of water. (2) Sediment concentration in the Lower Yellowstone watershed channels is more correlated to flow rate than precipitation, implying it is largely generated by flow processes, not runoff. (3) Minimizing tillage reduces sediment concentrations but promotes the washing away of nutrients into the channels. (4) Increasing channel conductivity increases flow, implying channels are net gainers of water by return flow. (5) However higher Total Nitrogen and Phosphorus with more conductivity implies return flow brings higher nutrient loads. These five results were presented at the 2009 American Water Resource Association, Montana Chapter Annual Conference in Missoula and form a research report manuscript aimed for publication in the Journal of American Water Resources Association.

Automated calibration and uncertainty estimation of complex distributed hydrologic models, such as SWAT, is a slow and computationally intensive process. Specifically, the statistical coherency of non-Bayesian uncertainty estimation methods currently in use is hotly debated. In response to these drawbacks, work has already been covered to show the potential for significant quickening of the calibration process and for making the uncertainty estimation more statistically coherent. Markov Chain Monte Carlo, MCMC, methods have been tested on synthetic and real world lumped models as proof of concept in making uncertainty analysis faster and statistically acceptable. To further quicken model calibration and uncertainty estimation, fast surrogate models have been demonstrated as adequate in mimicking the required responses of the slow but more and complex models used in analysis. Research on the feasibility of these response surface estimation methods (RSM) has been completed and results presented at the American Statistical Association annual conference (2009) for the Montana chapter, in Butte. A research paper manuscript on this work is currently going through internal moderation. Current and outstanding research is in the implementation of these quickening methods (RSM, MCMC, and parallel computing) to the SWAT modeling framework. If current research progress is sustained, the remaining time is ample to develop and test these ideas on the case study SWAT model, with significant insights into, and contribution to, computationally time-expensive modeling in general.

Student Fellowship: Tree-ring based reconstruction of Bighorn River Flow During the Last Millennium

Basic Information

Title:	Student Fellowship: Tree-ring based reconstruction of Bighorn River Flow During the Last Millennium
Project Number:	2009MT200B
Start Date:	3/1/2009
End Date:	12/31/2009
Funding Source:	104B
Congressional District:	At-Large
Research Category:	Climate and Hydrologic Processes
Focus Category:	Climatological Processes, Drought, Floods
Descriptors:	
Principal Investigators:	Bryan Swindell

Publications

There are no publications.

December 2009 Research Update
Bryan Swindell

My thesis research is about halfway finished. Fieldwork was conducted last summer and data analysis is underway. Although the original goal of the field season was to find suitable tree-ring collection sites in the Pryor Mountains of Wyoming, none could be found after days of searching. However, two promising tree-ring collection sites were discovered in the Crazy Mountains. One is located in the Upper Smith Creek drainage on the western side of the Range, and the other is located in the Big Timber Creek drainage on the eastern side of the Range.

A total of 40 approximately 500-year-old Douglas-fir trees were sampled at these sites. In addition, samples were collected from a small set of Douglas-fir trees growing in the Beartooth Mountains near Red Lodge. Counting and width measurement of the rings from all of these trees is almost complete. Data from these sites will be combined with data from several other sites sampled by other researchers in the Greater Yellowstone Ecosystem.

The next step will then be to look for a relationship between ring width and streamflow in the Bighorn Basin. This exercise will indicate if any of the sites are good predictors of streamflow. If a strong relationship between rings from any of these sites and streamflow is found, those trees will be used to statistically reconstruct the plausible annual flow volume of the Bighorn River as far back in time as the tree-ring record allows. Preliminary results should be available by May of 2010, with a final paper being ready by September.

Information Transfer Program Introduction

The Montana Water Center fills the unique role of coordinating Montana University System (MUS) water-related research, and disseminating and applying its findings for the benefit of the people of the state. And, as Montana is a headwaters state to two of the nation's major river drainage basins: the Missouri and the Columbia, how Montana manages its water and aquatic plants and animals can have far ranging impacts downstream. Obviously these are not closed systems. Montana's aquatic resources are also impacted by what comes into the state, be it acid rain, drought, aquatic nuisance species, or wind carried dust and debris that can increase snowpack melt. Of course, climate change is a growing concern and, as research is being done to determine the impact this will have on Montana, the Montana Water Center is part of a multi-disciplinary effort to prepare for what seems to be inevitable change. To prepare, people need to be informed, and the Center uses some of its USGS funding to provide forums and outlets for information exchange. During the period March 1, 2009 through February 28, 2010, the Montana Water Center drew on its USGS support to conduct programs listed under the Statewide Education and Outreach project.

Statewide Education and Outreach

Basic Information

Title:	Statewide Education and Outreach
Project Number:	2009MT201B
Start Date:	3/1/2009
End Date:	2/28/2010
Funding Source:	104B
Congressional District:	At-Large
Research Category:	Not Applicable
Focus Category:	Education, Water Quality, Water Quantity
Descriptors:	
Principal Investigators:	Steve Guettermann, Mary Jo Nehasil

Publications

There are no publications.

Supporting students to become water science professionals is a core mission of the Montana Water Center. To that end, the center worked closely this year with faculty researchers to engage students in water-related research, writing papers and professional presentations. Center staff frequently encouraged aquatic science, engineering and students in related disciplines to apply for student fellowships. This outreach increased the diversity of students with whom the center worked. Faculty researchers who received research funding from the Water Center are required to actively mentor students in the research projects. The Water Center also encouraged students engaged in water resource studies to present at conferences.

In addition to working with faculty and students, Water Center programs reached thousands of other water resource professionals, teachers, farmers, ranchers, engineers, drinking water and wastewater system operators and other professionals throughout the state. Specific information transfer activities include the following.

- * Published twelve Montana Water e-newsletters and distributed them monthly to almost 2,000 professionals, students and decision makers concerned with water resource management. Newsletter archives are posted at <http://water.montana.edu/newsletter/archives/default.asp>.

- * Completed a Montana Watersheds Coordination Council website redesign at <http://mtwatersheds.org/>. The site is better serving watershed groups throughout the state by highlighting organizational improvements and member communication.

- * Continued the web information network MONTANA WATER, at <http://water.montana.edu>. Known as Montana's clearinghouse for water information, this website includes an events page, news and announcement updates, an online library, water-resource forums and water source links, a Montana watershed projects database, an expertise directory, water facts and more.

- * With EPA funding, initiated four online web training modules for small drinking water system operators. The modules are: energy conservation, demand-side water conservation, water leak detection, and alternative energy use. Reviewers from around the country critiqued the modules. The center is incorporating those changes into the modules before they are disseminated for use.

- * With state and federal stimulus funding, the center began production of a series of water-science training modules for local decision makers. Surveys show that often decision makers are asked to make decisions that impact water quality and quantity, but frequently have no or little education, or understanding of, basic hydrology or other relevant water science topics that might be helpful for them to make informed decisions. These modules will help fill some of the gaps. Its major topics are wetlands, water data interpretation, ground water/surface water interaction, floodplain and riparian zone management, water quality impairment and protection, and recent changes to water law. The modules will be presented via webinars, as well as at conferences and other trainings, and be available online for individual study.

* Maintained and circulated a small library of paper documents related to Montana water topics.

* Conducted the statewide water research meeting on October 1-2, 2009 in Missoula, Montana. The theme of the 26th annual meeting was Waters that Cross Divides. It was a joint conference with the Montana Section of the American Water Resources Association and the River Center of the University of Montana. A field trip led by Water Center-funded researcher, Professor Andrew Wilcox, analyzed the Milltown Dam area just below the confluence of the Clark Fork and Blackfoot rivers, following removal of the Milltown Dam. The area is part of a major Superfund cleanup site. The conference attracted over 200 Montana researchers and policy makers and 50 students. Over forty researchers presented information on their latest findings along with nearly 30 poster displays. The web-based archive of this meeting is found at http://awra.org/state/montana/events/conf_archives.htm.

* Responded to numerous information requests on water topics ranging from invasive aquatic species to water rights to streamside setbacks to contaminants and pollutants in Montana's surface and ground water, and ways to better manage ground and surface water.

* Assisted elected and appointed officials, particularly those serving on the Montana Legislative Environmental Quality Council, the Water Policy Interim Committee (WPIC), and the Governor's Drought Advisory Committee, with water resource issues. Partly due to funding it received to work with local decision makers, the Water Center will continue to be involved with WPIC as issues about the state's water, and its use and management, become more important to the state legislature and Montanans.

* Sponsored and participated in Montana's 76th Annual Water School October 5-9, 2009 at Montana State University for 300 staff members of water and wastewater utilities. The school primarily helps prepare new system operators to pass the certification exam, and familiarizes participants with other resources they may find helpful in the future.

* Created and distributed 1,500 copies of the black-and-white Montana Water 2010 calendar to elected officials, water resource managers and other partners and supporters. Designed to educate the public about water issues and aquatic life, photographers from all over the state contributed to the calendar.

* Worked with the Montana Department of Environmental Quality and the Montana Department of Transportation to provide professional education to mitigate nonpoint source pollution. The Montana Watercourse provides comparable outreach to watershed groups, teachers, developers, and landowners.

USGS Summer Intern Program

None.

Student Support					
Category	Section 104 Base Grant	Section 104 NCGP Award	NIWR-USGS Internship	Supplemental Awards	Total
Undergraduate	2	0	0	0	2
Masters	6	0	0	0	6
Ph.D.	7	0	0	0	7
Post-Doc.	0	0	0	0	0
Total	15	0	0	0	15

Notable Awards and Achievements

Other notable work undertaken by the Montana Water Center includes:

The Whirling Disease Initiative The Whirling Disease Initiative was established by Act of Congress in 1997; it concluded on June 30, 2009. Its purpose was to conduct research to develop practical management solutions to maintain viable, self-sustaining wild trout fisheries in the presence of the whirling disease parasite. A final report for the federally funded Whirling Disease Initiative was published in October 2009, and funding has been discontinued. The final report is available at http://whirlingdisease.montana.edu/pdfs/wdi_final_2009.pdf . The Montana Water Center was the administrative entity that managed the program and coordinated outreach and educational activities.

In summer 2009 Trout Unlimited and the Whirling Disease Initiative, coordinated by the Montana Water Center, released *Whirling Disease in the United States: A Summary of Progress in Research and Management*. This publication reviews the complex life cycle of the parasite, biological and environmental factors influencing its spread and severity, and current prevention and management techniques. The text is copiously illustrated and augmented with a detailed bibliography. It should be most useful to field biologists and others who deal with aquatic nuisance species. The document is available for download from the Initiative website at <http://whirlingdisease.montana.edu/resources/publications.htm>.

The Whirling Disease Initiative was established to provide a rapid, science-based response to a serious fish health issue that threatened the wellbeing of highly valued fish populations and economically important fishery resources. Its response initially focused on providing a clear understanding of the *M. cerebralis* pathogen, its affinity for and the susceptibility of its fish and worm hosts, and developing technologies for rapid and accurate detection of the pathogen. The research agenda was broadened to include intensive study of biological and environmental factors influencing the establishment and severity of the pathogen in differing types of waters and different geographic regions.

The Initiative can claim notable accomplishments: * In-depth understanding of the biology of *Myxobolus cerebralis* in its two hosts * Establishment of the relative susceptibility of the North American salmonid species, and the lineages of *T. tubifex* * Synthesis of knowledge regarding infection and disease risk factors for watercourses * A suite of diagnostic techniques for assessing infection in different organisms and media * Description of disease immunology, and the limits of a vaccination approach, in fish * A synoptic understanding of the effects of disease in wild fish populations under different environmental circumstances.

While the research supported by the Whirling Disease Initiative uncovered no silver bullet to eliminate established whirling disease infections, successes in maintaining populations and fisheries have been attained. Much was learned and this information was effectively communicated to scientists, resource managers, and citizens interested in and dealing with this fish health challenge.

The Small Systems Technical Assistance Center The Small Systems Technical Assistance Center operated by the Water Center is the flagship of a nationwide network that helps small public water utilities provide safe, reliable and affordable drinking water. The Montana Water Center assists small drinking water operators throughout the country by providing continuing education via online download and CDs for system operators. To date, more than 50,000 water-utility workers have taken the Center's training courses nationwide. This year's projects include:

- developing live and electronic training courses on water-system energy efficiency, use of alternative energy sources, water loss testing, and water conservation.

- continued to work with the other TACs to develop a more comprehensive website and research and outreach presence to provide greater nationwide assistance to small public drinking water systems.

The Montana Watercourse Montana Watercourse, is part of the Montana Water Center. It is a statewide water education program that supports water resource decision making and stewardship by providing unbiased information, resources, tools and education to all water users.

This year the Montana Watercourse Montana successfully completed eight distinct programs that reached over 1,450 resource professionals, students and community members. Water rights trainings continue to provide application-based information that strengthens the connections among government entities, private landowners and brokers. At the three day 12th Annual Water Summit, teachers and students refined their ability to perform water quality monitoring tasks in relation to a variety of physical, chemical, social and cultural elements. During this report period, each of the four wetland and riparian buffer trunks was successfully delivered to the host institutions around the state. These trunks provide low-cost, hands-on opportunities for students to learn about critical habitats, and include a complete wetlands curriculum for the K-12 grade levels.

An annual report for the Montana Watercourse can be downloaded at <http://mtwatercourse.org/media/downloads/2009MTWCAnnualReport.pdf>.

Graduate Researcher Award Adam Sepulveda, an ecology doctoral student at the University of Montana, was awarded a trip to the National AWRA Conference in Seattle by the Montana Section of the AWRA for his student presentation at the state's water resources conference in Missoula, Montana, which the Montana Water Center co-sponsored. The title of his presentation was The Role of Movement to Stream Salamander X Fish Coexistence: On a Road to Nowhere? Much of Adam's work examines the importance of ecological linkages between headwater streams and downstream waters to the conservation and management of stream organisms, such as fish and salamanders.